ENERGY SPECTRA AND TRANSFERS IN MAGNETOHYDRODYNAMIC TURBULENCE

by

GAURAV DAR

DEPARTMENT OF PHYSICS

INDIAN INSTITUTE OF TECHNOLOGY KANPUR

January, 2000

ENERGY SPECTRA AND TRANSFERS IN MAGNETOHYDRODYNAMIC TURBULENCE

A Thesis Submitted

in Partial Fulfillment of the Requirements

for the Degree of

Doctor of Philosophy

by

GAURAV DAR

DEPARTMENT OF PHYSICS

INDIAN INSTITUTE OF TECHNOLOGY KANPUR

JANUARY 2000

CERTIFICATE

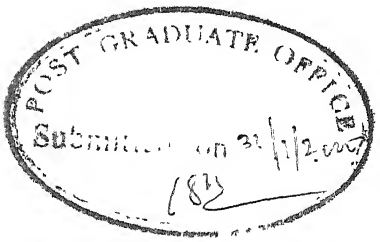

It is certified that the work contained in this thesis entitled "**Energy spectra and transfer in magnetohydrodynamic turbulence**", by **Gaurav Dar**, has been carried out under our supervision and that this work has not been submitted elsewhere for an degree.

Dr. Mahendra K. Verma
Assistant Professor
Department of Physics
Indian Institute of Technology
Kanpur

Dr. V Eswaran
Professor
Department of Mechanical Engine
Indian Institute of Technolog
Kanpur

January 2000

To

My Parents

Synopsis

The Magnetohydrodynamic (MHD) model describes plasmas as a collisional, electrically neutral, and a highly conducting fluid. In turbulent flows, fluctuations are present over a wide range of length scales (wavenumbers). The nonlinear terms in the MHD equations transfer energy between the wavenumbers of different sizes. Energy is transferred between velocity ($\mathbf{u}$) modes, between magnetic ($\mathbf{b}$) modes, and between velocity and magnetic modes. In this thesis we investigate these energy transfers and test the predictions of various MHD turbulence phenomenologies. Our study is restricted to two-dimensional MHD turbulence.

The energy spectrum in fluid turbulence is given by $E(k) = C < \epsilon >^{2/3} k^{-5/3}$, where $< \epsilon >$ is the average rate of energy dissipation and C is a universal constant. In MHD turbulence two classes of phenomenologies have been proposed: (1) The phenomenology by Kraichnan (1965), Iroshnikov (1963), Dobrowolony *et al.*(1980) [1–3] (together referred as KID) suggested that the energy spectra of $\mathbf{z}^{\pm}$ $(= \mathbf{u} \pm \mathbf{b})$ is $E^{\pm}(k) = (\Pi^{\pm} B_0)^{1/2} k^{-3/2}$, where $\mathbf{B_0}$ is the mean magnetic field, and $\Pi^{\pm}$ are the energy fluxes of $\mathbf{z}^{\pm}$. Additionally it was predicted that energy fluxes $\Pi^{\pm}$ are equal. An extension of KID phenomenology predicts that $\Pi^{+}/\Pi^{-} = m^{+}/m^{-}$ [4], where $m^{\pm}$ are the scaling exponent of the energy spectra $E^{\pm}(k) \sim k^{-m^{\pm}}$. (2) According to a different class of phenomenology [5–7], the energy spectra in MHD turbulence is Kolmogorov-like with $E^{\pm}(k) = C^{\pm}(\Pi^{\pm})^{4/3}(\Pi^{\mp})^{-2/3} k^{-5/3}$, and the constants $C^{\pm}$ are believed to be non-universal. These phenomenologies have been tested in simulations [8–13] and Solar Wind observations [14–16] and appear to favour Kolmogorov-like phenomenology, but there is still a lack of consensus among researchers. One of the objectives of this thesis is to investigate this issue further.

The interaction in MHD invloves three modes $\mathbf{k}$, $\mathbf{p}$, $\mathbf{q}$ satisfying the condition $\mathbf{k} + \mathbf{p} + \mathbf{q} =$ The *combined* energy transfer from any two modes to the third mode is known. In this thesi we develop a formalism to describe energy transfer between a pair of modes by the mediatio

of the third mode in the triad. We have used this formalism to study some important features of energy transfer.

The properties of energy transfer are an important component of turbulence studies. The total energy is known to cascade from low wavenumbers to the high wavenumbers. Some other aspects of energy transfer in MHD turbulence have also been studied, such as the nonlocal transfer between the high wavenumbers and the low wavenumbers [17–19] and the net energy transfer to a mode from all other modes [20, 21]. The predictions of some of these studies have not been rigorously tested. Additionally, several other interesting energy transfers have not been investigated as yet. In this thesis we have numerically studied some of these transfers, for example, the energy flux out of a velocity wavenumber-sphere, a magnetic wavenumber-sphere and various energy fluxes from velocity to the magnetic modes. We have also studied the fine-grained energy transfer between various velocity and magnetic wavenumber shells.

In the discussion given below we briefly describe the contents of each chapter, which includes its aim and its central results.

Chapter 1 contains a survey of the field. We also state the thesis problem here.

In **Chapter 2** we test the predictions of KID phenomenologies and the Kolmogorov-like phenomenology in direct numerical simulations of forced 2-D MHD turbulence. The phenomenologies are tested over a wide range of normalised cross helicity (normalised velocity-magnetic field correlations). To test the phenomenologies we plot the time-averaged energy spectra and the energy cascade rates. It is difficult to distinguish between the spectral exponents $-3/2$ and $-5/3$ predicted by KID phenomenology and Kolmogorov-like phenomenology respectively. Instead, following the approach of Verma *et al.* [11], we test the predictions of the energy cascade rates $\Pi^{\pm}$ by the KID and the Kolmogorov-like phenomenology. Our results of the energy cascade rates are inconsistent with the KID phenomenology and its extension by Grappin, but are in close agreement with the predictions of Kolmogorov-like phenomenology with $C^{\pm}$ having a small variation with the normalised cross-helicity σ_c. Using our simulation data we study the dependence of Kolmogorov constants on σ_c.

In **Chapter 3** we find a new approach for studying energy transfer in turbulence. We obtain a description of the energy transfer between a pair of modes in a triad by the mediation of the third mode. We find that the mode-to-mode energy transfer can be expressed as a sum of an 'effective' transfer and a 'circulating' transfer. These two have the property that the effective transfer causes a change in the modal energy, while the circulating transfer does not affect modal energy since the same amount of energy is transferred from $\mathbf{k}$ to $\mathbf{p}$. from $\mathbf{p}$ to $\mathbf{q}$, and from $\mathbf{q}$ back to $\mathbf{k}$. We have derived the expression for effective transfer between a pair of velocity modes, a pair of magnetic modes, and between a velocity and a magnetic mode. In each of these, the effective transfer between the two modes is mediated by the third mode of the triad. By applying the constraints of rotational invariance, galilean invariance, and finiteness, we show that the circulating transfer is equal to zero upto the linear order in a series. Using the expression for the effective transfer between modes, we define several energy cascade rates and shell-to-shell transfer rates (energy transfer between two wavenumber shells).

In **Chapter 4**, the energy cascade rates and the shell-to-shell transfer rates defined in Chapter 3 are computed by a direct numerical simulation of 2-D MHD turbulence. The cascade rates and shell-to-shell transfer rates are averaged over a quasi-steady state achieved by large-scale kinetic energy forcing. The picture of energy fluxes that emerges is quite complex — there is a forward cascade of magnetic energy, an inverse cascade of kinetic energy, a flux of energy from the kinetic to the magnetic field, and a reverse flux which transfers the energy back to the kinetic from the magnetic. The energy transfer between different wave number shells is also complex — local and nonlocal transfers possess opposing features — for example, energy transfer between some wave number shells occurs from kinetic to magnetic, while this transfer is reversed for some other shells. The net transfer of energy is from kinetic to magnetic. The results obtained from the flux studies and the shell-to-shell energy transfer studies are consistent with each other. Comparison of the simulation results with earlier analytical studies [18, 19] and numerical simulations [20] are also made.

The evolution of global quantities are presumed, by most researchers, to depend only on the initial value of the global quantities and their spectra. In **Chapter 5** we numerically study the effects of subtle changes in initial conditions, keeping the global quantities and their spectra unaltered, on the evolution of global quantities in two-dimensional MHD turbulence. We find that a change in the initial phases of complex Fourier modes of $\mathbf{z}^{\pm}$ while keeping the initial values of total energy, cross helicity, and Alfvén ratio (ratio of kinetic energy to magnetic energy) unchanged, has a significant effect on the evolution of cross helicity. On the other hand, the total energy and Alfvén ratio are insensitive to the initial phases.

The thesis is concluded in **Chapter 6** by a brief summary and the future research directions.

Acknowledgments

'(My) Life is a stage', said Shakespeare. It is time for curtains on one more scene. In each scene, new characters enter, some old and several new. The scene ends. The curtains come down. Another scene begins. The curtain rises. And a new set of characters appear on the stage. It is time to acknowledge the role played by the various characters in each scene on the stage of my life.

When I started a PhD I felt more like a sailor of the medieval times who, having set out on his maiden voyage, did not know whether he would complete the journey or he would be gobbled up by the limitless pit at the edge of the Earth. The experienced and wise navigators present on the ship must have given him some confidence. So has been the case with me. Like that sailor, it was to my supervisors I always turned, when the limitless pit appeared to be too close for my comfort. And like experienced navigators they always guided me to safety. I am grateful to my thesis supervisors for the time, the valuable help and the direction they always gave me in my research work. This thesis would not have taken shape without their guidance. I have always valued writing skills. To my annoyance, to begin with, I discovered that scientific writing was an entirely different genre. I am grateful that my supervisors very painstakingly set right all the wrongs that I had committed while writing papers and the thesis. At times I must have been lazy, forgetful, and disorganized. But I am grateful that they tolerated me.

The advice of my peer review committee, Dr. Ravi Shankar and Dr. Budhani was often useful and I thank them for their help. While Dr. Ravi Shankar was away on a sabbatical, Dr. Subrhamanyam had kindly consented to be a member of the committee. I also thank him.

We were able to perform our simulations only due to the kind assistance of Dr. R. K. Ghosh of the Computer Science and Engineering Dept. who allowed us the use of his

computer facilities. I also gratefully acknowledge the helpful discussions with Dr. Debasis Kundu of the Mathematics Dept. During the two months of stay at CDAC, Pune I parallelised my MHD turbulence code with the help of Dr. VCV Rao, Chaman and others in CDAC. Thanks are due to them.

Each human-being gets inspired by and learns from a myriad of sources. So was the case with me. My quest for knowledge began under the encouragement of my parents who regularly supplied me with books to read and inculcated in me the joy of reading and learning. My teachers served as role models for their achievements and scholarship. Many teachers had influenced me in ways, known and unknown to me. However, Arjun Mahey must deserve special mention for he was a rare breed of teachers who dared teach Physics in an English class and did it so successfully that it inspired me to take up physics in college. The desire to be creative, to teach and to reach out to the frontiers of knowledge is all due to my parents and to my school to whom I owe an immeasurable gratitude.

Books can be truly said to be agents of the information revolution. But well written books are the agents of a revolution of the spirit. They not only impart knowledge but send you in search of more. In my education, books like the Feynman lectures, Griffith's electrodynamics, and many more did just that and I am grateful to the writers of all these books.

Life is like a rainbow. Each colour has its own identity but it is the the togetherness of all the colour that adds beauty and meaning to the rainbow. My life at IIT has been like the rainbow with each colour depicting a different and a unique aspect of my stay here. To my friends here, I am thankful for adding colour to my life - Saurabh, Shobhit, Vivek, Alok, Magesh, Prasenjit, Narsimhan, Bijoy, Rajan, Panda. Companionship of my friends in other places too too is greatly valued by me - Sadiq, Kamilla (Gorillae), Raja (Piggy), Bharat, Chhachhi, Shiva, Vinita, Vandana, Vipin, and my entire class of St. Stephens. I learnt something from each of my friends. But above all Physics would not have been so much of fun without the presence of all these friends. It would take some adjusting to know what life

would be like without the long discussions on Science, politics, Art, etc. with Vivek. For the more immediate purpose I thank him for helping me with LaTeX. With Saurabh I spent very enjoyable moments of my seven years and shared a lot of personal thoughts, joys and sorrows. Shobhit cannot be forgotten for his infectious enthusiasm for everything, including eating several bhuttas at a time. With Alok I spent half the time climbing the Himalayas and the other half talking about it. I am thankful to him for making my stay memorable here. It has been a source of comfort to discuss our mutual worries with Magesh ! But in a more serious vain I also thank him for his eagerness to give help whenever I required it. Though far from IIT, it has been a pleasure communicating with Jeshma and I also thank her. I could fill pages thanking each of my friends. So, I collectively thank all of them and I apologize to those whose names I may have missed.

The graduate seminar had provided a unique possibility to grow. It had been a pleasure hearing the seminars of other enthusiastic PhD students — Rajan Gurjar, Sayan, Sujoy, Alok, Prasenjit,George, Sudhansu, Abir, Saurabh, Vivek, Prashanta, Panda, Rajan Pandey, Dalvi, Bala, Chandan.

The efforts of Dr. Mahendra Verma and Dr. Pankaj Jain were instrumental in the birth of a computer room for the department. What the primitive man must have felt after getting cooked food served on the table without first hunting for it would easily mirror my own feelings when the computer room came into existence. We no longer had to hunt for a computer in the overcrowded Computer Center. Life and work became more pleasurable after that. I thank both Dr. Verma and Dr. Pankaj Jain for their efforts.

I thank the staff of the Physics office for being of assistance from time to time. Thanks are also due to all the unacknowledged individuals whose work keeps the IIT machinery running smoothly.

Realization of ones ignorance is the first step towards gaining any meaningful knowledge. My interaction with the group composed of Dr. AP Shukla, Vivek, Prasenjit, Rahul and Manali stands out in this category. The discussions that we regularly had, week after week,

on Sociology of Science, history of science, and a host of other issues dealing with society have left an indelible mark on me. The contribution of this group to my growth has been significant.

Nothing of this would have ever been possible had it not been for the support of my parents. My father pointed out the various constellations to me when I had just learnt to speak, read out books to me, and took me to the mountains. He set me on the path of discovery. His example as a school-teacher has been an inspiration to me. My mothers support and care at the cost of her own comfort makes me wonder if I have the ability to follow her example. It is my parents who have shaped my personality and my dreams and the thesis can only be dedicated to them. My sister's and bua's love and concern for my well-being has been valuable to me at all times during my PhD.

Gaurav Dar,
IIT, Kanpur,
31st Jan 2008.

Contents

List of Tables

List of Figures

Chapter 1

Introduction

Turbulent flows are ubiquitous. They occur over various scales, from the scale of a laboratory to that of a cluster of galaxies, spanning a range of the order of 10^{25}. Turbulence in non-conducting fluids can be generated and studied in a variety of experimental setups in the laboratory, and also observational studies of turbulence can be carried out in naturally occurring flows such as the atmosphere. The Reynolds numbers required for generating MHD turbulence however are not usually achievable in a terrestrial laboratory. MHD turbulence exists in a variety of astrophysical flows such as in the Solar Wind, interstellar medium, stars, etc. The study of turbulence is important for these systems. For example, the molecular clouds form $20\% - 50\%$ of the interstellar gas in the milky way, and they are the sites of star formation. Turbulence in the molecular clouds is believed to play an important role in star formation [22]. In the Solar Wind, turbulence plays an important role in the evolution of energy, temperature, pressure, etc. [23]. Turbulence is believed to play an important role in the generation of large-scale magnetic field in the galaxy and other astrophysical objects [24].

A complete description of any of the flows discussed above (for example, the Solar Wind) requires inclusion of features like compressibility, inhomogeneity, shear, anisotropy, etc. However, in this thesis we will concern ourselves with the simplest model — the homogenous, incompressible MHD equation without any complications like shear and anisotropy.

and study some of the generic properties at the small scales. This model shows a rich behaviour which will be useful for understanding more realistic flows.

1.1 Problem definition

One of the most celebrated results in fluid turbulence is due to Kolmogorov(1941) [25]. He predicted that the energy spectrum in fluid turbulence is proportional to $k^{-5/3}$. For MHD turbulence. Kraichnan(1965) [1] and Iroshnikov(1963) [2] gave the first phenomenology and predicted both the kinetic and magnetic energy spectrum to be proportional to $k^{-3/2}$. Dobrowolny *et al.* [3] generalized Kraichnan-Iroshnikov arguments and still predicted a $k^{-3/2}$ spectrum Recently, several researchers have argued for a Kolmogorov-like $k^{-5/3}$ energy spectrum for MHD turbulence as well [5–7, 11, 13, 26, 27]. The Solar wind observations [14-16], and numerical simulations [11–13] appear to support Kolmogorov-like phenomenology rather than the phenomenology of Kraichnan-Iroshnikov-Dobrowolny (KID). In this thesis we have done an extensive numerical simulation to resolve the above controversy. To this end, we calculate both the energy spectrum and the energy cascade rates. Our simulation is based on the pseudo-spectral method and done in two-dimensions.

The interaction between wavenumbers in turbulence involves triads. In this thesis we have derived a very useful formula for calculating energy transfer rate from one mode of the triad to another, with the mediation of the third mode. This has been done for both fluids and MHD Using these formulae we have defined various energy fluxes and energy transfer rates between 'shells' These quantities give information about the energy transfer between different scales of the velocity field, the magnetic field, and between the scales of the velocity and the magnetic field. We have numerically computed these quantities from our simulation data. Our numerical results shed important light into the amplification of magnetic energy and locality of interactions.

Many researchers have studied the evolution of total energy and Cross-Helicity in terms of the initial Alfvén ratio ($\int \mathbf{u}^2 dx / \int \mathbf{b}^2 dx$), and normalised cross-helicity ($2\int (\mathbf{u}.\mathbf{b}) dx / \int (\mathbf{u}^2 +$

$\mathbf{b}^2)dx$, where $\mathbf{u}$ and $\mathbf{b}$ are the velocity and the magnetic fields respectively. There exists another quantity that can be varied keeping the initial Alfvén ratio and normalised cross-helicity fixed. This quantity is the Fourier 'phase'. We have studied the evolution of global quantities in terms of these quantities and found that the evolution of normalised cross-helicity sometimes depend on the initial phases, though the evolution of energy does not. This result is discussed towards the end of the thesis.

After the above brief discussion of the problem definition of our thesis, we turn to a description of some of the definitions and basic results of MHD turbulence which are related to our problem.

1.2 MHD equations

MHD is a fluid model for plasmas. In this model the plasma is collisional, electrically neutral, and highly conducting [28]. The simplest MHD flows are incompressible. There are two independent variables in the incompressible MHD equations — the velocity field $\mathbf{U}$, and the magnetic field $\mathbf{B}$. The MHD equations governing the evolution of $\mathbf{U}$ and $\mathbf{B}$ are

$$\frac{\partial \mathbf{U}}{\partial t} + (\mathbf{U}.\nabla)\mathbf{U} = -\frac{1}{\rho}\nabla p + \frac{1}{4\pi\rho}(\mathbf{B}.\nabla)\mathbf{B} + \nu\nabla^2\mathbf{U}, \tag{1.1}$$

$$\frac{\partial \mathbf{B}}{\partial t} + (\mathbf{U}.\nabla)\mathbf{B} = (\mathbf{B}.\nabla)\mathbf{U} + \mu\nabla^2\mathbf{B}, \tag{1.2}$$

$$\nabla.\mathbf{U} = 0 \tag{1.3}$$

$$\nabla.\mathbf{B} = 0 \tag{1.4}$$

where ν is the kinematic viscosity, μ is the magnetic diffusivity ($= c^2/(4\pi\sigma)$ with σ being the conductivity of the plasma and c being the velocity of light), ρ is the mass density, and p is the pressure which is a sum of the thermal pressure p_{th} and the magnetic pressure, $p_b = B^2/(8\pi)$. Eq. (1.3) is the equation of continuity for an incompressible fluid. For incompressible flows,

the pressure adjusts to maintain a constant mass density, and hence is not an independent quantity. The pressure p can be determined from the poisson's equation

$$\nabla^2 p = \nabla.(\mathbf{B}.\nabla)\mathbf{B} - \nabla.(\mathbf{U}.\nabla)\mathbf{U} \tag{1.5}$$

In the equations (1.1)-(1.2), the viscous and resistive terms $\nu\nabla^2\mathbf{U}$ and $\mu\nabla^2\mathbf{B}$ dissipate energy.

The MHD equations (1.1)-(1.4) are often written in a non-dimensional form. If the characteristic length scale is $\mathcal{L}$, the characteristic velocity scale is $\mathcal{U}$, the characteristic scale of the magnetic field is B, and the characteristic density scale is ρ_0, then the variables in equations (1.1)-(1.4) can be written in a non-dimensional form using $U' = U/\mathcal{U}$, $B' = B/B_0$, $t' = \mathcal{U}t/\mathcal{L}$, $\rho' = \rho/\rho_0$, and $p' = p/(\rho_0\mathcal{U}^2)$. The Eqs. (1.1)-(1.4) written in terms of these dimensionless variables are

$$\frac{\partial \mathbf{U}'}{\partial t'} + (\mathbf{U}'.\nabla')\mathbf{U}' = -\frac{\beta}{\rho'}\nabla' p + \frac{C_A^2}{U'^2}(\mathbf{B}'.\nabla')\mathbf{B}' + \frac{\nu}{\mathcal{U}\mathcal{L}}\nabla'^2\mathbf{U}', \tag{1.6}$$

$$\frac{\partial \mathbf{B}'}{\partial t'} + (\mathbf{U}'.\nabla')\mathbf{B}' = (\mathbf{B}'.\nabla')\mathbf{U}' + \frac{\mu}{\mathcal{U}\mathcal{L}}\nabla'^2\mathbf{B}', \tag{1.7}$$

$$\nabla'.\mathbf{U}' = 0 \tag{1.8}$$

$$\nabla'.\mathbf{B}' = 0 \tag{1.9}$$

where $C_A = B_0/\sqrt{4\pi\rho_0}$ and $\beta = C_s^2/\mathcal{U}^2$. The parameters $\mathcal{U}\mathcal{L}/\nu$ and $\mathcal{U}\mathcal{L}/\mu$ are the mechanical and the magnetic Reynolds numbers, respectively. For geometrically similar situations with identical Reynolds number and initial conditions the dimensionless variables $\mathbf{U}'(\mathbf{r}', t')$ and $\mathbf{B}'(\mathbf{r}', \mathbf{t}')$ are identical. At large Reynolds numbers ($> 10^4$ usually) the flow is turbulent.

In a turbulent flow $\mathbf{U}$ and $\mathbf{B}$ have random fluctuations over a wide range of spatial and temporal scales. It is useful to separate the fluctuations into a 'mean' $(\mathbf{U_0}, \mathbf{B_0})$ and a 'fluctuating' part $(\mathbf{u}, \mathbf{b})$, i.e., $\mathbf{U} = \mathbf{U_0} + \mathbf{u}$ and $\mathbf{B} = \mathbf{B_0} + \mathbf{b}$. The mean quantities can vary over long time scales and length scales. In the simplest situation the mean can be assumed to

be constant in space and time. A constant $\mathbf{U_0}$ can be eliminated from the MHD equations by shifting to a frame of reference moving with a velocity $\mathbf{U_0}$. However, a constant $\mathbf{B_0}$ cannot be eliminated from the MHD equations by a change of reference frame, and it, therefore, plays a dynamically significant role. In Section 1.4 we will describe some of the phenomenologies which attempt to describe the effect of $\mathbf{B_0}$ on the statistics of $\mathbf{u}$, $\mathbf{b}$. In a reference frame of the mean flow ($\mathbf{U_0} = 0$) the fluctuations $\mathbf{u}$, $\mathbf{b}$ satisfy the equations

$$\frac{\partial \mathbf{u}}{\partial t} - \frac{1}{4\pi\rho}(\mathbf{B_0}.\nabla)\mathbf{b} + (\mathbf{u}.\nabla)\mathbf{u} = -\frac{1}{\rho}\nabla p + \frac{1}{4\pi\rho}(\mathbf{b}.\nabla)\mathbf{b} + \nu\nabla^2\mathbf{u}, \tag{1.10}$$

$$\frac{\partial \mathbf{b}}{\partial t} - (\mathbf{B_0}.\nabla)\mathbf{u} + (\mathbf{u}.\nabla)\mathbf{b} = (\mathbf{b}.\nabla)\mathbf{u} + \mu\nabla^2\mathbf{b}, \tag{1.11}$$

$$\nabla.\mathbf{u} = 0 \tag{1.12}$$

$$\nabla.\mathbf{b} = 0 \tag{1.13}$$

The magnetic field can be expressed in Alfvénic units where we make the replacement $\mathbf{b}/\sqrt{4\pi\rho} \rightarrow \mathbf{b}$. The MHD equations in terms of the new $\mathbf{u}$ and $\mathbf{b}$ are

$$\frac{\partial \mathbf{u}}{\partial t} - (\mathbf{C_A}.\nabla)\mathbf{b} + (\mathbf{u}.\nabla)\mathbf{u} = -\frac{1}{\rho}\nabla p + (\mathbf{b}.\nabla)\mathbf{b} + \nu\nabla^2\mathbf{u}, \tag{1.14}$$

$$\frac{\partial \mathbf{b}}{\partial t} - (\mathbf{C_A}.\nabla)\mathbf{u} + (\mathbf{u}.\nabla)\mathbf{b} = (\mathbf{b}.\nabla)\mathbf{u} + \mu\nabla^2\mathbf{b}, \tag{1.15}$$

$$\nabla.\mathbf{u} = 0 \tag{1.16}$$

$$\nabla.\mathbf{b} = 0 \tag{1.17}$$

where $\mathbf{b}$ is in Alfvénic units in the above equation, and $\mathbf{C_A} = \mathbf{B_0}/\sqrt{4\pi\rho}$

In terms of the Elsässer variables $\mathbf{z}^{\pm} = \mathbf{u} \pm \mathbf{b}$, the MHD equations can be expressed as

$$\frac{\partial \mathbf{z}^{\pm}}{\partial t} \mp (\mathbf{C}_A.\nabla)\,\mathbf{z}^{\pm} + \left(\mathbf{z}^{\mp}.\nabla\right)\mathbf{z}^{\pm} = -\frac{1}{\rho}\nabla p + \nu_{+}\nabla^2\mathbf{z}^{\pm} + \nu_{-}\nabla^2\mathbf{z}^{\mp} \tag{1.18}$$

$$\nabla.\mathbf{z}^{\pm} = 0 \tag{1.19}$$

where $\nu^{\pm} \equiv (\nu \pm \mu)/2$. The $\mathbf{z}^{\pm}$ are the normal modes of the incompressible, inviscid ($\nu = 0$, $\mu = 0$) MHD equations; $\mathbf{z}^{+}$ propagates anti-parallel to $\mathbf{B}_0$, and $\mathbf{z}^{-}$ propagates parallel to $\mathbf{B}_0$ with the propagation speed of C_A. The nonlinear terms in the MHD equations vanish if either $\mathbf{z}^{+}$ or $\mathbf{z}^{-}$ is zero, i.e., if the system has pure modes. A turbulent flow is a mixture of $\mathbf{z}^{+}$ and $\mathbf{z}^{-}$. The nonlinearity modifies the Alfvénic fluctuations $\mathbf{z}^{\pm}$ and creates turbulence at high Reynolds numbers.

1.2.1 Important global quantities in MHD

The inviscid MHD equations possess some conserved global quantities. These conserved quantities are

1. the total energy per unit mass

$$E = \frac{1}{2}\int \left(u^2 + b^2\right) d\mathbf{x} = \frac{1}{4}\int \left\{(z^{+})^2 + (z^{-})^2\right\} d\mathbf{x}; \tag{1.20}$$

2 the velocity-magnetic field correlations (cross-helicity)

$$H_c = \int (\mathbf{u}.\mathbf{b}) d\mathbf{x} = \frac{1}{4}\int \left\{(z^{+})^2 - (z^{-})^2\right\} d\mathbf{x}; \tag{1.21}$$

3. the magnetic helicity in absence of B_0

$$H_m = \frac{1}{2}\int (\mathbf{a}.\mathbf{b}) d\mathbf{x}; \tag{1.22}$$

where $\mathbf{a}$ is the magnetic vector potential, i.e.,$\mathbf{b} = \nabla \times \mathbf{a}$. $H_m' = H_m + 2\mathbf{B}_0.\mathbf{A}_0$ is conserved

in presence of B_0 [15]. In 2-D, H_m is equal to zero, but the mean-square magnetic vector potential is conserved (in absence of B_0)

$$A = \int a^2 \mathrm{dx}. \tag{1.23}$$

The $\mathbf{z}^+$ energy, $E^+ = (1/2)\int (z^+)^2 \mathbf{dx}$ and the $\mathbf{z}^-$ energy, $E^- = (1/2)\int (z^-)^2 \mathbf{dx}$ are also conserved quantities but they can be expressed in terms of E and H_c. Note that the kinetic energy $E_u = (1/2)\int u^2 d\mathbf{x}$ and the magnetic energy $E_b = (1/2)\int b^2 d\mathbf{x}$ are not conserved. In the MHD equations (1.1)- (1.2) the term $(\mathbf{U}.\nabla)\mathbf{U}$ conserves the kinetic energy and $(\mathbf{U}.\nabla)\mathbf{B}$ conserves the magnetic energy. The terms $(\mathbf{B}.\nabla)\mathbf{B}$ in Eq. (1.1) and $(\mathbf{B}.\nabla)\mathbf{U}$ in Eq. (1.2) exchange energy between the velocity and the magnetic field by stretching the magnetic field lines (see reference [24]). The following dimensionless quantities are often studied in literature : the normalised cross helicity defined as $\sigma_c = 2H_c/E = (E^+ - E^-)/(E^+ + E^-)$, and the Alfvén ratio defined as $r_A = E_u/E_b$.

The evolution of the global quantities defined above has been studied in simulations [8, 9, 29–34]. The fields $\mathbf{u}$ and $\mathbf{b}$ usually show a tendency to align with each other in numerical simulations, i.e., σ_c increases [8, 9, 29, 30] — this is called dynamic alignment. However, the tendency for dynamic alignment is weaker for low values of σ_c and large Reynolds number [8]. The Alfvén ratio is found to decrease indicating the preferential decay of the magnetic energy compared to the kinetic energy — this is known as selective decay. Ting *et al.* [31] performed an extensive study over a range of initial values of r_A and σ_c and found distinct regimes of evolution. However, it has been believed so far that the evolution depends only on the initial value of the global quantities and their spectra. However, in Chapter 5 we will show that the evolution can be affected by some subtle features of the initial state. The values of σ_c and r_A can have an influence on the energy spectra (defined below) — this is a subject of investigation of Chapter 2.

1.2.2 Spectral analysis in MHD turbulence

Spectral analysis is very important in turbulence research. The velocity field $\mathbf{u}(\mathbf{x})$ can be expressed in terms of the Fourier components defined as

$$\mathbf{u}(\mathbf{k}) = (\frac{1}{2\pi})^d \int \mathbf{u}(\mathbf{x}) e^{i\mathbf{k}\cdot\mathbf{x}} d\mathbf{x}, \tag{1.24}$$

where d is the real space dimension. The relationship between the modal energy density in real space and energy density $E(\mathbf{k})$ in the Fourier space is given by

$$\frac{1}{2}\int_{unitvol} u^2(x) d\mathbf{x} = \int E^u(\mathbf{k}) d\mathbf{k}, \tag{1.25}$$

where $E^u(\mathbf{k}) = (1/2)|\mathbf{u}(\mathbf{k})|^2$. In case of isotropic turbulence, the directionally integrated $E^u(k)$

$$E^u(k) = \int_{|\mathbf{k}|=k} E^u(\mathbf{k}) d\mathbf{k}, \tag{1.26}$$

is a useful quantity. Similarly, the magnetic energy spectrum can be defined as

$$E^b(k) = \int_{|\mathbf{k}|=k} E^b(\mathbf{k}) d\mathbf{k}, \tag{1.27}$$

where $E^b(\mathbf{k}) = (1/2)|\mathbf{b}(\mathbf{k})|^2$, and the energy spectrum of the inward and the outward propagating Alfvén waves, i.e., fluctuations are defined as

$$E^{\pm}(k) = \int_{|\mathbf{k}|=k} E^{\pm}(\mathbf{k}) d\mathbf{k}. \tag{1.28}$$

where $E^{\pm}(\mathbf{k}) = (1/2)|\mathbf{z}^{\pm}(\mathbf{k})|^2$. In Chapter 2, we will study the energy spectra $E^{\pm}(\mathbf{k})$ using data from our numerical simulations.

The evolution equation for the kinetic energy spectrum $E^u(k)$ is obtained from the MHD equations (1.14)

$$\frac{\partial E^u(\mathbf{k})}{\partial t} + 2\nu k^2 E^u(\mathbf{k}) = \sum_{\mathbf{k+p+q=0}} \frac{1}{2} S^{uu}(\mathbf{k}|\mathbf{p},\mathbf{q}) + \sum_{\mathbf{k+p+q=0}} \frac{1}{2} S^{ub}(\mathbf{k}|\mathbf{p},\mathbf{q}) \tag{1.29}$$

where the nonlinear term $S^{uu}(\mathbf{k}|\mathbf{p},\mathbf{q})$ is

$$S^{uu}(\mathbf{k}|\mathbf{p},\mathbf{q}) \equiv -Re\,(i[\mathbf{k}.\mathbf{u}(\mathbf{q})][\mathbf{u}(\mathbf{k}).\mathbf{u}(\mathbf{p})] + i[\mathbf{k}.\mathbf{u}(\mathbf{p})][\mathbf{u}(\mathbf{k}).\mathbf{u}(\mathbf{q})]) \tag{1.30}$$

$$S^{ub}(\mathbf{k}|\mathbf{p},\mathbf{q}) \equiv -Re\,(i[\mathbf{k}.\mathbf{b}(\mathbf{q})][\mathbf{u}(\mathbf{k}).\mathbf{b}(\mathbf{p})] + i[\mathbf{k}.\mathbf{b}(\mathbf{p})][\mathbf{u}(\mathbf{k}).\mathbf{b}(\mathbf{q})]) \tag{1.31}$$

The interaction involves a triad $\mathbf{k}$, $\mathbf{p}$, $\mathbf{q}$ satisfying the condition $\mathbf{k}+\mathbf{p}+\mathbf{q}=\mathbf{0}$. The quantity $S^{uu}(\mathbf{k}|\mathbf{p},\mathbf{q})$ is the combined energy transfer from the modes $\mathbf{p}$ and $\mathbf{q}$ to mode $\mathbf{k}$ [35, 36]. The energy transfer *individually* from the modes $\mathbf{p}$ to $\mathbf{k}$ and from mode $\mathbf{q}$ to $\mathbf{k}$ are not known. In this thesis we will formulate an approach for calculating the energy transfer between two modes of the triad with the third mode mediating this transfer (see Chapter 3).

The nonlinear terms transfer energy between the various modes but conserve the overall energy. The loss of energy from a sphere in Fourier space to the modes outside is termed as the *energy cascade rate* (or energy flux)[1]. The study of energy cascades due to each of the nonlinear terms of Eqs. (1.14)-(1.15) is a major objective of this thesis. We shall discuss the known features of energy cascades later in this Introduction.

1.3 Fluid turbulence

Many current theories in turbulence have their foundation in the phenomenology proposed by Kolmogorov [25] and Obukhov [37] in the context of fluid turbulence. Other recent advances in fluid turbulence have also made an impact on the study of MHD turbulence. We will briefly discuss some of the aspects of fluid turbulence that are relevant to our work.

[1] the terms 'energy flux' and 'energy cascade rate' are synonymous and will be used interchangeably.

1.3.1 Scaling laws in fluid turbulence

Kolmogorov proposed a set of hypothesis [25] for fluid turbulence using which the energy spectra is obtained. The hypothesis can be stated as follows :

1. The energy flows from the energy-containing low wavenumbers to the energy-dissipating high wave numbers. There exists a range of wavenumbers, intermediate to the energy-containing wavenumbers (L), and the energy-dissipating wavenumbers (k_d), that stays in statistical equilibrium — it is called the 'inertial range'.

2. In the inertial range fluctuations of approximately same length $l \sim (k^{-1}$, participate in nonlinear energy transfer, i.e., energy transfer is local in wavenumber space. It also follows that the inertial range statistics are independent of statistics of the energy-containing low wavenumbers and the energy-dissipating high wavenumbers.

3. The statistical properties in the inertial range are isotropic.

4. In the inertial range, the energy flux $\Pi(k)$ is independent of the wavenumber and equal to the dissipation rate, $< \epsilon >$. The energy spectrum $E(k)$ in the inertial range depends only on the mean energy dissipation rate $< \epsilon >$ and the wavenumber k.

Under the above set of hypothesis, the energy spectrum in the inertial range is obtained using dimensional analysis. Since $[E(k)] = cm^3s^{-2}$, $[< \epsilon >] = cm^2s^{-3}$, and $[k] = cm^{-1}$, it follows that

$$E(k) = C < \epsilon >^{2/3} k^{-5/3} \tag{1.32}$$

where C is the universal Kolmogorov constant. According to the Kolmogorov's phenomenology, the energy spectrum in the above equation is *universal*, i.e., $E(k)$ has the same scaling exponent in all types of turbulent flows with arbitrary geometries. In experiments (see the references in [38]) no significant departure from the $E(k) \sim k^{-5/3}$ has been found.

A tacit assumption in Kolmogorov's phenomenology is that the dissipation rate has a uniform distribution in space. This is reflected in the use of mean dissipation rate $< \epsilon >$ in Eq. (1.32). However, the dissipation rate has large spatial and temporal fluctuations — a phenomenon called 'intermittency'. The scaling exponent of $E(k)$ which is equal to $-5/3$ in Eq. (1.32) is expected to get modified due to intermittency. Intermittency is frequently studied by means of the longitudinal structure functions of order p defined as

$$S_p(r) = \langle |[\mathbf{u}(\mathbf{x}+\mathbf{r}) - \mathbf{u}(\mathbf{x})].\hat{\mathbf{r}}|^p \rangle . \tag{1.33}$$

where the term 'longitudinal' implies that the velocity component along the line joining the two points is being considered. According to Kolmogorov's phenomenology, at inertial range separations, $1/k_d << r << L$, the structure functions S_p have a power law behaviour $S^p(r) \sim r^{\zeta_p}$ with $\zeta_p = p/3$. The spectral exponent m in $E(k) \sim k^{-m}$ is related to ζ_2 as $m = \zeta_2 + 1$ (see [38]). Experiments show that ζ_p deviates from $p/3$, and the deviation increases with p (see Frisch [38]), an effect that is believed to be due to intermittency. Several models have been proposed to model the intermittency in fluid turbulence (refer to Frisch [38] for a discussion of these models).

The elementary interactions in Navier-Stokes and MHD equations involve a wavenumber triad $\mathbf{k}$, $\mathbf{p}$, $\mathbf{q}$ with $\mathbf{k} + \mathbf{p} + \mathbf{q} = \mathbf{0}$. Researchers have investigated the following question: given a wavenumber k, which triads contribute most to the interactions ? (see Domaradzki [39]). One implicit assumption in most models is that the interactions are local, i.e., the triads with $k \sim p \sim q$ contribute most to the energy transfer to wavenumber k. The nonlocal triad interactions are those where $k \sim p >> q$. Locality has been investigated in several direct numerical simulations [39–43]. One of the conclusions from simulations is that the contribution of the nonlocal triads ($k \sim p >> q$) to the interactions is not small, but in such triads the dominant exchange of energy occurs between wavenumbers of similar magnitudes, i.e., between k and p [39, 40]. We will point out in Chapter 3 that the arguments used in these papers are ambiguous. We derive an expression for the 'effective energy transfer' that

eliminates the ambiguity. In Chapter 4, we have investigated the locality assumption using our new formalism.

Note that in Kolmogorov's phenomenology, the energy was assumed to flow from the low to the high wavenumbers. The kinetic energy is a conserved quantity in inviscid three-dimensional Navier-Stokes equation. The two-dimensional Navier-Stokes equation has an additional conserved quantity — the enstrophy $\int \omega^2 dx$, where $\omega = \nabla \times \mathbf{u}$ is the vorticity. The consequence of vorticity conservation is important. Assume that energy is being fed at wavenumber k_f. Using Absolute equilibrium theories (see [44] for a discussion of these theories), Kraichnan [45] argued that there is an inverse cascade of kinetic energy to wavenumbers less than k_f, and there is a forward cascade of enstrophy to wavenumbers greater than k_f. These predictions were thereafter confirmed in numerical simulations and experiments (see Frisch [38] and Nelkin [46] for the references). Kolmogorov-type analysis applied to enstrophy cascade leads to a k^{-3} in the wavenumber region $k_f << k << k_d$, while the usual analysis applied to the energy cascade yields a $k^{-5/3}$ spectra in the wavenumber region $k << k_f$ [45, 47]. The $k^{-5/3}$ spectrum has been observed for small wavenumbers in direct numerical simulations and also in recent experiments (see Frisch [38] and Nelkin [46] for references). In summary, the cascade of conserved quantities is a crucial component in the phenomenology of turbulence. For further discussion refer to Frisch [38] Lesieur [44], Kraichnan [48]; and Nelkin [46] provides a useful guide to references.

1.4 MHD turbulence : Phenomenology, Simulations, Solar Wind observations, and Analytical results

In this section we will discuss the MHD turbulence phenomenologies proposed so far and current status of simulation, analytical, and observational studies. For a review on this subject refer to Verma and Dar [27].

1.4.1 Energy spectrum: phenomenological results

The effect of the mean magnetic field on the energy spectra has been a matter of considerable debate. Broadly, there exist two view-points described below.

Kraichnan [1] and Iroshnikov [49] suggested that the mean magnetic field, or the magnetic field of the large-scale eddies, affect the energy transfer to the small scales, and that there is an equipartition of kinetic and magnetic energy at small-scales, and they have a $k^{-3/2}$ energy spectra. These arguments were restricted to the $\sigma_c = 0$ condition. Dobrowolny *et al.* [3] generalized the arguments to arbitrary σ_c and again found $E^{\pm}(k) \sim k^{-3/2}$. The phenomenology proposed by Kraichnan, Iroshnikov, and Dobrowolny *et al.* has been referred to as the KID phenomenology in our thesis. A different view-point was proposed by Marsch [5], Matthaeus and Zhou [6], Zhou and Matthaeus [7] according to which the energy spectra $E^{\pm}(k) \sim k^{-5/3}$ — this is the Kolmogorov-like phenomenology.

For any mode with length scale $l \sim k^{-1}$, we can define three time scales in the MHD equations: the Alfvén time scale $\tau_A = (C_A k)^{-1}$, and the two nonlinear time scales $\tau_{NL}^{\mp} = (k z_k^{\mp})^{-1}$. The two nonlinear time scales are not equal due to the structure of the nonlinear interactions. The KID and the Kolmogorov-like phenomenology differ in the choice of the interaction time scale.

Recall from Section 1.2, that $\mathbf{z}^+$ and $\mathbf{z}^-$ are two independent modes traveling anti-parallel and parallel to the mean magnetic field. In a turbulent flow $\mathbf{z}^+$ and $\mathbf{z}^-$ interact via the nonlinear term $(\mathbf{z}^{\mp}.\nabla)\mathbf{z}^{\pm}$ leading to a exchange of energy between the modes. In the phenomenologies the interactions are assumed to be local in wavenumber space. Let $\tau_k^{\mp}$ denote the time scale over which the interacting eddies $z^+(k)$ and $z^-(k)$ remain correlated. The variation $\delta z^{\pm}(k)$ in the amplitudes of the eddies over the time interval $\tau_k^{\pm}$ is

$$\delta z_k^{\pm} \approx \tau_k^{\pm} z_k^{+} z_k^{-} k. \tag{1.34}$$

Assuming random interactions, the amplitude variation in N such interactions will be

$$\Delta z_k^{\pm} \approx \sqrt{N}(\delta z_k^{\pm}). \tag{1.35}$$

Therefore, the number of interactions $N^{\pm}$ taken to obtain a variation equal to its initial amplitude $z_k^{\pm}$ is

$$N^{\pm} \approx \frac{1}{k^2(z^{\mp})^2(\tau_k^{\pm})^2}, \tag{1.36}$$

and the corresponding time $T^{\pm} = N_k^{\pm}\tau_k^{\pm}$ is

$$T^{\pm} \approx \frac{1}{k^2(z^{\mp})^2\tau_k^{\pm}} = \frac{(\tau_{NL}^{\pm})^2}{\tau_k^{\pm}}. \tag{1.37}$$

The time scale for energy transfer is assumed to be $T^{\pm}$. The energy fluxes $\Pi^{\pm}$ of $z^{\pm}(k)$ fluctuations, out of a sphere in k-space, can be estimated as

$$\Pi^{\pm} \approx \frac{(z_k^{\pm})^2}{T^{\pm}} \approx \tau_k^{\pm}(z_k^{\pm})^2(z_k^{\mp})^2k^2. \tag{1.38}$$

z_k^+ and z_k^- being oppositely traveling fluctuations, KID phenomenology assumes that they will get de-correlated in an Alfvén time scale. Hence $\tau_k \sim \tau_A \sim (C_A k)^{-1}$. Since $(z_k^{\pm})^2 \sim kE^{\pm}(k)$, we get

$$\Pi^+ \approx \Pi^- \approx \frac{1}{B_0}E^+(k)E^-(k)k^3, \tag{1.39}$$

for arbitrary σ_c value. For $\sigma_c = 0$ ($E^+ \sim E^-$), we get

$$E^{\pm}(k) \approx (B_0\Pi)^{1/2}k^{-3/2}. \tag{1.40}$$

It is assumed that in the absence of mean magnetic field, the magnetic field of the largest eddy would play the role of B_0.

In the Kolmogorov-like phenomenology the nonlinear time scale, $\tau_{NL}^{\pm}$ are taken to be the interaction time-scale for the $z_k^{\pm}$ eddies, i.e., $\tau_k^{\pm} \sim \tau_{NL}^{\pm} \sim (kz_k^{\mp})^{-1}$. Then, from Eq. (1.38) the fluxes $\Pi^{\pm}$ are

$$\Pi^{\pm} \approx (z_k^{\pm})^2(z_k^{\mp})k. \tag{1.41}$$

The above equation can be inverted to give

$$E^{\pm}(k) = C^{\pm}(\Pi^{\pm})^{4/3}(\Pi^{\mp})^{-2/3}k^{-5/3}. \tag{1.42}$$

Hence the spectral exponent is the same as the Kolmogorov's $-5/3$ scaling exponent in fluid turbulence. This phenomenology was given by Marsch [5], Matthaeus and Zhou [6], Zhou and Matthaeus [7]. In contrast to the Kolmogorov constant in fluid turbulence, the constants $C^{\pm}$ are expected to depend on the cross helicity and the Alfvén ratio [50].

The KID phenomenology predicts that the fluxes Π^{+} and Π^{-} are equal, whereas in the Kolmogorov-like phenomenology they are unequal. In order to construct a model within the KID phenomenology where $\Pi^{+} \neq \Pi^{-}$ Grappin *et al.* [4] proposed an extension to the KID phenomenology. They assume that the $\tau_{NL}^{\pm}$ in Eq. (1.37) is to be determined by including non-locality in the analysis. The nonlinear time scale $\tau_{NL}^{\pm} = kz_k^{\pm}$, if the interactions are local. Assuming non-locality, Grappin *et al.* replaced $\tau_{NL}^{\pm}$ in Eq. (1.37) by an average $\left\langle \tau_{NL}^{\pm} \right\rangle = \int_{\alpha/k}^{\alpha k} (kz_k^{\mp})^{-1} dk / \int_{\alpha/k}^{\alpha k} dk$, and obtained $m^{+} + m^{-} = 3$ and $\Pi^{+}/\Pi^{-} = m^{+}/m^{-}$, where $E^{\pm}(k) \sim k^{-m^{\pm}}$.

The Kolmogorov-like phenomenology is also a limiting case of a more generalized phenomenology constructed by Matthaeus and Zhou [6], and Zhou and Matthaeus [7], which yields

$$\Pi^{\pm} = \frac{A^2 E^{+}(k) E^{-}(k) k^3}{B_0 + \sqrt{k E^{\pm}(k)}}, \tag{1.43}$$

where A is a constant. Here the wavenumbers satisfying $\sqrt{kE^{\pm}(k)} >> B_0$ follow $-5/3$ spectrum and the wavenumbers $\sqrt{kE^{\pm}(k)} << B_0$ follow a $-3/2$ spectrum.

In both 2-D and 3-D MHD turbulence, there is a forward cascade of energy. The consequence of this result is that the phenomenologies discussed above for MHD turbulence based on energy cascade are valid for both 2-D and 3-D flows. Recall that in the earlier discussion of Section 1.3 we pointed out that 2-D fluid turbulence is fundamentally different from 3-D fluid turbulence.

1.4.2 Simulation results

Earlier theoretical [4] and numerical [8–10] work in this area claimed support for KID phenomenology and its extension to Grappin. The relationship $\Pi^+/\Pi^- = m^+/m^-$, with $m^+ + m^- = 3$ was found to be present in numerical calculations of the Eddy Damped Quasi-Normal Markovian approximation (EDQNM) closure scheme [4] (an introduction to EDQNM can be found in the book by Leslie [35] and Lesieur [44]). It was reported in numerical simulations of Biskamp and Welter [8] that $E(k) \sim k^{-3/2}$ for low σ_c values [8]. The exponents m^+ and m^- were found to be unequal and the relationship $m^+ + m^- = 3$ was found to hold approximately in numerical simulations [9, 10]. However, the errors involved in these simulations were too large to reach a definite conclusion. A clearer picture has been emerging from the work done during the last decade.

The KID phenomenology and the Kolmogorov-like phenomenology differ in their predictions regarding the scaling exponents of energy spectra and also in the relationship between the fluxes Π^+ and Π^-. While $\Pi^+ = \Pi^-$ in the KID phenomenology [see Eq. (1.39)], $\Pi^+ \neq \Pi^-$ for Kolmogorov-like phenomenology [see Eq. (1.41)]. Verma *et al.* [11] exploited this distinction between the two phenomenologies to make a comparison between them. In their simulation they found that $\Pi^+ \neq \Pi^-$, thus raising a doubt on the validity of KID phenomenology. In Kolmogorov-like phenomenology, at low σ_c values the constants C'^+ and C'^- in Eqs. (1.42) are expected to be equal and $E^+/E^- = (\Pi^+/\Pi^-)^2$. These equalities were found to hold in Verma *et al.*'s simulations [11] of decaying 2-D MHD turbulence. Grappin *et al.*'s [4] extension of KID phenomenology, where $\Pi^+/\Pi^- = m^+/m^-$ was not tested by Verma *et al.* in their simulations. Verma *et al.*'s simulations were done for decaying turbulence and the energy spectra and energy cascade rates were given without averaging. In our simulations we will average the fluxes and spectra over a steady-state which will reduce the errors, and we will also test Grappin *et al.*'s predictions.

These earlier simulations were not done at high enough Reynolds numbers. Con-

sequently, the inertial range obtained was not large enough for an accurate estimation of the spectral exponents. Much higher Reynolds numbers have been achieved in some of the recent numerical simulations done by Politano *et al.* [12], and Müller and Biskamp [13]. In addition, the phenomenon of Extended Self Similarity (ESS). which we describe below, is now used by researchers to extract the exponents with greater accuracy.

In the inertial range, the structure functions $S_p^{\pm}(r) = \left\langle |\delta z^{\pm}(r)|^{\zeta_p} \right\rangle$ follow a power law behaviour $S_p^{\pm}(r) \sim r^{\zeta_p}$, where $\delta z^{\pm}(r) = (\mathbf{z}^{\pm}(\mathbf{x}+\mathbf{r}) - \mathbf{z}^{\pm}(\mathbf{x}))$. By plotting $S_p^{\pm}(r)$ against $S_3^{\pm}(r)$, a power law $S_p^{\pm} \sim (S_3^{\pm})^{\zeta_p^{\pm}/\zeta_3^{\pm}}$ was found to exist over a much wider range [51]. This is called Extended Self Similarity (ESS) and it was earlier reported in fluid turbulence [52–55]. ESS has been found in simulations of MHD turbulence [12, 51] and Solar Wind observations [56, 57]. In fluid turbulence, $\zeta_3 = 1$ is an exact result [38, 58], so the ESS plot gives the exponents ζ_p directly. In MHD turbulence ζ_3 is not equal to one [12, 13]. So, only the ratio the exponents ζ_p/ζ_3 can be obtained by plotting $S_p^{\pm}(r)$ against $S_3^{\pm}(r)$.

Fortunately $\zeta_p^{\pm}$ can be calculated using mixed correlators $L^{\pm}(r) =< (\delta z^{\pm}(r))^2 \delta z^{\mp}(r) >$ for which an exact result is known. Politano *et al.* [59, 60] derived the following exact relationship,

$$< (\delta z^{\pm})^2 \delta z^{\mp} > -2 < z^{\pm}(x) z^{\pm}(x) z^{\mp}(x+r) >= -c_d \epsilon^{\pm} r \tag{1.44}$$

which can be simplified for large magnetic field to

$$< (\delta z^{\pm})^2 \delta z^{\mp} >= -c_d \epsilon^{\pm} r \tag{1.45}$$

The above relationship is analogous to $|\delta u(r)|^3 \sim r$ obtained from the Navier-Stokes equation for homogenous, isotropic fluid turbulence. The relationship (1.45) has been verified in a numerical simulation [12]. A power law $S_p^{\pm}(r) \sim [L^{\pm}(r)]^{\zeta_p^{\pm}}$ was found to extend well beyond the inertial range [12], and it was used to obtain the exponents $\zeta_p^{\pm}$.

The exponent $m^{\pm}$ in $E^{\pm}(k) \sim k^{-m^{\pm}}$ and the exponent $\zeta_2^{\pm}$ of the second order structure functions $S_2^{\pm}$ are related to each other by $m^{\pm} = \zeta_2^{\pm} + 1$. Using the relationship between

and $m^{\pm}$, it can be seen that $\zeta_2 = 1/2$ according to the KID phenomenology but is equal to 2/3 in the Kolmogorov-like phenomenology. In addition, $\zeta_p = p/3$ for the Kolmogorov-like phenomenology and $\zeta_p = p/4$ for the KID phenomenology. Hence, it may be expected that $\zeta_3 = 1$ for Kolmogorov-like and $\zeta_4 = 1$ for KID phenomenology. Using ESS the exponents $\zeta_2^{\pm}$ were obtained for 2-D MHD turbulence by Politano *et al.* [12] with greater accuracy than was possible earlier. They found that $\zeta_2^{+} = 0.69$ ($m^{+} = 1.69$) and $\zeta_2^{-} = 0.7$ ($m^{-} = 1.7$) [12]. Therefore, these results support the Kolmogorov-like phenomenology, which predicts that $m^{\pm} = 5/3$ [Eq. (1.42)], when we consider $\zeta_2^{\pm}$.

Politano *et al.* also observed that $\zeta_4 \simeq 1$, leading them to conclude that KID phenomenology is a valid description of MHD turbulence. However, we differ in our view regarding the implication of their results for two reasons: (1) KID phenomenology is not consistent with the Verma *et al.*'s observation that $\Pi^{+} \neq \Pi^{-}$ and $E^{+}/E^{-} \simeq (\Pi^{+}/\Pi^{-})^2$ which are consistent with the Kolmogorov-like phenomenology; (2) ζ_2 found in Politano *et al*'s simulation is close to the value expected by Kolmogorov-like phenomenology and the observed deviation is small ($\delta m^{+} \simeq 0.04$). A deviation of this magnitude can be expected to arise due to intermittency corrections. In this light, the result $\zeta_4 \simeq 1$ may be a fortuitous occurance arising by a deviation from the Kolmogorov value of $\zeta_4 = 4/3$ due to intermittency.

In another recent simulation of 3-D MHD turbulence performed by Müller and Biskamp [13], it was found that $m^{\pm} \simeq 5/3$. They concluded that their results support the validity of Kolmogorov-like phenomenology to MHD turbulence.

MHD turbulence is found to be intermittent. Numerical simulations [12, 13, 51] and Solar Wind observations [61–63] show that the exponents $\zeta_p^{\pm}$ are nonlinear functions of p, and the deviation from both $p/3$ and $p/4$ increases with p. In simulations, the probability distributions of $|\delta\mathbf{b}(r)| = |\mathbf{b}(\mathbf{x}+\mathbf{r}) - \mathbf{b}(\mathbf{x})|$ is found to have a tail [51, 64], which is longer for smaller scale separations r, [64] indicating small-scale intermittency. The probability distribution of $|\delta\mathbf{u}(r)| = |\mathbf{u}(\mathbf{x}+\mathbf{r}) - \mathbf{u}(\mathbf{x})|$ has a smaller tail and appears to be less intermittent than $|\delta\mathbf{b}(r)|$. Some models have been proposed to account for intermittency on the lines of models

earlier proposed for fluid turbulence, but all these models are under the framework of KID phenomenology. The predictions of She-Leveque (SL) model [65] for fluid turbulence compare well with the exponents ζ_p^b obtained in 3-D simulations of MHD turbulence [55]. However, the same predictions do not agree with the exponents ζ_p^v. The ζ_p's predicted by both the S-L model for fluid turbulence and its modification to MHD turbulence [66, 67] do not have a close agreement with the ζ_p's found in 2-D MHD turbulence simulations. It is clear that none of the present phenomenologies can explain the intermittent behaviour of MHD turbulence. In this thesis, we will not investigate intermittency. Rather, we will focus on resolving the controversy between the applicability of Kolmogorov-like and KID phenomenologies by testing their predictions for the energy spectra and the cascade rates.

1.4.3 Solar wind observations

The Solar wind provides a unique opportunity for *in situ* measurements of MHD turbulence properties. Researchers have used observational data to verify various turbulence theories. From the arguments of Matthaeus and Zhou [6], Zhou and Matthaeus [7], and Marsch [5], we see that the arguments of KID phenomenology are applicable when $B_0 >> \sqrt{kE^{\pm}(k)}$ (when k is in the inertial range); on the other hand Kolmogorov-like phenomenology is applicable when $B_0 << \sqrt{kE^{\pm}(k)}$. In the Solar Wind, $B_0 >> \sqrt{kE^{\pm}(k)}$ for k in the inertial range, and hence KID phenomenology should be applicable according to these authors. However, the energy spectra in the solar wind are found to be nearly proportional to $k^{-5/3}$ [15, 16, 14]. The Fig. 1.1, taken from reference [15], shows the total energy spectra to be proportional to $k^{-1.69\pm0.08}$ at 1 AU[2]. Hence, the Solar Wind observations show that there is some inconsistency in the phenomenological arguments given above. Verma [26] has attempted to resolve this contradiction by applying renormalization group treatment to MHD equations.

The Solar Wind is found to be intermittent [61–63]. The usual signatures of intermittency, namely, spectral exponents having a nonlinear dependence on p and a tail in the

[2]An astronomical unit (AU) is the mean distance between the Sun and the Earth which is approximately equal to 1.5×10^8 Km

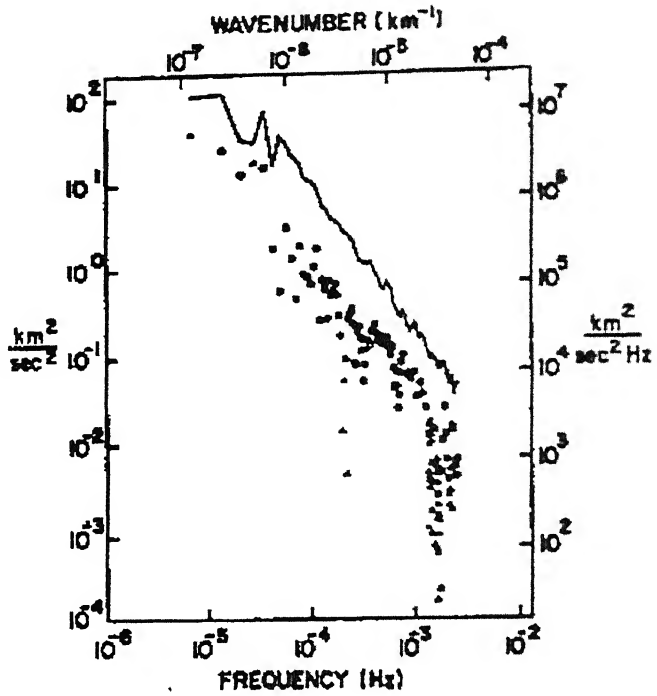

Figure 1.1: Total energy spectra $E(k) = E^+(k) + E^-(k)$ in the Solar wind at 1 AU (shown by the solid line) taken from Matthaeus and Goldstein [15].

probability distribution of $|\delta \mathbf{v}(r)|$ are found in Solar Wind data. The SL model for MHD is found to agree quite well with the Solar Wind data [61]. However, Grauer [66] has cautioned that the errors in the spectral exponents from the Solar Wind are too large to be certain about the agreement between SL model and the Solar Wind data.

We will discuss below the results of the analytical theories applied to MHD turbulence.

1.4.4 Analytical results

The Renormalization group (RG) approach (see McComb [68] for an introduction) was applied to MHD turbulence by Fournier *et al.* [69], Camargo and Tasso [70], Verma [26]. Fournier *et al.* found that RG of MHD is quite complex. There are various types of regimes where the transport coefficients, viscosity ν and resistivity μ, get renormalized either due to kinetic small scales or due to magnetic small scales. They also find a strong dimensional

dependence. Later, Camargo and Tasso [70] applied similar techniques, and showed that the effective (renormalized) viscosity and resistivity are, in general, non-negative. They mapped the effective transport parameters as a function of initial parameter.

Verma [26] constructed a self-consistent renormalization group scheme. Within this scheme the mean magnetic field was found to get renormalized, scaling as $k^{-1/3}$, while the magnetic energy scaled as $k^{-5/3}$. The Renormalization group (RG) calculation demonstrated that the magnetic field acting on the eddies $l \approx k^{-1}$ is not the magnetic field of the largest eddies but a renormalized field. This gives rise to a $k^{-5/3}$ spectrum instead of the $k^{-3/2}$ spectrum. These calculations were done by replacing the term $\mathbf{k}.\mathbf{C_A}$ in Eq. (1.14) with an isotropic term kC_A and also for $\sigma_c = 0$ and $r_A = 1$. These restrictions should be lifted in future for a more realistic calculation. However, this calculation provides support for the Kolmogorov-like phenomenology.

Kraichnan's Direct interaction approximation (refer to Leslie [35] for details) was applied to MHD by Verma and Bhattacharjee [50]. Assuming $E(k) \sim k^{-5/3}$ they computed the Kolmogorov constants $C^{\pm}$ [see Eq. (1.42)] and found that $C^{\pm}$ are not universal but depend on the Alfvén ratio. In our simulations we compute $C^{\pm}$ for different σ_c and show that they have a slight dependence on σ_c. Assuming a $k^{-5/3}$ spectra, these constants had also been calculated earlier [11, 71] in a decaying simulation of 2-D MHD turbulence; however, the errors involved were large.

The EDQNM scheme was applied to MHD turbulence by Grappin *et al.* [4], and the spectral exponents $m^{\pm}$ were obtained by numerically solving the EDQNM equations. They found that $m^+ \simeq m^-$ when $\sigma_c \simeq 0$, but as $\sigma_c \to 1$, the exponent $m^+ \to 3$, and $m^- \to 0$, and for any intermediate σ_c the $m^+ + m^- = 3$ and $\Pi^+/\Pi^- = m^+/m^-$. EDQNM thus gives results consistent with the phenomenology proposed by Grappin.

To conclude this section, numerical simulations [11–13], Solar Wind data [14–16], and also Renormalization group calculations [26] appear to support Kolmogorov-like phenomenology over the KID phenomenology, atleast for low σ_c. At high σ_c too, indications are that

KID phenomenology is not applicable [11]. However, further support is required by accurate measurements of spectral exponents or alternatively by testing the flux relationships predicted by the phenomenologies, and also by stronger theoretical arguments.

1.5 Energy cascades in MHD turbulence

In fluid turbulence the dynamics of energy transfer has been well studied. We had discussed in Section 1.3 that in 3-D fluid turbulence the kinetic energy is transferred from large scales to small scales, whereas in two dimensions there is an inverse cascade of kinetic energy from small scales to large scales [44]. Contrary to fluid turbulence, the direct numerical simulations (DNS) of MHD turbulence show that the *total* energy is transferred from large scales to small scales *both* in 2-D as well as 3-D turbulence [11, 71], and that there is a constant cascade rate of energy in the inertial range [11]. There have been theoretical predictions of the magnitude and directions of only a few of the various fluxes [17, 18, 72].

In Section 1.2.1 we had stated the conserved quantities for inviscid 2-D and 3-D MHD equations. If turbulence is being forced at the wavenumber k_f, then it is observed that in 2-D MHD turbulence, the mean-square vector potential A [Eq. (1.23)] has an inverse cascade to wavenumbers less than k_f, and in 3-D MHD turbulence the magnetic helicity [Eq. (1.22] has an inverse cascade. These cascades are predicted by Absolute Equilibrium theories [73], and closure calculations [17, 18], and have also been observed in numerical simulations [74, 75]. One consequence of the inverse cascade of A is that the magnetic energy spectrum $E^b(k) \sim k^{-1/3}$ for $k < k_f$ [75, 64]. This spectrum has been observed in numerical simulations [75]. In our simulations we do not force the magnetic energy (but force the kinetic energy), and hence the inverse cascade regime is not found.

The velocity field evolves due to two nonlinear terms $(\mathbf{u}.\nabla)\mathbf{u}$ and $(\mathbf{b}.\nabla)\mathbf{b}$ in Eq. (1.14), and the magnetic field evolves due to the terms $(\mathbf{u}.\nabla)\mathbf{b}$ and $(\mathbf{b}.\nabla)\mathbf{u}$ in Eq. (1.15) [see Section 1.2]. The term $(\mathbf{u}.\nabla)\mathbf{u}$ transfers kinetic energy between different scales of velocity fields; $(\mathbf{b}.\nabla)\mathbf{b}$ and $(\mathbf{b}.\nabla)\mathbf{u}$ transfer energy from the velocity field to the magnetic field and vice

versa; $(\mathbf{u}.\nabla)\mathbf{b}$ transfers magnetic energy between different scales of magnetic fields. Recently Ishizawa and Hattori [20] studied some of the kinetic and magnetic energy transfers arising from the non-linear terms. In this thesis (Chapter 4) we have carried out a detailed investigation of the various energy cascades and shell-to-shell energy transfers in 2-D MHD turbulence.

Pouquet *et al.* [17] studied the energy transfer between large and small scales using 3-D EDQNM closure calculations. They found that the large scales of the magnetic field gain energy in the presence of small-scale residual helicity (which is the difference between kinetic helicity and magnetic helicity)[3]. The large scale magnetic field, in turn, was found to enhance the energy exchange between the small-scale magnetic and the velocity fields. This energy exchange resulted in equipartition of small-scale kinetic and magnetic energies. By drawing an analogy between the MHD equation for the magnetic field [see Eq. (1.2)] and the vorticity equation[4], Batchelor [72] argued that the transfer between kinetic and magnetic energies takes place primarily at small scales. A similar conjecture was made by Pouquet and Patterson [21]. They also conjectured that an inverse cascade of energy from small-scale to large-scale magnetic field is the mechanism responsible for the ehancement of large-scale magnetic energy. Contrary to the prediction from 3-D EDQNM of Pouquet *et al.* [17], simulations of decaying turbulence showed that it is the magnetic helicity and *not* the residual helicity which is important for the growth of large-scale magnetic field [21].

In a 2-D EDQNM study, Pouquet [18] obtained eddy viscosities for MHD turbulence. She found that the small-scale magnetic energy acts like a negative eddy viscosity on the large-scale magnetic energy. The inverse cascade of A, and hence the ehnancement of large-scale magnetic energy, was conjectured to arise due to the destablization of the of large-scale magnetic field by the small-scale magnetic field. She also found that the small-scale kinetic energy has the effect of a positive eddy viscosity on the large-scale magnetic energy. Ishizawa

[3]The kinetic helicity is defined as $\int \mathbf{v}.\boldsymbol{\omega}\mathbf{dx}$ and magnetic helicity is given by Eq. (1.22)

[4]The equation for the vorticity evolution can be obtained by taking the curl of the Navier-Stokes equation (see Lumley [76])

and Hattori [19] resolved the calculations further and obtained eddy viscosity due to each of the nonlinear terms in Eqs. (1.1)-(1.2) of Chapter 1. They found that the eddy viscosity due to $(\mathbf{b}.\nabla)\mathbf{u}$ is positive leading to a transfer of energy from large-scale magnetic field to small-scale magnetic field. In their calculation, energy was also found to be transferred from the small-scale velocity field to the large-scale magnetic field. Both, Pouquet's [18] and Ishizawa and Hattori's [19] calculations give a non-local energy transfer from small-scale velocity field to the large-scale velocity field.

In a recent work Ishizawa and Hattori [20] employed the wavelet basis to investigate energy transfer in 2-D MHD turbulence. There are some similarities between the observations made by us in this thesis and those in the work of Ishizawa and Hattori[5]. Using our formalism we do a thorough investigation of all the energy transfers (Chapter 4). The wavelet basis used by Ishizawa and Hattori [20] is a useful tool for investigating spectral properties and energy transfer properties in different regions of the flow. In Ishizawa's work, the flow was divided into a turbulent and a coherent region which are distinguished by the level of vorticity fluctuations in that region — turbulence is known to have high levels of vorticity fluctuations [76]. They found that the energy transfer between velocity/magnetic scales occurs more efficiently in the turbulent region and less efficiently in the coherent region.

In some of the above mentioned studies [17, 21] a distinction was not made between the energies transferred to a mode from the kinetic and the magnetic fields. Also, the energy transferred into a mode $\mathbf{k}$ from different wave number regions was not separately considered—only the *net* energy transfer into a wave number $\mathbf{k}$ was computed [20, 21]. The EDQNM closure calculations dealt mainly with nonlocal energy transfers, i.e., between large scales and small scales [17–19]. In another study, Frick and Sokoloff [77] solved a shell model of MHD turbulence and calculated only those fluxes transferring the kinetic energy between the velocity modes, and the magnetic energy between the magnetic modes.

In our simulations we investigate the (1) various energy fluxes arising within and between

[5]However, we became aware of Ishizawa's results only after the completion of our work

the velocity and magnetic fields, and (2) the fine-grained (considering many wave number shells) energy transfer between magnetic and kinetic shells. This will give a more informed picture of the physics of energy transfer in MHD turbulence.

In 3-D MHD turbulent flows, beyond a critical magnetic Reynolds number, the magnetic field can grow and reach a steady state [21, 78–80] — this is called the *dynamo effect*, and is believed to be the mechanism responsible for the generation of magnetic fields within astrophysical objects like the sun, earth and galaxies. The non-linear energy transfer in MHD turbulence is important for understanding the growth process of magnetic energy in a dynamo. The magnetic helicity is believed to play a crucial role in the generation of large-scale magnetic field [81, 24]. In two-dimensional flows there is no magnetic helicity; the magnetic energy cannot be sustained in two-dimensional MHD turbulence. Although, it is not possible to indefinitely maintain a steady state magnetic field in two-dimensional turbulence [82], a steady state can be achieved for a *finite* period of time [18]. This, coupled with the similarity in physics of the E^+ and E^- energy cascades in 2-D and 3-D, allows us to probe the non-linear energy transfer in real MHD flows through 2-D simulations. In Chapter 4, we have calculated the energy flux into a magnetic-mode sphere. We have investigated the contribution to this flux from the fluid-mode sphere, from the modes outside this sphere, and from the modes outside the magnetic-mode sphere. Our results shed light into the amplification of magnetic energy. The methods used here are completely generalizable to the 3-D case and can be used to directly study the dynamo problem at a later date.

1.6 Topics beyond the scope of this thesis

In this thesis we investigate the energy spectra and the energy cascades for the simplest example of incompressible MHD turbulence. We do not include a mean-magnetic field, shear, current sheets, etc. in our simulations.

Most astrophysical plasmas (for example, the Solar Wind) evolve in presence of a mean magnetic field. Turbulence with a finite $\mathbf{B}_0$ is anisotropic due to a preferred direction in

space making it simultaneously harder to study and richer in its physics. The mean magnetic field affects both the energy cascade and the energy spectrum. The Solar wind observations show that the intensity of fluctuations transverse to the mean magnetic field is larger than the intensity parallel to the mean magnetic field [83]. Thus, the energy spectra for the fluctuations transverse and parallel to $\mathbf{B_0}$ will not be the same. The energy spectra will also have an angular dependence. The energy cascades have been investigated to some degree and interesting observations have been made. Numerical simulations and perturbative calculations show that energy cascade occurs more efficiently between the modes transverse to $\mathbf{B}_0$ and less efficiently between modes parallel to $\mathbf{B_0}$ [84, 85]. For more details on the investigation of turbulence with $\mathbf{B_0}$, the reader is referred to Shebalin *et al.* [84], Oughton *et al.* [85], Montgomery and Turner [86], Oughton *et al.* [87], Mattaeus *et al.* [88], and Kinney and Mcwilliams [89].

1.7 Outline of the thesis

In Chapter 2 we will compare the predictions of various turbulence phenomenologies with the numerical results of our forced, 2-D MHD turbulence simulations. After showing that the Kolmogorov phenomenology is preferred over KID phenomenology, we will study the dependence of the Kolmogorov's constants on the normalised cross-helicity values.

In Chapter 3 we will devise an approach for describing the energy transfer between a pair of modes of the triad where we will introduce the idea of an 'effective' transfer. We will show how the effective transfer can be used to re-define shell-to-shell energy transfer [39], and also define energy cascade rates.

In Chapter 4 we will numerically compute the shell-to-shell energy transfer rates and energy cascade rates defined in Chapter 3 for forced 2-D MHD turbulence.

In Chapter 5 we will study the evolution of global quantities for different initial conditions. We will show that the evolution of global quantities can sometimes depend on subtle features of the initial state.

In Chapter 6 we will conclude with a summary of our findings and state some of the possible future investigations.

Chapter 2

A numerical validation of MHD turbulence phenomenologies.

2.1 Introduction

In Chapter 1 we described the existing MHD turbulence phenomenologies. Kraichnan, Iroshnikov, and Dobrowolny *et al.* (KID) [1–3] predicted that the energy spectrum exponent is -3/2 (Eq. (1.40) of Chapter 1). Their phenomenology predicts $\Pi^+ = \Pi^-$ independent of E^+/E^- ratio. In contrast to this phenomenology, Marsch, Matthaeus and Zhou, Zhou and Matthaeus [5–7] argued that the energy spectra $E^{\pm}(k) \sim k^{-5/3}$ (Eq. (1.42) of chapter 1). An extension of the KID phenomenology due to Grappin *et al.* [90] predicted that the fluxes $\Pi^{\pm}$ and the exponents $m^{\pm}$ in $E^{\pm}(k) \sim k^{-m^{\pm}}$ satisfy the relationship $\Pi^+/\Pi^- = m^+/m^-$.

As discussed in the introduction, the solar wind observations indicate that the spectral indices are closer to $-5/3$ than to $-3/2$ [14, 15]. Various attempts using numerical simulations have been made to test which one of the phenomenologies is correct. In simulations of Pouquet *et al.* [9], Politano *et al.* [10], and Verma *et al.* [11], reliable estimates of the spectral exponents could not be obtained. Biskamp and Welter [8] concluded that the $-3/2$ scaling is valid. However, Verma *et al.* [11] studied the energy fluxes and found that Π^+ differs significantly from Π^-, in contradiction to the predictions of KID phenomenology [Eq. (1.39) of Chapter 1]; For small σ_c they also found that $E^+/E^- \simeq (\Pi^+/\Pi^-)^2$, as predicted by Kolmogorov like-phenomenology [from Eq. (1.42) of Chapter 1]. From these observations

Verma *et al.* concluded that Kolmogorov's phenomenology is preferred over KID's phenomenology. Recently large Reynolds number simulations were done by Politano *et al.* [12] for 2-D MHD turbulence, and by Müller and Biskamp [13] for 3-D MHD turbulence. They found that the spectral indices are closer to $-5/3$ than to $-3/2$. However, these results are limited to $\sigma_c \simeq 0$ fluctuations.

Analytically Grappin *et al.* [90] applied EDQNM closure scheme to MHD equations and found that $\Pi^+/\Pi^- = m^+/m^-$. These predictions have not been observed in the solar wind. Recently, RG calculations of Verma [26] shows that Eq. (1.42) of Kolmogorov-like phenomenology is a consistent solution of RG equations, but KID's formula [(1.40)] is not.

In this chapter we will investigate the energy fluxes (also termed as energy cascade rate) and energy spectra to test which of the phenomenologies is closer to numerical results for large σ_c cases. From the spectra and fluxes we will also calculate some of the constants. Our method is the same as that of Verma *et al.* [11]. However, we time-average the energy spectra and the fluxes over a steady state which improves the quality of data and also test Grappin *et al.*'s phenomenology.

The plan of this chapter is as follows: In Section 2.2 we define energy spectra and energy fluxes. In Section 2.3.1 we describe the simulation method used in this thesis. In the present chapter and in Chapter 4 we study forced turbulence. The description of the forcing employed in the simulations is given in Section 2.3.2. Section 2.4 contains the results. The discussion follows in Section 2.5.

2.2 Energy spectra and energy flux expressions

In this section we will define the quantities which we compute and study in this chapter. Energy flux is defined as the energy lost by a sphere Fourier space. In this section we will give the expressions for the fluxes corresponding to $\mathbf{z}^\pm$ energies. We had described in Chapter 1 that the energy densities of $\mathbf{z}^\pm$, denoted by $E^\pm$, are defined as

$$E^{\pm} = \frac{1}{2}\int_{unitvol} |\mathrm{z}^{\pm}|^2 \mathrm{dx}, \tag{2.1}$$

can be expressed in terms of the Fourier components $\mathrm{z}^{\pm}(\mathrm{k})$ as

$$E^{\pm} = \frac{1}{2}\int |\mathrm{z}^{\pm}(\mathrm{k})|^2 \mathrm{dk}. \tag{2.2}$$

where we define the quantity $E^{\pm}(\mathrm{k}) \equiv |\mathrm{z}^{\pm}(\mathrm{k})|^2/2$ as the modal energy spectra, and

$$E^{\pm}(k) = \frac{1}{2}\int_{|\mathrm{k}|=k} |\mathrm{z}^{\pm}(\mathrm{k})|^2 \mathrm{dk} \tag{2.3}$$

is the omni-directional energy spectra. In this chapter our interest is in evaluating $E^{\pm}(k)$. We have performed our simulations in two-dimensions with periodic boundary conditions. We choose our box-size to be 2π. For such flows the wavenumber space is $k_x = (2\pi/L)n_x$, and $k_y = (2\pi/L)n_y$, where n_x, n_y are integers. For discrete wave number space, the omni-directional energy spectra in Eq. (2.3) can be written as

$$E^{\pm}(k) = \sum_{k-1/2}^{k+1/2} E^{\pm}(\mathrm{k}). \tag{2.4}$$

The energy flux of $E^{\pm}$ can be obtained from the MHD equation using its definition. The equation for the evolution of $E^{\pm}(\mathrm{k})$ can be derived from the MHD equations (1.18) of Chapter 1.

$$\frac{\partial E^{\pm}(\mathrm{k})}{\partial t} + 2\nu^{\pm}k^2 E^{\pm}(\mathrm{k}) + 2\nu^{\mp}k^2 E^{\pm}(\mathrm{k}) = -\frac{1}{2}\sum_{\mathrm{p}}^{\mathrm{k+p+q=0}} Re\left(i\left[\mathrm{k}.\mathrm{z}^{\mp}(\mathrm{q})\right]\left[\mathrm{z}^{\pm}(\mathrm{k}).\mathrm{z}^{\pm}(\mathrm{p})\right]\right). \tag{2.5}$$

Integrating the above equation from $k = 0$ to $k = K$, the right hand side of the equation gives energy flux out of the sphere K to the modes outside. Hence, the fluxes $\Pi^{\pm}$ are equal

to

$$\Pi^{\pm}(K) = -\sum_{\mathbf{k}}\sum_{\mathbf{p}} Re\left(i\left[\mathbf{k}.\mathbf{z}^{\mp}(\mathbf{q})\right]\left[\mathbf{z}^{\pm}(\mathbf{k}).\mathbf{z}^{\pm}(\mathbf{p})\right]\right). \tag{2.6}$$

where $\mathbf{k}+\mathbf{p}+\mathbf{q}=\mathbf{0}$. We will compute the above energy fluxes in our numerical simulations.

In this chapter we will discuss the properties of the energy spectra $E^{\pm}(k)$ and the energy fluxes $\Pi^{\pm}(K)$. Then we will calculate the Kolmogorov's constants using these quantities. Our analysis will be carried out for a range of normalised cross-helicity σ_c values (defined in Section 1.2.1 of Chapter 1).

2.3 Simulation details

2.3.1 Numerical method

In our simulations we use the MHD equations given in terms $\mathbf{z}^{+}$ and $\mathbf{z}^{-}$, i.e.,

$$\begin{aligned}\frac{\partial \mathbf{z}^{\pm}}{\partial t} \mp (\mathbf{B}_0.\nabla)\,\mathbf{z}^{\pm} + \left(\mathbf{z}^{\mp}.\nabla\right)\mathbf{z}^{\pm} &= -\nabla p + \nu_{\pm}\nabla^2\mathbf{z}^{\pm} + \nu_{\mp}\nabla^2\mathbf{z}^{\mp} \\ &\quad + \left(\nu_{\pm}/k_{eq}^2\right)\nabla^4\mathbf{z}^{\pm} + \left(\nu_{\mp}/k_{eq}^2\right)\nabla^4\mathbf{z}^{\mp} + \mathbf{F}^{\pm}, \end{aligned}\tag{2.7}$$

$$\nabla.\mathbf{z}^{\pm} = 0. \tag{2.8}$$

The terms $\mathbf{F}^{\pm}$ are the forcing functions. The corresponding forcing functions for the $\mathbf{u}$ and the $\mathbf{b}$ fields are related to $\mathbf{F}^{\pm}$, i.e., $\mathbf{F}^{u} = (\mathbf{F}^{+}+\mathbf{F}^{-})/2$, and $\mathbf{F}^{b} = (\mathbf{F}^{+}-\mathbf{F}^{-})/2$ respectively. In our simulations we force only the velocity and not the magnetic field (i.e., $\mathbf{F}^{\mathbf{b}} = \mathbf{0}$). Consequently, we get $\mathbf{F}^{+} = \mathbf{F}^{-} = \mathbf{F}^{\mathbf{u}} = \mathbf{F}$.

In the numerical simulations we time evolve Eq. (2.7) in spectral space. Taking the Fourier transform of the above equations, we write

$$\frac{\partial \mathbf{z}_{\mathbf{k}}^{\pm}}{\partial t} = \mathbf{M}_{\mathbf{k}}^{\pm} - \mathbf{D}_{\mathbf{k}}^{\pm} + \mathbf{F}_{\mathbf{k}}^{\pm}, \tag{2.9}$$

$$\mathbf{k}.\mathbf{z}_{\mathbf{k}}^{\pm} = 0, \tag{2.10}$$

where

$$\mathbf{M}_{\mathbf{k}}^{\pm} = \left\{ \left(\mathbf{z}^{\mp} . \nabla \right) \mathbf{z}^{\pm} \right\}_{\mathbf{k}} - i\mathbf{k} p_{\mathbf{k}}, \tag{2.11}$$

is the Fourier transform of the nonlinear terms, and

$$\mathbf{D}_{\mathbf{k}}^{\pm} = \nu^{\pm} k^2 \left(1 + \left(\frac{k}{k_{eq}} \right)^2 \right) \mathbf{z}_{\mathbf{k}}^{\pm} + \nu^{\mp} k^2 \left(1 + \left(\frac{k}{k_{eq}} \right)^2 \right) z_{\mathbf{k}}^{\mp} \tag{2.12}$$

is the Fourier transform of the dissipative terms. The variables $\mathbf{z}_{\mathbf{k}}^{\pm}$, $\left\{ \mathbf{z}^{\mp} . \nabla \mathbf{z}^{\pm} \right\}_{\mathbf{k}}$, $p_{\mathbf{k}}$ are the Fourier transforms. $p_{\mathbf{k}}$ is determined using the incompressibility constraint.

The Eq. (2.9) is time evolved using the Adam-Bashforth scheme for the nonlinear terms and Crank-Nicholson for the dissipative terms. Both these schemes have an accuracy of $O(\Delta t^2)$. Using the two schemes we obtain $\mathbf{z}^{\pm}$ at time step $n+1$ from $\mathbf{z}^{\pm}$ at time step n and $n-1$ using

$$\frac{\mathbf{z}_{\mathbf{k}}^{\pm(n+1)} - \mathbf{z}_{\mathbf{k}}^{\pm(n)}}{\Delta t} = \left(\frac{3}{2} \mathbf{M}_{\mathbf{k}}{}^{\pm(n)} - \frac{1}{2} \mathbf{M}_{\mathbf{k}}{}^{\pm(n-1)} \right) - \frac{\Delta t}{2} \left(\mathbf{D}_{\mathbf{k}}^{\pm(n+1)} + \mathbf{D}_{\mathbf{k}}^{\pm(n)} \right) + \mathbf{F}_{\mathbf{k}}{}^{\pm(n)}. \tag{2.13}$$

The nonlinear terms are usually computed using the pseudo-spectral method [91] which we illustrate below. For the 2-D case, $\mathbf{u}$ and $\mathbf{b}$ do not have any component along the z-axis, and there is also no variation along z-axis, i.e., $\mathbf{u} = (u_x(x,y,t), u_y(x,y,t), 0)$, and $\mathbf{b} = (b_x(x,y,t), b_y(x,y,t), 0)$. The x and y-components of Elsässer variables in a 2-D MHD equation are

$$\begin{aligned} \frac{\partial z_x^{\pm}}{\partial t} \mp (\mathbf{B}_0 . \nabla) z_x^{\pm} + \frac{\partial}{\partial x}(z_x^{\mp} z_x^{\pm}) + \frac{\partial}{\partial y}(z_y^{\mp} z_x^{\pm}) &= -\frac{\partial p}{\partial x} + \nu_{\pm} \nabla^2 z_x^{\pm} + \nu_{\mp} \nabla^2 z_x^{\mp} \\ &\quad + \left(\nu_{\pm}/k_{eq}^2 \right) \nabla^4 z_x^{\pm} + \left(\nu_{\mp}/k_{eq}^2 \right) \nabla^4 z_x^{\mp} + F_x^{\pm} \end{aligned} \tag{2.14}$$

$$\begin{aligned} \frac{\partial z_y^{\pm}}{\partial t} \mp (\mathbf{B}_0 . \nabla) z_y^{\pm} + \frac{\partial}{\partial x}(z_x^{\mp} z_y^{\pm}) + \frac{\partial}{\partial y}(z_y^{\mp} z_y^{\pm}) &= -\frac{\partial p}{\partial y} + \nu_{\pm} \nabla^2 z_y^{\pm} + \nu_{\mp} \nabla^2 z_y^{\mp} \\ &\quad + \left(\nu_{\pm}/k_{eq}^2 \right) \nabla^4 z_y^{\pm} + \left(\nu_{\mp}/k_{eq}^2 \right) \nabla^4 z_y^{\mp} + F_y^{\pm} \end{aligned} \tag{2.15}$$

In Fourier space the nonlinear terms involve a convolution sum. For example, the term $\frac{\partial}{\partial x}(z_x^{\mp} z_x^{\pm})$ will be expressed in the Fourier space as the convolution sum $\sum_{\mathbf{p}} ik_x z_x^{\mp}(\mathbf{p}) z_x^{\pm}(\mathbf{k}-\mathbf{p})$ (also see the Fourier space MHD equation written in the introduction). To compute this term for each $\mathbf{k}$ by direct summation requires $O(N^2)$ operations, where N is the number of grid points in Fourier space. The number of operations is reduced to $O(Nlog.N)$ by using the pseudo-spectral method. The $\mathbf{z}^{\pm}$ are transformed from Fourier space to real space using inverse Fast Fourier transforms. The products $z_x^{\mp} z_x^{\pm}$, etc. are formed in real space. The resulting product is transformed back to the Fourier space using a forward fast Fourier transform and then the Fourier transformed derivative $\partial/\partial x$ is obtained by multiplying the transformed product by ik_x. The number of operations required is thus reduced to $O(Nlog.N)$ [1]. In the above procedure the aliasing error is known to modify the convolution sum by adding the contribution of higher wavenumbers to the lower wavenumbers [91]. In order to remove the aliasing errors arising in the pseudo-spectral method we use square truncation wherein all the modes with $|k_x| \geq N/3$ or $|k_y| \geq N/3$ are set equal to zero [91].

In direct numerical simulations hyperviscosity $\nu k^4/k_{eq}^2$ and hyper-resistivity $\mu k^4/k_{eq}^2$ is added to the equations. It damps the higher wavenumbers while not modifying the lower wavenumbers. In this way, it becomes possible to simulate higher Reynolds number turbulence. In general higher orders of hyperviscosity $\nu k^{2p+2}/k_{eq}^{2p}$ are often used. However, much higher orders of hyperviscosity need to be avoided as it has been pointed out by Biskamp *et al.* [92] that the effect of hyperviscosity on the inertial range is large for high values of p. We have used the value of $p = 1$ in all our simulations.

The simulations are carried out in a periodic box of size $2\pi \times 2\pi$. All the quantities are non-dimensionalised using the initial total energy and length scale of 2π.

[1] the vorticity-vector potential form of the 2-D MHD equations which is seemingly simpler, is infact more expensive computationally. A larger number of FFT's are required to compute the nonlinear terms in the vorticity-vector potential formulation

2.3.2 Steady state

The normalised cross helicity σ_c is defined as $\sigma_c = 2H_c/E$, where $H_c = E^+ - E^-$ is the cross helicity and E is the total energy. In decaying turbulence the total energy decays due to the viscous and resistive dissipation, whereas σ_c often shows the tendency to increase with time. We shall discuss the issue of increase of cross-helicity in greater detail in Chapter 5. In simulations it is observed that the decay rate of the majority species E^+ (if $\sigma_c > 0$) is larger than the decay rate of the minority species E^-. Therefore, H_c decreases with time. To obtain a steady state we inject kinetic energy and cross-helicity (H_c) at a rate such that both E and σ_c are maintained at a statistically steady value.

At each time step we construct $\mathbf{F}$ as an uncorrelated random function that is divergence free (i.e., $\nabla.\mathbf{F} = 0$). The x-component of $\mathbf{F}$ is determined at every time step by

$$F_x = \left(\frac{k_y}{k}\right)\sqrt{\Delta t}\mathcal{F}e^{i\phi}, \tag{2.16}$$

where $\mathcal{F}^2$ is equal to the average energy input rate per mode, and phase ϕ is a uniformly distributed random variable between 0 and 2π. The y-component of the forcing function is obtained by using the condition of zero divergence, i.e.,

$$F_y = -\left(\frac{k_x}{k}\right)\sqrt{\Delta t}\mathcal{F}e^{i\phi}, \tag{2.17}$$

We force all the modes in the annulus $4 < k < 5$. The value of $\mathcal{F}^2$ is determined from the average rate of the total energy input.

The simulation method described above is common to all our simulations described in this thesis. The specific values of ν's, μ's, k_{eq}, and the forcing parameters for each simulation will be stated in the next section.

2.4 Results

In this section we will study the energy spectra $E^{\pm}(k)$ and the energy fluxes $\Pi^{\pm}$ over a range of σ_c values. Using these results we will carry out a comparative test of KID and the

Kolmogorov phenomenologies and compute the appropriate constants.

We have obtained a steady state for the approximate σ_c values listed in Table 2.1. The Alfven ratio in he steady state are also shown in the table. Note that in our simulations higher σ_c states also have a higher r_A. We have performed all the runs at a unit Prandtl number ($\nu = \mu$). The values of ν and the hyper-viscosity parameter k_{eq} are also shown in the table. The fluxes and energy spectra are averaged in the steady state over a time interval t_{avg}.

Runs	σ_c	ν	k_{eq}	r_A	dt	t_{avg}
R1	0.1	5×10^{-6}	16	0.2	5×10^{-4}	6
R4	0.4	5×10^{-6}	16	0.5	2.5×10^{-4}	6
R7	0.7	5×10^{-6}	16	0.65	2.5×10^{-4}	6
R9	0.9	5×10^{-6}	14	0.8	2.5×10^{-4}	6
R95	0.95	5×10^{-6}	14	0.9	2.5×10^{-4}	3

Table 2.1: The parameters for our simulations and the steady state values of σ_c and r_A.

The compensated energy spectra , $E^{\pm}(k)k^{\alpha}$ with $\alpha = 5/3$ and $3/2$ have been plotted in Figs. 2.1-2.5 for the runs R1-R95. From these plots of $E^{\pm}k^{\alpha}$ we are unable to distinguish between the $-3/2$ and $-5/3$ exponents, as the inertial range is not wide enough. Even though the exponents $m^{\pm}$ cannot be accurately determined from these plots, it is clear that m^{+} and m^{-} are close to each other, i.e., $m^{+} \sim m^{-}$. For low σ_c fluctuations, the spectral exponents have been measured by Politano *et al.* [12] to be close to $-5/3$, with $m^{+} = -1.69$ and $m^{-} = -1.7$, as predicted by Kolmogorov-like phenomenology. In the same simulations of Politano *et al.* [12], the structure function of fourth order, i.e., $|\Delta z^{\pm}(r)|^4$ were found to be proportional to r, in accordance with the predictions of KID phenomenology. However, we have argued in Chapter 1 (see Section 1.4.2) that the predictions of KID phenomenology regarding the fluxes are not in agreement with simulations, and hence the agreement of ζ_4

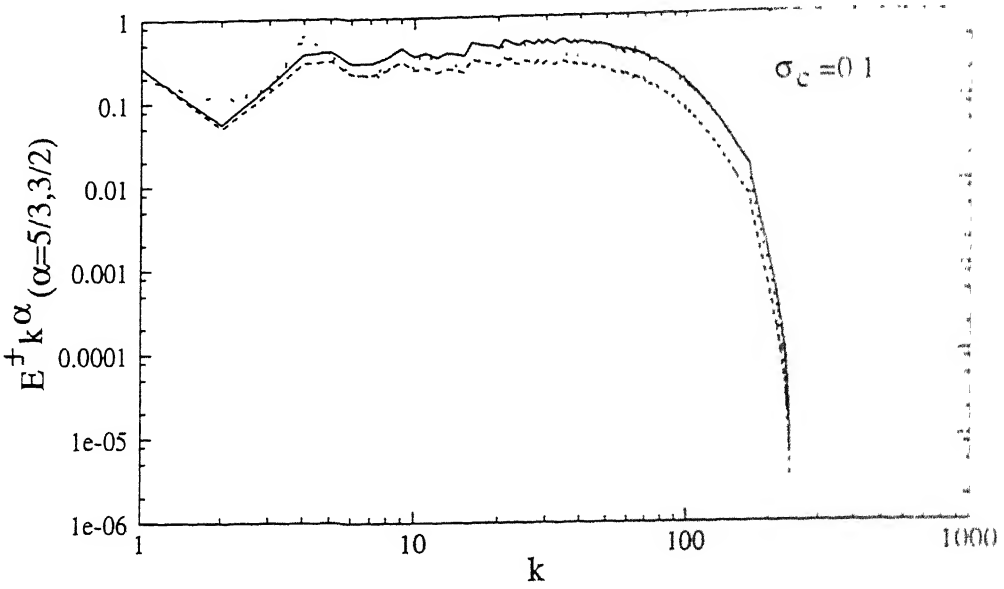

Figure 2.1: $E^{\pm}(k)k^{\alpha}$ versus k for run R1 with $\sigma_c = 0.1$. The solid (E^+) and closely spaced dotted line (E^-) corresponds to $\alpha = 5/3$, and dashed (E^+) and widely spaced dotted line (E^-) correspond to $\alpha = 3/2$.

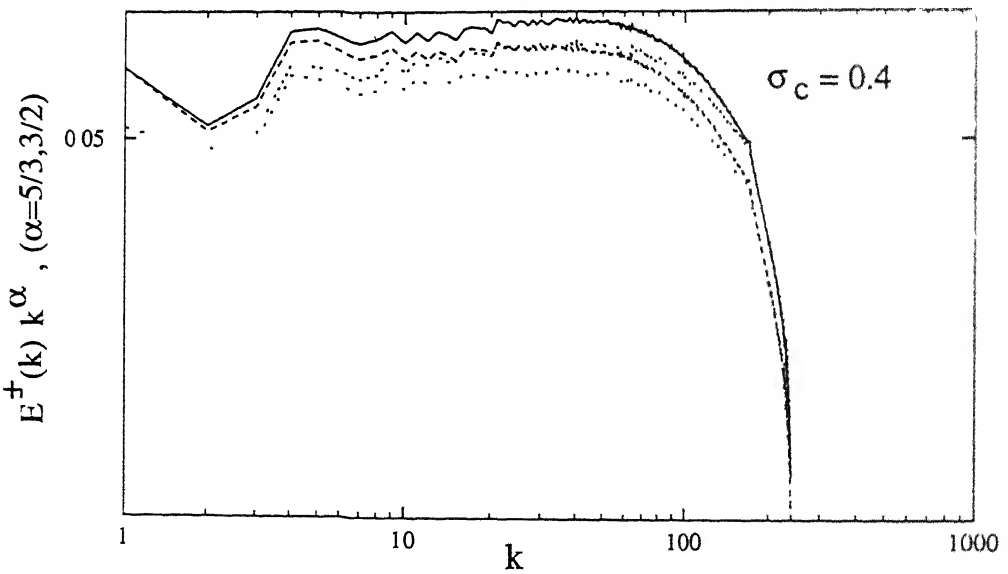

Figure 2.2: $E^{\pm}(k)k^{\alpha}$ versus k for run R4 with $\sigma_c = 0.4$.

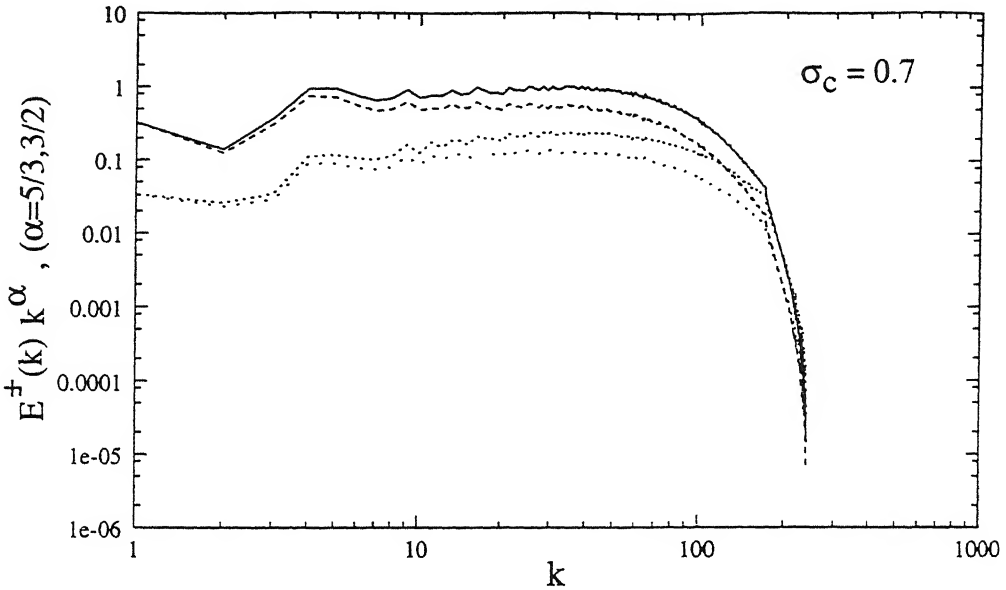

Figure 2.3: $E^{\pm}(k)k^{\alpha}$ versus k for run R7 with $\sigma_c = 0.7$.

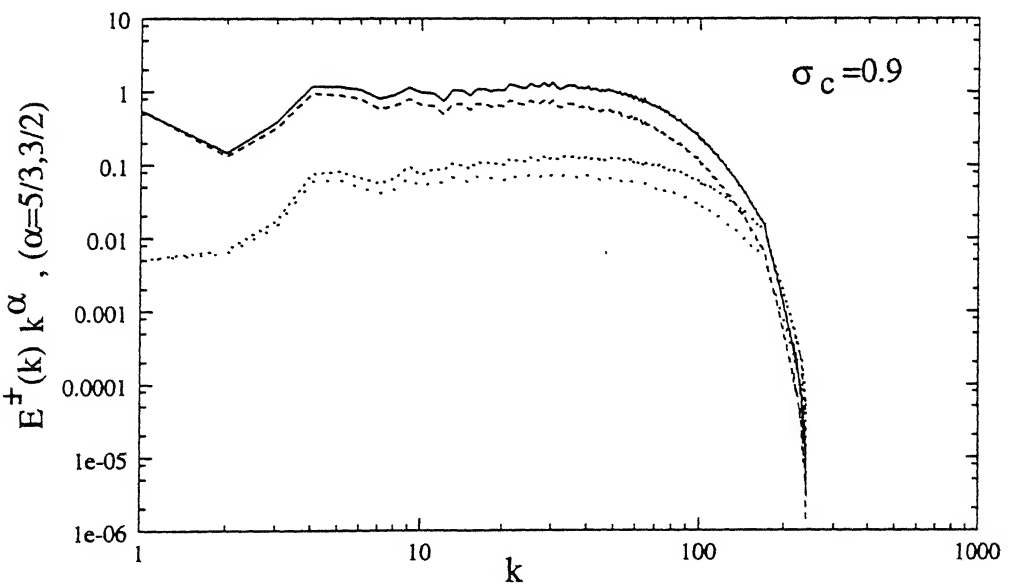

Figure 2.4: $E^{\pm}(k)k^{\alpha}$ versus k for run R9 with $\sigma_c = 0.9$.

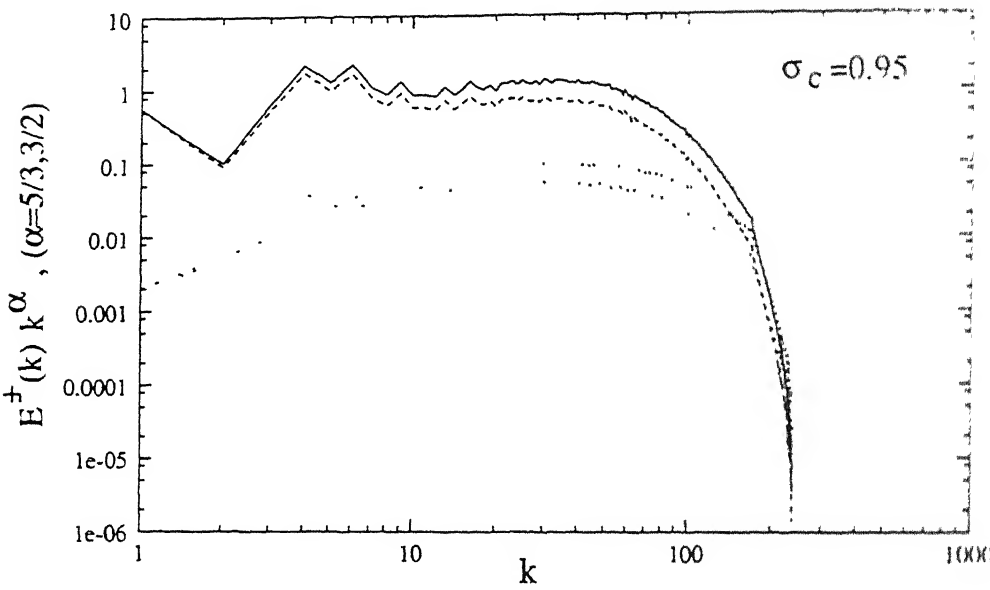

Figure 2.5: $E^{\pm}(k)k^{\alpha}$ versus k for run R95 with $\sigma_c = 0.95$.

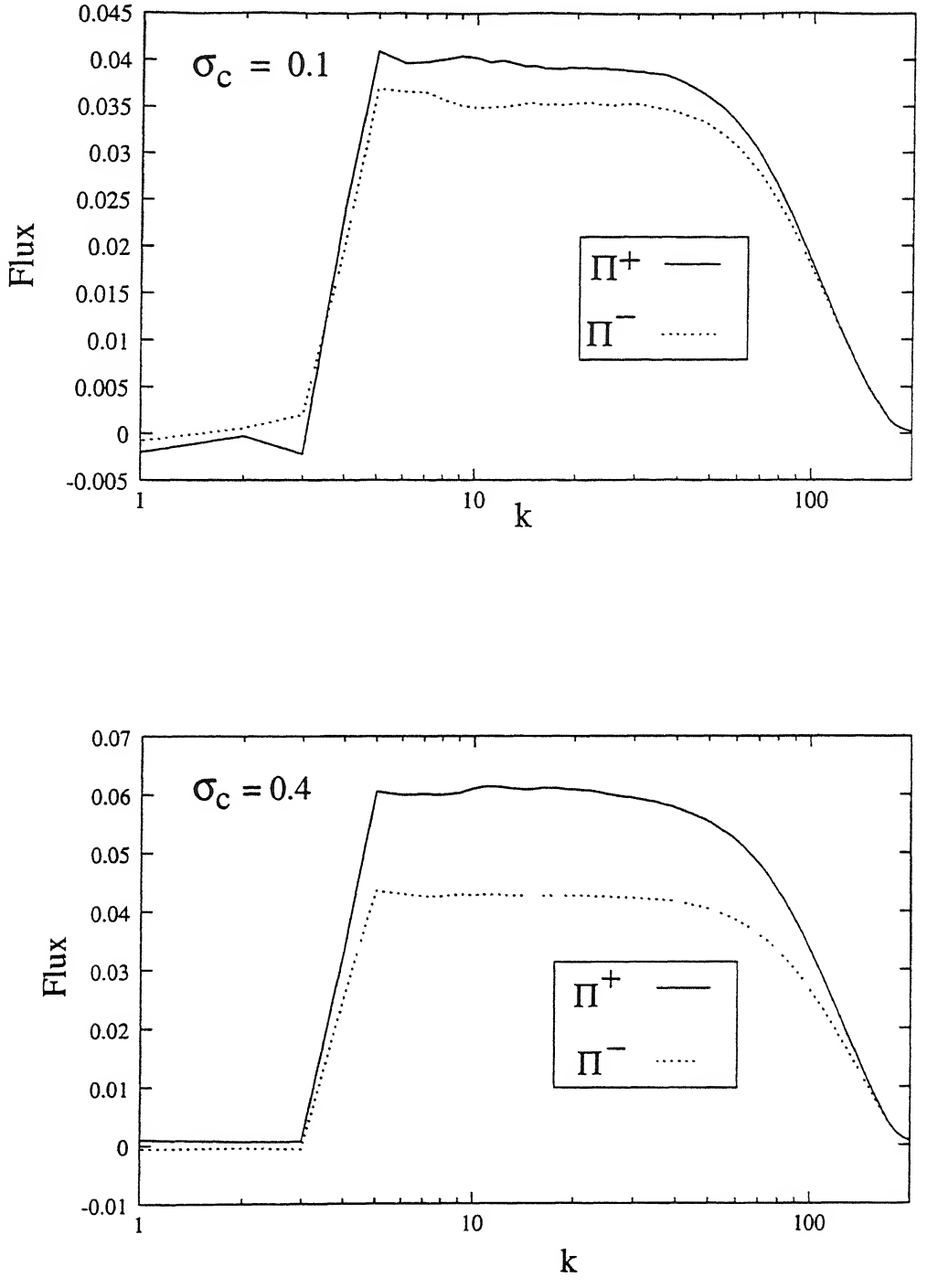

Figure 2.6: The fluxes $\Pi^{\pm}$ for (a) run R1 and with steady state $\sigma_c \simeq 0.1$, and (b) run R4 with steady state $\sigma_c \simeq 0.4$.

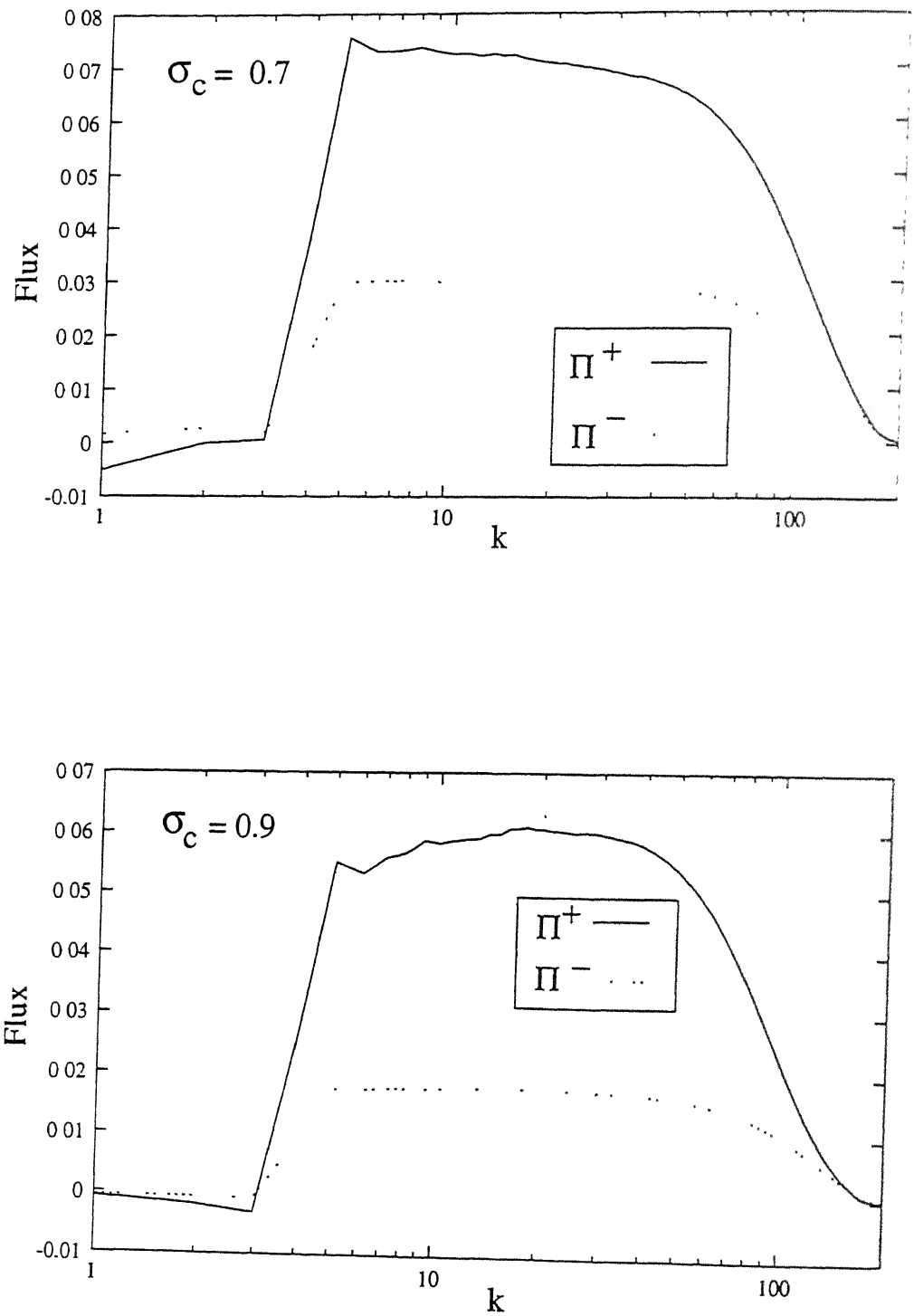

Figure 2.7: The fluxes $\Pi^{\pm}$ for (a) run R4 and with steady state $\sigma_c \simeq 0.7$. and (b) run R9 with steady state $\sigma_c \simeq 0.9$.

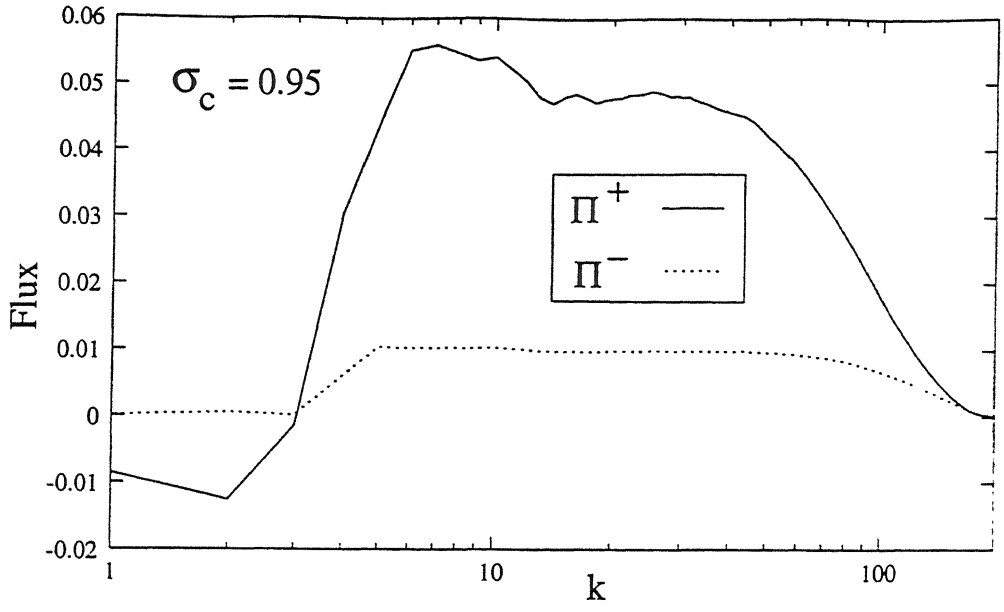

Figure 2.8: The fluxes $\Pi^{\pm}$ for run R95 with steady state $\sigma_c \simeq 0.95$.

in KID phenomenology and simulations observed by Politano *et al.* [12] may be fortuitous. The small deviation of $m^{\pm}$ from $-5/3$ observed in Politano's simulation can arise because of intermittency.

For high σ_c fluctuations attempts have been made to measure $m^{\pm}$ from the spectral plots [9–11], but no conclusive statements were made from these measurements. Instead of measuring the spectral exponents directly, Verma *et al.* [11] had tested the predictions of KID and Kolmogorov phenomenologies regarding the fluxes Π^+ and Π^-. We will follow their approach.

We have plotted the fluxes for runs R1-R95 in Figs.2.6-2.8. We find that $\Pi^- \neq \Pi^-$ for all the σ_c's listed in Table 2.2. They become increasingly unequal with an increase in σ_c. As an example, for $\sigma_c = 0.4$, the ratio $\Pi^+/\Pi^- = 1.08$, and for $\sigma_c = 0.95$, $\Pi^+/\Pi^- = 4$. These observations had earlier been made by Verma *et al.* [11] in their simulations. Since $\Pi^+ \neq \Pi^-$, they had concluded from these results that KID phenomenology is not applicable to MHD turbulence. However, an extension of KID phenomenology due to Grappin *et al.* [4] predicts inequality of fluxes. This phenomenology was not tested by Verma *et al.*. According to

Grappin's phenomenology [4] $\Pi^+/\Pi^- = m^+/m^-$. However, we observe that our simulations do not support this prediction, since $m^+ \simeq m^-$ but $\Pi^+ \neq \Pi^-$. Thus, the flux asymmetry observed in the simulations cannot be explained successfully by any of the existing models based on KID phenomenology.

Inequality of fluxes Π^+ and Π^- is consistent with the predictions of Kolmogorov's phenomenology [5–7]. For low values of σ_c, the constants C^+ and C^- (in Eq. (1.42) of Chapter 1) should be expected to be nearly equal. It follows from Eq. (1.42) of Chapter 1 that the relationship $E^+/E^- = (\Pi^+/\Pi^-)^2$ will hold. From Table 2.2, where we have tabulated these ratios, we find that our simulations confirm this prediction of the Kolmogorov like phenomenology. For highest $\sigma_c(= 0.95)$ in our simulations (see Table 2.2) we find that E^+/E^- and $(\Pi^+/\Pi^-)^2$ differ approximately by a factor of two. The predictions of Kolmogorov-like phenomenology will be consistent with our simulation results if C^+ and C^- are unequal for high σ_c cases. Earlier Verma and Bhattacharjee [50] had applied DIA to calculate the Kolmogorov constant for MHD turbulence. They show in their calculations that the $C^\pm$ depend on Alfvén ratio and argue that it will also depend on σ_c.

On the basis of the results of reference [12, 11] and our own results, there is justification for supporting the view that $E^\pm(k)$ follow Kolmogorov's $-5/3$ scaling at all values of σ_c.

In the Kolmogorov-like phenomenology for MHD turbulence the energy spectrum for $z^\pm$ is given as

$$E^\pm(k) = C^\pm (\Pi^\pm)^{4/3} (\Pi^\mp)^{-2/3} k^{-5/3}, \tag{2.18}$$

where $C^\pm$ are the Kolmogorov's constants. From the above equation we can write $C^\pm$ as

$$C^\pm = \frac{E^\pm(k) k^{5/3}}{(\Pi^\pm)^{4/3} (\Pi^\mp)^{-2/3}}. \tag{2.19}$$

In fluid turbulence the Kolmogorov constant are found to be universal. We had pointed out above that in MHD turbulence the constants may depend on σ_c. Now we will study the dependence of $C^\pm$ on σ_c. Verma *et al.* [11] had previously obtained $C^\pm$ from decaying

simulations. However, because of the large fluctuations in the energy spectrum and the fluxes there were large errors in the values of these constants. In our simulations $E^{\pm}(k)k^{5/3}$ and $\Pi^{\pm}$ will be averaged over the steady state and $C^{\pm}$ then calculated from Eq. (2.19).

Run	σ_c	$E^+(k)k^{5/3}$	$E^-(k)k^{5/3}$	Π^+	Π^-	C^+	C^-	C^-/C^+	E^+/E^-	$(\Pi^+/\Pi^-$
R1	0.1	0.48	0.41	0.041	0.038	4.0	4.1	1.03	1.2	1.2
R4	0.4	0.64	0.38	0.06	0.042	3.3	4.0	1.2	1.7	2.0
R7	0.7	0.95	0.23	0.07	0.03	3.0	4.4	1.4	4.1	5.4
R9	0.9	1.18	0.23	0.06	0.017	3.3	4.2	1.3	5.1	12.4
R95	0.95	1.25	0.09	0.048	0.01	3.3	5.7	1.7	13.9	23.0

Table 2.2: The $E^{\pm}(k)k^{5/3}$ and $\Pi^{\pm}$ obtained from the simulations, and the Kolmogorov's constants $C^{\pm}$ calculated from these values. The errors in $C^{\pm}$ due to the fluctuations are indicated in text.

The constants $C^{\pm}$ were obtained using Eq. (2.19) by first performing a fit of a constant function, i.e., $f(x) = constant$ to $E^{\pm}k^{5/3}$ vs. k and to $\Pi^{\pm}(k)$ vs. k. The fit was performed in the inertial range over a wavenumber interval typically equal to 20. The best estimates of $C^{\pm}$ thus computed are given in Table 2.2. The worst error estimate of $C^{\pm}$ were computed by considering the maximum error in $E^{\pm}k^{5/3}$ and $\Pi^{\pm}(k)$. The error in $C^{\pm}$ calculated in this manner was roughly in the range of 0.4 to 0.8 for the various σ_c cases. The following observations can be made from Table 2.2.

The constant C^+ and C^- are unequal at high values of σ_c, i.e., $C^+ \neq C^-$, and C^- is larger than C^+ — these results are consistent with those from Verma *et al.'s* [11] decaying simulations. At $\sigma_c \simeq 0$ (R1 in Table 2.2), $C^+ \simeq C^- = C$ as expected with $C \simeq 4$. The constant C^- does not show a tendency to vary upto $\sigma_c = 0.9$. However, beyond $\sigma_c = 0.9$, C^- has a dependence on σ_c. It increases from a value of 4.2 ± 0.5 at $\sigma_c = 0.9$ to a value

5.7 ± 0.8 at $\sigma_c = 0.95$. On the contrary C^+ varies at low σ_c values — it is equal to 4 ± 0.4 at $\sigma_c = 0.1$ and decreases to 3.3 ± 0.3 at $\sigma_c = 0.4$. At higher σ_c values, C^+ does not show any dependence on σ_c, and is roughly 3.3 ± 0.8. Therefore, C^- is independent of σ_c for low σ_c's and C^+ is independent of σ_c at high σ_c's. Verma *et al.* [11] had earlier found that for low σ_c case $C^+ \simeq C^- \simeq 5 - 7$, and for high σ_c case $C^+ \simeq 4 - 5$ and $C^- \simeq 8 - 10$. Their results differ from our present results; this may be due to large error bars in their simulations.

The ratio E^+/E^- can be obtained from the definition $\sigma_c = (E^+ - E^-)/(E^+ + E^-)$. The value E^+/E^- corresponding to the σ_c's of Run R1-R95 are listed in Table 2.2. The ratio C^-/C^+ is also shown in the table. In Fig. 2.9 we have plotted C^-/C^+ versus E^+/E^- for $\sigma_c = 0.$ to 0.7. From the figure there appears to be a linear relationship between C^-/C^+ and E^+/E^- at low values of σ_c. The data points for higher values of σ_c do not appear to follow this linear dependence between C^-/C^+ and E^+/E^- (not shown in the figure). The best fit between the two parameters is found to be $C^-/C^+ = (0.09 \pm 0.01)(E^+/E^-) + (0.93 \pm 0.03)$.

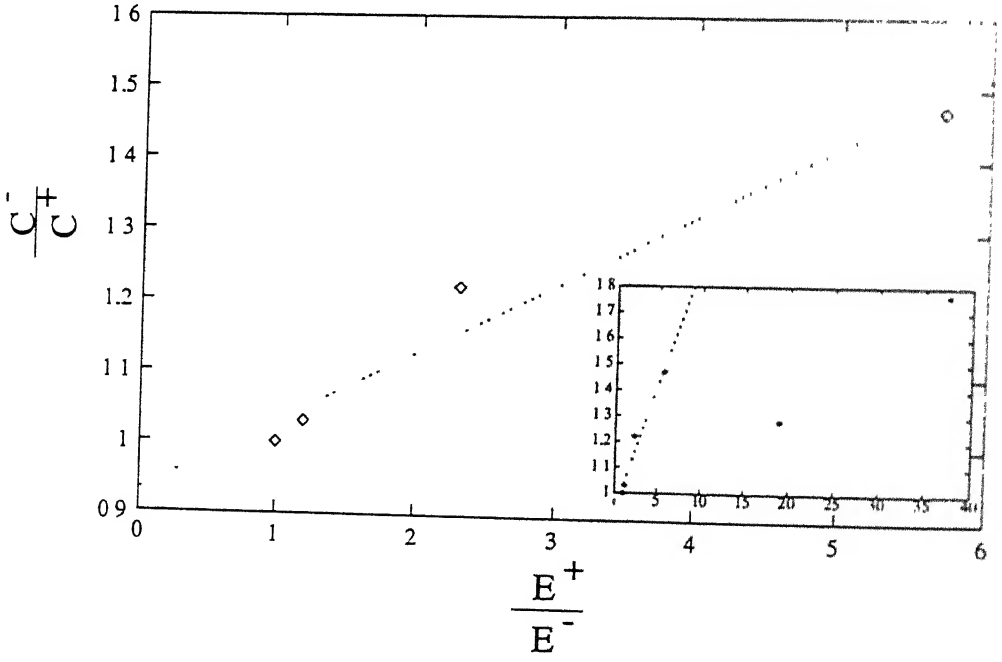

Figure 2.9: Plot of C^-/C^+ vs. E^+/E^-. $E^\pm$ refer to the global energies. The diamonds are the computed values for $\sigma_c = 0.1$ to 0.7 and the straight line is the best fit line through the points $[C^-/C^+ = (0.09 \pm 0.01)(E^+/E^-) + (0.93 \pm 0.03)]$. The figure inset shows the data from $\sigma_c = 0.$ to 0.95.

2.5 Discussion

In this chapter we studied the numerical results of energy spectra $E^{\pm}(k)$ and fluxes $\Pi^{\pm}$ in 2-D MHD turbulence with kinetic forcing. From the energy spectra, it was difficult to distinguish between -3/2 and -5/3 exponents as predicted by the KID phenomenology and the Kolmogorov-like phenomenology, respectively. The spectral exponents m^+ and m^- however were found to be close to each other. The predictions regarding fluxes were earlier tested by Verma *et al.* in a decaying simulation, and KID phenomenology was found to be inconsistent with the numerical results. We performed the same test in a forced simulation and found KID phenomenology to be inconsistent with the numerical results, as expected from earlier results of Verma *et al.* [11]. Note, however, that our simulations were done in the steady state. We have time-averaged the energy spectra and the fluxes resulting in less errors compared to Verma *et al.* [11]. We found that Grappin *et al.'s* extension of KID phenomenology was also not consistent with the numerical results. We concluded that KID phenomenology [1–3, 90] cannot explain the numerical results. However, as observed by Verma *et al.* [11], we also find that $E^+/E^- \simeq (\Pi^+/\Pi^-)^2$, upto a factor of atmost two. Therefore, we tend to believe that Kolmogorov-like phenomenology is more suitable for MHD turbulence. Our belief is reinforced by recent high Reynolds number simulations by Politano *et al.* [12], and Müller and Biskamp [13]. Unfortunately, these high Reynolds number simulations have been done only for small σ_c. A similar analysis should be carried out for large σ_c. Recently, Verma [26] has shown that the $k^{-5/3}$ spectra predicted by Kolmogorov-like phenomenology is a consistent solution of RG equations of MHD. This approach is based on renormalisation of mean magnetic field. Unfortunately, this approach also assumes $\sigma_c = 0$, $r_A = 1$. Generalization of the above RG argument is needed for $\sigma_c \neq 0$ cases.

The Kolmogorov's $-5/3$ scaling had recently been observed in high Reynolds number simulations [12, 13] for low σ_c cases, and a theoretical reasoning had also been provided in RG calculations in support of $-5/3$ scaling [26]. For high σ_c cases our simulation results

preferred Kolmogorov-like phenomenology over KID type phenomenologies. From all the earlier evidences and our simulation results we concluded that Kolmogorov like phenomenology probably provides the correct description for MHD turbulence.

We computed the Kolmogorov's constants for various σ_c cases from 0.1 to 0.95. We found that C^+ varies at low values of σ_c but stays constant beyond $\sigma_c \simeq 0.4$, while C^- stays constant upto $\sigma_c \simeq 0.9$ and varies beyond that. The value of C^+ of C^- in their constant regimes were approximately equal to 3.3 ± 0.8 and 4.2 ± 0.5 respectively (the worst error estimates are quoted). These constants were earlier evaluated by Verma *et al* [11] in a decaying simulation. However, in their simulations the fluctuations in $\Pi^\pm$ and $E^\pm(k)k^{5/3}$ were too large to provide the trend of the constants with variation in σ_c. In our simulations, we have averaged the energy spectra and fluxes over the steady state maintained by forcing and obtained a clearer picture of the variation of the constants with σ_c.

The Kolmogorov's constants are also expected to depend upon the Alfvén ratio [50]. It is desirable to obtain both σ_c and r_A dependence of $C^\pm$. However, we have not studied this dependence in our numerical simulations. In all our numerical simulations $r_A = 0.2 - 0.9$ and we could not vary it independently of σ_c. The reason for this is the difficulty in obtaining the desired steady state Alfvén ratio in simulations. It is not clear to us at the moment whether it is possible to maintain a desired level of Alfvén ratio by external forcing.

In this chapter we studied some properties of the energy fluxes (cascade rates) of $\mathbf{z}^\pm$ energies and using these properties we attempted to see which of the MHD turbulence phenomenologies is correct. In our analysis we ignored various energy fluxes and energy transfer rates related to $\mathbf{u}$ and $\mathbf{b}$. These fluxes are very important for magnetic field amplification observed in astrophysical objects. In the next chapter we will develop a formalism for studying energy transfer properties between the various scales of $\mathbf{u}$ and $\mathbf{b}$ fields. In the following chapter we will use that formalism for studying energy fluxes (cascade rates) and shell-to-shell energy transfer rates in numerical simulations of 2-D MHD turbulence.

Chapter 3

A new approach to study energy transfer in turbulence

3.1 Introduction

In fluid and MHD turbulence eddies of various sizes interact amongst themselves; energy is exchanged among them in this process. These interactions arise due to the nonlinearity present in these systems. The interactions involve wavenumber triads $(\mathbf{k},\mathbf{p},\mathbf{q})$ with $\mathbf{k}+\mathbf{p}+\mathbf{q}=\mathbf{0}$. The complete nonlinear energy transfer term consist of all possible combinations of wavenumber triads that satisfy this triangle equality.

The *combined energy transfer* computation to a mode from the other two modes of a triad has generally been considered to be fundamental. This formalism has played an important role in furthering our understanding of locality in fluid turbulence [39–42], and also in analysing subgrid scale eddy viscosity [93, 94]. In this formalism, Batchelor [72] first suggested a formula for the energy transfer in fluid turbulence between two regions in Fourier space, and Domaradzki and Rogallo [39] calculated shell-to-shell energy transfer rates. Taking energy energy transfer between shells as an example, we will show in Section 3.3, that this formalism has certain limitations.

In this chapter we present a scheme to calculate the energy transfer between two modes in a triad interaction. Using this scheme we can calculate the energy transfer between two shells, cascade rates, and also study locality of energy transfer.

One of the main objectives of this thesis is to study cascade rates and shell-to-shell transfer rates in MHD turbulence. The formulae for the combined energy transfer rate were used to study energy transfer in MHD turbulence [11, 17–20]. However, several cascade rates cannot be calculated using this formalism. Our formalism of "mode-to-mode" transfer enables us to calculate all these energy transfer rates between the spheres and the shells.

This chapter is organized into the following sections. In Section 3.2 we will state the known results regarding the combined energy transfer between velocity modes of a triad. In Section 3.3 we will present a discussion on the formulae which are used for studying energy transfer between shells in fluid turbulence. In Section 3.4 we will formulate a way of studying energy transfer between a pair of modes within a triad, with the third mode of the triad meditating the transfer. This new method is used to re-define shell-to-shell transfer in Section 3.5. The known results of energy transfer in a MHD triad are discussed in Section 3.6 and the "mode-to-mode" transfers in MHD in Section 3.7. The results of Section 3.7 are used in Section 3.8 to define shell-to-shell transfer rates and the energy cascade rates in MHD turbulence. The conclusion to this chapter follows in Section 3.9.

3.2 Energy transfer in a triad: Known results

The Navier Stokes equation in real space are written as

$$\frac{\partial \mathbf{u}}{\partial t} + (\mathbf{u}.\nabla)\mathbf{u} = -\nabla p + \nu \nabla^2 \mathbf{u}, \tag{3.1}$$

where $\mathbf{u}$ is the velocity field, and ν is the fluid kinematic viscosity. In Fourier space, the kinetic energy equations for a Fourier mode is

$$\frac{\partial E^u(\mathbf{k})}{\partial t} + 2\nu k^2 E^u(\mathbf{k}) = \sum_{\mathbf{k+p+q=0}} \frac{1}{2} S^{uu}(\mathbf{k}|\mathbf{p},\mathbf{q}), \tag{3.2}$$

where $E^u(\mathbf{k}) \equiv |\mathbf{u}(\mathbf{k})|^2/2$ is the kinetic energy in Fourier space for mode $\mathbf{k}$. The nonlinear terms $S^{uu}(\mathbf{k}|\mathbf{p},\mathbf{q})$ is

$$S^{uu}(\mathbf{k}|\mathbf{p},\mathbf{q}) \equiv -Re\,(i[\mathbf{k}.\mathbf{u}(\mathbf{q})][\mathbf{u}(\mathbf{k}).\mathbf{u}(\mathbf{p})] + i[\mathbf{k}.\mathbf{u}(\mathbf{p})][\mathbf{u}(\mathbf{k}).\mathbf{u}(\mathbf{q})]) \tag{3.3}$$

This term represents the combined transfer of kinetic energy from mode $\mathbf{p}$ and $\mathbf{q}$ to mode $\mathbf{k}$ [44]. Note that the wavenumber triad $\mathbf{k}$, $\mathbf{p}$, and $\mathbf{q}$ should satisfy the condition $\mathbf{k}+\mathbf{p}+\mathbf{q}=0$. This nonlinear term satisfies the following detailed conservation properties

$$S^{uu}(\mathbf{k}|\mathbf{p},\mathbf{q}) + S^{uu}(\mathbf{p}|\mathbf{k},\mathbf{q}) + S^{uu}(\mathbf{q}|\mathbf{k},\mathbf{p}) = 0. \tag{3.4}$$

The quantity $S^{uu}(\mathbf{k}|\mathbf{p},\mathbf{q})$ represents the nonlinear energy transfer from the *two modes* $\mathbf{p}$ and $\mathbf{q}$ to mode $\mathbf{k}$. It would be useful to know the exact energy transfer between *any two modes*, say from $\mathbf{p}$ to $\mathbf{k}$. In Section 3.4 we will explore this idea further.

3.3 Shell-to-Shell energy transfer in fluid turbulence

We had mentioned in the last section that the combined energy transfer from modes $\mathbf{p}$ and $\mathbf{q}$ to mode $\mathbf{k}$ is given by $S^{uu}(\mathbf{k}|\mathbf{p},\mathbf{q})$. Using this result researchers [39] have discussed energy transfer between two shells. The quantity

$$T^{uu}_{mn} = \frac{1}{2}\sum_{\mathbf{k}\in m}\sum_{\mathbf{p}\in n} S^{uu}(\mathbf{k}|\mathbf{p},\mathbf{q}). \tag{3.5}$$

is usually interpreted as the rate of energy transfer from shell n to shell m [39, 72]. Note that $\mathbf{k}$-sum is over shell m, $\mathbf{p}$-sum over shell n, and $\mathbf{q} = -\mathbf{k}-\mathbf{p}$. However, Domaradzki [39] points out that it may not be correct to interpret the formula (3.5) as the shell-to-shell energy transfer. The argument is as follows:

In energy transfer between two shells m and n, two types of wavenumber triads are involved in the energy transfer (see Fig. 3.1 shown below). In triad of type I the wavenumbers $\mathbf{p}$, $\mathbf{q}$ are located in one shell, and $\mathbf{k}$ is located in the other. In type II, wavenumber $\mathbf{k}$ is in one shell, $\mathbf{p}$ *or* $\mathbf{q}$ in the other shell, and the third wavenumber is located outside the two shells. In Eq. (3.5) the summation is carried over both kinds of triads. However, it is easy to to see

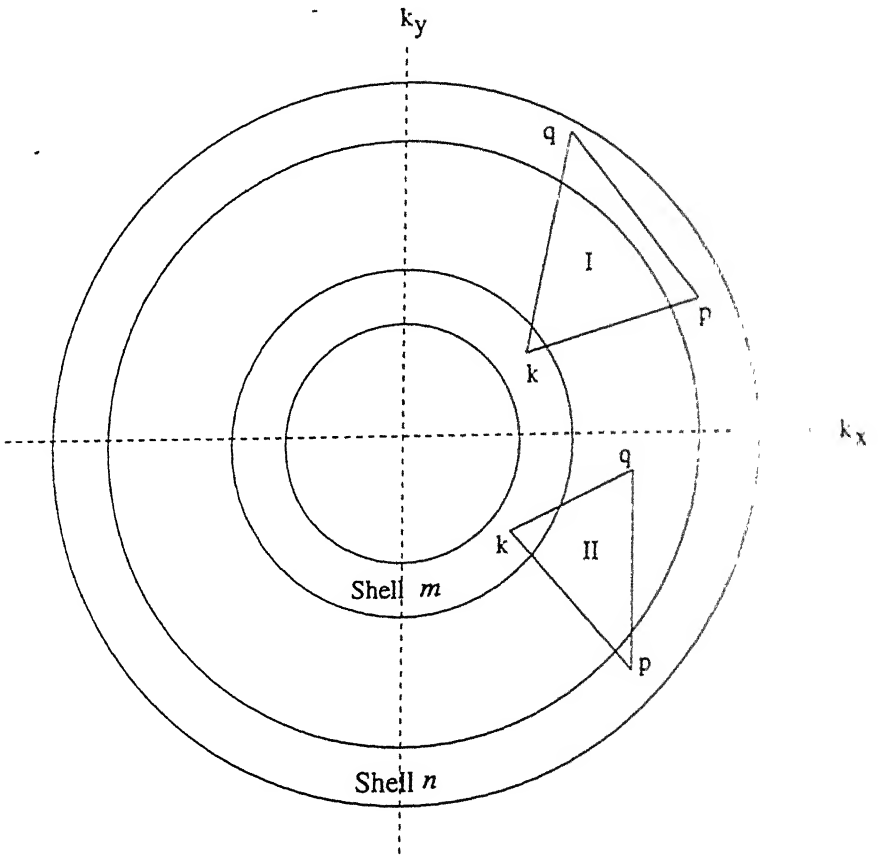

Figure 3.1: two types of triads involved in transfer between shell m and shell n. Mode q could be either inside a shell or could be located outside the shells.

that the energy transfer from shell n to shell m takes place through both the **k-p** and **k-q** legs of triad I but only through the **k-p** leg of triad II. Hence Batchelor's and Domaradzki's formalism do not yield correct shell-to-shell energy transfers (as pointed out by Batchelor and Domaradzki themselves).

3.4 "Mode-to-Mode" energy transfer in a triad

The nonlinear interaction in the Navier-Stokes and the MHD equations are intrinsically three-mode interactions. The expressions for the energy transfer to one mode of the triad from the other two were presented in Section 3.2. In this section we shall explore the possibility of obtaining an expression for the energy transfer between any two modes *within* a triad —

we will call it the *mode-to-mode transfer*. We emphasize that this approach is still within framework of the triad interaction — that is, the triad is still the fundamental interaction of which the mode-to-mode transfer is a part. The energy transfer between two modes of a triad by the mediation of the third mode is sought here.

We shall first consider only the Navier-Stokes equation. In a later section, the discussion will be generalised to the MHD equation.

3.4.1 Definition of Mode-to-Mode transfer in a triad

Consider a triad **k**, **p**, **q** shown in the figure below. The quantity $\mathcal{R}^{uu}(\mathbf{k}|\mathbf{p}|\mathbf{q})$ in Fig. 3.2

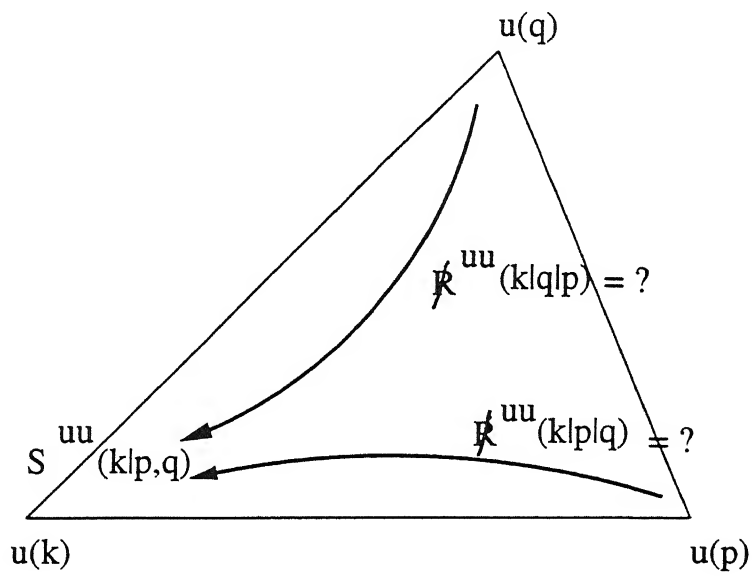

Figure 3.2: The mode-to-mode energy transfers $\mathcal{R}^{uu}$'s sought to be determined.

denotes the energy transferred from mode **p** to mode **k** with mode **q** playing the role of a mediator. We wish to obtain an expression for $\mathcal{R}^{uu}$.

$\mathcal{R}^{uu}$'s should satisfy the following relationships :

1. The sum of $\mathcal{R}^{uu}(\mathbf{k}|\mathbf{p}|\mathbf{q})$ and $\mathcal{R}^{uu}(\mathbf{k}|\mathbf{q}|\mathbf{p})$, which represent energy transfer from mode **p** to mode **k** and from mode **q** to mode **k** respectively, should be equal to the total energy transferred to mode **k** from modes **p** and **q**, i.e., $S^{uu}(\mathbf{k}|\mathbf{p},\mathbf{q})$ [see Eq. (3.3)]. Thus,

$$\mathcal{R}^{uu}(\mathbf{k}|\mathbf{p}|\mathbf{q}) + \mathcal{R}^{uu}(\mathbf{k}|\mathbf{q}|\mathbf{p}) = S^{uu}(\mathbf{k}|\mathbf{p},\mathbf{q}), \tag{3.6}$$

$$\mathcal{R}^{uu}(\mathbf{p}|\mathbf{k}|\mathbf{q}) + \mathcal{R}^{uu}(\mathbf{p}|\mathbf{q}|\mathbf{k}) = S^{uu}(\mathbf{p}|\mathbf{k},\mathbf{q}). \tag{3.7}$$

$$\mathcal{R}^{uu}(\mathbf{q}|\mathbf{k}|\mathbf{p}) + \mathcal{R}^{uu}(\mathbf{q}|\mathbf{p}|\mathbf{k}) = S^{uu}(\mathbf{q}|\mathbf{k},\mathbf{p}). \tag{3.8}$$

2. The energy transferred from mode $\mathbf{p}$ to mode $\mathbf{k}$, i.e., $\mathcal{R}^{uu}(\mathbf{k}|\mathbf{p}|\mathbf{q})$, will be equal and opposite to the energy transferred from mode $\mathbf{k}$ to mode $\mathbf{p}$ i.e., $\mathcal{R}^{uu}(\mathbf{p}|\mathbf{k}|\mathbf{q})$, (also see Fig. 3.3. Thus,

$$\mathcal{R}^{uu}(\mathbf{k}|\mathbf{p}|\mathbf{q}) + \mathcal{R}^{uu}(\mathbf{p}|\mathbf{k}|\mathbf{q}) = 0. \tag{3.9}$$

$$\mathcal{R}^{uu}(\mathbf{k}|\mathbf{q}|\mathbf{p}) + \mathcal{R}^{uu}(\mathbf{q}|\mathbf{k}|\mathbf{p}) = 0. \tag{3.10}$$

$$\mathcal{R}^{uu}(\mathbf{p}|\mathbf{q}|\mathbf{k}) + \mathcal{R}^{uu}(\mathbf{q}|\mathbf{p}|\mathbf{k}) = 0. \tag{3.11}$$

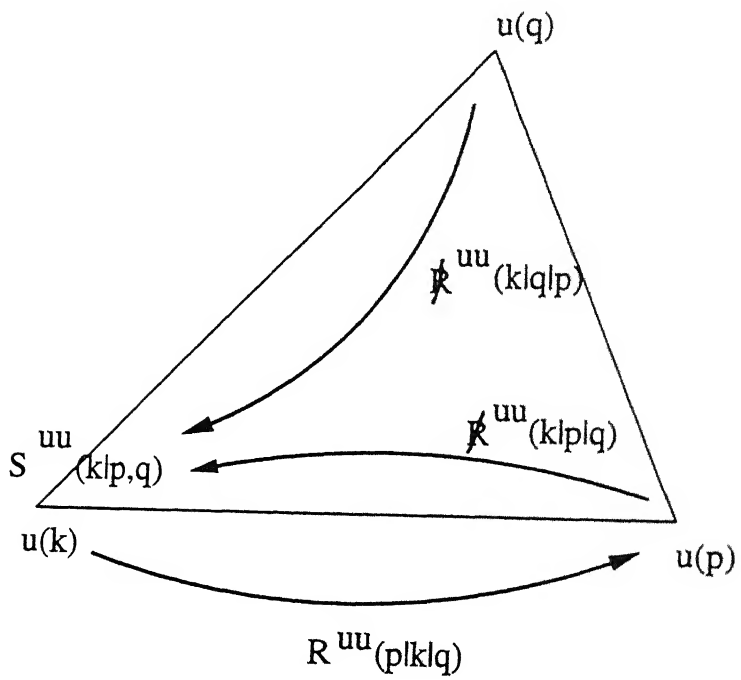

Figure 3.3: Relationship between the $\mathcal{R}^{uu}$'s. Transfer $\mathbf{u(k)} \rightarrow \mathbf{u(p)}$ is physically the same as the transfer $\mathbf{u(p)} \rightarrow \mathbf{u(k)}$. Sum of transfers from $\mathbf{u(q)} \rightarrow \mathbf{u(k)}$ and $\mathbf{u(p)} \rightarrow \mathbf{u(k)}$ is equal to the combined transfer.

There are six equations and six unknowns. However, the value of the determinant formed

from the Eqs. (3.6)-(3.11) is zero. Therefore we cannot find unique $\mathcal{R}^{uu}$'s given just these equations. However, it is reasonable to expect that there is a *definite* amount of energy transfer from one mode to the other mode, say from mode $\mathbf{k}$ to mode $\mathbf{p}$ given $\mathbf{u(k)}$, $\mathbf{u(p)}$, $\mathbf{u(q)}$. Since Eqs. (3.6)-(3.11) do not yield a unique $\mathcal{R}^{uu}$, we need to use constraints based on invariance, symmetries, etc. to get a definite $\mathcal{R}^{uu}$ using Eqs. (3.6)-(3.11).

3.4.2 Solutions of equations of mode-to-mode transfer

One solution of Eqs. (3.6)-(3.11) is

$$\mathcal{S}^{uu}(\mathbf{k}|\mathbf{p}|\mathbf{q}) \equiv -Re\,(i[\mathbf{k}.\mathbf{u}(\mathbf{q})][\mathbf{u}(\mathbf{k}).\mathbf{u}(\mathbf{p})])\,, \tag{3.12}$$

From the definition of $\mathcal{S}^{uu}(\mathbf{k}|\mathbf{p}|\mathbf{q})$, it directly follows that $\mathcal{S}^{uu}$'s satisfy the following conditions.

$$\mathcal{S}^{uu}(\mathbf{k}|\mathbf{p}|\mathbf{q}) + \mathcal{S}^{uu}(\mathbf{k}|\mathbf{q}|\mathbf{p}) = S^{uu}(\mathbf{k}|\mathbf{p}.\mathbf{q}), \tag{3.13}$$

$$\mathcal{S}^{uu}(\mathbf{p}|\mathbf{k}|\mathbf{q}) + \mathcal{S}^{uu}(\mathbf{p}|\mathbf{q}|\mathbf{k}) = S^{uu}(\mathbf{p}|\mathbf{k}.\mathbf{q}), \tag{3.14}$$

$$\mathcal{S}^{uu}(\mathbf{q}|\mathbf{k}|\mathbf{p}) + \mathcal{S}^{uu}(\mathbf{q}|\mathbf{p}|\mathbf{k}) = S^{uu}(\mathbf{q}|\mathbf{k}.\mathbf{p}). \tag{3.15}$$

Using the triad relationship $\mathbf{k}+\mathbf{p}+\mathbf{q}=\mathbf{0}$, and the incompressibility constraint $[\mathbf{k}.\mathbf{u}(\mathbf{k})=\mathbf{0}]$, it can be seen that $\mathcal{S}^{uu}$'s, etc. also satisfy the following conditions

$$\mathcal{S}^{uu}(\mathbf{k}|\mathbf{p}|\mathbf{q}) + \mathcal{S}^{uu}(\mathbf{p}|\mathbf{k}|\mathbf{q}) = 0, \tag{3.16}$$

$$\mathcal{S}^{uu}(\mathbf{k}|\mathbf{q}|\mathbf{p}) + \mathcal{S}^{uu}(\mathbf{q}|\mathbf{k}|\mathbf{p}) = 0, \tag{3.17}$$

$$\mathcal{S}^{uu}(\mathbf{p}|\mathbf{q}|\mathbf{k}) + \mathcal{S}^{uu}(\mathbf{q}|\mathbf{p}|\mathbf{k}) = 0. \tag{3.18}$$

Comparing Eqs. (3.13)-(3.18) with Eqs. (3.6)-(3.11), it is clear that the set of $\mathcal{S}^{uu}$'s is *one instance* of the $\mathcal{R}^{uu}$'s, i.e., $\mathcal{R}^{uu}(\mathbf{k}|\mathbf{p}|\mathbf{q}) = \mathcal{S}^{uu}(\mathbf{k}|\mathbf{p}|\mathbf{q})$. However, this is not a unique solution.

If another solution $\mathcal{R}^{uu}(\mathbf{k}|\mathbf{p}|\mathbf{q})$ differs from $\mathcal{S}^{uu}(\mathbf{k}|\mathbf{p}|\mathbf{q})$ by an arbitrary function X_Δ, i.e., $\mathcal{R}^{uu}(\mathbf{k}|\mathbf{p}|\mathbf{q}) = \mathcal{S}^{uu}(\mathbf{k}|\mathbf{p}|\mathbf{q}) + X_\Delta$, then by inspection we can easily see that every possible

solution of Eqs. (3.6)-(3.11) must be of the form

$$\mathcal{R}^{uu}(\mathbf{k}|\mathbf{p}|\mathbf{q}) = \mathcal{S}^{uu}(\mathbf{k}|\mathbf{p}|\mathbf{q}) + X_\Delta \tag{3.19}$$

$$\mathcal{R}^{uu}(\mathbf{k}|\mathbf{q}|\mathbf{p}) = \mathcal{S}^{uu}(\mathbf{k}|\mathbf{q}|\mathbf{p}) - X_\Delta \tag{3.20}$$

$$\mathcal{R}^{uu}(\mathbf{p}|\mathbf{k}|\mathbf{q}) = \mathcal{S}^{uu}(\mathbf{p}|\mathbf{k}|\mathbf{q}) - X_\Delta \tag{3.21}$$

$$\mathcal{R}^{uu}(\mathbf{p}|\mathbf{q}|\mathbf{k}) = \mathcal{S}^{uu}(\mathbf{p}|\mathbf{q}|\mathbf{k}) + X_\Delta \tag{3.22}$$

$$\mathcal{R}^{uu}(\mathbf{q}|\mathbf{k}|\mathbf{p}) = \mathcal{S}^{uu}(\mathbf{q}|\mathbf{k}|\mathbf{p}) + X_\Delta \tag{3.23}$$

$$\mathcal{R}^{uu}(\mathbf{q}|\mathbf{p}|\mathbf{k}) = \mathcal{S}^{uu}(\mathbf{q}|\mathbf{p}|\mathbf{k}) - X_\Delta \tag{3.24}$$

Note that X_Δ can depend upon the wavenumber triad $\mathbf{k}$, $\mathbf{p}$, $\mathbf{q}$, and the Fourier components $\mathbf{u}(\mathbf{k})$, $\mathbf{u}(\mathbf{p})$, $\mathbf{u}(\mathbf{q})$. X_Δ needs to be determined from other symmetry and invariance arguments to uniquely fix $\mathcal{R}^{uu}$.

In Appendix A we have attempted to determine X_Δ. We construct X_Δ by observing that it can depend on $\mathbf{k}$, $\mathbf{p}$, $\mathbf{q}$, $\mathbf{u}(\mathbf{k})$, $\mathbf{u}(\mathbf{p})$, $\mathbf{u}(\mathbf{q})$; and it must satisfy rotational invariance, galilean invariance, and it should be finite. In our procedure we write down a general scalar function of $\mathbf{k}$, $\mathbf{p}$, $\mathbf{q}$, $\mathbf{u}(\mathbf{k})$, $\mathbf{u}(\mathbf{p})$, and $\mathbf{u}(\mathbf{q})$ with undetermined coefficients. The coefficients can be written as a series in the scalars of the type $\mathbf{k}.\mathbf{p}$, $\mathbf{k}.\mathbf{u}(\mathbf{p})$, $\mathbf{u}(\mathbf{k}).\mathbf{u}(\mathbf{p})$ with unknown constants. By imposing invariance,and finiteness constraints we have shown that, upto the linear order in these scalars, the coefficients must vanish, giving $X_\Delta = 0$. Unfortunately, we have not been able to determine the higher order coefficients. Hence, from the analysis of Appendix A we cannot show for definite that X_Δ will vanish. However, we believe that X_Δ is equal to zero. When $X_\Delta = 0$, we get a simple relationship,

$$\mathcal{R}^{uu} = \mathcal{S}^{uu}, \tag{3.25}$$

giving the energy transfer between a pair of modes in a triad with the third mode mediating

the transfer, as simply $\mathcal{S}^{uu}$. But if $X_\Delta \neq 0$ then the energy transfer picture is more complex and the energy transfer between a pair of modes will be given by Eqs. (3.19)-(3.24) where X_Δ is unknown.

We will now give a physical interpretation to the two parts of $\mathcal{T}^{uu}$'s, i.e., $\mathcal{S}^{uu}$'s and X_Δ. We see from Fig. 3.4 that $\mathcal{S}^{uu}(\mathbf{k}|\mathbf{p}|\mathbf{q}) + X_\Delta$ gets transferred from $\mathbf{p}$ to $\mathbf{k}$, $\mathcal{S}^{uu}(\mathbf{q}|\mathbf{k}|\mathbf{p}) + X_\Delta$

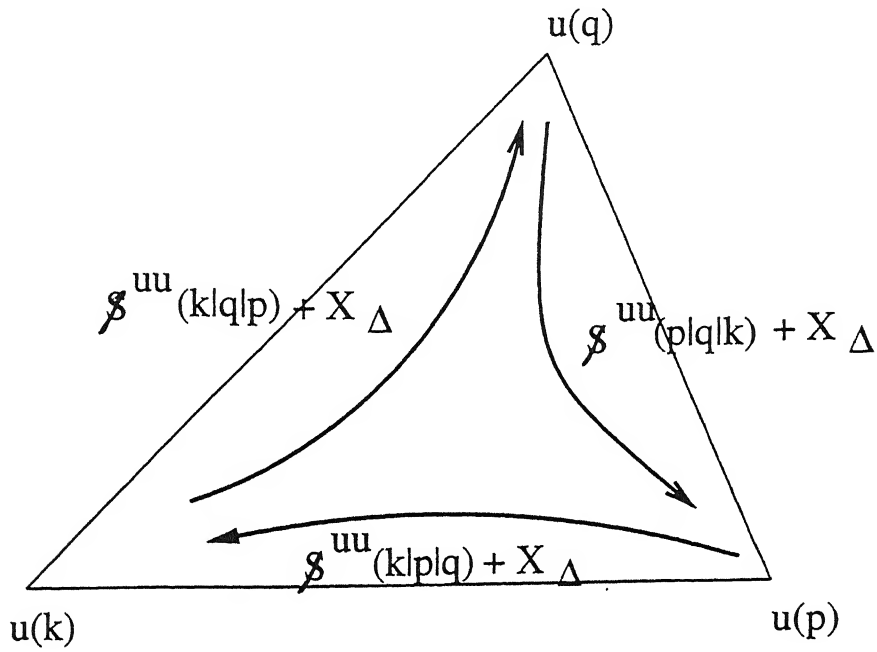

Figure 3.4: Mode-to-mode transfer can be expressed as a sum of circulating transfer and effective mode-to-mode transfer.

gets transferred from $\mathbf{k}$ to $\mathbf{q}$, $\mathcal{S}^{uu}(\mathbf{p}|\mathbf{q}|\mathbf{k}) + X_\Delta$ gets transferred from $\mathbf{q}$ to $\mathbf{p}$. The quantity X_Δ flows along $\mathbf{p} \to \mathbf{k} \to \mathbf{q} \to \mathbf{p}$, circulating around the entire triad without changing the energy of any of the modes. Therefore we will call it the *Circulating transfer*. Of the total energy transfer between two modes, $\mathcal{S}^{uu} + X_\Delta$, only $\mathcal{S}^{uu}$ can bring about a change in modal energy. X_Δ transferred from mode $\mathbf{p}$ to mode $\mathbf{k}$ is transferred back to mode $\mathbf{p}$ via mode $\mathbf{q}$, i.e. the mode $\mathbf{p}$ transfers X_Δ *directly* to mode $\mathbf{k}$, and mode $\mathbf{p}$ transfers X_Δ back to $\mathbf{k}$ *indirectly* through mode $\mathbf{q}$. Thus the energy that is effectively transferred from mode $\mathbf{p}$ to mode $\mathbf{k}$ is just $\mathcal{S}^{uu}(\mathbf{k}|\mathbf{p}|\mathbf{q})$. Therefore $\mathcal{S}^{uu}(\mathbf{k}|\mathbf{p}|\mathbf{q})$ can be be termed as the "*effective mode-to-mode transfer*" from mode $\mathbf{p}$ to mode $\mathbf{k}$.

In summary, we have attempted to obtain an expression for the energy transfer rate $\mathcal{R}^{uu}$ between two modes in a triad. To leading order in a series expansion we can show that $\mathcal{R}^{uu} = \mathcal{S}^{uu}$. But the ambiguity in $\mathcal{R}^{uu}$ remains because of the lack of a complete proof. However, the important conclusion is that the mode-to-mode energy transfer can be expressed as $\mathcal{R}^{uu} = \mathcal{S}^{uu} + X_\Delta$ where $\mathcal{S}^{uu}$ is the 'effective mode-to-mode transfer' and X_Δ is the 'circulating transfer'. In the next section we will further develop the notion of effective transfers by applying it to energy transfer between shells.

3.5 Shell-to-Shell energy transfer and Cascade rates using "mode-to-mode" formalism

In Section 3.3 we had pointed out the problem in treating the expression in Eq. (3.5) as the shell-to-shell transfer. This expression, commonly taken to be the shell-to-shell transfer, actually gives the energy transferred to shell m from both shell n and the modes $\mathbf{q}$. In this section we will make use of the idea of "circulating" and "effective mode-to-mode transfer" (see Fig. 3.4) to redefine shell-to-shell transfer.

Consider energy transfer between shells m and n in the figure below. The mode $\mathbf{k}$ is in shell m, the mode $\mathbf{p}$ is in shell n, and $\mathbf{q}$ could be inside or outside the shells. In terms of the mode-to-mode transfer $\mathcal{R}^{uu}(\mathbf{k}|\mathbf{p}|\mathbf{q})$ from mode $\mathbf{p}$ to mode $\mathbf{k}$, the energy transfer from shell n to shell m can be defined as

$$T^{uu}_{mn} = \sum_{\mathbf{k}\in m} \sum_{\mathbf{p}\in n} \mathcal{R}^{uu}(\mathbf{k}|\mathbf{p}|\mathbf{q}) \tag{3.26}$$

where the $\mathbf{k}$-sum is over shell m, $\mathbf{p}$-sum is over shell n, and $\mathbf{k}+\mathbf{p}+\mathbf{q}=\mathbf{0}$. The quantity $\mathcal{R}^{uu}$ can be written as a sum of an effective transfer $\mathcal{S}^{uu}(\mathbf{k}|\mathbf{p}|\mathbf{q})$ and a circulating transfer X_Δ. We know from the last section that the circulating transfer does not contribute to the energy change of modes. From Fig. 3.5 we can see that X_Δ flows from shell m to shell n and then flows back to m indirectly through the mode $\mathbf{q}$. Therefore the effective energy transfer from

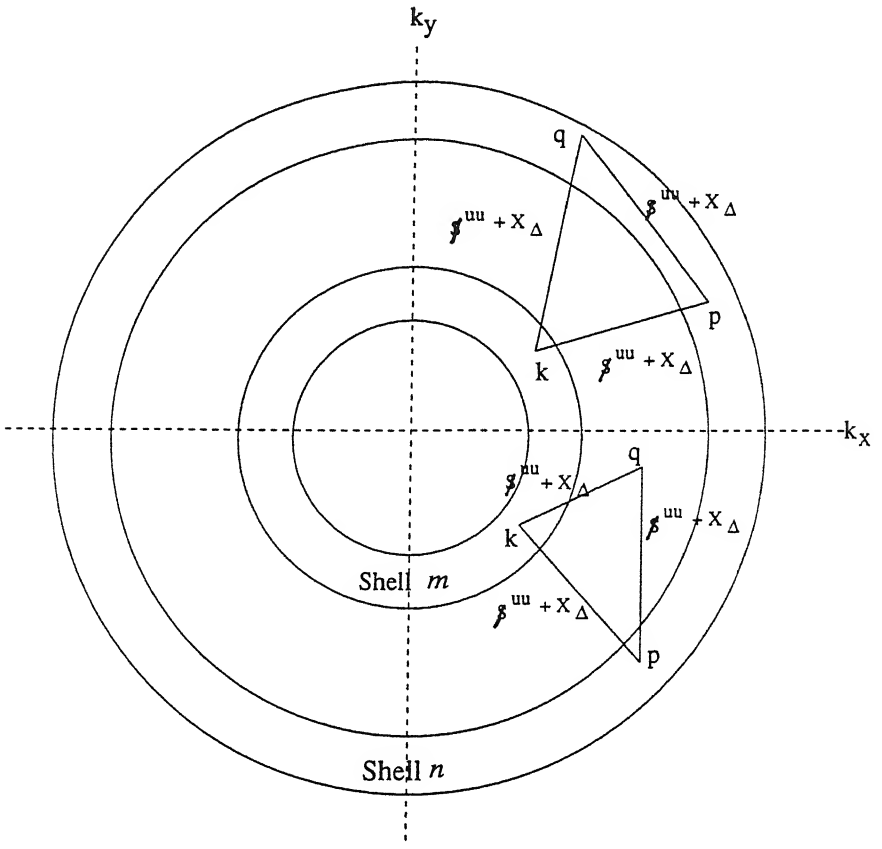

Figure 3.5: The circulating transfer and mode-to-mode transfer from shell n to shell m with the arrows pointing towards the direction of energy transfer.

shell m to shell n is just $\mathcal{S}^{uu}(\mathbf{k}|\mathbf{p}|\mathbf{q})$ summed over all $\mathbf{k}$ in shell m and all $\mathbf{p}$ in shell n, i.e.,

$$T^{uu}_{mn} = \sum_{\mathbf{k}\epsilon m}\sum_{\mathbf{p}\epsilon n}\mathcal{S}^{uu}(\mathbf{k}|\mathbf{p}|\mathbf{q}), \tag{3.27}$$

where $\mathcal{S}^{uu}(\mathbf{k}|\mathbf{p}|\mathbf{q})$ is the effective mode-to-mode transfer.

If $X_\Delta = 0$ then the effective transfer between two shells given by this equation will be the same as the same as the total energy transfer between them given by Eq. (3.26). However, if X_Δ is non-zero then the two are not equal. The effective shell-to-shell transfer [Eq. (3.27)] differs from the total transfer [Eq. (3.26)] by the contribution of the circulating transfer. We have argued earlier that the circulating transfer does not result in the energy change of any of the modes. Hence, from the physical point of view the effective shell-to-shell transfer is a very relevant quantity to study. In the next chapter we have studied the effective shell-to-shell

transfers in numerical simulations.

3.5.1 Energy cascade rates

The kinetic energy cascade rate (Π) (or flux) in fluid turbulence is defined as the rate of loss of kinetic energy by a sphere in k-space to the modes outside. In literature, the energy flux in fluid turbulence has been computed using $S^{uu}(\mathbf{k}|\mathbf{p},\mathbf{q})$ [35, 95]. Kraichnan [95] shows that by direct integration of Eq. (3.2) that the kinetic energy lost from a sphere of radius K by nonlinear convective transfers is

$$\Pi(K) = -\sum_{|\mathbf{k}|<K}\sum_{|\mathbf{p}|>K}\frac{1}{2}S^{uu}(\mathbf{k}|\mathbf{p},\mathbf{q}). \tag{3.28}$$

Although the energy cascade rate in fluid turbulence can be found by the above formula, the mode-to-mode approach provides a more natural way of looking at the energy transfers. In later sections we will obtain expressions for mode-to-mode transfer in MHD turbulence and define various fluxes which are not accessible to the conventional approach

Here, we will obtain an expression for the flux in terms of the effective mode-to-mode energy transfer. Since $\mathcal{R}^{uu}(\mathbf{k}|\mathbf{p}|\mathbf{q})$ represents energy transfer from $\mathbf{p}$ to $\mathbf{k}$ with $\mathbf{q}$ as the mediator, we may alternatively write the energy loss from a sphere as

$$\Pi(K) = -\sum_{|\mathbf{k}|<K}\sum_{|\mathbf{p}|>K}\mathcal{R}^{uu}(\mathbf{k}|\mathbf{p}|\mathbf{q}). \tag{3.29}$$

where mode $\mathbf{k}$ is inside the sphere, $\mathbf{p}$ is outside the sphere, and $\mathbf{q} = -\mathbf{k} - \mathbf{p}$. The mode-to-mode transfer $\mathcal{R}^{uu}(\mathbf{k}|\mathbf{p}|\mathbf{q})$ consists of a circulating part and an effective part. From Fig. 3.6 we see that the net amount of circulating transfer leaving the sphere is zero. Thus the circulating transfer makes no contribution to the the energy flux from the sphere. Therefore, it can be removed from Eq. (3.29). Hence, the resultant expression for the flux can be written as

$$\Pi(K) = -\sum_{|\mathbf{k}|<K}\sum_{|\mathbf{p}|>K}\mathcal{S}^{uu}(\mathbf{k}|\mathbf{p}|\mathbf{q}). \tag{3.30}$$

with a summation over the effective mode-to-mode transfer. As expected, the expressions in

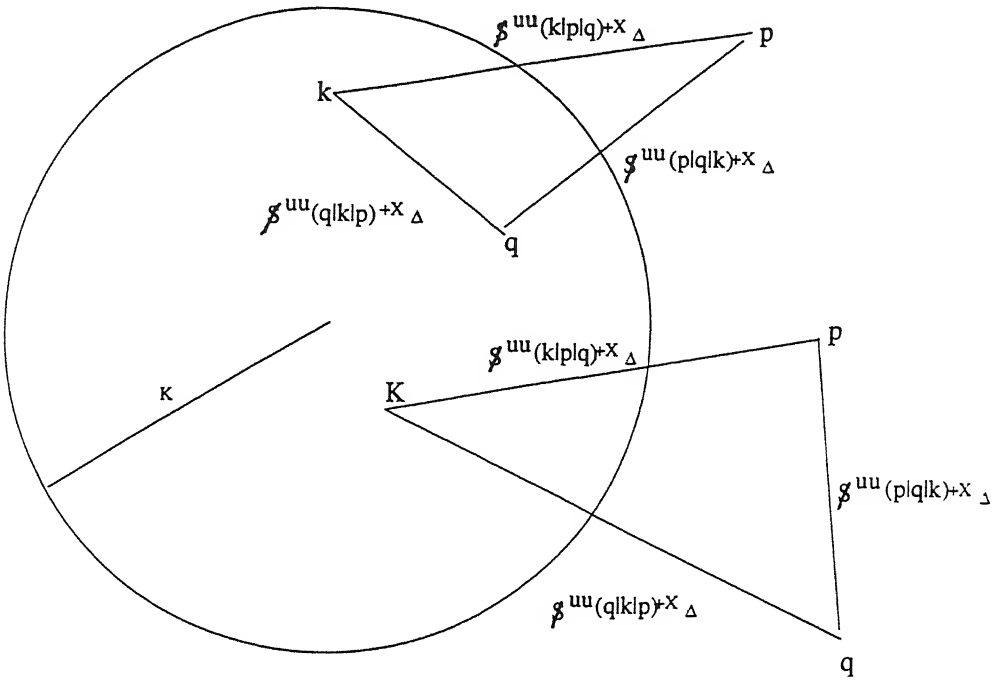

Figure 3.6: The circulating transfer X_Δ does not contribute to the energy flux out of the sphere K.

Eqs. (3.28) and (3.30) are equivalent as proved in Appendix B.

3.6 Energy transfer in a MHD triad: known results

The MHD equations in real space are written as

$$\frac{\partial \mathbf{u}}{\partial t} + (\mathbf{u}.\nabla)\mathbf{u} = -\nabla p + (\mathbf{b}.\nabla)\mathbf{b} + \nu\nabla^2\mathbf{u}, \tag{3.31}$$

and

$$\frac{\partial \mathbf{b}}{\partial t} + (\mathbf{u}.\nabla)\mathbf{b} = (\mathbf{b}.\nabla)\mathbf{u} + \mu\nabla^2\mathbf{b}, \tag{3.32}$$

where $\mathbf{u}$ and $\mathbf{b}$ are the velocity and magnetic fields respectively, and ν and μ are the fluid kinematic viscosity and magnetic diffusivity, respectively. In Fourier space, the kinetic energy and magnetic energy evolution equations for a Fourier mode are

$$\frac{\partial E^u(\mathbf{k})}{\partial t} + 2\nu k^2 E^u(\mathbf{k}) = \sum_{\mathbf{k}+\mathbf{p}+\mathbf{q}=0} \frac{1}{2} S^{uu}(\mathbf{k}|\mathbf{p},\mathbf{q}) + \sum_{\mathbf{k}+\mathbf{p}+\mathbf{q}=0} \frac{1}{2} S^{ub}(\mathbf{k}|\mathbf{p},\mathbf{q}), \tag{3.33}$$

$$\frac{\partial E^b(\mathbf{k})}{\partial t} + 2\mu k^2 E^b(\mathbf{k}) = \sum_{\mathbf{k}+\mathbf{p}+\mathbf{q}=0} \frac{1}{2} S^{bb}(\mathbf{k}|\mathbf{p},\mathbf{q}) + \sum_{\mathbf{k}+\mathbf{p}+\mathbf{q}=0} \frac{1}{2} S^{bu}(\mathbf{k}|\mathbf{p},\mathbf{q}), \tag{3.34}$$

where $E^u(\mathbf{k}) = |\mathbf{u}(\mathbf{k})|^2/2$ is the kinetic energy, and $E^b(\mathbf{k}) = |\mathbf{b}(\mathbf{k})|^2/2$ is the magnetic energy. The four nonlinear terms $S^{uu}(\mathbf{k}|\mathbf{p},\mathbf{q})$, $S^{ub}(\mathbf{k}|\mathbf{p},\mathbf{q})$ $S^{bb}(\mathbf{k}|\mathbf{p},\mathbf{q})$ and $S^{bu}(\mathbf{k}|\mathbf{p},\mathbf{q})$ are

$$S^{uu}(\mathbf{k}|\mathbf{p},\mathbf{q}) \equiv -Re\,(i[\mathbf{k}.\mathbf{u}(\mathbf{q})][\mathbf{u}(\mathbf{k}).\mathbf{u}(\mathbf{p})] + i[\mathbf{k}.\mathbf{u}(\mathbf{p})][\mathbf{u}(\mathbf{k}).\mathbf{u}(\mathbf{q})]), \tag{3.35}$$

$$S^{bb}(\mathbf{k}|\mathbf{p},\mathbf{q}) \equiv -Re\,(i[\mathbf{k}.\mathbf{u}(\mathbf{q})][\mathbf{b}(\mathbf{k}).\mathbf{b}(\mathbf{p})] + i[\mathbf{k}.\mathbf{u}(\mathbf{p})][\mathbf{b}(\mathbf{k}).\mathbf{b}(\mathbf{q})]), \tag{3.36}$$

$$S^{ub}(\mathbf{k}|\mathbf{p},\mathbf{q}) \equiv Re\,(i[\mathbf{k}.\mathbf{b}(\mathbf{q})][\mathbf{u}(\mathbf{k}).\mathbf{b}(\mathbf{p})] + i[\mathbf{k}.\mathbf{b}(\mathbf{p})][\mathbf{u}(\mathbf{k}).\mathbf{b}(\mathbf{q})]), \tag{3.37}$$

$$S^{bu}(\mathbf{k}|\mathbf{p},\mathbf{q}) \equiv Re\,(i[\mathbf{k}.\mathbf{b}(\mathbf{q})][\mathbf{b}(\mathbf{k}).\mathbf{u}(\mathbf{p})] + i[\mathbf{k}.\mathbf{b}(\mathbf{p})][\mathbf{b}(\mathbf{k}).\mathbf{u}(\mathbf{q})]), \tag{3.38}$$

These terms are conventionally taken to represent the nonlinear transfer from modes $\mathbf{p}$ and $\mathbf{q}$ to mode $\mathbf{k}$ [36, 44]. Note that the wavenumber triad $\mathbf{k}$, $\mathbf{p}$, and $\mathbf{q}$ should satisfy the condition $\mathbf{k}+\mathbf{p}+\mathbf{q}=0$. The term $S^{uu}(\mathbf{k}|\mathbf{p},\mathbf{q})$ represents the net transfer of kinetic energy from modes $\mathbf{p}$ and $\mathbf{q}$ to mode $\mathbf{k}$. Likewise the term $S^{ub}(\mathbf{k}|\mathbf{p},\mathbf{q})$ is the net magnetic energy transferred from modes $\mathbf{p}$ and $\mathbf{q}$ to the kinetic energy in mode $\mathbf{k}$, whereas $S^{bu}(\mathbf{k}|\mathbf{p},\mathbf{q})$ is the net kinetic energy transferred from modes $\mathbf{p}$ and $\mathbf{q}$ to the magnetic energy in mode $\mathbf{k}$. The term $S^{bb}(\mathbf{k}|\mathbf{p},\mathbf{q})$ represents the transfer of magnetic energy from modes $\mathbf{p}$ and $\mathbf{q}$ to mode $\mathbf{k}$. All these transfer terms are represented in the Fig. 3.7 shown below.

Stanisic [36] showed that the nonlinear terms satisfy the following detailed conservation properties:

$$S^{uu}(\mathbf{k}|\mathbf{p},\mathbf{q}) + S^{uu}(\mathbf{p}|\mathbf{k},\mathbf{q}) + S^{uu}(\mathbf{q}|\mathbf{k},\mathbf{p}) = 0, \tag{3.39}$$

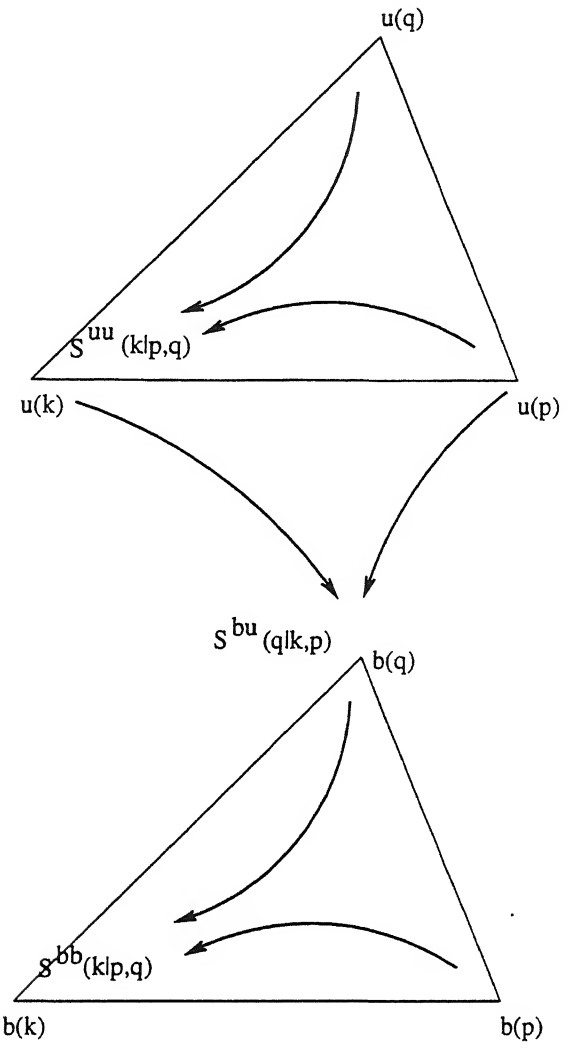

Figure 3.7: The combined energy transfers in a triad. $S^{uu}(\mathbf{k}|\mathbf{p},\mathbf{q})$: $\mathbf{u}(\mathbf{p})$ and $\mathbf{u}(\mathbf{q}) \rightarrow \mathbf{u}(\mathbf{k})$: $S^{bu}(\mathbf{q}|\mathbf{k},\mathbf{p})$: $\mathbf{u}(\mathbf{k})$ and $\mathbf{u}(\mathbf{p}) \rightarrow \mathbf{b}(\mathbf{q})$; $S^{bb}(\mathbf{k}|\mathbf{p},\mathbf{q})$: $\mathbf{b}(\mathbf{p})$ and $\mathbf{b}(\mathbf{q}) \rightarrow \mathbf{b}(\mathbf{k})$.

$$S^{bb}(\mathbf{k}|\mathbf{p},\mathbf{q}) + S^{bb}(\mathbf{p}|\mathbf{k},\mathbf{q}) + S^{bb}(\mathbf{q}|\mathbf{k},\mathbf{p}) = 0, \tag{3.40}$$

and

$$S^{ub}(\mathbf{k}|\mathbf{p},\mathbf{q}) + S^{ub}(\mathbf{p}|\mathbf{k},\mathbf{q}) + S^{ub}(\mathbf{q}|\mathbf{k},\mathbf{p}) + S^{bu}(\mathbf{k}|\mathbf{p},\mathbf{q}) + S^{bu}(\mathbf{p}|\mathbf{k},\mathbf{q}) + S^{bu}(\mathbf{q}|\mathbf{k},\mathbf{p}) = 0. \tag{3.41}$$

The Eq. (3.39) implies that kinetic energy is transferred conservatively between the velocity modes of a wavenumber triad, and the Eq. (3.40) implies that magnetic energy is also trans-

ferred conservatively between the magnetic modes of a wavenumber triad. The Eq. (3.41) implies that the cross transfers of kinetic and magnetic energy, $S^{ub}(\mathbf{k}|\mathbf{p},\mathbf{q})$ and $S^{bu}(\mathbf{k}|\mathbf{p},\mathbf{q})$, within a triad are also energy conserving.

The quantities $S^{uu}(\mathbf{k}|\mathbf{p},\mathbf{q})$, $S^{ub}(\mathbf{k}|\mathbf{p},\mathbf{q})$, $S^{bb}(\mathbf{k}|\mathbf{p},\mathbf{q})$, and $S^{bu}(\mathbf{k}|\mathbf{p},\mathbf{q})$ represent the nonlinear energy transfer from the *two modes* $\mathbf{p}$ and $\mathbf{q}$ to mode $\mathbf{k}$. It would be useful to know the energy transfer between *any two modes*, say from $\mathbf{p}$ to $\mathbf{k}$. This issue will be explored in the next section.

3.7 "Mode-to-Mode" energy transfers in MHD Equations

In Section 3.4 we had presented a new approach to describe the energy transfer between two modes of a triad with the help of the third mode, in the Navier-Stokes equation. In the same spirit we will now attempt to find the mode-to-mode energy transfers in MHD. In MHD turbulence there will be three kinds of mode-to-mode transfer within a wavenumber triad $\mathbf{k}$, $\mathbf{p}$, $\mathbf{q}$: kinetic energy transfer from $\mathbf{u}(\mathbf{p})$ to $\mathbf{u}(\mathbf{k})$; magnetic energy transfer from $\mathbf{b}(\mathbf{p})$ to $\mathbf{b}(\mathbf{k})$; and transfer of kinetic energy from $\mathbf{u}(\mathbf{p})$ to magnetic energy in $\mathbf{b}(\mathbf{k})$. We denote these three transfers by $\mathcal{R}^{uu}(\mathbf{k}|\mathbf{p}|\mathbf{q})$, $\mathcal{R}^{bb}(\mathbf{k}|\mathbf{p}|\mathbf{q})$, and $\mathcal{R}^{bu}(\mathbf{k}|\mathbf{p}|\mathbf{q})$ respectively, where the index $\mathbf{q}$ indicates that the energy transfer between modes $\mathbf{p}$ and $\mathbf{k}$ is mediated by the mode $\mathbf{q}$. Since the nonlinear interactions fundamentally involve three-modes, the energy transfer between a pair of modes should depend on the third mode. The mode-to-mode transfers $\mathcal{R}^{uu}$, $\mathcal{R}^{bb}$, and $\mathcal{R}^{bu}$ are schematically illustrated in the figure below.

In this section we will obtain a description for each of these transfers.

3.7.1 Velocity mode to velocity mode energy transfers

In Section 3.4 we discussed the mode-to-mode transfer, R^{uu}, between velocity mode to velocity mode in fluid flows. In this section we will find R^{uu} for MHD flows. The transfer of kinetic energy between the velocity modes is brought about by the term $(\mathbf{u}.\nabla)\mathbf{u}$ both in

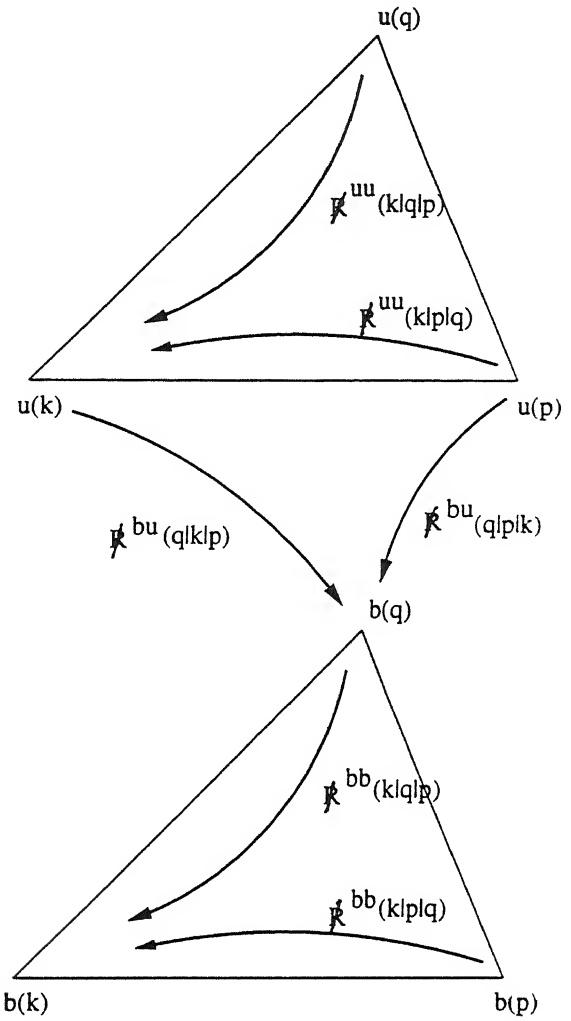

Figure 3.8: The mode-to-mode energy transfers sought to be determined.

the Navier Stokes equation and MHD equations. Hence, the expression for the combined kinetic energy transfer to a mode from the other two modes of the triad is also same for the two. i.e., the combined transfer to $\mathbf{u(k)}$ from $\mathbf{u(p)}$ and $\mathbf{u(q)}$ is given by $S^{uu}(\mathbf{k}|\mathbf{p},\mathbf{q})$ [see Eq. (3.3) and Eq. (3.35)]. Consequently, R^{uu} 's for MHD will satisfy the constraints given in Eqs. (3.6)-(3.11) for the corresponding R^{uu} 's for fluids. As a result. $R^{uu}(\mathbf{k}|\mathbf{p},\mathbf{q})$ in MHD can be expressed as a sum of a circulating transfer X_Δ and the effective transfer $\mathcal{S}^{uu}(\mathbf{k}|\mathbf{p}|\mathbf{q})$ given by Eq. (3.12), i.e.,

$$\mathcal{R}^{uu}(\mathbf{k}|\mathbf{p}|\mathbf{q}) = \mathcal{S}^{uu}(\mathbf{k}|\mathbf{p}|\mathbf{q}) + X_\Delta \tag{3.42}$$

A detailed discussion can be found in the earlier Section 3.4.2.

3.7.2 Magnetic mode to Magnetic mode energy transfers

This section contains a discussion on the magnetic energy transfer from mode b(p) to b(k) in the triad (k,p,q) [see Fig. 3.8]. This transfer which is denoted by $\mathcal{R}^{bb}$ k p q , which should satisfy the following relationships (refer to Fig. 3.9 for a pictorial description of these relationships):

1. The sum of the mode-to-mode energy transfers from b(p) to b(k) and from b(q) to b(k) should be equal to $S^{bb}(\mathbf{k}|\mathbf{p},\mathbf{q})$ [Eq. (3.36) in Section 3.6], which is the combined energy transfer to b(k) from b(p) and b(q). Thus,

$$\mathcal{R}^{bb}(\mathbf{k}|\mathbf{p}|\mathbf{q}) + \mathcal{R}^{bb}(\mathbf{k}|\mathbf{q}|\mathbf{p}) = S^{bb}(\mathbf{k}|\mathbf{p},\mathbf{q}), \tag{3.43}$$

$$\mathcal{R}^{bb}(\mathbf{p}|\mathbf{k}|\mathbf{q}) + \mathcal{R}^{bb}(\mathbf{p}|\mathbf{q}|\mathbf{k}) = S^{bb}(\mathbf{p}|\mathbf{k},\mathbf{q}), \tag{3.44}$$

$$\mathcal{R}^{bb}(\mathbf{q}|\mathbf{k}|\mathbf{p}) + \mathcal{R}^{bb}(\mathbf{q}|\mathbf{p}|\mathbf{k}) = S^{bb}(\mathbf{q}|\mathbf{k},\mathbf{p}), \tag{3.45}$$

and

2. the energy transfer from b(k) to b(p), $\mathcal{R}^{bb}(\mathbf{k}|\mathbf{p}|\mathbf{q})$, and the transfer from b(p) to b(k), $\mathcal{R}^{bb}(\mathbf{p}|\mathbf{k}|\mathbf{q})$, should be equal but opposite in sign.

$$\mathcal{R}^{bb}(\mathbf{k}|\mathbf{p}|\mathbf{q}) + \mathcal{R}^{bb}(\mathbf{p}|\mathbf{k}|\mathbf{q}) = 0, \tag{3.46}$$

$$\mathcal{R}^{bb}(\mathbf{k}|\mathbf{q}|\mathbf{p}) + \mathcal{R}^{bb}(\mathbf{q}|\mathbf{k}|\mathbf{p}) = 0, \tag{3.47}$$

$$\mathcal{R}^{bb}(\mathbf{p}|\mathbf{q}|\mathbf{k}) + \mathcal{R}^{bb}(\mathbf{q}|\mathbf{p}|\mathbf{k}) = 0. \tag{3.48}$$

The above equations cannot uniquely determine $\mathcal{R}^{bb}(\mathbf{k}|\mathbf{p}|\mathbf{q})$ since the value of the determinant formed from these equations is zero. While discussing the mode-to-mode energy transfers in Navier Stokes equation in Section 3.4 we got the same result for $\mathcal{R}^{uu}(\mathbf{k}|\mathbf{p}|\mathbf{q})$.

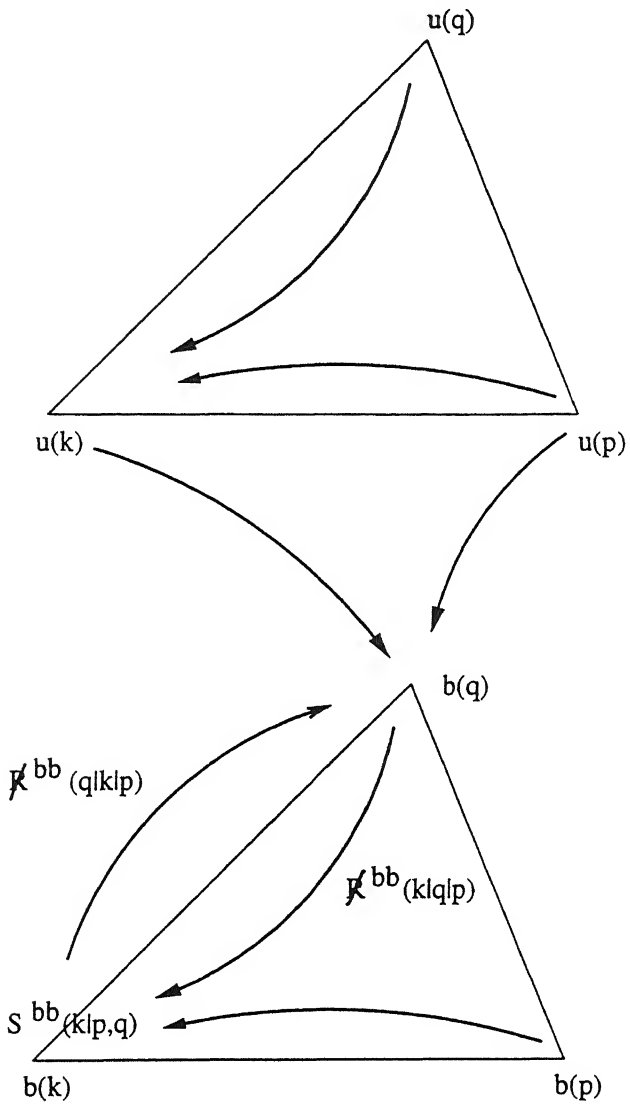

Figure 3.9: Relationship between the $\mathcal{R}^{bb}$'s. Transfer $\mathbf{b(k)} \rightarrow \mathbf{b(p)}$ is equal and opposite to the transfer $\mathbf{b(p)} \rightarrow \mathbf{b(k)}$ since both are physically the same. Sum of transfers from $\mathbf{b(q)} \rightarrow \mathbf{b(k)}$ and $\mathbf{b(p)} \rightarrow \mathbf{b(k)}$ is equal to the combined transfer.

Following the reasoning in that section, we can extract physically meaningful information from Eqs. (3.43)-(3.48).

The combined energy transfer to $\mathbf{b(k)}$ from $\mathbf{b(p)}$ and $\mathbf{b(q)}$ is given by Eq. (3.36) of Section 3.6. We denote the first term on the right hand side of that equation by $\mathcal{S}^{bb}(\mathbf{k}|\mathbf{p}|\mathbf{q})$, i.e.,

$$\mathcal{S}^{bb}(\mathbf{k}|\mathbf{p}|\mathbf{q}) \equiv -Re\,(i[\mathbf{k}.\mathbf{u}(\mathbf{q})][\mathbf{b}(\mathbf{k}).\mathbf{b}(\mathbf{p})])\,, \tag{3.49}$$

By replacing $\mathcal{S}^{bb}(\mathbf{k}|\mathbf{p}|\mathbf{q})$ for $\mathcal{R}^{bb}(\mathbf{k}|\mathbf{p}|\mathbf{q})$ in Eqs. (3.43)-(3.48) we find that $\mathcal{S}^{bb}(\mathbf{k}|\mathbf{p}|\mathbf{q})$ is a solution of these equations, i.e.,

$$\mathcal{S}^{bb}(\mathbf{k}|\mathbf{p}|\mathbf{q}) + \mathcal{S}^{bb}(\mathbf{k}|\mathbf{q}|\mathbf{p}) = S^{bb}(\mathbf{k}|\mathbf{p},\mathbf{q}), \tag{3.50}$$

$$\mathcal{S}^{bb}(\mathbf{p}|\mathbf{k}|\mathbf{q}) + \mathcal{S}^{bb}(\mathbf{p}|\mathbf{q}|\mathbf{k}) = S^{bb}(\mathbf{p}|\mathbf{k},\mathbf{q}), \tag{3.51}$$

$$\mathcal{S}^{bb}(\mathbf{q}|\mathbf{k}|\mathbf{p}) + \mathcal{S}^{bb}(\mathbf{q}|\mathbf{p}|\mathbf{k}) = S^{bb}(\mathbf{q}|\mathbf{k},\mathbf{p}), \tag{3.52}$$

and

$$\mathcal{S}^{bb}(\mathbf{k}|\mathbf{p}|\mathbf{q}) + \mathcal{S}^{bb}(\mathbf{p}|\mathbf{k}|\mathbf{q}) = 0, \tag{3.53}$$

$$\mathcal{S}^{bb}(\mathbf{k}|\mathbf{q}|\mathbf{p}) + \mathcal{S}^{bb}(\mathbf{q}|\mathbf{k}|\mathbf{p}) = 0, \tag{3.54}$$

$$\mathcal{S}^{bb}(\mathbf{p}|\mathbf{q}|\mathbf{k}) + \mathcal{S}^{bb}(\mathbf{q}|\mathbf{p}|\mathbf{k}) = 0. \tag{3.55}$$

Thus, $\mathcal{S}^{bb}(\mathbf{k}|\mathbf{p}|\mathbf{q})$ is a solution of the equations (3.43)- (3.48). By inspection it can be seen that *all* solutions of the equations can be expressed as

$$\mathcal{R}^{bb}(\mathbf{k}|\mathbf{p}|\mathbf{q}) = \mathcal{S}^{bb}(\mathbf{k}|\mathbf{p}|\mathbf{q}) + Y_\Delta, \tag{3.56}$$

$$\mathcal{R}^{bb}(\mathbf{k}|\mathbf{q}|\mathbf{p}) = \mathcal{S}^{bb}(\mathbf{k}|\mathbf{q}|\mathbf{p}) - Y_\Delta, \tag{3.57}$$

$$\mathcal{R}^{bb}(\mathbf{p}|\mathbf{k}|\mathbf{q}) = \mathcal{S}^{bb}(\mathbf{p}|\mathbf{k}|\mathbf{q}) - Y_\Delta, \tag{3.58}$$

$$\mathcal{R}^{bb}(\mathbf{p}|\mathbf{q}|\mathbf{k}) = \mathcal{S}^{bb}(\mathbf{p}|\mathbf{q}|\mathbf{k}) + Y_\Delta, \tag{3.59}$$

$$\mathcal{R}^{bb}(\mathbf{q}|\mathbf{k}|\mathbf{p}) = \mathcal{S}^{bb}(\mathbf{q}|\mathbf{k}|\mathbf{p}) + Y_\Delta, \tag{3.60}$$

$$\mathcal{R}^{bb}(\mathbf{q}|\mathbf{p}|\mathbf{k}) = \mathcal{S}^{bb}(\mathbf{q}|\mathbf{p}|\mathbf{k}) - Y_\Delta, \tag{3.61}$$

where Y_Δ is an arbitrary scalar function dependent on the wavenumber triad $\mathbf{k}$, $\mathbf{p}$, $\mathbf{q}$ and the Fourier components $\mathbf{u}(\mathbf{k})$, $\mathbf{u}(\mathbf{p})$, $\mathbf{u}(\mathbf{q})$, $\mathbf{b}(\mathbf{k})$, $\mathbf{b}(\mathbf{p})$, $\mathbf{b}(\mathbf{q})$ at those wavenumbers. To

determine the unique form of this function we need to impose additional constraints, similar to those used in Appendix A for determining a similar function of mode-to-mode energy transfer between velocity modes in fluid turbulence (see Section 3.4.2). We will impose symmetry, invariance, and some other constraints to determine Y_Δ (see Appendix B for derivation). The exact form of Y_Δ is however not crucial to our formalism.

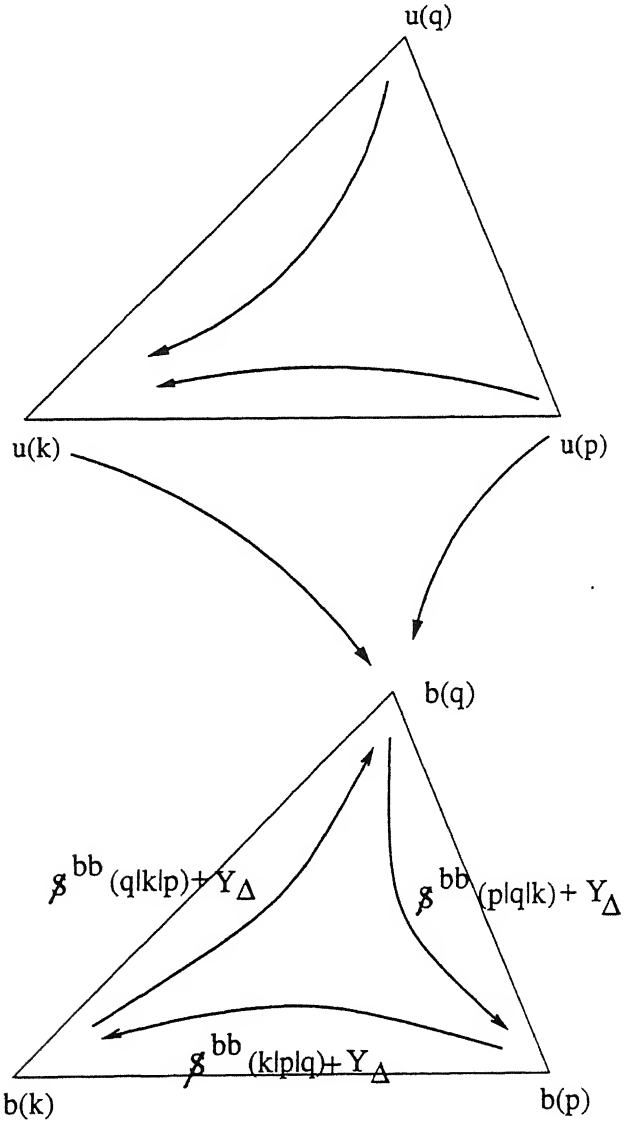

Figure 3.10: Energy transfer between a pair of magnetic modes in a triad can be expressed as a sum of circulating transfer and effective mode-to-mode transfer.

The solutions in Eqs. (3.56)-(3.61) have been schematically illustrated in Fig. 3.10. We see from the figure that Y_Δ is transferred from $\mathbf{b(p)} \rightarrow \mathbf{b(k)} \rightarrow \mathbf{b(q)}$ and back to $\mathbf{b(p)}$, i.e., it circulates around the triad without causing any change in modal energy — it is a thus a circulating transfer. The magnetic energy *effectively* transferred from $\mathbf{b(p)}$ to $\mathbf{b(k)}$ is just $\mathcal{S}^{bb}(\mathbf{k|p|q})$[1],i.e.,

$$\mathcal{R}^{bb}_{eff}(\mathbf{k|p|q}) = \mathcal{S}^{bb}(\mathbf{k|p|q}). \tag{3.62}$$

The effective mode-to-mode transfer $\mathcal{S}^{bb}(\mathbf{k|p|q})$ from $\mathbf{b(p)}$ to $\mathbf{b(k)}$ is mediated by the *sloshy mode* $\mathbf{u(q)}$.

In the next section we will use $\mathcal{R}^{bb}_{eff}$ to calculate effective energy transfer rate between the magnetic modes inside two shells and the effective cascade rate of magnetic energy.

3.7.3 Velocity mode to Magnetic mode energy transfers

In Section 3.7.1 and Section 3.7.2 we discussed mode-to-mode energy transfer between a pair of velocity modes and between a pair of magnetic modes in a wavenumber triad, respectively. In the same spirit, this section is devoted to finding the energy transfer between the $\mathbf{u(p)}$ and $\mathbf{b(k)}$, $\mathcal{R}^{ub}(\mathbf{k|p|q})$, within the triad $(\mathbf{k}, \mathbf{p}, \mathbf{q})$ illustrated in Fig. 3.8. We will follow the same sequence of steps as in the two sections 3.7.1 and 3.7.2.

$\mathcal{R}^{ub}$'s will satisfy the following relationships: (see Fig. 3.11 for an illustration of these relationships):

1. Since $\mathcal{R}^{ub}(\mathbf{k|p|q})$ and $\mathcal{R}^{ub}(\mathbf{k|q|p})$ are the mode-to-mode energy transfers from $\mathbf{b(p)}$ to $\mathbf{u(k)}$ and from $\mathbf{b(q)}$ to $\mathbf{u(k)}$, the sum of the two should be equal to $S^{ub}(\mathbf{k|p,q})$, the combined energy transfer to $\mathbf{u(k)}$ from $\mathbf{b(p)}$ and $\mathbf{b(q)}$. Therefore, we get

$$\mathcal{R}^{ub}(\mathbf{k|p|q}) + \mathcal{R}^{ub}(\mathbf{k|q|p}) = S^{ub}(\mathbf{k|p,q}). \tag{3.63}$$

$$\mathcal{R}^{ub}(\mathbf{p|k|q}) + \mathcal{R}^{ub}(\mathbf{p|q|k}) = S^{ub}(\mathbf{p|k,q}), \tag{3.64}$$

[1]the idea of circulating transfer and effective mode-to-mode transfer in a triad was introduced in Section 3.4.2 — a detailed discussion can be found in that section.

$$\mathcal{R}^{ub}(\mathbf{q}|\mathbf{k}|\mathbf{p}) + \mathcal{R}^{ub}(\mathbf{q}|\mathbf{p}|\mathbf{k}) = S^{ub}(\mathbf{q}|\mathbf{k},\mathbf{p}). \tag{3.65}$$

$$\mathcal{R}^{bu}(\mathbf{k}|\mathbf{p}|\mathbf{q}) + \mathcal{R}^{bu}(\mathbf{k}|\mathbf{q}|\mathbf{p}) = S^{bu}(\mathbf{k}|\mathbf{p},\mathbf{q}), \tag{3.66}$$

$$\mathcal{R}^{bu}(\mathbf{p}|\mathbf{k}|\mathbf{q}) + \mathcal{R}^{bu}(\mathbf{p}|\mathbf{q}|\mathbf{k}) = S^{bu}(\mathbf{p}|\mathbf{k},\mathbf{q}), \tag{3.67}$$

$$\mathcal{R}^{bu}(\mathbf{q}|\mathbf{k}|\mathbf{p}) + \mathcal{R}^{bu}(\mathbf{q}|\mathbf{p}|\mathbf{k}) = S^{bu}(\mathbf{q}|\mathbf{k},\mathbf{p}). \tag{3.68}$$

2. $\mathcal{R}^{ub}(\mathbf{k}|\mathbf{p}|\mathbf{q})$ denotes the energy transfer from $\mathbf{b}(\mathbf{p})$ to $\mathbf{u}(\mathbf{k})$. $\mathcal{R}^{bu}(\mathbf{p}|\mathbf{k}|\mathbf{q})$ is physically the same transfer but seen as a transfer from $\mathbf{u}(\mathbf{k})$ to $\mathbf{b}(\mathbf{p})$. Therefore,

$$\mathcal{R}^{ub}(\mathbf{k}|\mathbf{p}|\mathbf{q}) + \mathcal{R}^{bu}(\mathbf{p}|\mathbf{k}|\mathbf{q}) = 0. \tag{3.69}$$

$$\mathcal{R}^{ub}(\mathbf{k}|\mathbf{q}|\mathbf{p}) + \mathcal{R}^{bu}(\mathbf{q}|\mathbf{k}|\mathbf{p}) = 0, \tag{3.70}$$

$$\mathcal{R}^{ub}(\mathbf{p}|\mathbf{q}|\mathbf{k}) + \mathcal{R}^{bu}(\mathbf{q}|\mathbf{p}|\mathbf{k}) = 0. \tag{3.71}$$

$$\mathcal{R}^{bu}(\mathbf{k}|\mathbf{p}|\mathbf{q}) + \mathcal{R}^{ub}(\mathbf{p}|\mathbf{k}|\mathbf{q}) = 0, \tag{3.72}$$

$$\mathcal{R}^{bu}(\mathbf{k}|\mathbf{q}|\mathbf{p}) + \mathcal{R}^{ub}(\mathbf{q}|\mathbf{k}|\mathbf{p}) = 0, \tag{3.73}$$

$$\mathcal{R}^{bu}(\mathbf{p}|\mathbf{q}|\mathbf{k}) + \mathcal{R}^{ub}(\mathbf{q}|\mathbf{p}|\mathbf{k}) = 0. \tag{3.74}$$

The solutions of these equations are not unique and the expression for the energy transfer between modes cannot be obtained from the above equations alone. We have encountered this situation earlier while discussing energy transfer between a pair of velocity modes in Sections 3.4 and 3.7.1, and a pair of magnetic modes in Section 3.7.2. Like in those sections, we will now explore the solutions of the above equations.

We define the following quantities :

$$\mathcal{S}^{ub}(\mathbf{k}|\mathbf{p}|\mathbf{q}) \equiv -Re\,(i[\mathbf{k}.\mathbf{b}(\mathbf{q})][\mathbf{u}(\mathbf{k}).\mathbf{b}(\mathbf{p})])\,, \tag{3.75}$$

$$\mathcal{S}^{bu}(\mathbf{k}|\mathbf{p}|\mathbf{q}) \equiv -Re\,(i[\mathbf{k}.\mathbf{b}(\mathbf{q})][\mathbf{b}(\mathbf{k}).\mathbf{u}(\mathbf{p})])\,, \tag{3.76}$$

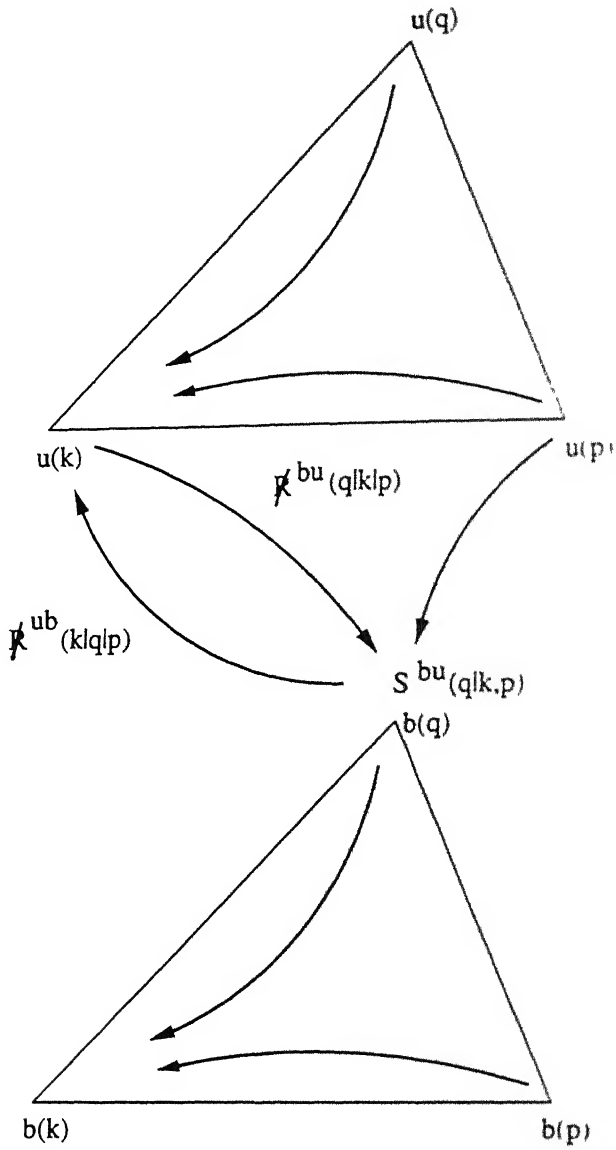

Figure 3.11: Relationship between the $\mathcal{R}^{ub}$'s, $\mathcal{R}^{bu}$'s. Energy transfer from $\mathbf{b(q)} \rightarrow \mathbf{u(k)}$ is physically the same as the transfer $\mathbf{u(k)} \rightarrow \mathbf{b(q)}$. Sum of transfers from $\mathbf{u(k)} \rightarrow \mathbf{b(q)}$ and $\mathbf{u(p)} \rightarrow \mathbf{b(q)}$ is equal to the combined transfer.

Replacing $\mathcal{S}^{ub}$ and $\mathcal{S}^{bu}$ for $\mathcal{R}^{ub}$ and $\mathcal{R}^{bu}$ respectively in Eqs. (3.63)-(3.74) we find that the $\mathcal{S}$'s are a solution to those equations, i.e.,

$$\mathcal{S}^{ub}(\mathbf{k}|\mathbf{p}|\mathbf{q}) + \mathcal{S}^{ub}(\mathbf{k}|\mathbf{q}|\mathbf{p}) = S^{ub}(\mathbf{k}|\mathbf{p},\mathbf{q}), \tag{3.77}$$

$$\mathcal{S}^{ub}(\mathbf{p}|\mathbf{k}|\mathbf{q}) + \mathcal{S}^{ub}(\mathbf{p}|\mathbf{q}|\mathbf{k}) = S^{ub}(\mathbf{p}|\mathbf{k},\mathbf{q}), \tag{3.78}$$

$$\mathcal{S}^{ub}(\mathrm{q|k|p}) + \mathcal{S}^{ub}(\mathrm{q|p|k}) = S^{ub}(\mathrm{q|k,p}). \tag{3.79}$$

$$\mathcal{S}^{bu}(\mathrm{k|p|q}) + \mathcal{S}^{bu}(\mathrm{k|q|p}) = S^{bu}(\mathrm{k|p,q}), \tag{3.80}$$

$$\mathcal{S}^{bu}(\mathrm{p|k|q}) + \mathcal{S}^{bu}(\mathrm{p|q|k}) = S^{bu}(\mathrm{p|k,q}), \tag{3.81}$$

$$\mathcal{S}^{bu}(\mathrm{q|k|p}) + \mathcal{S}^{bu}(\mathrm{q|p|k}) = S^{bu}(\mathrm{q|k,p}), \tag{3.82}$$

and

$$\mathcal{S}^{ub}(\mathrm{k|p|q}) + \mathcal{S}^{bu}(\mathrm{p|k|q}) = 0, \tag{3.83}$$

$$\mathcal{S}^{ub}(\mathrm{k|q|p}) + \mathcal{S}^{bu}(\mathrm{q|k|p}) = 0, \tag{3.84}$$

$$\mathcal{S}^{ub}(\mathrm{p|q|k}) + \mathcal{S}^{bu}(\mathrm{q|p|k}) = 0, \tag{3.85}$$

$$\mathcal{S}^{bu}(\mathrm{k|p|q}) + \mathcal{S}^{ub}(\mathrm{p|k|q}) = 0, \tag{3.86}$$

$$\mathcal{S}^{bu}(\mathrm{k|q|p}) + \mathcal{S}^{ub}(\mathrm{q|k|p}) = 0, \tag{3.87}$$

$$\mathcal{S}^{bu}(\mathrm{p|q|k}) + \mathcal{S}^{ub}(\mathrm{q|p|k}) = 0. \tag{3.88}$$

The $\mathcal{S}^{ub}$'s are just a single instance of the the $\mathcal{R}^{ub}$'s. It can be seen by inspection that *all* solutions can be expressed in the form :

$$\mathcal{R}^{bu}(\mathrm{k|p|q}) = \mathcal{S}^{bu}(\mathrm{k|p|q}) + Z_{\Delta}, \tag{3.89}$$

$$\mathcal{R}^{bu}(\mathrm{k|q|p}) = \mathcal{S}^{bu}(\mathrm{k|q|p}) - Z_{\Delta}, \tag{3.90}$$

$$\mathcal{R}^{bu}(\mathrm{p|k|q}) = \mathcal{S}^{bu}(\mathrm{p|k|q}) - Z_{\Delta}, \tag{3.91}$$

$$\mathcal{R}^{bu}(\mathrm{p|q|k}) = \mathcal{S}^{bu}(\mathrm{p|q|k}) + Z_{\Delta}, \tag{3.92}$$

$$\mathcal{R}^{bu}(\mathrm{q|k|p}) = \mathcal{S}^{bu}(\mathrm{q|k|p}) + Z_{\Delta}, \tag{3.93}$$

$$\mathcal{R}^{bu}(\mathbf{q}|\mathbf{p}|\mathbf{k}) = \mathcal{S}^{bu}(\mathbf{q}|\mathbf{p}|\mathbf{k}) - Z_\Delta. \tag{3.94}$$

$$\mathcal{R}^{ub}(\mathbf{k}|\mathbf{p}|\mathbf{q}) = \mathcal{S}^{ub}(\mathbf{k}|\mathbf{p}|\mathbf{q}) + Z_\Delta. \tag{3.95}$$

$$\mathcal{R}^{ub}(\mathbf{k}|\mathbf{q}|\mathbf{p}) = \mathcal{S}^{ub}(\mathbf{k}|\mathbf{q}|\mathbf{p}) - Z_\Delta. \tag{3.96}$$

$$\mathcal{R}^{ub}(\mathbf{p}|\mathbf{k}|\mathbf{q}) = \mathcal{S}^{ub}(\mathbf{p}|\mathbf{k}|\mathbf{q}) - Z_\Delta. \tag{3.97}$$

$$\mathcal{R}^{ub}(\mathbf{p}|\mathbf{q}|\mathbf{k}) = \mathcal{S}^{ub}(\mathbf{p}|\mathbf{q}|\mathbf{k}) + Z_\Delta. \tag{3.98}$$

$$\mathcal{R}^{ub}(\mathbf{q}|\mathbf{k}|\mathbf{p}) = \mathcal{S}^{ub}(\mathbf{q}|\mathbf{k}|\mathbf{p}) + Z_\Delta. \tag{3.99}$$

$$\mathcal{R}^{ub}(\mathbf{q}|\mathbf{p}|\mathbf{k}) = \mathcal{S}^{ub}(\mathbf{q}|\mathbf{p}|\mathbf{k}) - Z_\Delta. \tag{3.100}$$

where Z_Δ is an arbitrary function dependent on $\mathbf{k}$, $\mathbf{p}$, $\mathbf{q}$, $\mathbf{u}(\mathbf{k})$, $\mathbf{u}(\mathbf{p})$, $\mathbf{u}(\mathbf{q})$, $\mathbf{b}(\mathbf{k})$, $\mathbf{b}(\mathbf{p})$, $\mathbf{b}(\mathbf{q})$. These solutions are pictorially represented in Fig. 3.12 below.

We are already familiar with such solutions from the earlier discussion on mode-to-mode transfers between the velocity modes and between the magnetic modes. From Fig. 3.12 we see that Z_Δ transfers energy from $\mathbf{u}(\mathbf{p}) \to \mathbf{b}(\mathbf{k}) \to \mathbf{u}(\mathbf{q}) \to \mathbf{b}(\mathbf{p}) \to \mathbf{u}(\mathbf{k}) \to \mathbf{b}(\mathbf{q}) \to$ and back to $\mathbf{u}(\mathbf{p})$ without resulting in a change in modal energy. Hence, following the discussions in Section 3.7.1 and Section 3.7.2, we can interpret the quantity Z_Δ as a circulating transfer. The $\mathcal{S}^{bu}$ can be interpreted as the effective mode-to-mode transfers. For example, $\mathcal{S}^{bu}(\mathbf{k}|\mathbf{p}|\mathbf{q})$ is the effective transfer from $\mathbf{u}(\mathbf{p})$ to $\mathbf{b}(\mathbf{k})$,i.e,

$$\mathcal{R}^{bu}_{eff}(\mathbf{k}|\mathbf{p}|\mathbf{q}) = \mathcal{S}^{bu}(\mathbf{k}|\mathbf{p}|\mathbf{q}), \tag{3.101}$$

which is mediated by the *magnetic mode* $\mathbf{b}(\mathbf{q})$.

In the next section, we will use the effective mode-to-mode transfer to define, (a) shell-to-shell transfers between the velocity and the magnetic modes, and (b) cascade rates between the velocity and the magnetic modes.

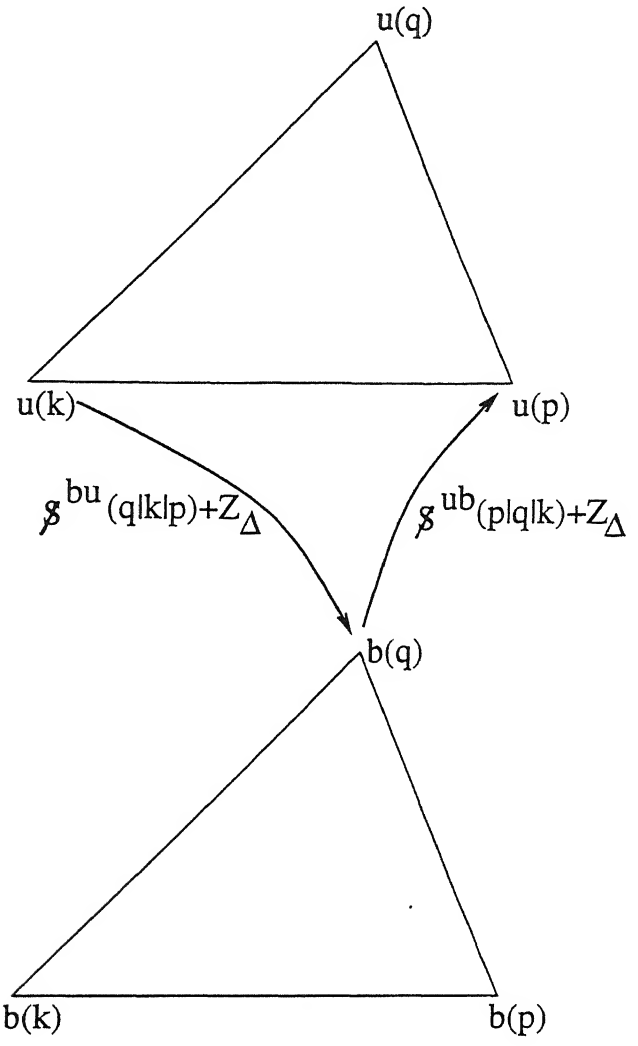

Figure 3.12: Energy transfer between a velocity and a magnetic mode in a triad can be expressed as a sum of circulating transfer and effective mode-to-mode transfer.

3.8 Shell-to-Shell energy transfer and cascade rates in MHD turbulence

In Section 3.5 we had defined the effective shell-to-shell transfer and the cascade rates in fluid turbulence in terms of the effective mode-to-mode transfer rate between a pair of modes in a wavenumber triad. In this section, we will extend the formulation of Section 3.5 to define shell-to-shell transfer rates and cascade rates in MHD turbulence.

In this thesis we will use the term u-shell (b-shell) to represent a shell in k-space con-

taining velocity (magnetic) modes. The term u-sphere (b-sphere) will be used to represent a sphere in k-space containing velocity (magnetic) modes. Thus, the energy associated with a u-sphere (b-sphere) is kinetic (magnetic) energy.

3.8.1 Shell-to-Shell energy transfer rates

In Section 3.5 we had defined the effective shell-to-shell transfer rates between two u shells in Fourier space. The expression for the effective mode-to-mode transfer between two velocity modes is the same for both Fluid and MHD flows [see Section 3.4.2 and 3.7.1]. Hence, the effective shell-to-shell transfer rates between two u-shells in MHD will also be defined by Eq. (3.27) of Section 3.5, i.e.,

$$T^{uu}_{mn} = \sum_{\mathbf{k}\in m}\sum_{\mathbf{p}\in n} \mathcal{S}^{uu}(\mathbf{k}|\mathbf{p}|\mathbf{q}). \tag{3.102}$$

The quantity $\mathcal{R}^{bb}(\mathbf{k}|\mathbf{p}|\mathbf{q})$ gives the energy transfer rate from $\mathbf{b}(\mathbf{p})$ to $\mathbf{b}(\mathbf{k})$ mediated by $\mathbf{q}$. Hence the energy transfer rate from n^{th} b-shell to the m^{th} b-shell can be obtained by summing $\mathcal{R}^{bb}(\mathbf{k}|\mathbf{p}|\mathbf{q})$ over every $\mathbf{p}$ in the the n^{th} b-shell and over every $\mathbf{k}$ in the m^{th} b-shell. From Section 3.7.2 we know that $\mathcal{R}^{bb} = \mathcal{S}^{bb}(\mathbf{k}|\mathbf{p}|\mathbf{q}) + Y_\Delta$, where $\mathcal{S}^{bb}(\mathbf{k}|\mathbf{p}|\mathbf{q})$ is the effective mode-to-mode transfer from $\mathbf{b}(\mathbf{p})$ to $\mathbf{b}(\mathbf{k})$, and Y_Δ is a circulating transfer. Thus, Y_Δ is transferred from $\mathbf{b}(\mathbf{p})$ in shell n to $\mathbf{b}(\mathbf{k})$ in shell m and then back to $\mathbf{b}(\mathbf{p})$ via the mode $\mathbf{b}(\mathbf{q})$. Therefore, the *effective* shell-to-shell transfer transfer rate from the n^{th} to the m^{th} b-shell is

$$T^{bb}_{mn} = \sum_{\mathbf{k}\in m}\sum_{\mathbf{p}\in n} \mathcal{S}^{bb}(\mathbf{k}|\mathbf{p}|\mathbf{q}). \tag{3.103}$$

We can also define shell-to-shell transfers rates between a u-shell and a b-shell. $\mathcal{R}^{bu}(\mathbf{k}|\mathbf{p}|\mathbf{q})$ is the energy transfer rate from $\mathbf{u}(\mathbf{p})$ to $\mathbf{b}(\mathbf{k})$ mediated by mode $\mathbf{q}$. Hence the energy transfer rate from the the n^{th} u-shell to the m^{th} b-shell can be calculated by summing $\mathcal{R}^{bu}(\mathbf{k}|\mathbf{p}|\mathbf{q})$ over every $\mathbf{p}$ in the n^{th} u-shell and over every $\mathbf{k}$ in m^{th} b-shell. We have shown in Section 3.7.3 that $\mathcal{R}^{bu}(\mathbf{k}|\mathbf{p}|\mathbf{q}) = \mathcal{S}^{bu}(\mathbf{k}|\mathbf{p}|\mathbf{q}) + Z_\Delta$, where $\mathcal{S}^{bu}(\mathbf{k}|\mathbf{p}|\mathbf{q})$ is the effective mode-to-mode transfer

from the mode $\mathbf{u(p)}$ to the mode $\mathbf{b(k)}$ in the triad $\mathbf{k}$, $\mathbf{p}$, $\mathbf{q}$, and Z_Δ is the circulating transfer which is transferred along $\mathbf{u(p)} \rightarrow \mathbf{b(k)} \rightarrow \mathbf{u(q)} \rightarrow \mathbf{b(p)} \rightarrow \mathbf{u(k)} \rightarrow \mathbf{b(q)} \rightarrow \mathbf{u(p)}$. Hence, Z_Δ is transferred from the mode $\mathbf{u(p)}$ in shell n to $\mathbf{b(k)}$ in shell m and then flows back to $\mathbf{u(p)}$ via the modes $\mathbf{u(q)} \rightarrow \mathbf{b(p)} \rightarrow \mathbf{u(k)} \rightarrow \mathbf{b(q)} \rightarrow \mathbf{u(p)} \rightarrow \mathbf{u(p)}$. Therefore, we interpret the quantity obtained by summing $\mathcal{S}^{bu}(\mathbf{k}|\mathbf{p}|\mathbf{q})$ over every $\mathbf{p}$ in the n^{th} u-shell and every $\mathbf{k}$ in the m^{th} b-shell as the *effective* shell-to-shell transfer, i.e.,

$$T^{bu}_{mn} = \sum_{\mathbf{k}\in m} \sum_{\mathbf{p}\in n} \mathcal{S}^{bu}(\mathbf{k}|\mathbf{p}|\mathbf{q}) \tag{3.104}$$

is the effective transfer from the the n^{th} u-shell to the m^{th} b-shell. The energy transfer rate from the n^{th} b-shell to the m^{th} u-shell, $T^{ub}_{mn} = -T^{bu}_{mn}$.

In Appendix A-C, we have argued that the circulating transfer $X_\Delta = 0$, $Y_\Delta = 0$, and $Z_\Delta = 0$ to the first order in the expansion coefficients. If $X_\Delta = 0$, $Y_\Delta = 0$, $Z_\Delta = 0$, then the effective shell-to-shell transfers will be the same as the total shell-to-shell transfers. We had pointed out is Section 3.5 that the circulating transfer, if nonzero, does not contribute to a change in energy of any shell, and hence from the physical point of view the effective shell-to-shell transfers is of greater significance than the total shell-to-shell transfers. We have numerically computed the effective shell-to-shell transfers given by Eqs. (3.102)-(3.104) in numerical simulations of 2-D MHD turbulence and gained important insights into the energy transfer process. The results of the simulations will be discussed in the next chapter.

3.8.2 Energy cascade rates

There are various types of cascade rates (energy fluxes) in MHD turbulence. We have schematically shown these transfers in Fig. 3.13. In this section we will derive the formulae to calculate these cascade rates within the framework of effective transfers.

In Section 3.5.1, we derived an expression for kinetic energy flux in terms of the mode-to-mode transfer [Eq. (3.26)]. We showed that the circulating transfer X_Δ does not contribute to the flux. Hence, the kinetic energy flux can be expressed by Eq. (3.30) in terms of the

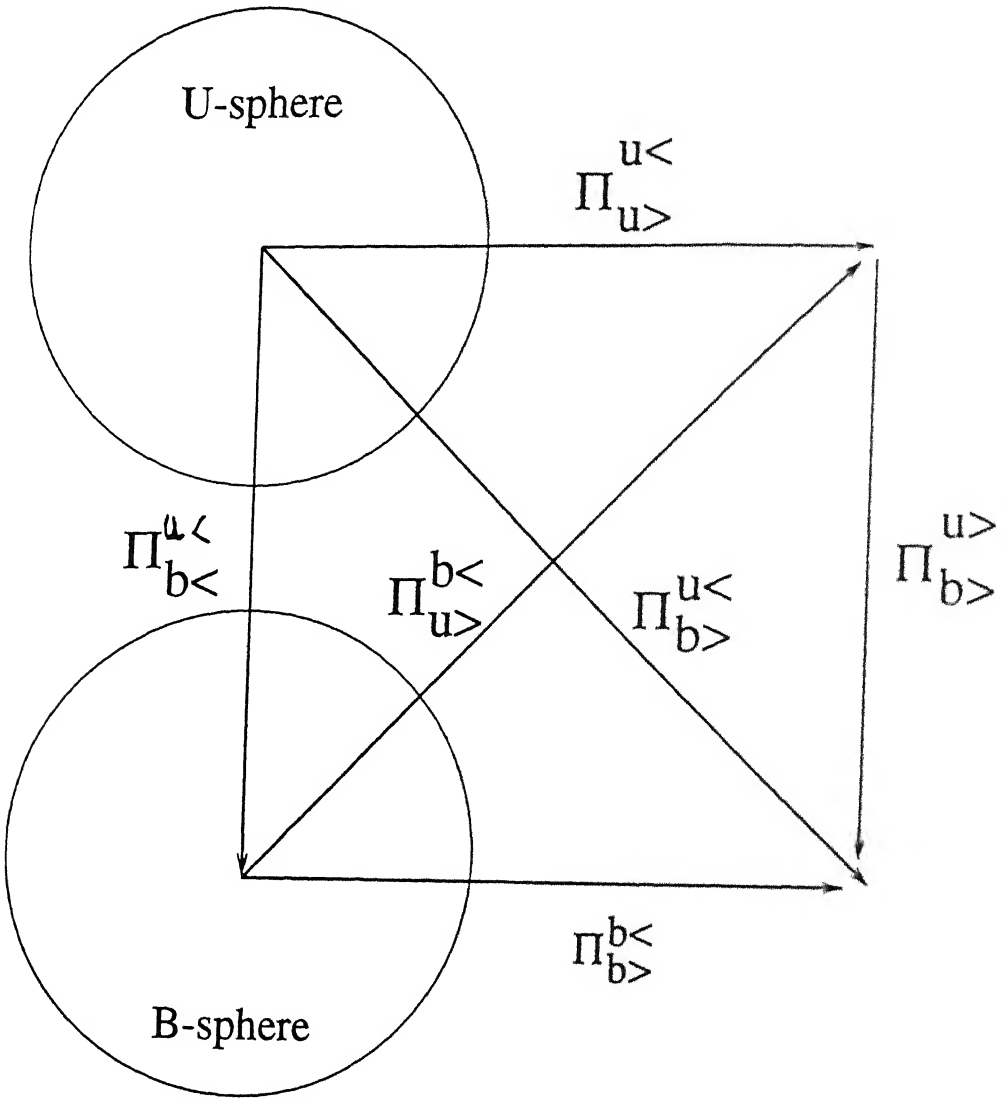

Figure 3.13: The various energy fluxes defined in this section are shown. The arrows indicate the directions of energy transfers corresponding to a positive flux. These fluxes are computed in numerical simulations and the results are given in Chapter 4.

effective mode-to-mode transfer $\mathcal{S}^{uu}(\mathbf{k}|\mathbf{p}|\mathbf{q})$. The kinetic energy flux $\Pi^{u<}_{u>}$ (the energy transfer rate from the u-sphere to outside the same sphere) in MHD will also be given by the same equation, i.e.,

$$\Pi^{u<}_{u>}(K) = \sum_{|\mathbf{p}|<K} \sum_{|\mathbf{k}|>K} \mathcal{S}^{uu}(\mathbf{k}|\mathbf{p}|\mathbf{q}). \tag{3.105}$$

The magnetic energy flux $\Pi^{b<}_{b>}(K)$ is defined as the rate of energy lost by the b-sphere to the modes outside the b-sphere. Since $\mathcal{R}^{bb}(\mathbf{k}|\mathbf{p}|\mathbf{q})$ is the mode-to-mode transfer from $\mathbf{b}(\mathbf{p})$ to $\mathbf{b}(\mathbf{k})$, $\Pi^{b<}_{b>}(K)$ can be obtained by summing $\mathcal{R}^{bb}(\mathbf{k}|\mathbf{p}|\mathbf{q})$ over every mode $\mathbf{p}$ inside the b-sphere and every mode $\mathbf{k}$ *outside* the b-sphere, i.e.,

$$\Pi^{b<}_{b>}(K) = \sum_{|\mathbf{p}|<K} \sum_{|\mathbf{k}|>K} \mathcal{R}^{bb}(\mathbf{k}|\mathbf{p}|\mathbf{q}). \tag{3.106}$$

Like for the kinetic energy flux, the circulating transfer Y_Δ will not contribute to the magnetic energy flux in Eq. (3.106). We briefly explain this as follows: let us take the mode $\mathbf{b}(\mathbf{q})$ to be outside the b-sphere. Then if the mode $\mathbf{b}(\mathbf{k})$ loses Y_Δ to mode $\mathbf{b}(\mathbf{p})$ then it will also gain Y_Δ from mode $\mathbf{b}(\mathbf{q})$, and hence Y_Δ will not contribute to the magnetic energy flux. Therefore, we can write the magnetic energy flux in Eq. (3.106) as

$$\Pi^{b<}_{b>}(K) = \sum_{|\mathbf{p}|<K} \sum_{|\mathbf{k}|>K} \mathcal{S}^{bb}(\mathbf{k}|\mathbf{p}|\mathbf{q}). \tag{3.107}$$

where $\mathcal{S}^{bb}(\mathbf{k}|\mathbf{p}|\mathbf{q})$ is given by Eq. (3.49) of Section 3.7.2.

The energy transfer between the kinetic energy and magnetic energy can be described by four types of fluxes. We shall define these fluxes below.

There is a transfer of energy from a u-sphere of radius K to the b-sphere of the same radius. The rate of loss of energy from the u-sphere to the corresponding b-sphere can be calculated by by summing $\mathcal{R}^{bu}(\mathbf{k}|\mathbf{p}|\mathbf{q})$ over every mode inside the b-sphere and the u-sphere. Following the definition of the effective shell-to-shell transfer T^{bu}_{mn} we can define the effective flux from the u-sphere to the b-sphere as

$$\Pi^{u<}_{b<}(K) = \sum_{|\mathbf{p}|<K} \sum_{|\mathbf{k}|<K} \mathcal{S}^{bu}(\mathbf{k}|\mathbf{p}|\mathbf{q}). \tag{3.108}$$

by summing the effective mode-to-mode transfer, $\mathcal{S}^{bu}(\mathbf{k}|\mathbf{p}|\mathbf{q})$, from $\mathbf{u}(\mathbf{p})$ to $\mathbf{b}(\mathbf{k})$, over the modes inside the u-sphere and the b-sphere.

There is a transfer of energy from the u-sphere to the magnetic modes outside the corresponding b-sphere. The rate of loss of the the energy from the u-sphere to the modes outside the b-sphere can be obtained by summing $\mathcal{R}^{bu}(\mathbf{k}|\mathbf{p}|\mathbf{q})$ over every mode inside the u-sphere and every mode outside the b-sphere. The corresponding effective flux can be calculated using

$$\Pi^{u<}_{b>}(K) = \sum_{|\mathbf{p}|<K} \sum_{|\mathbf{k}|>K} \mathcal{S}^{bu}(\mathbf{k}|\mathbf{p}|\mathbf{q}). \tag{3.109}$$

Similarly, there is a transfer of magnetic energy from a b-sphere to velocity modes outside the u-sphere. The rate of loss of energy from the b-sphere to the modes outside the u-sphere can be calculated by

$$\Pi^{b<}_{u>}(K) = \sum_{|\mathbf{p}|<K} \sum_{|\mathbf{k}|>K} \mathcal{S}^{ub}(\mathbf{k}|\mathbf{p}|\mathbf{q}). \tag{3.110}$$

There is a transfer of energy from modes outside the u-sphere to the modes outside the b-sphere. The rate of loss of energy by the modes outside the u-sphere to the modes outside the b-sphere can be obtained by

$$\Pi^{u>}_{b>}(K) = \sum_{|\mathbf{p}|>K} \sum_{|\mathbf{k}|>K} \mathcal{S}^{bu}(\mathbf{k}|\mathbf{p}|\mathbf{q}). \tag{3.111}$$

The total effective flux is defined as the total energy (kinetic+magnetic) lost by the K-sphere to the modes outside, i.e.,

$$\Pi_{tot}(K) = \Pi^{u<}_{u>}(K) + \Pi^{b<}_{b>}(K) + \Pi^{u<}_{b>}(K) + \Pi^{b<}_{u>}(K). \tag{3.112}$$

A schematic illustration of the effective fluxes defined in Eqs. (3.105)-(3.111) was given in Fig. 3.13. If the circulating transfer is zero, then each of the effective fluxes will be the same as the corresponding total fluxes. In the next chapter we will present the results of the detailed study of these fluxes in numerical simulations of 2-D MHD turbulence.

3.9 Conclusion

In literature we find a description of energy transfer rates from two modes in a triad to the third mode, i.e., from $\mathbf{u(p)}$ and $\mathbf{u(q)}$ to $\mathbf{u(k)}$. Here we have constructed new formulae to describe energy transfer rates between a pair of modes in the triad (mode-to-mode transfer), say from $\mathbf{u(p)}$ to $\mathbf{u(k)}$. The third mode in the triad acts as a mediator in the transfer process.

The mode-to-mode energy transfer in our formalism can be expressed as a combination of an "effective transfer" *and* a "circulating transfer". In Appendices A-C we have shown by imposing galilean invariance, symmetry and some other constraints that the circulating transfer should be zero. A completely general proof is not available at present. However even if the circulating transfer happens to be nonzero, it will not result in a change of modal energy, since the amount of circulating transfer gained by mode $\mathbf{k}$ from mode $\mathbf{p}$ is also lost by mode $\mathbf{k}$ to mode $\mathbf{q}$ (see Figs. 3.4, 3.10, 3.12). Only the effective transfer is responsible for modal energy change. As the circulating transfer does not have any observable effect on the energy of the modes, it may be correct to ignore it from the study of energy transfer.

Using the notion of effective mode-to-mode transfer and the circulating transfer we defined effective shell-to-shell energy transfer rates and energy fluxes in fluid turbulence [see Eq. (3.27) and Eq. (3.30)] and in MHD turbulence [see Eqs. (3.102)-(3.104) and Eqs. (3.105)-(3.111)]. Some of these energy transfers can be obtained only using the "mode-to-mode" energy transfer formulae. In the next chapter we will present the results of our numerical study of the effective shell-to-shell energy transfer rates and energy fluxes in 2-D MHD turbulence.

Chapter 4

Energy transfers in two-dimensional magnetohydrodynamic turbulence

4.1 Introduction

Turbulence is characterised by the existence of a range of spatial scales. Energy is transferred between these scales. Some of the features of energy transfer are well established, while a few other have been a matter of controversy, and some others have not been investigated at all. A detailed account of these issues was given in Chapter 1.

The following features of energy transfer in MHD turbulence have been conclusively established. The total energy (kinetic+magnetic) cascades from the large scales to the small scales in both 2-D and 3-D MHD turbulence [11]. Fluxes associated with z^+ and z^- energies are also found to cascade to the small scales [11].

We know from our earlier discussion that the magnetic energy of a mode evolves due to two nonlinear terms in the MHD equations — $[\mathbf{b}.(\mathbf{u}.\nabla)\mathbf{b}]$ and $[\mathbf{b}.(\mathbf{b}.\nabla)\mathbf{u}]$ — the first exchanges magnetic energy between different scales of the velocity field, and the second exchanges magnetic and kinetic energy between different scales. The kinetic energy similarly evolves due to two nonlinear terms — $[\mathbf{u}.(\mathbf{u}.\nabla)\mathbf{u}]$ and $[\mathbf{u}.(\mathbf{b}.\nabla)\mathbf{b}]$ — the first one exchanges kinetic energy between different scales and the second exchanges energy between the magnetic and the velocity fields. The kinetic and magnetic energy transfers arising from each of these non-linear terms above have not been investigated in detail either analytically or numerically

till very recently [20]. It is the purpose of this chapter to do a detailed investigation of energy transfer in 2-D MHD turbulence. To this end we will numerically compute the effective energy fluxes and the effective shell-to-shell energy transfer rates using Eqs. (3.105)-(3.111) and Eqs. (3.102)-(3.104) of Chapter 3. Recently, Ishizawa and Hattori [20] studied some of the energy transfer properties in 2-D MHD turbulence using wavelets. They computed the net energy transfer to a wavelet from all other wavelets. In contrast, we have calculated the energy cascade rates and detailed shell-to-shell energy transfers. While discussing our simulation results we will point out results common to both our simulations.

Non-local aspects of energy transfer in 2-D and 3-D MHD turbulence have been studied using EDQNM closure calculations [17–19]. For 2-D MHD turbulence, EDQNM calculations of both Pouquet [18], and Ishizawa and Hattori [19] give a transfer of kinetic energy from the small-scale to large-scale velocity field. Pouquet [18] also predicted magnetic energy transfer from small-scale magnetic field to large-scale magnetic field, and another transfer from large-scale magnetic field to small-scale velocity field. However, the conclusions of Ishizawa and Hattori are exactly the opposite [19], and are also confirmed by means of a direct numerical simulation [20]. The reason for the difference in the conclusion of these EDQNM results was discussed in Chapter 1 (see Section 1.5). Pouquet *et al.* [17] have also studied 3-D MHD turbulence using EDQNM closure calculation, as described in Chapter 1.

In some of the studies [17, 21], distinction was not made between the energies transferred to a mode from the kinetic and the magnetic fields. Also, the energy transferred into a mode $\mathbf{k}$ from different wave number regions were not separately considered [20, 21] — only the *net* energy transfer into a wave number $\mathbf{k}$ is generally computed. The EDQNM closure calculations [17–19] dealt mainly with coarse-grained energy transfer (between large scales and small scales). In another study, Frick and Sokoloff [77] solved a shell model of MHD turbulence and calculated the kinetic energy flux resulting from the interaction of the velocity modes, and magnetic energy flux arising from the interaction of the magnetic modes. In our simulations we investigate the (1) various energy fluxes arising within and between the

velocity and magnetic fields, and (2) the fine-grained (considering many wave number shells) energy transfer between magnetic and kinetic energies. This will give a more informed picture of the physics of energy transfer in MHD turbulence.

This chapter is organized as follows. In Section 4.2 we will describe the numerical technique to compute the fluxes from the velocity to the magnetic field, and the shell-to-shell energy transfers. The numerical method to solve the MHD equations has been described in Chapter 1. In Section 4.3 we will list the parameters for our numerical simulation. We perform the numerical simulation by forcing the large-scale velocity field. The steady state thus obtained in our simulations is discussed in Section 4.4. The various fluxes and shell-to-shell energy transfer rates are averaged over this steady state. Results of the fluxes obtained in the simulations is given in Section 4.5. In Section 4.6 we present the results for the shell-to-shell energy transfer rates. A discussion of the results follows in Section 4.7

4.2 Numerical computation of fluxes

In this section we describe the numerical technique used by us to compute the fluxes in Eqs. (3.108)-(3.111) of Chapter 3. To compute the fluxes we employ a method similar to that used by Domaradzki and Rogallo [39]. We outline this method below using $\Pi_{u>}^{b<}(K)$ as an example. In Eq. (3.110) of Chapter 3 we substitute the expression for $\mathcal{S}^{bu}(\mathbf{k}|\mathbf{p}|\mathbf{q})$ [Eq. (3.75) of Chapter 3] :

$$\Pi_{u>}^{b<}(K) = \sum_{|\mathbf{k}|>K} \sum_{|\mathbf{p}|<K} Re\,(i[\mathbf{k}.\mathbf{b}(\mathbf{q})][\mathbf{u}(\mathbf{k}).\mathbf{b}(\mathbf{p})])\,. \tag{4.1}$$

A straightforward summation over $\mathbf{k}$ and $\mathbf{p}$ involves $O(N^2)$ operations, where N is the size of the grid, and would thus involve a prohibitive computational cost for high Reynolds number simulations. Instead, the pseudo-spectral method can be used to compute Eq. (4.1) in $O(N log N)$ operations. It involves the following procedure.

We define two 'truncated' variables $\mathbf{u}^>$ and $\mathbf{b}^<$ as follows

$$\mathbf{u}^>(\mathbf{k}) = \left\{ \begin{array}{ll} 0 & \text{if } |\mathbf{k}| < K' \\ \mathbf{u}(\mathbf{k}) & \text{if } |\mathbf{k}| > K' \end{array} \right\}, \tag{4.2}$$

and

$$\mathbf{b}^<(\mathbf{p}) = \left\{ \begin{array}{ll} \mathbf{b}(\mathbf{p}) & \text{if } |\mathbf{p}| < K' \\ 0 & \text{if } |\mathbf{p}| > K' \end{array} \right. \tag{4.3}$$

The Eq. (4.1) written in terms of $\mathbf{u}^>$ and $\mathbf{b}^<$ reads as follows

$$\Pi^{b<}_{u>}(K') = \sum_{\mathbf{k}} \sum_{\mathbf{p}} Re\,(i[\mathbf{k}.\mathbf{b}(\mathbf{k}-\mathbf{p})][\mathbf{u}^>(\mathbf{k}).\mathbf{b}^<(\mathbf{p})])\,. \tag{4.4}$$

The above equation may be written as

$$\Pi^{b<}_{u>}(K') = Re\left[\sum_{\mathbf{k}} ik_j u_i^>(\mathbf{k}) \sum_{\mathbf{p}} b_j(\mathbf{k}-\mathbf{p}) b_i^<(\mathbf{p})\right]. \tag{4.5}$$

The $\mathbf{p}$ summation in the equation above can be recognized as a convolution sum. The right hand side of Eq. (4.5) can be conveniently and efficiently evaluated by the pseudo-spectral method, using the truncated variables $\mathbf{u}^>$ and $\mathbf{b}^<$. This procedure has to be repeated for every value of wavenumber K' for which the flux needs to be computed. The rest of the fluxes defined in Eqs. (3.108)-(3.111) and also the shell-to-shell transfer rates defined in Eqs. (3.102)-(3.104) of Chapter 3 are similarly computed.

4.3 Simulation parameters

In our numerical simulations, the large-scale velocity field is forced with white-noise forcing. The simulations are performed with hyperviscosity and hyper-resistivity characterised by the wavenumber k_{eq}. The parameters for the simulations are given below:

- Grid size = 512×512.
- $\nu = \mu = 5 \times 10^{-6}$.
- $k_{eq} = 14$.
- $dt = 5 \times 10^{-4}$.

- Forced wavenumbers k_f : $4 \leq k_f \leq 5$.
- Average total energy input rate $\simeq 0.1$. The parameter $\mathcal{F}$ in the forcing function [Eqs. (2.16)-(2.17) of Chapter 2] is fixed by this rate of energy input
- Magnetic energy input rate = 0.
- Steady state values of

$$r_A = \frac{\int \mathbf{u}^2 dx}{\int \mathbf{b}^2 dx} \simeq 0.5, \tag{4.6}$$

$$\sigma_c = \frac{2\int(\mathbf{u}.\mathbf{b})dx}{\int(\mathbf{u}^2 + \mathbf{b}^2)dx}. \simeq 0.1. \tag{4.7}$$

Usually the cross-helicity has a tendency to grow. In order to keep the cross-helicity low in our simulations, we had to adjust the injection rate of cross-helicity during the course of our simulations.

4.4 Generation of steady state

The computational time required to obtain a statistically steady state on a grid of size 512^2 is enormous. So to obtain a steady state in simulations on this grid we proceed in stages. We run on a grid of size 64^2 till a seemingly statistical steady state is achieved. This steady state field is then used as the initial condition to achieve a steady state in a simulation on a grid of size 128^2 and so on to grids 256^2 and then 512^2.

It is theoretically expected that in 2-D, in the long term, the magnetic energy *will* decay [82] even if the kinetic energy is stationary — this is called the anti-dynamo theorem. In our simulations we found that the fields remain steady for significantly long period after which it will decay (Fig. 4.1). Since the $N = 512^2$ simulations are computationally expensive, we have instead shown the decay of magnetic energy for a $N = 128^2$ simulation.

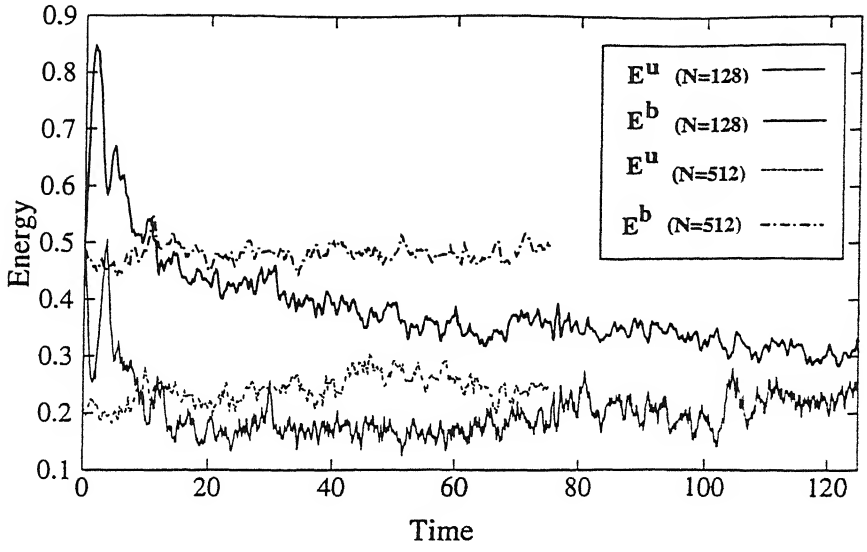

Figure 4.1: Evolution of the total kinetic energy and the magnetic energy for simulations on grid sizes 512^2 and 128^2. For 512^2 a quasi-steady magnetic energy is obtained over the period of the simulation. It is demonstrated in the 128^2 simulation that a quasi-steady magnetic energy eventually decays - a quasi-steady magnetic energy is obtained from $t = 60$ to 100.

The magnetic energy is found to have a quasi-steady state over the time interval extending from approximately $t = 20 - 30$ and it decays over the remaining period, as is theoretically expected. For the $N = 512^2$ simulation too, after the period of stationarity, the simulations should show decay of magnetic energy. So, strictly speaking, our steady state is only a quasi-steady state. In Fig. 4.1 we show the magnetic and kinetic energy in a quasi-steady state. The Alfvén ratio (the ratio of kinetic to magnetic energy) is found to fluctuate between the values 0.4 and 0.56. Hence over the steady state, magnetic energy dominates over the kinetic energy. The value of normalised cross-helicity is low (close to zero) in the steady state. We compute the fluxes and the shell-to-shell transfer rates over this quasi-steady state once in every unit of non-dimensional time. The fluxes and shell-to-shell transfer rates shown in this chapter are averages over 15 time units.

4.5 Energy fluxes in 2-D MHD simulations

In our numerical simulations we have computed all the energy fluxes defined in Eqs. (3.105)-(3.111) of Chapter 3. These fluxes are schematically shown in Fig. 3.13 of Chapter 3. In this we section we discuss these energy fluxes (cascade rates).

In Fig. 4.2 we show all the fluxes. The total flux Π_{tot} is positive indicating that there is a net loss of energy from the K-sphere to modes outside for all K. In the wavenumber region $25 < K < 50$, the total flux is seen to be approximately constant. This wave number region is the inertial range.

The net transfer from kinetic to magnetic energy is a sum of the fluxes $\Pi^{u<}_{b<}(K)$, $\Pi^{u<}_{b>}(K)$, $\Pi^{u>}_{b<}[= -\Pi^{b<}_{u>}(K)]$, and $\Pi^{u>}_{b>}(K)$. In our 512^2 simulations, the sphere of radius $K_{max} = 241$ encloses all the modes. We observe from Fig. 4.2 that the fluxes $\Pi^{u<}_{b>}(K_{max})$, $\Pi^{u>}_{b<}(K_{max})$ and $\Pi^{u>}_{b>}(K_{max})$ are zero, as there are no modes outside this sphere of maximum radius K_{max}. The flux $\Pi^{u<}_{b<}(K_{max})$ is found to be positive (see Fig. 4.2), indicating that there is a net transfer from kinetic energy to magnetic energy; since the magnetic modes are not being forced, it is this transfer that keeps the magnetic energy constant in quasi-steady state.

We now describe features of the fluxes $\Pi^{u<}_{b<}$, $\Pi^{u<}_{b>}$, $\Pi^{b<}_{u>}$, $\Pi^{u>}_{b>}$, $\Pi^{u<}_{u<}$, and $\Pi^{b<}_{b<}$ observed in our simulations and plotted in Fig. 4.2. We remind the reader that the u-modes within a wave number sphere are called the u-sphere and the b-modes within the wave number sphere are called the b-sphere. First, we discuss the fluxes that transfer energy between the u-modes and the b-modes. We find that the flux $\Pi^{u<}_{b<}(K)$ is positive — hence, kinetic energy is lost by a u-sphere to the corresponding b-sphere. The flux $\Pi^{u<}_{b>}(K)$ is also positive. It means that a u-sphere loses energy to the modes outside the b-sphere. We find that the flux $\Pi^{b<}_{u>}(K)$ is negative, which implies that the b-sphere gains energy from modes outside the u-sphere. Thus, all these fluxes result in a transfer of kinetic energy to magnetic energy. However, $\Pi^{u>}_{b>}(K)$ is negative, implying that there is some feedback of energy from modes outside the b-sphere to modes outside the u-sphere. The *net* transfer, however, is from kinetic to magnetic.

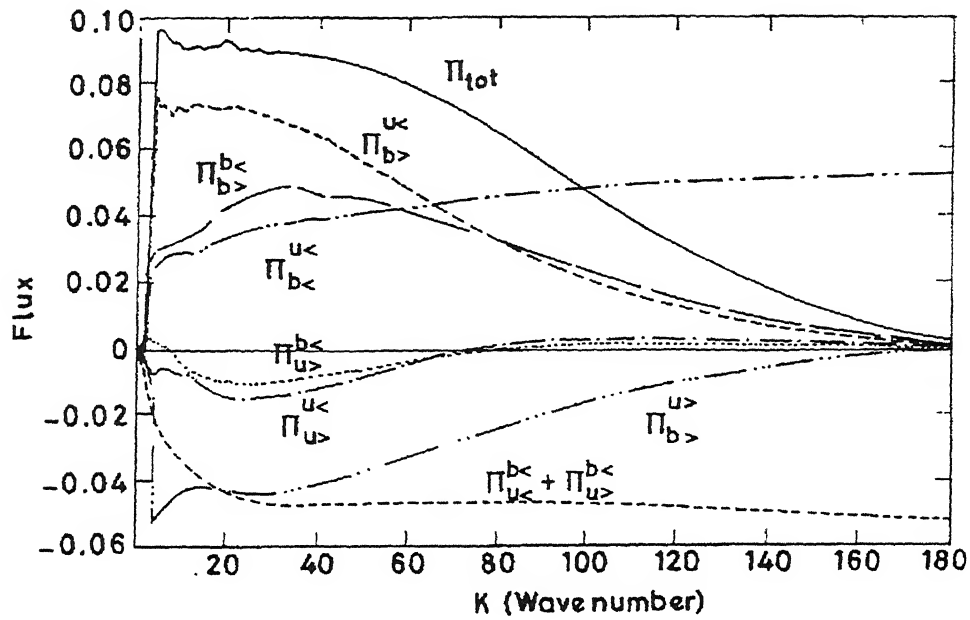

Figure 4.2: The simulation results of fluxes. The following fluxes have been plotted : the total flux (Π_{tot}), the kinetic energy flux from u-sphere to outside u-sphere $\Pi^{u<}_{u>}$, the magnetic energy flux from b-sphere to outside b-sphere $\Pi^{b<}_{b>}$, the energy flux from u-sphere to b-sphere $\Pi^{u<}_{b<}$, the energy flux from u-sphere to modes outside the b-sphere $\Pi^{u<}_{b>}$, the energy flux from b-sphere to modes outside the u-sphere $\Pi^{b<}_{u>}$, the energy flux from modes outside u-sphere to modes outside the b-sphere $\Pi^{u>}_{b>}$, and the net flux out of a b-sphere ($\Pi^{b<}_{u<} + \Pi^{b<}_{u>}$) have been plotted in this figure.

We shall later show that the flux $\Pi^{u>}_{b>}(K)$ plays a crucial role in driving the kinetic-to-kinetic flux $\Pi^{u<}_{u>}(K)$.

The energy gained by the b-spheres is found to be constant for the approximate range $20 \leq K \leq K_{max}$. This can be seen from the plot of $\Pi^{b<}_{u<}(K) + \Pi^{b<}_{u>}$ (which is the negative of the total transfer of kinetic energy to the modes within the b-sphere). The constancy of the flux implies that a b-sphere of radius K and that of radius of $K + \Delta K$ get the same amount of energy from the u-modes. Thus there is no *net* energy transfer from the u-modes into a b-shell (of thickness ΔK) beyond approximately $K = 20$. We therefore conclude that the *net* energy transfer from u-modes to the b-sphere occurs within the $K \leq 20$ sphere.

We find that there is a kinetic energy gain by the u-sphere from u-modes outside due to the fact that flux $\Pi^{u<}_{u>}(K)$ is negative — this is consistent with the numerical simulations of Ishizawa and Hattori [20]. This behaviour of kinetic energy is known as an 'inverse cascade' in literature and is reminiscent of the inverse cascade of kinetic energy in 2-D fluid turbulence [44] and of mean square vector potential in 2-D MHD turbulence [18, 75]. However, note that the kinetic energy in 2-D MHD turbulence is not an inviscid invariant. Fig. 4.2 shows that the inverse cascade of kinetic energy exists in the wave number range $K \leq 60$. Even the modes that are being forced ($4 \leq k \leq 5$) gain energy from higher wave numbers u-modes. The source of this energy is the flux $\Pi^{b>}_{u>}(K)[= -\Pi^{u>}_{b>}(K)]$ which transfers energy from higher b-modes to the higher u-modes and thus effectively forces them.

We observe from Fig. 4.2 that there is a loss of magnetic energy from the b-sphere to the b-modes outside [see $\Pi^{b<}_{b>}(K)$] — this was also observed in the numerical simulations of Ishizawa and Hattori [20]. Our observation of a forward cascade of magnetic energy contradicts the result of the EDQNM closure calculations which predicts an inverse cascade of magnetic energy [18].

The flux $\Pi^{b<}_{b>}(K)$ is found to be constant in the inertial range. Using similar reasoning to that given above, we can conclude that the net magnetic energy transfer to a wave number shell in the inertial range is zero. However, in this case it would imply that the *entire* energy gained by the shell (of thickness ΔK) from the b-sphere of radius K is lost *completely* to the modes outside the region $K + \Delta K$. Thus the magnetic energy *cascades* down to higher wave numbers independent of the transfers between kinetic and magnetic energy. This flux of magnetic energy is sustained by the fluxes $\Pi^{u<}_{b<}(K)$ and $\Pi^{u>}_{b<}(K)$, both of which transfer kinetic energy into the small b-spheres.

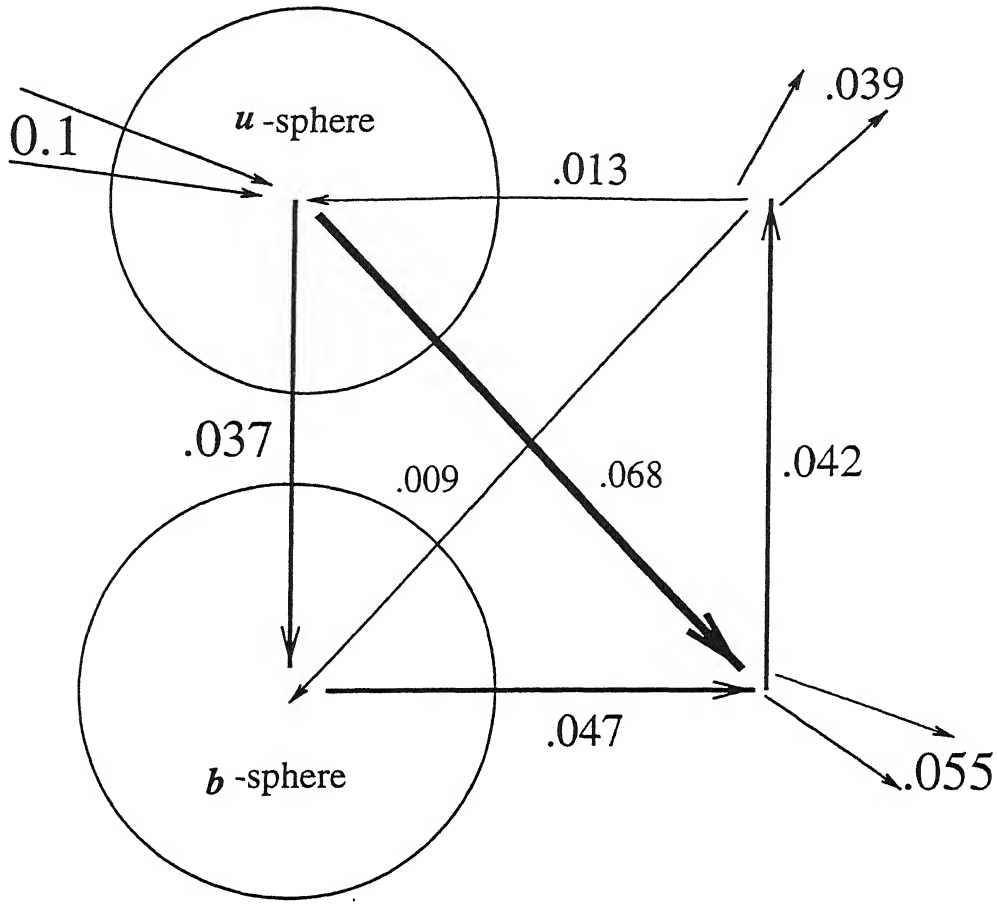

Figure 4.3: The schematic illustration of the directions and the magnitudes of the fluxes plotted in Fig. 4.2 (also see Fig. 3.13 of Chapter 3). Also shown are the magnitudes of the kinetic energy input rate due to forcing, and the total dissipation of kinetic and magnetic energy. The fluxes are shown for $K = 20$ but are representative of the entire inertial range. All quantities have been time-averaged. The fluctuations of the fluxes (except $\Pi_{b<}^{u<}$) and the dissipation rate are approximately equal to 0.005. The fluctuations in $\Pi_{b<}^{u<}$ are higher and is approximately 0.01 .

Figure 4.3 schematically illustrates the energy fluxes of Fig. 4.2 for a K' sphere of radius $K' = 20$, which is within the inertial range. The energy input due to forcing and the small inverse cascade $[\Pi^{u<}_{u>}(K')]$ into the u-sphere from higher u-modes, provide the energy input into the u-sphere. This energy is transferred into and outside the b-sphere by $\Pi^{u<}_{b<}(K')$ and $\Pi^{u<}_{b>}(K')$, the latter transfer being the most significant of all transfers (see Figs. 4.2 and 4.3). The energy transferred into the b-sphere from the u-sphere $[\Pi^{u<}_{b<}(K')]$, and a negligible input from the modes outside the u-sphere $[-\Pi^{b<}_{u>}(K')]$, cascades down to the higher wave number b-modes. In the higher b-modes, this cascaded energy $[\Pi^{b<}_{b>}(K')]$, together with the transfer from the u-sphere, is partly dissipated and partly fed back to the high wave number u-modes. This feedback to the kinetic energy is mostly dissipated, though a small inverse cascade takes some energy back into the u-sphere. This is the qualitative picture of the energy transfer in 2-D MHD turbulence.

The net transfer to each of the four corners of the Fig. 4.3 sum to zero within the statistical error (which is computed from the standard deviation of the sampled data). This is consistent with a quasi-steady-state picture.

The results presented here for the quasi-steady-state in a forced turbulence remain qualitatively valid even for a decaying case — the direction of the various fluxes for the decaying case are identical to that for the forced simulation; but as the energy decays, the magnitudes of all the fluxes reduce.

The fluxes give us information about the overall energy transfer from a wave number sphere or outside-sphere to another sphere or outside-sphere. To obtain a more detailed account of the energy transfer, energy exchange between the wave number shells are now studied. In the following section we present a discussion on the shell-to-shell energy transfer rates in MHD turbulence.

4.6 Shell-to-Shell energy transfer-rate studies

Significant details of energy transfers are revealed by calculating the shell-to-shell energy transfer rates T^{uu}_{mn}, T^{bb}_{mn}, T^{bu}_{mn}, and between different shells defined in Eqs. (3.102)-(3.104) of Chapter 3. We partition the k-space into shells at wave numbers $k_n (n = 1, 2, 3. ...) = 1, 16, 19.02, 22.62, ..., 2^{(n+14)/4}$. The first shell extends from $k_1 = 1$ to $k_2 = 16$ — a division of the wave number space into smaller shells at the large scales will contain too few modes: the second shell extends from $k_2 = 16$ to $k_3 = 19.02$, ..., the m^{th} shell extends from k_m to $k_{(m+1)}$. Thus, the effective shell-to-shell energy transfer rate from the n^{th} u-shell to the m^{th} u-shell [Eq. (3.102) of Chapter 3] can be written as,

$$T^{uu}_{mn} = \sum_{k_m<k<k_{m+1}} \sum_{k_n<p<k_{n+1}} \sum_{\mathbf{q}}^{\Delta} \mathcal{S}^{uu}(\mathbf{k}|\mathbf{p}|\mathbf{q}), \tag{4.8}$$

and the effective shell-to-shell energy transfer rate from the n^{th} b-shell to the m^{th} b-shell [Eq. (3.103) of Chapter 3] can be written as

$$T^{bb}_{mn} = \sum_{k_m<k<k_{m+1}} \sum_{k_n<p<k_{n+1}} \sum_{\mathbf{q}}^{\Delta} \mathcal{S}^{bb}(\mathbf{k}|\mathbf{p}|\mathbf{q}). \tag{4.9}$$

and the effective shell-to-shell energy transfer rate from the n^{th} u-shell to the m^{th} b-shell, as defined in Eq. (3.104) of Chapter 3, can be written as,

$$T^{bu}_{mn} = \sum_{k_m<k<k_{m+1}} \sum_{k_n<p<k_{n+1}} \sum_{\mathbf{q}}^{\Delta} \mathcal{S}^{bu}(\mathbf{k}|\mathbf{p}|\mathbf{q}). \tag{4.10}$$

We categorise the energy transfer between u-shells and the b-shells as being *homologous* if the transfers are between the corresponding shells (of the same wave number range $k_n < k < k_{n+1}$, say). Transfers between different shells are therefore *non-homologous*. Further, transfers (kinetic-to-magnetic, kinetic-to-kinetic, and magnetic-to-magnetic) involving shells which are close in wave number space are called *local* transfers, as is the convention. Two shells are considered close if the wave number ratio of the larger shell to the smaller shell is less than 2 (in this study this would include the shells between $n + 4$ to $n - 4$ from the n^{th} shell). Transfers involving shells more distant are called *non-local*.

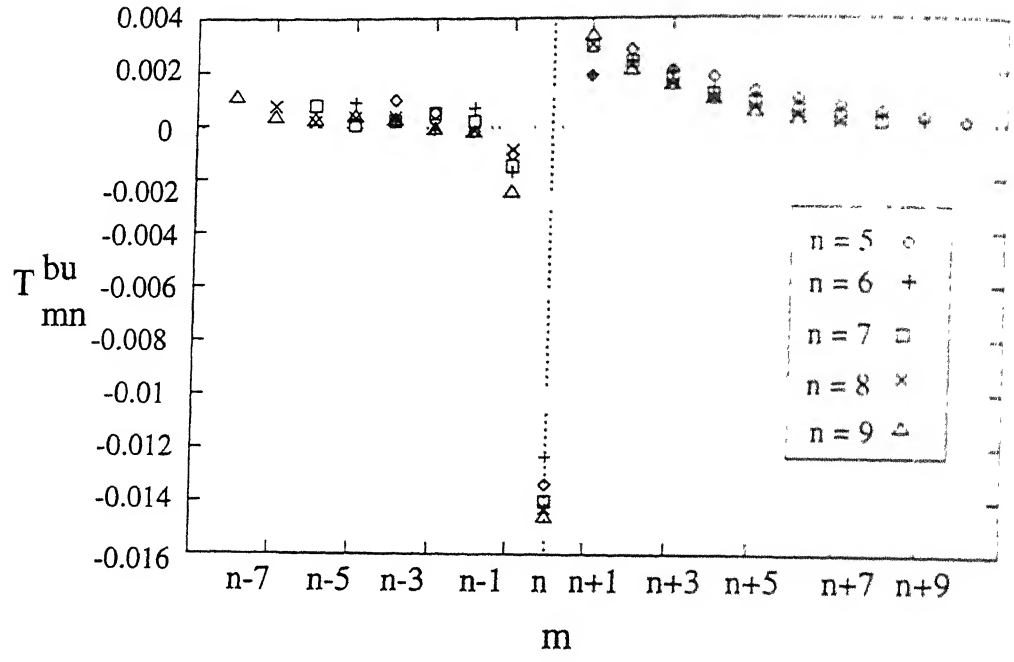

Figure 4.4: The energy transfer rate T^{bu}_{mn} from the n^{th} u-shell to the m^{th} b-shell. The loss of energy from the n^{th} u-shell to the m^{th} b-shell is defined to be positive.

In Fig. 4.4 we plot the energy transfer rates T^{bu}_{mn} between u-shells and b-shells. It is evident from the figure that the transfer rates between shells in the inertial range are virtually independent of the individual values of the indices m and n, and only dependent on their differences. This means that the transfer rates in the inertial range are *self-similar*. The differences in T^{bu}_{mn} for various n are smaller than the standard deviation of the sampled data, indicating that the perceived self-similarity is statistically significant.

We now discuss our simulation results for the non-homologous transfer rates between u-shells and b-shells. In Fig. 4.4 we have shown these transfer rates from the n^{th} u-shell to the m^{th} b-shell by plotting T^{bu}_{mn} versus m for various values of n. We find that for all m, except for $m = n-1$ and n, T^{bu}_{mn} is positive. This implies that a u-shell loses energy to all the b-shells but gains energy from the $(n-1)^{th}$ and n^{th} b-shells. The quantity T^{bu}_{mn} is found to be small for $m < n$ in comparison with the transfer for $m > n$. Consequently, energy

from a u-shell is mainly transferred to the b-shells at higher wave numbers. We had found earlier that the flux $\Pi^{u>}_{b<}(K)$ is much smaller in magnitude to the flux $\Pi^{u<}_{b>}(K)$. The fluxes and the transfer rates are consistent with each other. From Fig. 4.4 we also find that the energy transfer rate T^{bu}_{1n} from the n^{th} u-shell to the 1^{st} b-shell is positive, implying that the 1^{st} b-shell gains energy from the u-shells — this is a nonlocal transfer of energy from the large u-modes to the small b-modes. The inverse cascade $\Pi^{b<}_{u<}$ observed in Section 4.5 (see Fig. 4.2) is due to this nonlocal transfer.

The homologous transfers are found to transfer energy from b-shells to u-shells (see Fig. 4.4); this is in contrast to the net energy transfer and a majority of the non-homologous transfers which are from kinetic to magnetic. We find that the energy gained by a u-shell through the homologous transfers is larger than the *total* loss of energy by the u-shell through non-homologous transfers. Consequently, there is a *net* gain of energy by the u-shells in the inertial range. In Section 4.5 it was shown that the magnetic energy outside a b-sphere is lost to kinetic energy outside the u-sphere. It is now clear that this transfer arises primarily due to the homologous transfers from magnetic to kinetic.

The Fig. 4.4 shows energy transfer rates T^{bu}_{mn}, to b-shells from u-shells indexed as $n = 5, 6, 7, 8, 9$. In Fig. 4.5 we show the transfer rates T^{bu}_{mn} from the $n = 1$ u-shell to all the b-shells. Recall that the first u-shell is comprised of small wave number modes, $k = 1$ to 16. Comparing the magnitudes of T^{bu}_{mn} to the b-shells from the first u-shell (see Fig. 4.5) and from the u-shells at higher wavenumbers (see Fig. 4.4), we see that the energy transfer rate from the 1^{st} u-shell dominates the transfers from all other u-shells. Hence, there is a large amount of *non-local* transfer from the first u-shell to the b-shells. In Section 4.5 we had claimed that there is no net kinetic energy transfer into any inertial range b-shell. Now we show this explicitly in Fig. 4.6 by plotting the net kinetic energy transferred into a b-shell ($=\sum_n T^{bu}_{mn}$) versus the shell index m ($\diamond$ in the figure). From the figure, the net energy transferred into the

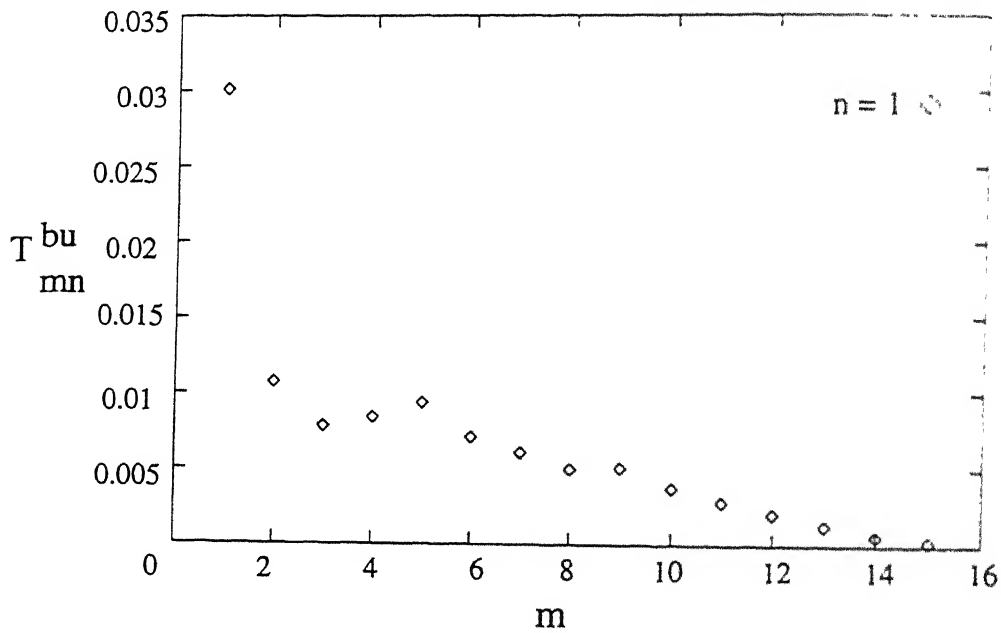

Figure 4.5: The energy transfer rate from the 1^{st} u-shell to the b-shells.

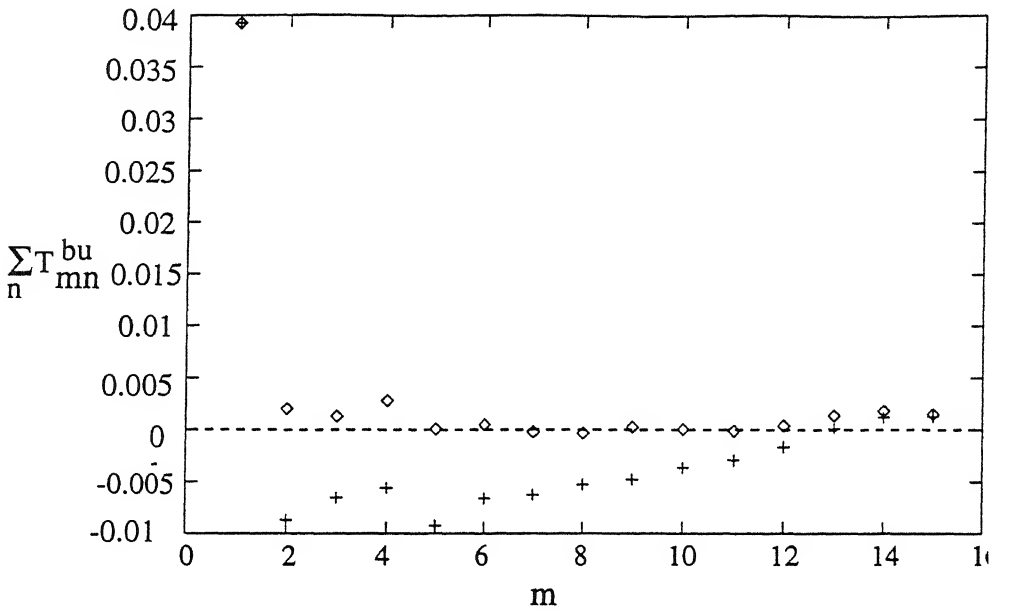

Figure 4.6: The diamonds ($\diamond$) represent the net energy transfer into a b-shell from all the u-shells. The pluses ($+$) represent the net energy transfer into a b-shell from all u-shells except the 1^{st} one.

inertial range b-shell can be seen to be nearly zero. We also plot in Fig. 4.6 the net kinetic energy transfer into a b-shell from all u-shells, *except* the first ($+$ in the figure). This quantity is now no longer zero and has a significant magnitude. Therefore, the non-local transfer from the first shell plays an important part in balancing the other kinetic energy transfers into an inertial range b-shell.

We have also computed the transfer rates of magnetic energy T^{bb}_{mn} from n^{th} to m^{th} b-shell. In Fig. 4.7 we have plotted the quantity T^{bb}_{mn} versus m for different values of n in the inertial range. We find that the differences in $T^{bb}_{(n+\Delta n)n}$ for any fixed $\Delta n(=n-m)$ are smaller than the standard deviation of their statistical fluctuations computed from the sampled data. Hence we can conclude that T^{bb}_{mn} is *self-similar* in the inertial range, dependent only on the difference Δn and independent of the location of the shell n. We find that the transfer rates

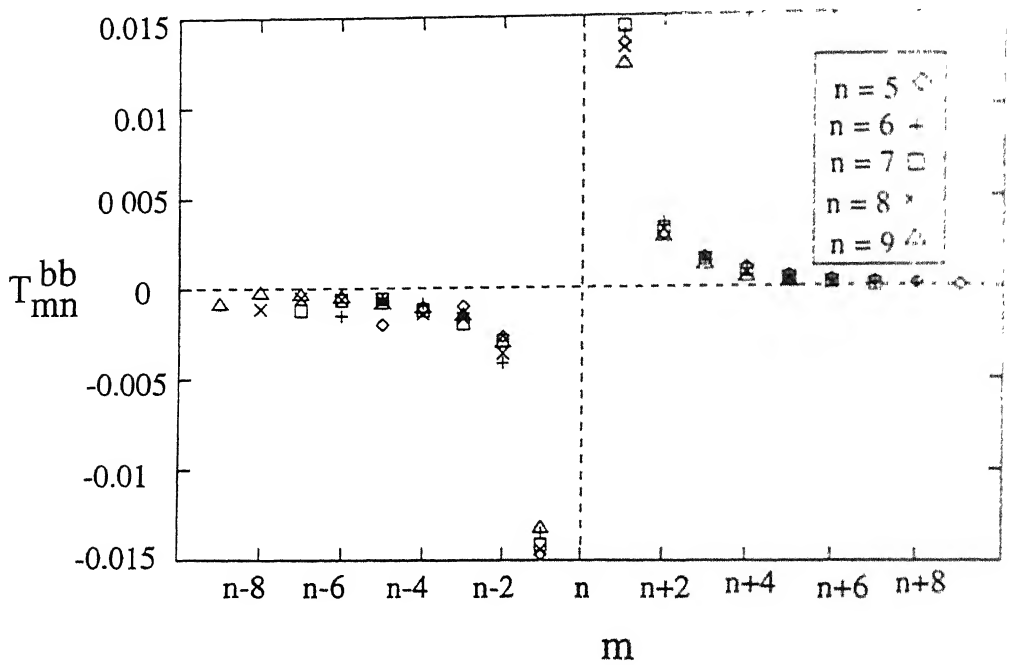

Figure 4.7: The energy transfer rate T^{bb}_{mn} from the n^{th} b-shell to the m^{th} b-shell. The loss of energy from the n^{th} b-shell to the m^{th} b-shell is defined to be positive.

T^{bb}_{mn} are negative for $m < n$ and they are positive for $m > n$ (see Fig. 4.7). Hence a b-shell gains energy from the b-shells of smaller wave numbers and loses energy to the b-shells of larger wave numbers. Since T^{bb}_{mn} is self-similar, the energy lost from a shell $(n - \Delta n)$ to n is equal to the energy lost from n to the shell $(n + \Delta n)$. Thus, the net magnetic energy transfer into any inertial range shell is zero, and the energy cascades from the smaller wave numbers to the higher wave numbers.

We now discuss the simulation results for the kinetic energy transfer rates T^{uu}_{mn} from the n^{th} to the m^{th} shell. The results are shown in Fig. 4.8 where we have plotted T^{uu}_{mn} versus m for various values of n. We find that the most dominant transfers are from the n^{th} u-shell to $m = n \pm 1$. From the sign of these transfers we see that kinetic energy is gained from $(n-1)^{th}$

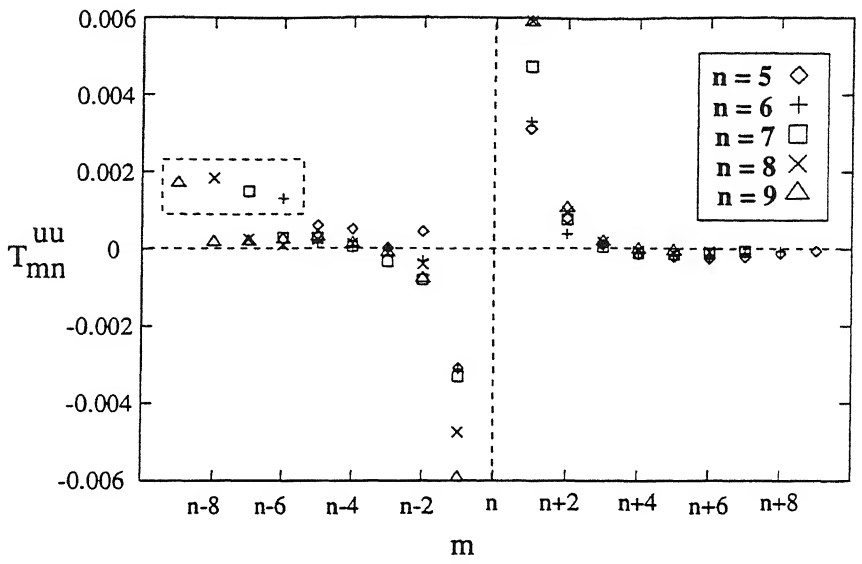

Figure 4.8: The energy transfer rate T^{uu}_{mn} from the n^{th} u-shell to the m^{th} u-shell. The loss of energy from the n^{th} b-shell to the m^{th} b-shell is defined to be positive. The boxed points represent energy transfer from the n^{th} u-shell to the 1^{st} u-shell.

shell and lost to $(n+1)^{th}$ shell. This means that the *local* transfers from the adjacent shells result in a *forward* cascade of energy towards the *large* wave numbers. The transfers from other shells are largely negligible except for the transfer to the shell $m = 1$ (shown boxed on the left of the figure), which represents a loss from high wave number modes to the $m = 1$ shell. This *non-local* transfer (to the first shell) produces an *inverse* cascade to the *small* wave numbers, observed earlier in Section 4.5. Now it is clear that this inverse cascade is due to non-local transfers. The local and non-local transfers are seen to possess altogether different features: the former is a forward cascade which seems largely self-similar, while the latter is an inverse cascade *only* to the first shell.

We schematically illustrate in Fig. 4.9 the energy transfer between shells. In this figure we show directions of the most significant transfers in the inertial range. The arrows indicate the directions of the transfers, and thickness of the arrows indicates the approximate relative

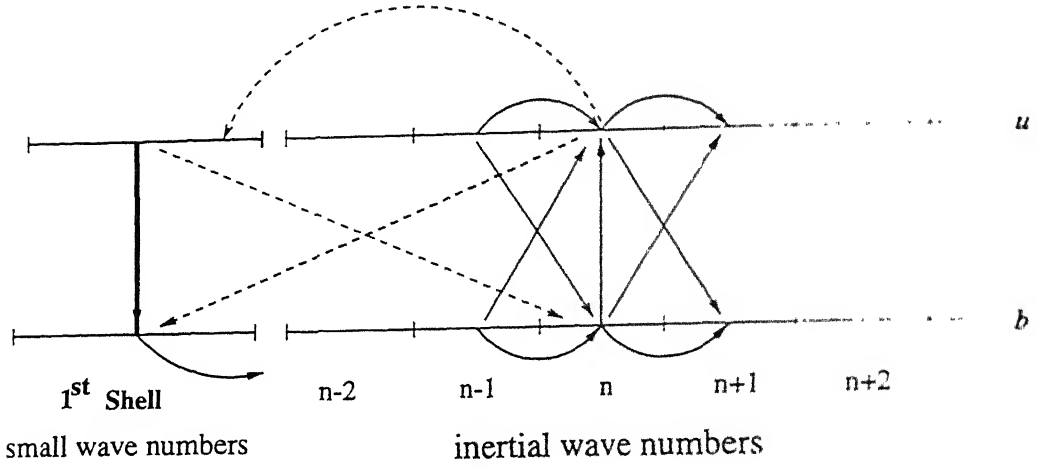

Figure 4.9: A schematic representation of the direction and the magnitude of energy transfer between u-shells and b-shells. The relative magnitudes of the different transfers has been represented by the thickness of the arrows. The non-local transfers with the 1st shell have been shown by dashed lines.

magnitudes. Since the local transfer rates are self-similar, the transfers from any other shells in the inertial range will also show the same pattern. An inertial range b-shell gains significant amount of energy from the smaller u-shells through both local and non-local transfers, and it also locally gains energy from the smaller b-shells (T^{bb}_{mn}). The energy gained by a b-shell from the smaller b-shells is *exclusively* lost to the larger b-shells and the energy gained from the u-shells is mainly lost through homologous transfer (T^{bu}_{nn}) to the corresponding u-shell. A small fraction of the energy is also lost to the larger u-shells. In addition to the energy from the b-shells, a u-shell also gains energy from smaller u-shells by *local* transfer. The energy of u-shells is mainly lost locally to higher b-shells and u-shells, but a significant amount is also transferred to smaller u-modes (T^{uu}_{mn}) by a *non-local* inverse cascade.

As illustrated in Fig. 4.9, there is a transfer of energy from the first u-shell to the first

b-shell. This is the most significant gain of magnetic energy from the kinetic energy. Under steady state the magnetic energy gained by the first shell gets transferred to the higher b-shells. This transfer yields the forward cascade of magnetic energy discussed in Section 4.5

To summarise, we find that there are various types of energy transfers in MHD turbulence: local, nonlocal, homologous, and non-homologous. The main local transfers are the forward magnetic energy transfer and the forward kinetic energy transfer, the homologous transfer from the magnetic to the kinetic energy (all in the inertial range). There is nonlocal transfer from inertial range u-shells to the first b-shell and the first u-shell, and from the first u-shell to the b-shells. There is a transfer from kinetic energy to magnetic energy in the first shell.

In this section we had extensively described various cascade rates (fluxes) and shell-to-shell energy transfer rates. It is clear that the complete picture is quite complex. Infact, some of the features we have seen contradicts earlier conjectures and results. These differences are discussed in the next section.

4.7 Discussion

We have investigated the features of kinetic and magnetic energy transfer between scales at low values of cross-helicity in a quasi-steady state of forced 2-D MHD turbulence. A summary of the results is given below. For the following discussion refer to Figs. 4.3 and 4.9.

1) There is a net transfer of energy from the kinetic to the magnetic.

2) There is an energy transfer to the large-scale magnetic field from the large-scale velocity field (u-sphere to b-shere flux $\Pi_{b<}^{u<}$ in Fig.4.2), and also from the small-scale velocity field (flux from b-sphere to modes outside the u-sphere $\Pi_{u>}^{b<}$ in Fig.4.2). The former transfer is of a greater magnitude than the latter. The latter transfer has also been observed in numerical simulations and EDQNM calculations of Ishizawa and Hattori [19, 20]. The magnetic field enhancement is primarily caused by a transfer from the u-sphere to the b-sphere. Indeed the first few b-modes get most of this energy.

3) Other significant transfers, not noted in earlier work, are from the large-scale velocity field to the small-scale magnetic field (u-sphere to outside the b-sphere) and an interesting reverse transfer from the small-scale magnetic field to the small-scale velocity field (from modes outside the b-sphere to modes outside u-sphere).

4) There is an *inverse* cascade in the velocity field – this is consistent with the observation of Ishizawa and Hattori arising from numerical simulations [20] and is also consistent with the EDQNM closure calculations [18, 19]. This inverse cascade of kinetic energy is driven by the reverse transfer of energy from magnetic to the velocity field at the small scales. Although the flux study points to an inverse cascade of kinetic energy, the shell-to-shell energy transfer rates reveal the following feature. There exists both an inverse and a forward transfer of kinetic energy. The inverse transfer is primarily *nonlocal*, coming from the larger wave numbers to the first few modes. The forward cascade is *local*, i.e., between same sized eddies and is self-similar in the inertial range.

5) There is a *forward* cascade of magnetic energy towards the small scales. This is consistent with other recent numerical simulations [20]. EDQNM closure calculations also yield a magnetic energy transfer to the small-scales [19]. The magnetic energy transfer is primarily *local* and is found to be self-similar in the inertial range.

6) In the inertial range we found a dichotomy between the homologous transfers (defined as the transfers between kinetic and magnetic energy shells of same wave numbers) and non-homologous transfers (which are the transfers between shells of different wave numbers). These transfers are more complex than had been anticipated [18] and are summarised and discussed in detail in Section 4.6 (also see Fig. 4.9). From point (1) of this section we recall that the magnetic energy enhancement is mainly caused by the energy transfer to the large-scale magnetic field from the large-scale velocity field. This observation is important in lieu of the interest that exists regarding the physical mechanism responsible for the enhancement of magnetic energy. Pouquet [18] found that the large-scale magnetic energy is destablised by the small-scale magnetic energy. In context of 3-D turbulence, Pouquet and Patterson [21]

conjectured that energy is redistributed between the small-scale magnetic and kinetic energies and that the the enhancement of large-scale magnetic energy is due to an inverse cascade of magnetic energy from small-scale to large-scale magnetic field — we, infact find a forward cascade of magnetic energy. In a more recent work, Ishizawa and Hattori [19] attributed the enhancement of large-scale magnetic energy to energy transfer from small-scale velocity field to the large-scale magnetic field. We have also found such a transfer in our simulation. However, the strength of this transfer is much smaller as compared to the strength of energy transfer from large scale velocity field to the large scale magnetic field (from u-sphere to b-sphere).

The EDQNM closure calculations yield a net transfer of energy to the large-scale magnetic field from the small-scales (magnetic+kinetic) [18, 19]. In our simulations, the energy lost by the large-scale magnetic field to the small-scale magnetic field is much larger than the energy gained by the large-scale magnetic field from the small-scale velocity field. Hence, contrary to the predictions of EDQNM calculations, the large-scale magnetic field loses energy to the small-scales. A similar observation was also made by Ishizawa and Hattori in their simulations [20]. Thus, it appears that EDQNM calculations do not yield the correct strengths of the various transfers.

The picture obtained by us for the energy fluxes and the shell-to-shell transfers are consistent and complement each other. The fluxes and the transfer rates discussed here could find applications in the dynamo problem. In astrophysical objects, like galaxies and the sun, the magnetic field is thought to have arisen due to the amplification of a seed magnetic field. It must be borne in mind that our caclulations are two-dimsensional and devoid of magnetic helicity and kinetic helicity. A three-dimensional calculation (with the inclusion of magnetic and kinetic helicities) of various fluxes and shell-to-shell energy transfer rates will yield important insights on some unresolved issues concerning enhancement of magnetic energy.

In all the numerical simulations of previous chapters, an initial state was time evolved

using MHD equations. In the next chapter we will discuss the influence of the details of the initial state on the time evolution of some global quantities.

Chapter 5

Initial condition sensitivity of global quantities in magnetohydrodynamic turbulence

5.1 Introduction

In earlier chapters we had studied energy spectra and energy transfers using direct numerical simulations. Global quantities could affect the energy spectra and transfers. In Chapter 2, we had also considered the effect of global quantities like normalised cross-helicity on the energy spectra and certain energy fluxes. In this chapter we will study the influence of some fine details of the initial condition (to be specified below) on evolution of global quantities.

In fluid turbulence, the evolution of the velocity $\mathbf{u}(\mathbf{x})$ at a given position or of a given Fourier component $\mathbf{u}(\mathbf{k})$ is known to be sensitive to the details of the initial conditions, e.g., phases of $\mathbf{u}(\mathbf{k})$ (to be defined rigorously later). However, the evolution of global quantities like total energy are generally presumed to depend only on initial values of total energy and energy spectrum. The averaging over many modes appear to wash out the effects of the initial phases after a reasonably long time. The total energy in simulations with the same initial energy and spectrum, but with the modes chosen randomly, evolve along nearby trajectories: this is demonstrated in Fig. 5.1. It has been a common belief that in MHD turbulence also, the evolution of global quantities, e.g., total energy and cross helicity, depends only on the

initial values of global quantities and their spectra. The evolution of global quantities have earlier been studied by Ting et al. [31], Matthaeus et al. [29], Biskamp and Welter [8], Pouquet et al. [9] in which they found dynamic alignment and various other phenomena

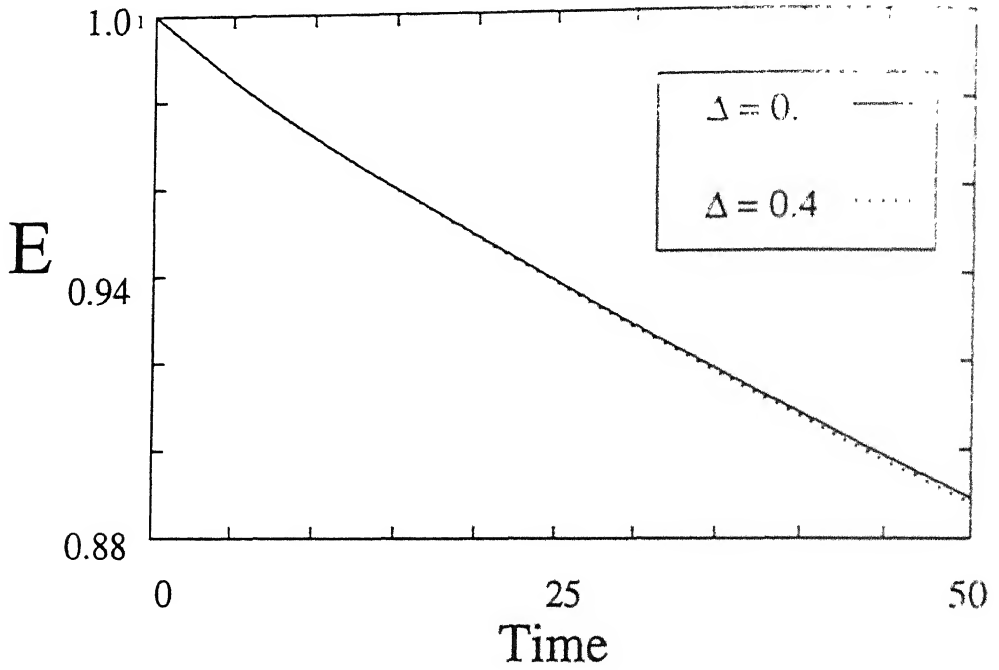

Figure 5.1: Energy evolution for fluids. The two cases shown here differ only in the phases of the initial conditions. The modes in the runs were $|\mathbf{u}(\mathbf{k})| \exp^{i(\theta_k + \Delta)}$ with $\Delta = 0.0$ and 0.4.

In this chapter we show numerically that under certain conditions in 2D MHD turbulence, the evolution of global quantities may not depend solely only on their initial values, but may depend significantly on more subtle features like the phases of complex Fourier modes (to be defined below) of the initially prescribed fields of the dynamical variables. In other words, a knowledge of the gross initial features as specified by the global quantities is not sufficient under all conditions to determine the evolution of global quantities. We only choose phases as a convenient way of demonstrating the inadequacy of specifying the initial global quantities and spectra alone for computing the evolution of certain global quantities. We find that the evolution of cross helicity shows sensitivity to the initial phases in simulations with small values of initial cross helicity.

The relevant global quadratic quantities for this chapter are

$$E^+ = \frac{1}{2}\int_{unit\ vol.} \left(\mathbf{z}^+\right)^2 d\mathbf{v} = \frac{1}{2}\sum_{\mathbf{k}} \left(\left|\mathbf{z}^+(\mathbf{k})\right|^2\right), \tag{5.1}$$

$$E^- = \frac{1}{2}\int_{unit\ vol} \left(\mathbf{z}^-\right)^2 d\mathbf{v} = \frac{1}{2}\sum_{\mathbf{k}} \left(\left|\mathbf{z}^-(\mathbf{k})\right|^2\right), \tag{5.2}$$

the magnetic energy,

$$\begin{aligned} E_b &= \frac{1}{2}\int_{unit\ vol.} \mathbf{b}^2 d\mathbf{v} \\ &= \frac{1}{8}\sum_{\mathbf{k}} \left(\left|\mathbf{z}^+(\mathbf{k})\right|^2 + \left|\mathbf{z}^-(\mathbf{k})\right|^2 - 2Re\left(\mathbf{z}^+(\mathbf{k})\cdot\tilde{\mathbf{z}}^-(\mathbf{k})\right)\right). \end{aligned} \tag{5.3}$$

and the fluid energy,

$$\begin{aligned} E_u &= \frac{1}{2}\int_{unit\ vol.} \mathbf{u}^2 d\mathbf{v} \\ &= \frac{1}{8}\sum_{\mathbf{k}} \left(\left|\mathbf{z}^+(\mathbf{k})\right|^2 + \left|\mathbf{z}^-(\mathbf{k})\right|^2 + 2Re\left(\mathbf{z}^+(\mathbf{k})\cdot\tilde{\mathbf{z}}^-(\mathbf{k})\right)\right). \end{aligned} \tag{5.4}$$

where $\tilde{\mathbf{z}}^+$ and $\tilde{\mathbf{z}}^-$ are complex conjugates of $\mathbf{z}^+$ and $\mathbf{z}^-$ respectively. The total energy is $E = (E^+ + E^-)/2$ and the cross helicity is $H_c = (E^+ - E^-)/2$.

The plan of the chapter is as follows. In Section 5.2 we define the problem which we tackle in this chapter. In Section 5.3 we describe the numerical procedure and the method of generating initial conditions for the different runs whose evolution is then compared in Section 5.4. The discussion follows in Section 5.5. The contents of this chapter are taken from the paper by Dar *et al.* [96].

5.2 Initial condition dependence.

We denote the complex Fourier modes $\mathbf{z}^{\pm}(\mathbf{k})$ by $|\mathbf{z}^{\pm}(\mathbf{k})|\exp(i\theta^{\pm}_{\mathbf{k}})$, where $\theta^{\pm}_{\mathbf{k}}$ are the phases of the modes. All the three global inviscid invariants E, H_c, and A are independent of phases. while the Alfvén ratio r_A depends on the phase difference $\theta^+_{\mathbf{k}} - \theta^-_{\mathbf{k}}$. Ting *et al.* [31] found that the Alfvén ratio affects the evolution of global quantities; it follows from their observations that the initial phase difference $\theta^+_{\mathbf{k}} - \theta^-_{\mathbf{k}}$ would affect the global evolution. In this paper

we demonstrate numerically that even keeping this initial phase difference fixed, change of absolute value of the initial phases $\theta_{\mathbf{k}}^{+}$ affects the global evolution.

In our simulations we investigate the effects of the initial phases on the temporal evolution of total energy E, normalised cross helicity σ_c, and Alfvén ratio r_A. The temporal evolution of σ_c has been the subject of investigation in a number of earlier studies [8, 9, 29, 31]. In several of these studies, σ_c has been observed to increase with time [8, 9, 29], a behaviour termed as dynamic alignment. However, Biskamp and Welter [8] observed in their simulations that the tendency towards dynamic alignment decreases with the increase in Reynolds number, and σ_c could even decrease at high enough Reynolds number [8]. Ting *et al.* [31] too observed a few cases of decreasing σ_c for small values of initial σ_c and E/A. In these earlier studies the effects of absolute phases had not been studied.

5.3 Simulation approach and initial conditions

We solve the 2-D incompressible MHD equations with hyperviscosity in Eqs. (2.7) of Chapter 2. The numerical algorithm applied to solve these equations has been discussed earlier in Section 2.3 of Chapter 2. For the simulations discussed in this chapter we choose $\nu = \mu = 5 \times 10^{-4}$ for runs on a grid of size 512×512, and we choose $\nu = \mu = 10^{-3}$ for runs on a grid of size 256×256. The hyperviscosity related parameter $k_{\mathbf{eq}}$ is chosen to be 20 for runs on both the grids. The time step dt used for these runs is 10^{-3}. The simulations are carried up to the final time $t_{final} = 50$.

The simulations are performed for various initial sets of σ_c and r_A values. The initial conditions are generated by first fixing r_A, σ_c, E. The chosen value of r_A determines the phase difference $\theta_{\mathbf{k}}^{+} - \theta_{\mathbf{k}}^{-}$. The initial E and σ_c determine $|\mathbf{z}^{\pm}(\mathbf{k})|$. Note that the absolute phase $\theta_{\mathbf{k}}^{+}$ is still a free parameter. Only modes within the annular region $1/2 \leq |\mathbf{k}| < 3/2$ are non-zero and each of the modes within this region receives equal energy (i.e., $|\mathbf{z}^{\pm}(\mathbf{k})|^2 = E^{\pm}/M$, where M is the number of modes in the shell). The initial states are generated thus for only half the modes - the remaining half are conjugate to them.

Run	N	Seed	r_A	Δ	$\sigma_c(t=0)$	$\sigma_c(t=50)$	σ_c increases/decreases
mhd1	512	50	1.5	0.	0.1	0.06	decreases
mhd1*	512	50	1.5	0.4	0.1	0.13	increases
mhd1**	512	575	1.5	0.	0.1	0.20	increases
mhd2	512	50	5.0	0.	0.1	0.22	increases
mhd2*	512	50	5.0	0.3	0.1	0.05	decreases
mhd2**	512	575	5.0	0.	0.1	0.13	increases
mhd3	256	50	5.0	0.	0.5	0.87	increases
mhd3*	256	50	5.0	0.4	0.5	0.88	increases
mhd4	64	50	1.5	0.	0.1	0.02	decreases
mhd4*	64	50	1.5	0.6	0.1	0.34	increases
mhd4**	64	50	1.5	1.0	0.1	0.17	increases
mhd5	64	50	2.0	0.	0.1	- 0.02	decreases
mhd5*	64	50	2.0	0.2	0.1	- 0.01	decreases
mhd5**	64	50	2.0	0.4	0.1	0.22	increases
mhd6	64	50	1.0	0.	0.5	0.79	increases
mhd6*	64	50	1.0	0.2	0.5	0.74	increases
mhd6**	64	50	1.0	0.4	0.5	0.72	increases

Table 5.1: Initial values of the random number generator seed Δ, σ_c and r_A for runs performed on grid of size $N \times N$. The initial and the final values (at $t_{final} = 50$) of σ_c are also shown.

The phase sensitivity of the evolution of σ_c, E, and r_A are studied by comparison of pa of simulations in which initial $\theta^+_{\mathbf{k}}$ are different. We change the initial phases in two ways. one case we change $\theta^+_{\mathbf{k}}$ uniformly for all the modes by an amount Δ, while in the other ca the phases are changed by using a different random seed in the random number generat The initial global quantities E, H_c, r_A, and their spectra remain unchanged under these pha changes. The evolution of σ_c for a variety of initial σ_c, r_A and Δ values are shown in Tab 5.1 (pairs of simulations are shown together; for example, mhd1 differs from mhd1* only that its initial $\mathbf{z}^{\pm}(\mathbf{k})$ fields have to be shifted from the latter's by $\Delta = 0.4$).

The $N = 512$ runs with $t_{final} = 50$ are very time intensive. Hence only the small init σ_c runs, which we found to be sensitive to the phases, were carried out for N=512. A lar number of runs were performed on N=64 to explore a wider range of initial conditions. A these results showed behaviour consistent with the results discussed below which are base on the high resolution runs N=256 and 512.

5.4 Results

In this section we will discuss the results of the simulations for the initial conditions descril in Table 5.1.

In our simulations, the small σ_c runs showed the most significant dependence on initi phase $\theta^+_{\mathbf{k}}$. For $\sigma_c = 0.1$ and $r_A = 1.5$, we choose Δ to be 0.0 and 0.4 in mhd1 and mhd respectively. It is seen in Fig. 5.2 that phase shifting has a marked effect on the evolution σ_c. For $\Delta = 0.0$ (mhd1) σ_c increases from its initial value of 0.1 to its final value of 0.12 whereas for $\Delta = 0.4$ (mhd1*), σ_c decreases to a final value of 0.06. The total energy (Fig. 5.3 and the Alfvén ratio (Fig. 5.4) do not appear to be affected much by the phase shift. We als compare two simulations (mhd1 and mhd1** in Table 5.1.) in which the initial phases ar generated using different random seeds. For these cases also the effect on the evolution σ_c (Fig. 5.2) is significant, but the corresponding effects on the evolution of the total energ (Fig. 5.3) and r_A (Fig. 5.4) are not noticeable.

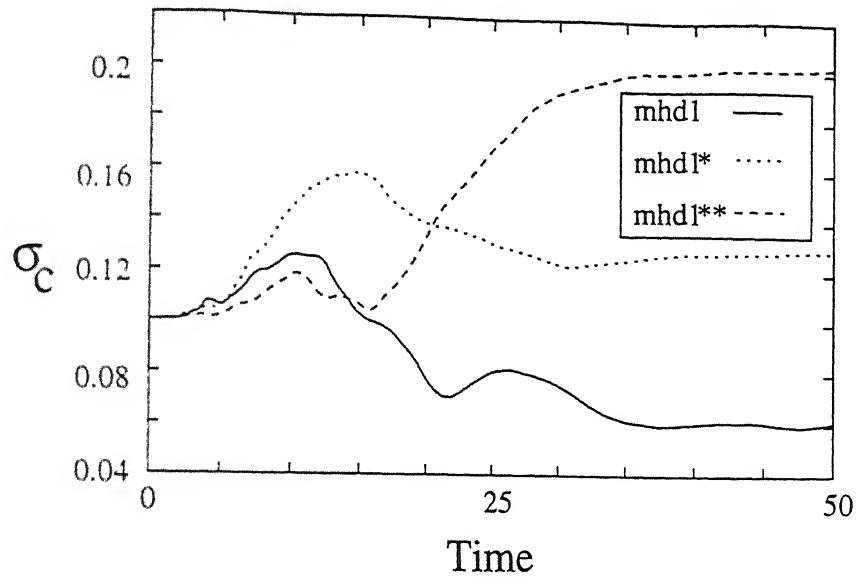

Figure 5.2: Normalised cross helicity (σ_c) evolution for initial $\sigma_c = 0.1$, $r_A = 1.5$. The curves shown correspond to mhd1, mhd1*, and mhd1** in Table 5.1.

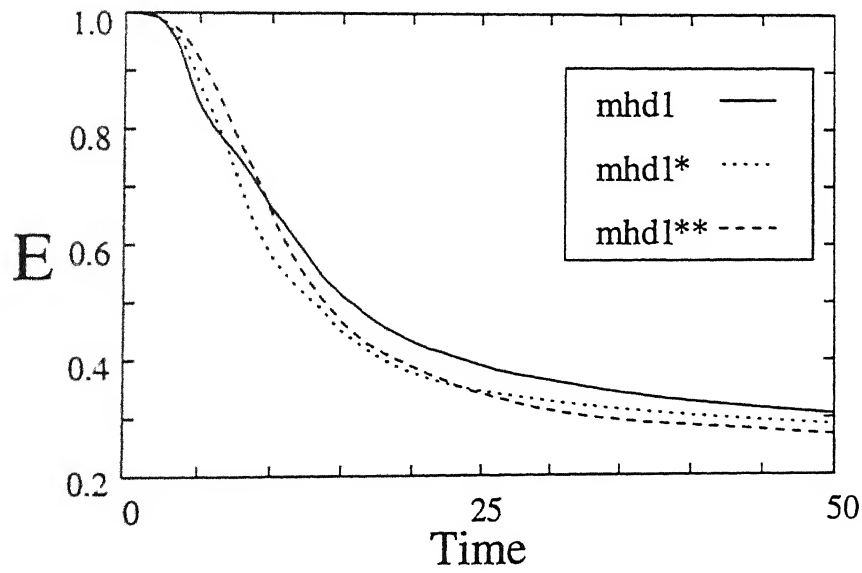

Figure 5.3: Evolution of total energy (E) for same initial conditions as in Fig. 5.2. See Table 5.1 for description of mhd1, mhd1*, and mhd1**.

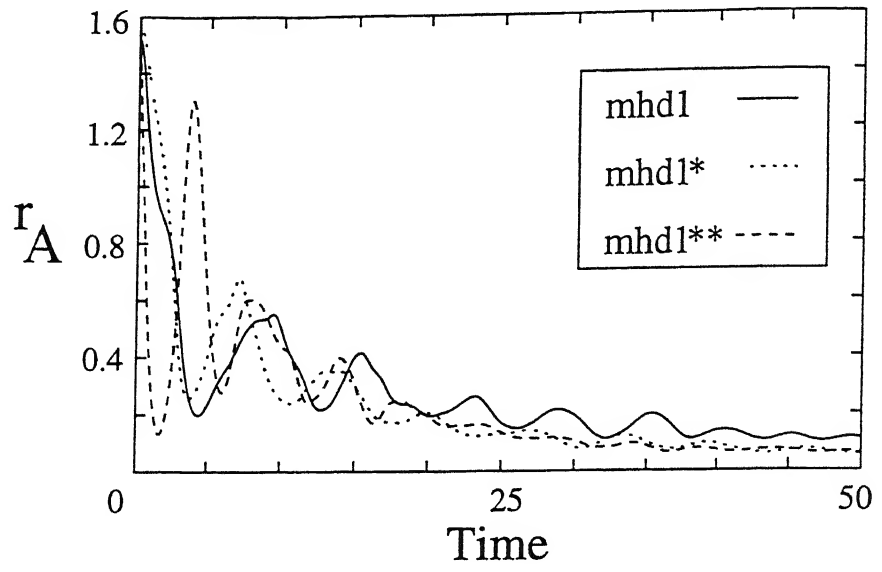

Figure 5.4: Evolution of Alfvén ratio (r_A) for same initial conditions as in Fig. 5.2. Look at Table 5.1 for description of mhd1, mhd1*, and mhd1**.

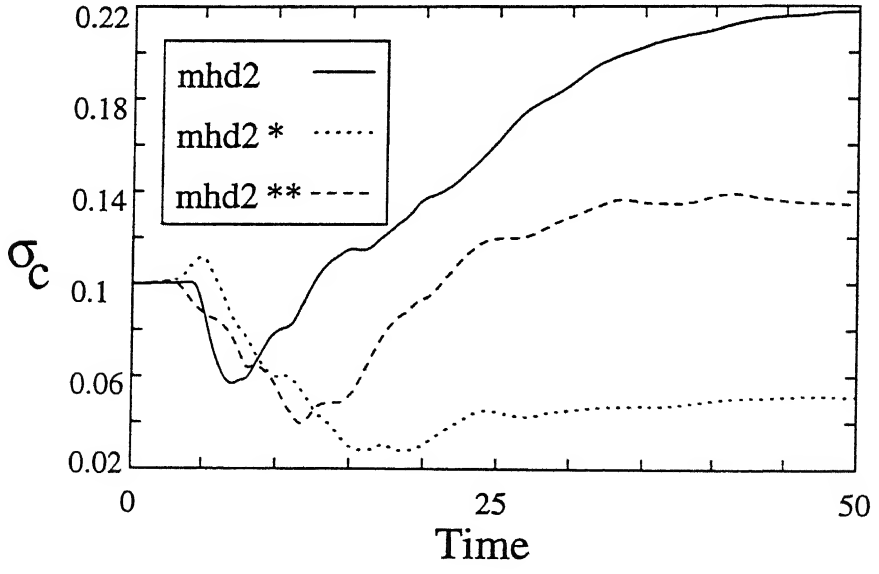

Figure 5.5: Normalised cross helicity (σ_c) evolution for initial $\sigma_c = 0.1$, $r_A = 5.0$. The curves shown correspond to mhd2, mhd2*, and mhd2** in Table 5.1

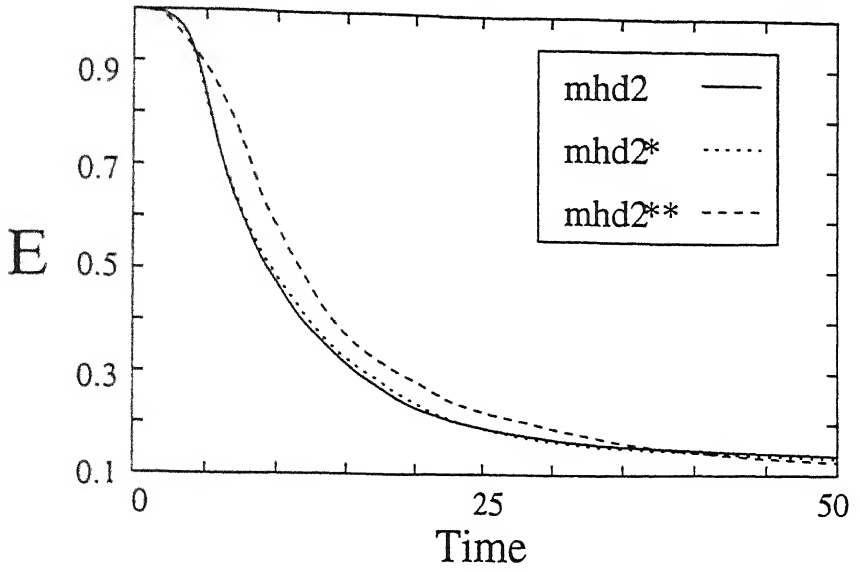

Figure 5.6: Evolution of total energy (E) for same initial conditions as in Fig. 5.5. Look at Table 5.1 for description of mhd2, mhd2*, and mhd2**.

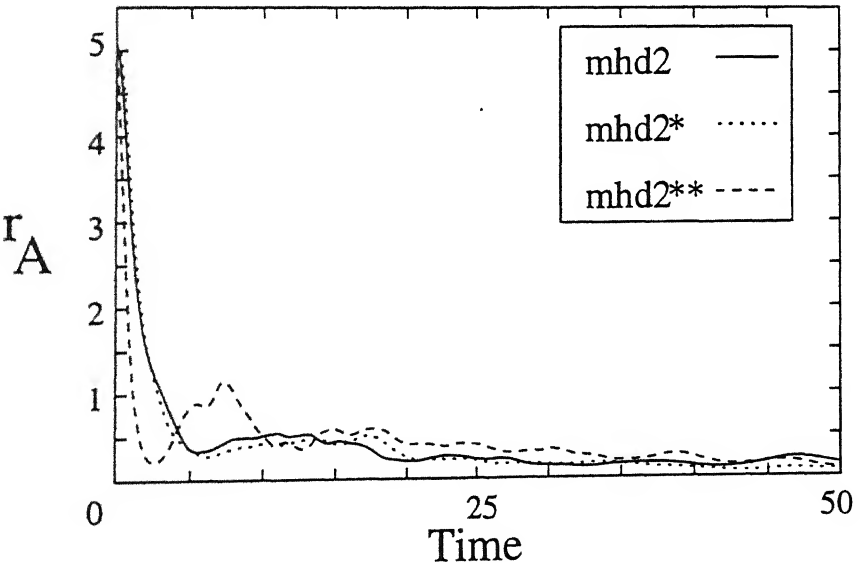

Figure 5.7: Evolution of Alfvén ratio (r_A) for same initial conditions as in Fig. 5.5. Look at Table 5.1 for description of mhd2, mhd2*, and mhd2**.

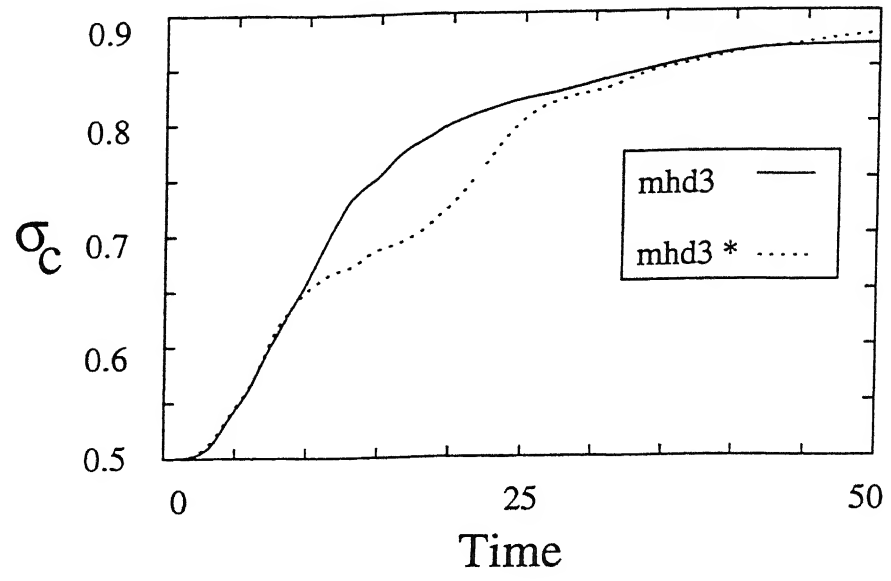

re 5.8: Normalised cross helicity (σ_c) evolution for initial $\sigma_c = 0.5$ and $r_A = 5.0$. The es shown correspond to mhd3, mhd3* in Table 5.1.

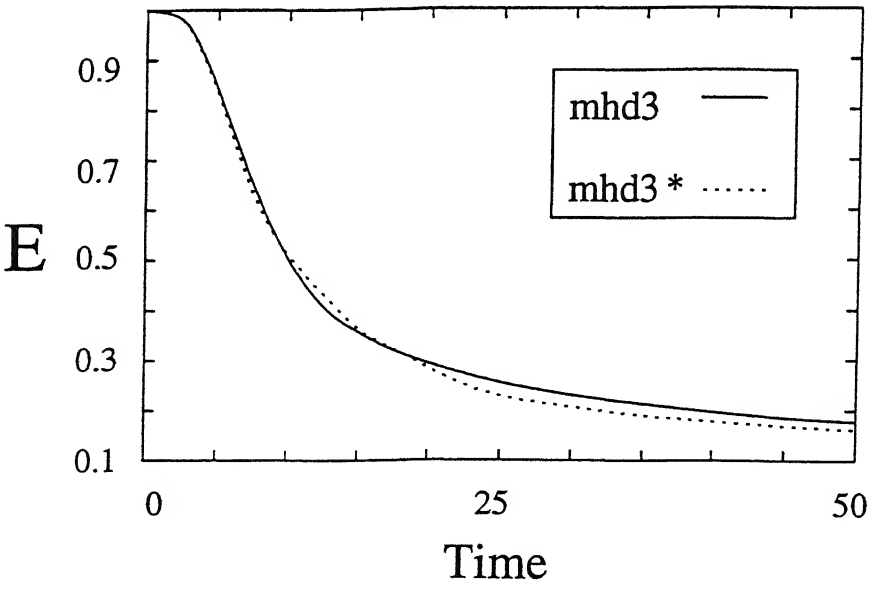

e 5.9: Evolution of total energy (E) for same initial conditions as in Fig. 5.8. Look at 5.1 for description of mhd3, mhd3*.

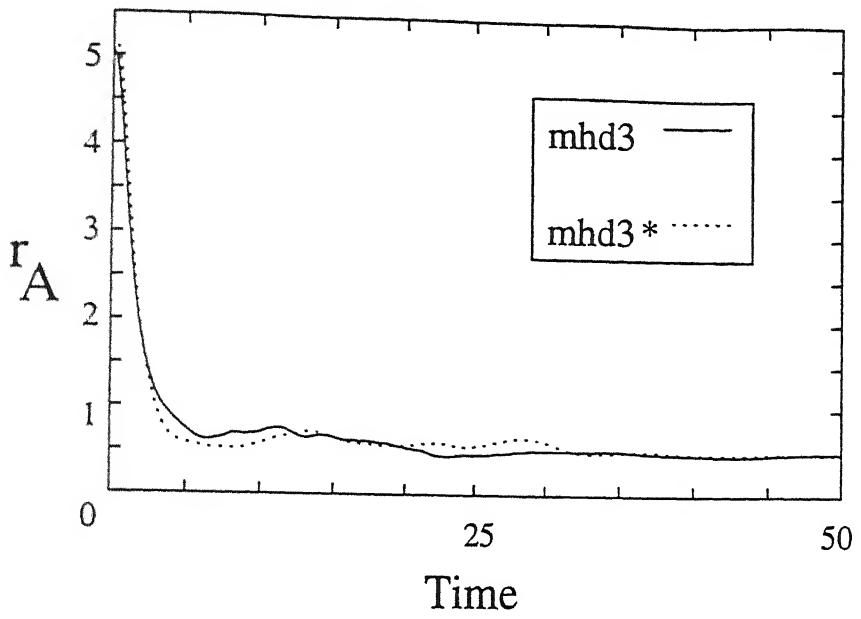

Figure 5.10: Evolution of Alfvén ratio for same initial conditions as in Fig. 5.8. Look at Table 5.1 for description of mhd3, mhd3*.

We also studied the effects of initial phases for the same initial σ_c, but with a large initial $r_A(5.0)$. The runs mhd2 and mhd2* show the effects of changing Δ, while mhd2 and mhd2** show the effects of different random number generator seeds. The results obtained for this case are similar to the run for initial condition with $r_A = 1.5$. In Fig. 5.5 it is seen that for initial value of $\Delta = 0.0$ (mhd2), σ_c increases and for initial $\Delta = 0.3$, σ_c decreases. The effect of changing Δ on the total energy (Fig. 5.6) and r_A (Fig. 5.7) is seen to be small. Similar results are obtained if we change the seed of the random number generator (compare mhd2 and mhd2**). Hence, σ_c (Fig. 5.5) is sensitive to the change in the initial phases whereas the total energy (Fig. 5.6) and r_A (Fig. 5.7) are not sensitive. Earlier, Ting *et al.* [31] had observed a decrease in σ_c for small initial σ_c.

We also perform runs at higher initial values of σ_c (mhd3 and mhd3* in Table 5.1). The effect of phase shifting for initial $\sigma_c = 0.5$ and $r_A = 5.0$ is shown in Figs. 5.8, 5.9, 5.10. It is seen in Fig. 5.8 that the changes in evolution caused by phase shifting are relatively smaller for high initial σ_c values as compared to small initial σ_c discussed above. From Fig. 5.9 it can be seen that the effect of Δ on total energy is also small and r_A (Fig. 5.10) remains

ensitive to the change in Δ. We have performed more runs than have been shown here in all cases σ_c was seen to increase for high σ_c values. This increase in σ_c is consistent h simulations performed earlier for high σ_c values [8, 9, 29–31].

5 Discussion

m the numerical results presented here we conclude that phases of the initial modes play an ortant role in the evolution of σ_c, atleast for cases with small initial σ_c values. For higher ues of σ_c, phases do not appear to affect the evolution of σ_c by any significant amount. In he runs the total energy and r_A were seen not to have any significant dependence on the ses.

The origin of the phase effects discussed here is not clear at this moment. We need to mine the evolution more carefully before reaching any definite conclusion. These studies ld find applications in understanding the solar wind observations in which σ_c has been erved to decrease [14, 15, 97, 98].

It has been demonstrated in the paper that the evolution of normalised cross helicity ignificantly affected by subtle features of the initial condition especially at low initial s helicities. This observation will require us to be more circumspect in drawing conclu- s based on arbitrary initial conditions and to exercise more care in choosing the initial litions in MHD turbulence.

Chapter 6

Conclusions

This thesis dealt primarily with two aspects of turbulence : 1) The scaling behaviour of energy spectra, and 2) the features of energy transfer between the velocity scales, the magnetic scales, and between the velocity and the magnetic scales. We briefly summarize our findings below and then we discuss a few future research directions.

6.1 Summary of results

We compared the predictions of the Kraichnan-Iroshnikov-Dobrowolony's phenomenology and the Kolmogorov-like phenomenology in our simulations. It was difficult to distinguish between the scaling exponents $-3/2$ and $-5/3$ from the plots of the energy spectra obtained from our simulations. So, following the approach suggested earlier by Verma *et al.* [11] we compared the fluxes Π^+ and Π^- since the KID phenomenology and Kolmogorov-like phenomenology make different predictions for the ratio of Π^+/Π^-. In our simulations we averaged our results over a steady state obtained by forcing small wavenumber modes, therefore giving better accuracy compared to Verma *et al*'s simulations. We also compared the results of Grappin's extension [4] of KID phenomenology with our simulations. We found that the KID phenomenology and its extension by Grappin are inconsistent with the simulation results, but the predictions of Kolmogorov-like phenomenology are in reasonably close agreement. Hence, our results favour the Kolmogorov-like phenomenology where the energy spectra is

proportional to $k^{-5/3}$. In addition to our own results, the Kolmogorov-like phenomenology is also supported by the Solar Wind data [14–16], higher Reynolds number simulations in 2-D and 3-D [12, 13], and a recent RG calculation [26]. We have studied the dependence of the Kolmogorov constants $C^{\pm}$ with σ_c (or E^+/E^-) and found that there is an approximate linear relationship between C^-/C^+ and (E^+/E^-). The constant $C^{\pm}$ are independent of σ_c over a wide range, and have a dependence on it only at low values (for C^+) and at high values for (for C^-).

An important component of turbulence phenomenologies and its description is the energy transfer between wavenumbers. The MHD and Navier-Stokes equations show that energy is transferred, in spectral space, to a mode $\mathbf{k}$ from modes $\mathbf{p}$ and $\mathbf{q}$ such that the three wavenumbers satisfy the condition $\mathbf{k}+\mathbf{p}+\mathbf{q}=\mathbf{0}$. The method for computing the *combined* energy transfer into mode $\mathbf{k}$ from the other two modes is well known. We devised an approach for describing the 'mode-to-mode' energy transfer between two modes of this triad, *mediated* by the third mode. We found that the mode-to-mode energy transfer is expressible as a sum of an 'effective transfer' and a 'circulating transfer'. These two have the property that the effective transfer contributes to the modal energy change, whereas the circulating transfer does not alter the modal energy because the energy transferred from $\mathbf{k}$ to $\mathbf{p}$ gets transferred from $\mathbf{p}$ to $\mathbf{q}$ and then back to $\mathbf{k}$ from $\mathbf{q}$. By imposing the requirements of rotational invariance, galilean invariance, finiteness, and retaining only certain linear terms in the series we showed that the circulating transfer is equal to zero. However, in absence of a complete proof, the value of the circulating transfer remains uncertain. Still, we have drawn important conclusions in terms of effective energy transfer which is independent of the circulating transfer. We introduced the idea of effective mode-to-mode transfer for energy transfer between a (1) pair of velocity modes, (2) a pair of magnetic modes, and (3) between a velocity and a magnetic mode in the triad. Using effective mode-to-mode transfer we defined energy fluxes and shell-to-shell transfers which cannot be defined in the older approach where only the combined transfer is known. The energy fluxes and shell-to-shell energy transfer rates were studied in a numerical

simulation of 2-D MHD turbulence and important conclusions were drawn.

We studied the energy fluxes and shell-to-shell energy transfer rates in a numerical simulation of 2-D MHD turbulence where white-noise velocity forcing is included at low wavenumbers. The results of energy cascade rates and the shell-to-shell transfer rates were obtained by averaging over a quasi-steady state. Several interesting observations were made in our simulations.

From the simulations we drew conclusions about the direction of energy transfer between different scales, and their relative magnitudes. The details of the energy transfers are explained in the conclusion of Chapter 4 and are pictorially represented in Figs. 4.3 and 4.9 of the same chapter. The most important outcome of our study can be stated in the following points : (1) Enhancement of magnetic energy occurs due to the energy transfer to the large-scale magnetic field from the large-scale velocity field, (2) there is a forward cascade of magnetic energy from the large-scale magnetic field to the small-scale magnetic field. Our results are important since they clarify some of the proposals made earlier regarding the physical mechanism for the generation of large-scale magnetic field. Pouquet [18] had found that the large-scale magnetic energy is destablised by the small-scale magnetic energy. Ishizawa and Hattori [19] proposed that the large-scale magnetic energy is enhanced due to energy transfer from the small-scale velocity field to the large-scale magnetic field. Although we find such a transfer, the dominant transfer to the large-scale magnetic energy is from the large-scale kinetic energy. Pouquet and Patterson [21] proposed in context of 3-D turbulence that there an inverse cascade of energy from small-scale to large-scale magnetic field. However, our numerical calculations give a forward cascade in 2-D turbulence. A simulation should be done to verify whether this feature is also present in 3-D turbulence.

Interestingly, we found an inverse cascade of kinetic energy to large-scale velocity field from small-scale velocity field, which was driven by the transfer of energy to the small-scale velocity field from the large-scale magnetic field. The inverse cascade was a result of *non-local* transfer to the large wavenumber velocity modes. Interestingly, the *local* transfer

had a forward cascade from the large-scale velocity field to the small-scale velocity field. By studying the energy transfer to a wavenumber-shell from all other wavenumber shells, we found that the 'homologous' (energy transfer between shells at same wavenumbers) transfers were responsible for the reverse transfer from magnetic to velocity field. The 'non-homologous' (energy transfer between shells at different wavenumbers) transfers were from the velocity to the magnetic field (see Chapter 4).

Numerical simulations of MHD turbulence are performed by time evolving an initial state. The initial condition is generated by fixing the global quantities, and the phases are generated randomly. It has been assumed till now that the random phases will have no influence on the evolution of global quantities. We found that evolution of σ_c can depend significantally on the random set of initial Fourier phases, atleast when σ_c is low. Hence we show that one should be careful in drawing conclusions based on simulations with arbitrary initial conditions and care must be exercised in choosing the initial condition.

6.2 Future research directions

In this thesis we have not considered the effect of a mean-magnetic field on the energy spectra and the fluxes. The turbulence phenomenologies assume isotropy. However, $\mathbf{B}_0$ is expected to introduce anisotropy in the energy spectra. A mean magnetic field is known to affect energy cascades in turbulence [84, 85]. However, the effect of $\mathbf{B}_0$ on the various energy cascades and shell-to-shell transfer rates was not investigated in this thesis. Since, most astrophysical plasmas are immersed in an external magnetic field it is important to study the effect of such a field on the energy transfers.

The dependence of the Kolomogorov constant $C^{\pm}$ only on σ_c was investigated. However, $C^{\pm}$ are also expected to depend on r_A. In future simulations, the effect of r_A should be studied.

The chief source of magnetic energy enhancement in 2-D is large-scale kinetic energy transfer to large-scale magnetic energy ($\Pi_{b<}^{u<}$). Our conjecture is that in 3-D too one probably

will observe such behaviour. Considering the implications of the results to dynamo theories, we believe that similar analysis for 3-D simulations will yield many important insights. We could not do the above analysis because of lack of computational power . We hope that the problem will be taken up in the future. Our study has been performed over a quasi steady state period with a low Alfvén ratio. In order to understand the build-up of magnetic energy starting from a seed value it is important to perform a similar study at high Alfvén ratio. We have done some preliminary decaying simulations for large Alfvén ratio in which the magnetic field increases, then saturates and finally decays. The growth of magnetic energy in the early phase is particularly interesting. A careful study in this direction is being carried out and will be reported at a later date.

In some of the popular models, like the α-dynamo [81], the mean magnetic field gets amplified in presence of helical fluctuations. The 2-D turbulence simulations discussed here does not have any helicity. The numerical verification of α-dynamo and similar models requires 3-D and somewhat complex field and geometry configurations. Still, we clearly see an increase in magnetic energy in the early phases. This mimics the magnetic energy enhancement in galaxies and the universe. Hence, our study presented here could possibly find application in the galactic dynamo.

The fluxes also find important applications in various phenomenological studies. For example, Verma *et al.* [99] estimated the turbulent dissipation rates in the Solar Wind and obtained the temperature variation of the Solar Wind as a function of distance. The various cascade rates discussed here could be useful for various astrophysical studies. For example, $\Pi^{u<}_{b<}$ and $\Pi^{u<}_{b>}$ can be used for studying the variation of r_A of the Solar Wind.

Recent numerical and analytical results appear to show that Kolmogorov-like phenomenology is applicable to MHD turbulence. Our results support this belief. Still higher resolution 2-D and 3-D numerical simulations and more exhaustive analytic calculations are necessary for drawing definite conclusions.

We have shown that very rich physics is present in energy transfer. We have investigated

some of its aspects. Full 3-D simulations will yield many valuable insights which will help us understand many complex processes, e.g.. MHD dynamo, local vs. nonlocal transfers, etc.

To conclude, we have discovered some important results in MHD turbulence. Yet, many more questions remain to be answered, and some new questions have been posed.

Appendix A

Derivation of the circulating transfer between the velocity modes in a triad

In Section 3.4 of Chapter 3 we showed that the mode-to-mode transfer is given by $\mathcal{T}^{uu} = \mathcal{S}^{uu} + X_\Delta$. We interpreted X_Δ as a circulating transfer and $\mathcal{S}^{uu}$ [Eq. (3.12)] as an effective mode-to-mode transfer. In this appendix we shall determine the circulating transfer X_Δ for fluid and MHD turbulence, using symmetry considerations. In the first section we shall discuss X_Δ in fluid turbulence and in the next section we will discuss the MHD turbulence.

A.1 X_Δ in fluid turbulence

The energy transfer between pair of modes should be invariant under a rotation (because it is a scalar), and galilean transformation, and it should be finite for all values of $\mathbf{k}$, $\mathbf{p}$, $\mathbf{q}$, $\mathbf{u(k)}$, $\mathbf{u(p)}$, $\mathbf{u(q)}$. We will determine the form of the circulating transfer by imposing these and a few other symmetry constraints.

We construct a scalar expression for X_Δ dependent on $\mathbf{k}$, $\mathbf{p}$, $\mathbf{q}$, $\mathbf{u(k)}$, $\mathbf{u(p)}$, $\mathbf{u(q)}$, and which is cubic in $\mathbf{u}$ and linear in $\mathbf{k}$, $\mathbf{p}$ or $\mathbf{q}$, to satisfy the for dimensional reasons. We write the general expression for such a scalar as

$$\begin{aligned} X_\Delta = Re(\ & [\mathbf{k}.\mathbf{u(q)}]\ \{[\mathbf{u(k)}.\mathbf{u(p)}]\alpha + [\mathbf{u(k)}.\mathbf{u(q)}]\beta + [\mathbf{u(p)}.\mathbf{u(q)}]\gamma + \\ & [\mathbf{u(k)}.\mathbf{u(k)}]\delta + [\mathbf{u(p)}.\mathbf{u(p)}]\nu + [\mathbf{u(q)}.\mathbf{u(q)}]\mu\} + \\ & [\mathbf{k}.\mathbf{u(p)}]\ \{[\mathbf{u(k)}.\mathbf{u(p)}]\eta + [\mathbf{u(k)}.\mathbf{u(q)}]\zeta + [\mathbf{u(p)}.\mathbf{u(q)}]\epsilon + \end{aligned}$$

$$
\begin{aligned}
& [\mathbf{u(k).u(k)}]\kappa + [\mathbf{u(p).u(p)}]\lambda + [\mathbf{u(q).u(q)}]\theta\} + \\
[\mathbf{p.u(k)}] \quad & \{[\mathbf{u(k).u(p)}]\psi + ... + [\mathbf{u(p).u(q)}]\omega + ... + [\mathbf{u(q).u(q)}]\lambda\} + \\
[\mathbf{p.u(q)}] \quad & \{[\mathbf{u(k).u(p)}]\tau + ... + [\mathbf{u(p).u(q)}]\phi + ... + [\mathbf{u(q).u(q)}]\varphi\} + \\
[\mathbf{q.u(k)}] \quad & \{[\mathbf{u(k).u(p)}]\sigma + ... + [\mathbf{u(p).u(q)}]\xi + ... + [\mathbf{u(q).u(q)}]\varsigma\} + \\
[\mathbf{q.u(p)}] \quad & [[\mathbf{u(k).u(p)}]\pi + [\mathbf{u(k).u(q)}]\rho + ... + [\mathbf{u(q).u(q)}]\varrho\}) \qquad \text{(A.1)}
\end{aligned}
$$

where all the coefficients α, β, etc. are atmost non-dimensional functions of the wavenumbers $\mathbf{k}$, $\mathbf{p}$, $\mathbf{q}$ and of $\mathbf{u(k)}$, $\mathbf{u(p)}$, $\mathbf{u(q)}$. '*Re*' in the expression in Eq. (A.1) indicates the real part of the expression. We should have infact written X_Δ as a linear combination of the real and the imaginary parts of the entire expression in the above equation. However, we will only consider the real part explicitly. The imaginary part can be treated in the same manner and the following conclusions, although explicitly stated for the real part will also be valid for the imaginary part. The most general expression should also contain terms of the kind $Re[\mathbf{k.u(q)}]Re[\mathbf{u(k).u(p)}]$, $Re[\mathbf{k.u(q)}]Im[\mathbf{u(k).u(p)}]$, and $Im[\mathbf{k.u(q)}]Im[\mathbf{u(k).u(p)}]$. However, we will explain below that such terms should not be present in X_Δ on account of galilean invariance. Hence, from the outset we do not include such terms. The task now is to determine the coefficients in Eq. (A.1).

The interactions involves all three modes of the triad, i.e., if the Fourier coefficients of any of the wavenumbers is zero, interaction between the modes is turned off. The mode-to-mode transfer should respect this fundamental feature of the triad interactions. Therefore, if $\mathbf{u(k)}$, $\mathbf{u(p)}$ or $\mathbf{u(q)}$ approach zero, X_Δ should approach zero as well. We have just argued above that α, β, etc., in Eq. (A.1) are independent of the magnitude of $\mathbf{u(k)}$, $\mathbf{u(p)}$, $\mathbf{u(q)}$. By inspecting Eq. (A.1) for X_Δ, we find that a few terms in the expression are independent of the magnitude of atleast one of the Fourier components. For example, the term $[\mathbf{k.u(q)}][\mathbf{u(k).u(q)}]\beta$ is independent of $\mathbf{u(p)}$. Such terms should be dropped from the expression of circulating transfer. After dropping such terms, we obtain

$$
\begin{aligned}
X_\Delta \; = Re(\; & [\mathbf{k.u(q)}][\mathbf{u(k).u(p)}]\alpha + [\mathbf{k.u(p)}][[\mathbf{u(k).u(q)}]\zeta + \\
\end{aligned}
$$

$$[\mathbf{p}.\mathbf{u}(\mathbf{k})][[\mathbf{u}(\mathbf{p}).\mathbf{u}(\mathbf{q})]\omega + [\mathbf{p}.\mathbf{u}(\mathbf{q})][[\mathbf{u}(\mathbf{k}).\mathbf{u}(\mathbf{p})]\tau +$$
$$[\mathbf{q}.\mathbf{u}(\mathbf{k})][[\mathbf{u}(\mathbf{p}).\mathbf{u}(\mathbf{q})]\xi + [\mathbf{q}.\mathbf{u}(\mathbf{p})][[\mathbf{u}(\mathbf{k}).\mathbf{u}(\mathbf{q})]\rho) \quad (A.2)$$

The requirement of finiteness of the mode-to-mode transfer imposes restrictions on the form of X_Δ. In Eq. (A.1) the dimensional terms are $[\mathbf{k}.\mathbf{u}(\mathbf{q})][[\mathbf{u}(\mathbf{k}).\mathbf{u}(\mathbf{p})]$, $[\mathbf{k}.\mathbf{u}(\mathbf{p})][[\mathbf{u}(\mathbf{k}).\mathbf{u}(\mathbf{q})]$, etc. and they are finite for all values of $\mathbf{k}$, $\mathbf{p}$, $\mathbf{q}$, $\mathbf{u}(\mathbf{k})$, $\mathbf{u}(\mathbf{p})$, $\mathbf{u}(\mathbf{q})$. The coefficients α, β, etc. are 'dimensionless scalars'. Therefore they can be written as

$$\alpha = f[\frac{\mathbf{k}.\mathbf{p}}{kp}, \frac{\mathbf{k}.\mathbf{p}}{kq}, ..., \frac{\mathbf{k}.\mathbf{u}(\mathbf{p})}{k|\mathbf{u}(\mathbf{p})|}, \frac{\mathbf{k}.\mathbf{u}(\mathbf{p})}{k|\mathbf{u}(\mathbf{q})|}, ..., \frac{\mathbf{u}(\mathbf{k}).\mathbf{u}(\mathbf{p})}{|\mathbf{u}(\mathbf{k})||\mathbf{u}(\mathbf{p})|}, \frac{\mathbf{u}(\mathbf{k}).\mathbf{u}(\mathbf{p})}{|\mathbf{u}(\mathbf{k})||\mathbf{u}(\mathbf{q})|}, ...] \quad (A.3)$$

where the arguments of the function have been non-dimensionalised. Consider triads in which one of the wavenumbers, say $\mathbf{q}$, tends to zero. Then the terms like $\mathbf{k}.\mathbf{p}/kq$ with $\mathbf{q}$ in the denominator diverge. Similarly if one of the Fourier coefficients, say $\mathbf{u}(\mathbf{q})$, is equal to zero, then the arguments $\frac{\mathbf{k}.\mathbf{u}(\mathbf{p})}{k|\mathbf{u}(\mathbf{q})|}$ and $\frac{\mathbf{u}(\mathbf{k}).\mathbf{u}(\mathbf{p})}{|\mathbf{u}(\mathbf{k})||\mathbf{u}(\mathbf{q})|}$, etc. diverge. Hence terms which depend on the magnitude of vectors must be dropped. Only the arguments which depend on the angles between vectors, e.g., $\frac{\mathbf{k}.\mathbf{u}(\mathbf{p})}{k|\mathbf{u}(\mathbf{p})|}$, $\frac{\mathbf{u}(\mathbf{k}).\mathbf{u}(\mathbf{p})}{|\mathbf{u}(\mathbf{k})||\mathbf{u}(\mathbf{p})|}$, should be included. Therefore, all the dimensionless coefficients should be a function of only these arguments, i.e., $\alpha = f[\frac{\mathbf{k}.\mathbf{p}}{kp}, ..., \frac{\mathbf{k}.\mathbf{u}(\mathbf{p})}{k|\mathbf{u}(\mathbf{p})|}, ..., \frac{\mathbf{u}(\mathbf{k}).\mathbf{u}(\mathbf{p})}{|\mathbf{u}(\mathbf{k})||\mathbf{u}(\mathbf{p})|}, ...]$.

We now write the coefficient α, ζ, etc. in the form

$$\alpha = \alpha^{(0)} + \alpha^{(1)} + \alpha^{(2)} + \alpha^{(3)} + \alpha^{(4)} + \alpha^{(5)} \quad (A.4)$$

where $\alpha^{(0)}$ is a constant, and

$$\alpha^{(1)} = \alpha_1^{(1)}\frac{\mathbf{k}.\mathbf{p}}{kp} + \alpha_2^{(1)}\frac{\mathbf{k}.\mathbf{q}}{kq} + \alpha_3^{(1)}\frac{\mathbf{p}.\mathbf{q}}{pq}, \quad (A.5)$$

$$\alpha^{(2)} = \alpha_1^{(2)}\frac{\mathbf{k}.\mathbf{u}(\mathbf{p})}{k|\mathbf{u}(\mathbf{p})|} + \alpha_2^{(2)}\frac{\mathbf{k}.\mathbf{u}(\mathbf{q})}{k|\mathbf{u}(\mathbf{q})|} + \alpha_3^{(2)}\frac{\mathbf{p}.\mathbf{u}(\mathbf{k})}{p|\mathbf{u}(\mathbf{k})|} + \alpha_4^{(2)}\frac{\mathbf{p}.\mathbf{u}(\mathbf{q})}{p|\mathbf{u}(\mathbf{q})|} + \alpha_5^{(2)}\frac{\mathbf{q}.\mathbf{u}(\mathbf{k})}{q|\mathbf{u}(\mathbf{k})|} + \alpha_6^{(2)}\frac{\mathbf{q}.\mathbf{u}(\mathbf{p})}{q|\mathbf{u}(\mathbf{p})|}, \quad (A.6)$$

$$\alpha^{(3)} = \alpha_1^{(3)}\frac{\mathbf{u}(\mathbf{k}).\mathbf{u}(\mathbf{p})}{|\mathbf{u}(\mathbf{k})||\mathbf{u}(\mathbf{p})|} + \alpha_2^{(3)}\frac{\mathbf{u}(\mathbf{k}).\mathbf{u}(\mathbf{q})}{|\mathbf{u}(\mathbf{k})||\mathbf{u}(\mathbf{q})|} + \alpha_3^{(3)}\frac{\mathbf{u}(\mathbf{p}).\mathbf{u}(\mathbf{q})}{|\mathbf{u}(\mathbf{p})||\mathbf{u}(\mathbf{q})|}. \quad (A.7)$$

The quantities $\alpha^{(1)}, \alpha^{(2)}, \alpha^{(3)}$ are 'linear' in the scalars of the type $\mathbf{k}.\mathbf{p}/kp$, $\mathbf{k}.\mathbf{u}(\mathbf{p})/k|\mathbf{u}(\mathbf{p})|$, and $\mathbf{u}(\mathbf{k}).\mathbf{u}(\mathbf{p})/|\mathbf{u}(\mathbf{k})||\mathbf{u}(\mathbf{p})|$ respectively. The quantity $\alpha^{(4)}$ contains terms like $(\mathbf{k}.\mathbf{p})^2/k^2p^2$,

$[\mathbf{k}.\mathbf{u}(\mathbf{p})]^2/k^2([\mathbf{u}(\mathbf{p}).\mathbf{u}(\mathbf{p})]$, etc. which are higher order in these scalars. All the other coefficients ζ, γ, ω, etc. in Eq. (A.1) can be similarly divided into linear and non-linear terms.

We now study the consequences of galilean invariance of X_Δ on Eq. (A.1). Consider two frames of reference S and S' with S moving with respect to S' with velocity $\mathbf{U_0}$. We denote the Fourier coefficient of velocity in frame S and S' by $\mathbf{u}(\mathbf{k})$ and $\mathbf{u}'(\mathbf{k})$ respectively. The relationship between $\mathbf{u}(\mathbf{k})$ and $\mathbf{u}'(\mathbf{k})$ is given by

$$\mathbf{u}'(\mathbf{k}) = \mathbf{u}(\mathbf{k}) \exp^{i(\mathbf{k}\,\mathbf{U_0})t} + \mathbf{U_0}\delta(\mathbf{k}). \tag{A.8}$$

The second term is non-zero only for the $\mathbf{k} = 0$ modes. In the subsequent discussion relating to galilean invariance we can drop this term for sake of simplicity without affecting the derivation. The transformation rule for scalars of the type $\mathbf{k}.\mathbf{p}$, $\mathbf{k}.\mathbf{u}(\mathbf{p})$, $\mathbf{u}(\mathbf{k}).\mathbf{u}(\mathbf{p})$ between the two frames of references S and S' can be deduced from the transformation property of $\mathbf{u}(\mathbf{k})$.

$$\mathbf{k}'.\mathbf{u}'(\mathbf{q}') = \mathbf{k}.\mathbf{u}(\mathbf{q}) \exp^{i(\mathbf{q}\,\mathbf{U_0})t} \tag{A.9}$$

$$\mathbf{u}'(\mathbf{k}').\mathbf{u}'(\mathbf{p}') = \mathbf{u}(\mathbf{k}).\mathbf{u}(\mathbf{p}) \exp^{i(\mathbf{k}+\mathbf{p}).\mathbf{U_0}t} \tag{A.10}$$

It follows from the above two transformation rules that $\mathbf{k}.\mathbf{u}(\mathbf{q})$ and $\mathbf{u}(\mathbf{k}).\mathbf{u}(\mathbf{p})$ are not invariant under a change of reference frame. However, a product of these quantities can be seen to be invariant

$$\begin{aligned}[\mathbf{k}'.\mathbf{u}'(\mathbf{q}')][\mathbf{u}'(\mathbf{k}').\mathbf{u}'(\mathbf{p}')] &= [\mathbf{k}.\mathbf{u}(\mathbf{q})][\mathbf{u}(\mathbf{k}).\mathbf{u}(\mathbf{p})] \exp^{i(\mathbf{k}+\mathbf{p}+\mathbf{q}).\mathbf{U_0}t} \\ &= [\mathbf{k}.\mathbf{u}(\mathbf{q})][\mathbf{u}(\mathbf{k}).\mathbf{u}(\mathbf{p})] \end{aligned} \tag{A.11}$$

using $\mathbf{k}+\mathbf{p}+\mathbf{q}=\mathbf{0}$. However,

$$Re[\mathbf{k}'.\mathbf{u}'(\mathbf{q}')]Re[\mathbf{u}'(\mathbf{k}').\mathbf{u}'(\mathbf{p}')] \neq Re[\mathbf{k}.\mathbf{u}(\mathbf{q})]Re[\mathbf{u}(\mathbf{k}).\mathbf{u}(\mathbf{p})], \tag{A.12}$$

$$Re[\mathbf{k}'.\mathbf{u}'(\mathbf{q}')]Im[\mathbf{u}'(\mathbf{k}').\mathbf{u}'(\mathbf{p}')] \neq Re[\mathbf{k}.\mathbf{u}(\mathbf{q})]Im[\mathbf{u}(\mathbf{k}).\mathbf{u}(\mathbf{p})], \tag{A.13}$$

and

$$Im[\mathbf{k}'.\mathbf{u}'(\mathbf{q}')]Im[\mathbf{u}'(\mathbf{k}').\mathbf{u}'(\mathbf{p}')] \neq Im[\mathbf{k}.\mathbf{u}(\mathbf{q})]Im[\mathbf{u}(\mathbf{k}).\mathbf{u}(\mathbf{p})] \tag{A.14}$$

Thus, we have shown that the terms of the kind given in the above three equations are not galilean invariant.

Clearly, the invariance under Galilean transformation demands that all of the vectors $\mathbf{u}(\mathbf{k})$, $\mathbf{u}(\mathbf{p})$, $\mathbf{u}(\mathbf{q})$ appear either once, twice, or n times in the scalar. A scalar of the type $[\mathbf{k}.\mathbf{u}(\mathbf{q})][\mathbf{u}(\mathbf{k}).\mathbf{u}(\mathbf{q})]$ having two or more repeated wavenumber indices is not invariant since the term appearing in the exponential is not zero for such a scalar. The transformation properties of any quantity formed from the scalars like $\mathbf{k}.\mathbf{p}$, $\mathbf{k}.\mathbf{u}(\mathbf{p})$, $\mathbf{u}(\mathbf{k}).\mathbf{u}(\mathbf{p})$ can be obtained in a similar manner. If the quantity is not galilean invariant then it should not be included in the expression for mode-to-mode transfer.

We have shown above that scalars of the type $\mathbf{k}.\mathbf{u}(\mathbf{q})$ and $\mathbf{u}(\mathbf{k}).\mathbf{u}(\mathbf{p})$ are not Galilean invariant [Eqs. (A.9) and (A.10)]. It follows that $\alpha^{(2)}$,$\beta^{(2)}$, etc., $\alpha^{(3)}$, $\beta^{(3)}$, etc. are not Galilean invariant. To preserve the Galilean invariance of X_Δ, the coefficients $\alpha^{(2)}$ and $\alpha^{(3)}$ should be dropped from Eq. (A.4). However, the nonlinear quantity $\alpha^{(4)}$ can be constructed in a Galilean invariant form. Currently, we have dropped these higher order terms. Our derivation of X_Δ therefore has the limitation of being strictly valid only upto the linear order. A complete proof containing all order of terms in X_Δ is beyond the scope of this thesis and is left for future work. After dropping the terms $\alpha^{(2)}, \alpha^{(3)}, \alpha^{(4)}$, the Eq. (A.4) reduces to

$$\alpha = \alpha^{(0)} + \alpha^{(1)} \tag{A.15}$$

Using equations (A.4) and (A.15) we now write X in Eq. (A.2) as,

$$\begin{aligned} X_\Delta \; = Re(\; & [\mathbf{k}.\mathbf{u}(\mathbf{q})][\mathbf{u}(\mathbf{k}).\mathbf{u}(\mathbf{p})]\{\alpha_0 + \alpha_1\frac{\mathbf{k}.\mathbf{p}}{kp} + \alpha_2\frac{\mathbf{k}.\mathbf{q}}{kq} + \alpha_3\frac{\mathbf{p}.\mathbf{q}}{pq}\} + \\ & [\mathbf{k}.\mathbf{u}(\mathbf{p})][\mathbf{u}(\mathbf{k}).\mathbf{u}(\mathbf{q})]\{\zeta_0 + \zeta_1\frac{\mathbf{k}.\mathbf{p}}{kp} + \zeta_2\frac{\mathbf{k}.\mathbf{q}}{kq} + \zeta_3\frac{\mathbf{p}.\mathbf{q}}{pq}\} + \\ & [\mathbf{p}.\mathbf{u}(\mathbf{k})][\mathbf{u}(\mathbf{p}).\mathbf{u}(\mathbf{q})]\{\omega_0 + \omega_1\frac{\mathbf{k}.\mathbf{p}}{kp} + \omega_2\frac{\mathbf{k}.\mathbf{q}}{kq} + \omega_3\frac{\mathbf{p}.\mathbf{q}}{pq}\} + \end{aligned}$$

$$[\mathbf{p}.\mathbf{u}(\mathbf{q})][\mathbf{u}(\mathbf{k}).\mathbf{u}(\mathbf{p})]\{\tau_0+\tau_1\frac{\mathbf{k}.\mathbf{p}}{kp}+\tau_2\frac{\mathbf{k}.\mathbf{q}}{kq}+\tau_3\frac{\mathbf{p}.\mathbf{q}}{pq}\}+$$
$$[\mathbf{q}.\mathbf{u}(\mathbf{k})][\mathbf{u}(\mathbf{p}).\mathbf{u}(\mathbf{q})]\{\xi_0+\xi_1\frac{\mathbf{k}.\mathbf{p}}{kp}+\xi_2\frac{\mathbf{k}.\mathbf{q}}{kq}+\xi_3\frac{\mathbf{p}.\mathbf{q}}{pq}\}+$$
$$[\mathbf{q}.\mathbf{u}(\mathbf{p})][\mathbf{u}(\mathbf{k}).\mathbf{u}(\mathbf{q})]\{\rho_0+\rho_1\frac{\mathbf{k}.\mathbf{p}}{kp}+\rho_2\frac{\mathbf{k}.\mathbf{q}}{kq}+\rho_3\frac{\mathbf{p}.\mathbf{q}}{pq}\}) \qquad (A.16)$$

We have dropped the superscript '1' from $\alpha_1^{(1)}, \alpha_2^{(1)}, \alpha_3^{(1)}$. Using the incompressibility relationship $\mathbf{q}.\mathbf{u}(\mathbf{q}) = \mathbf{0}$ we obtain $\mathbf{p}.\mathbf{u}(\mathbf{q}) = -(\mathbf{k}+\mathbf{q}).\mathbf{u}(\mathbf{q}) = -\mathbf{k}.\mathbf{u}(\mathbf{q})$. Therefore, fourth term in the above equation can be absorbed into the first term. Similarly, using the relationships $\mathbf{q}.\mathbf{u}(\mathbf{p}) = -\mathbf{k}.\mathbf{u}(\mathbf{p})$ and $\mathbf{q}.\mathbf{u}(\mathbf{k}) = -\mathbf{p}.\mathbf{u}(\mathbf{k})$, the last term can be combined with the second term and the fifth term combined with the third term. Now, we can write

$$X_\Delta = Re(\ [\mathbf{k}.\mathbf{u}(\mathbf{q})][\mathbf{u}(\mathbf{k}).\mathbf{u}(\mathbf{p})]\{\alpha_0+\alpha_1\frac{\mathbf{k}.\mathbf{p}}{kp}+\alpha_2\frac{\mathbf{k}.\mathbf{q}}{kq}+\alpha_3\frac{\mathbf{p}.\mathbf{q}}{pq}\}+$$
$$[\mathbf{k}.\mathbf{u}(\mathbf{p})][\mathbf{u}(\mathbf{k}).\mathbf{u}(\mathbf{q})]\{\zeta_0+\zeta_1\frac{\mathbf{k}.\mathbf{p}}{kp}+\zeta_2\frac{\mathbf{k}.\mathbf{q}}{kq}+\zeta_3\frac{\mathbf{p}.\mathbf{q}}{pq}\}+$$
$$[\mathbf{p}.\mathbf{u}(\mathbf{k})][\mathbf{u}(\mathbf{p}).\mathbf{u}(\mathbf{q})]\{\omega_0+\omega_1\frac{\mathbf{k}.\mathbf{p}}{kp}+\omega_2\frac{\mathbf{k}.\mathbf{q}}{kq}+\omega_3\frac{\mathbf{p}.\mathbf{q}}{pq}\}) \qquad (A.17)$$

by making the replacements $(\alpha-\tau)\to\alpha$, $(\zeta-\rho)\to\zeta$ and $(\omega-\xi)\to\omega$.

The quantity X_Δ represents the energy circulating in the anti-clockwise direction, i.e., X_Δ flows along $\mathbf{p}\to\mathbf{k}\to\mathbf{q}\to\mathbf{p}$ [see Fig. 3.4 in Section 3.4.2]. We will now denote the circulating transfer along $\mathbf{p}\to\mathbf{k}$ by $X(\mathbf{k}|\mathbf{p}|\mathbf{q})$, transfer along $\mathbf{k}\to\mathbf{q}$ by $X(\mathbf{q}|\mathbf{k}|\mathbf{p})$ and so on for the circulating transfer between each pair of modes. The above X_Δ is the circulating transfer from $\mathbf{p}$ to $\mathbf{k}$, i.e., $X(\mathbf{k}|\mathbf{p}|\mathbf{q}|) \equiv X_\Delta$. Then by symmetry the circulating transfer from $\mathbf{q}$ to $\mathbf{k}$ can be written as

$$X(\mathbf{k}|\mathbf{q}|\mathbf{p}) = Re(\ [\mathbf{k}.\mathbf{u}(\mathbf{p})][\mathbf{u}(\mathbf{k}).\mathbf{u}(\mathbf{q})]\{\alpha_0+\alpha_1\frac{\mathbf{k}.\mathbf{q}}{kq}+\alpha_2\frac{\mathbf{k}.\mathbf{p}}{kp}+\alpha_3\frac{\mathbf{p}.\mathbf{q}}{pq}\}+$$
$$[\mathbf{k}.\mathbf{u}(\mathbf{q})][\mathbf{u}(\mathbf{k}).\mathbf{u}(\mathbf{p})]\{\zeta_0+\zeta_1\frac{\mathbf{k}.\mathbf{q}}{kq}+\zeta_2\frac{\mathbf{k}.\mathbf{p}}{kp}+\zeta_3\frac{\mathbf{p}.\mathbf{q}}{pq}\}+$$
$$[\mathbf{q}.\mathbf{u}(\mathbf{k})][\mathbf{u}(\mathbf{p}).\mathbf{u}(\mathbf{q})]\{\omega_0+\omega_1\frac{\mathbf{k}.\mathbf{q}}{kq}+\omega_2\frac{\mathbf{k}.\mathbf{p}}{kp}+\omega_3\frac{\mathbf{p}.\mathbf{q}}{pq}\}), \qquad (A.18)$$

and the circulating transfer from p to k is

$$\begin{aligned} X(\mathbf{p}|\mathbf{k}|\mathbf{q}) = Re\{ & [\mathbf{p}.\mathbf{u}(\mathbf{q})][\mathbf{u}(\mathbf{k}).\mathbf{u}(\mathbf{p})]\{\alpha_0 + \alpha_1\frac{\mathbf{k}.\mathbf{p}}{kp} + \alpha_2\frac{\mathbf{p}.\mathbf{q}}{pq} + \alpha_3\frac{\mathbf{k}.\mathbf{q}}{kq}\} + \\ & [\mathbf{p}.\mathbf{u}(\mathbf{k})][\mathbf{u}(\mathbf{p}).\mathbf{u}(\mathbf{q})]\{\zeta_0 + \zeta_1\frac{\mathbf{k}.\mathbf{p}}{kp} + \zeta_2\frac{\mathbf{p}.\mathbf{q}}{pq} + \zeta_3\frac{\mathbf{k}.\mathbf{q}}{kq}\} + \\ & [\mathbf{k}.\mathbf{u}(\mathbf{p})][\mathbf{u}(\mathbf{k}).\mathbf{u}(\mathbf{q})]\{\omega_0 + \omega_1\frac{\mathbf{k}.\mathbf{p}}{kp} + \omega_2\frac{\mathbf{p}.\mathbf{q}}{pq} + \omega_3\frac{\mathbf{k}.\mathbf{q}}{kq}\}) \end{aligned} \tag{A.19}$$

From Fig. 3.4 in Chapter 3. $X(\mathbf{k}|\mathbf{p}|\mathbf{q})$ flows along the anti-clockwise direction while $X(\mathbf{k}|\mathbf{q}|\mathbf{p})$ and $X(\mathbf{p}|\mathbf{k}|\mathbf{q})$ flows along the clockwise direction. The former should therefore be equal and opposite to the latter two transfers, i.e.,

$$X(\mathbf{k}|\mathbf{p}|\mathbf{q}) + X(\mathbf{k}|\mathbf{q}|\mathbf{p}) = 0. \tag{A.20}$$

and

$$X(\mathbf{k}|\mathbf{p}|\mathbf{q}) + X(\mathbf{p}|\mathbf{k}|\mathbf{q}) = 0. \tag{A.21}$$

Substitution of expressions $X(\mathbf{k}|\mathbf{p}|\mathbf{q})$, $X(\mathbf{k}|\mathbf{q}|\mathbf{p})$, $X(\mathbf{p}|\mathbf{k}|\mathbf{q})$ [Eqs. (A.17)-(A.19)] into the first of these two relationships yields

$$\begin{aligned} & [\mathbf{k}.\mathbf{u}(\mathbf{q})][\mathbf{u}(\mathbf{k}).\mathbf{u}(\mathbf{p})]\{(\alpha_0 + \zeta_0) + (\alpha_1 + \zeta_2)\frac{\mathbf{k}.\mathbf{p}}{kp} + (\alpha_2 + \zeta_1)\frac{\mathbf{k}.\mathbf{q}}{kq} + (\alpha_3 + \zeta_3)\frac{\mathbf{p}.\mathbf{q}}{pq}\} \\ & [\mathbf{k}.\mathbf{u}(\mathbf{p})][\mathbf{u}(\mathbf{k}).\mathbf{u}(\mathbf{q})]\{(\zeta_0 + \alpha_0) + (\zeta_1 + \alpha_2)\frac{\mathbf{k}.\mathbf{p}}{kp} + (\zeta_2 + \alpha_1)\frac{\mathbf{k}.\mathbf{q}}{kq} + (\zeta_3 + \alpha_3)\frac{\mathbf{p}.\mathbf{q}}{pq}\} \\ & [\mathbf{p}.\mathbf{u}(\mathbf{k})][\mathbf{u}(\mathbf{p}).\mathbf{u}(\mathbf{q})]\{(\omega_1 - \omega_2)\frac{\mathbf{k}.\mathbf{p}}{kp} + (\omega_2 - \omega_1)\frac{\mathbf{k}.\mathbf{q}}{kq}\} = 0. \end{aligned} \tag{A.22}$$

and

$$\begin{aligned} & [\mathbf{k}.\mathbf{u}(\mathbf{q})][\mathbf{u}(\mathbf{k}).\mathbf{u}(\mathbf{p})]\{(\alpha_2 - \alpha_3)\frac{\mathbf{k}.\mathbf{q}}{kq} + (\alpha_3 - \alpha_2)\frac{\mathbf{p}.\mathbf{q}}{pq}\} \\ & + [\mathbf{k}.\mathbf{u}(\mathbf{p})][\mathbf{u}(\mathbf{k}).\mathbf{u}(\mathbf{q})]\{(\zeta_0 + \omega_0) + (\zeta_1 + \omega_1)\frac{\mathbf{k}.\mathbf{p}}{kp} + (\zeta_2 + \omega_3)\frac{\mathbf{k}.\mathbf{q}}{kq} + (\zeta_3 + \omega_2)\frac{\mathbf{p}.\mathbf{q}}{pq}\} \\ & + [\mathbf{p}.\mathbf{u}(\mathbf{k})][\mathbf{u}(\mathbf{p}).\mathbf{u}(\mathbf{q})]\{(\omega_0 + \zeta_0) + (\omega_1 + \zeta_1)\frac{\mathbf{k}.\mathbf{p}}{kp} + (\omega_2 + \zeta_3)\frac{\mathbf{k}.\mathbf{q}}{kq} + (\omega_3 + \zeta_2)\frac{\mathbf{p}.\mathbf{q}}{pq}\} = 0. \end{aligned} \tag{A.23}$$

Each of the three terms in the two equations above has a different functional dependence on $\mathbf{u(k)}$, $\mathbf{u(p)}$, $\mathbf{u(q)}$. If we only rotate $\mathbf{u(k)}$ about $\mathbf{k}$ without changing its magnitude then each of the terms will change by a different factor depending on the direction of $\mathbf{u(p)}$, $\mathbf{u(q)}$ which can be independently chosen. Since the sum of three terms should be zero and each term can change a different factor, each of the terms should be individually zero. In addition, this should hold for all wavenumber triads. Therefore each term inside the curly bracket should also be individually zero. This condition gives the the following relationships between the constants: $\alpha_0 + \zeta_0 = 0, \alpha_1 + \zeta_2 = 0, \alpha_2 + \zeta_1 = 0, \alpha_3 + \zeta_3 = 0, \omega_1 - \omega_2 = 0$ from Eq. (A.22), and $\omega_0 + \zeta_0 = 0, \alpha_2 - \alpha_3 = 0, \zeta_1 + \omega_1 = 0, \zeta_2 + \omega_3 = 0, \zeta_3 + \omega_2 = 0$ from Eq. (A.23).

We now consider the following geometry - the wavenumber triad form an isosceles triangle with $|\mathbf{p}| = |\mathbf{q}|$, and the Fourier modes $\mathbf{u(p)}$ and $\mathbf{u(q)}$ are perpendicular to the plane of $\mathbf{k}$, $\mathbf{p}$, $\mathbf{q}$ and are equal in magnitude. For this geometry the clockwise and the anti-clockwise direction are equivalent. There is no preferred direction along which the circulating transfer may flow. Therefore, for the geometry shown the circulating transfer should be zero. We may now write the circulating transfer [Eq. (A.17)] for this geometry as

$$\begin{aligned} X &= Re\Big([\mathbf{p.u(k)}][\mathbf{u(p).u(q)}]\{(\omega_1+\omega_2)\frac{\mathbf{k.p}}{kp} + \omega_3\frac{\mathbf{p.q}}{pq} + a\}\Big) \\ &= 0 \end{aligned} \tag{A.24}$$

With $\mathbf{u(p)}$ and $\mathbf{u(q)}$ fixed perpendicular to the plane of the triad, X should be zero for all wavenumber triads which form an isosceles triangle. For X to be zero for every such geometry, each term inside the curly bracket should be equated to zero giving the additional relationships: $\omega_1 = -\omega_2, \omega_3 = 0, \omega_0 = 0$.

We have obtained 17 relationships between the constants α, ζ, etc. These equations may be solved to get the values of all these constants. It can be verified that the only solution of these equations is α's= 0, ζ's= 0, ω's= 0, $a = b = c = 0$.

Therefore we get $X = 0$. It follows that the mode-to-mode transfer $\mathcal{R}^{uu} = \mathcal{S}^{uu}$.

We have thus determined the mode-to-mode transfer. The proof used rotational in-

variance, galilean invariance, finiteness of mode-to-mode transfer, and symmetry of X with respect to k, p, q, u(k), u(p), u(q). However, in the series we have taken only linear terms in k.p, k.u(p), u(k).u(p). A complete proof containing all orders of terms is beyond the scope of this thesis. It may be possible to obtain a completely general proof by finding some symmetries which we have ignored in our proof. Otherwise a novel approach may be required.

A.2 X_Δ in MHD turbulence

The circulating transfer between the velocity modes in MHD can also be shown to be equal to zero to linear order terms in $\mathbf{k.p}, \mathbf{k.u(p)}, \mathbf{u(k).u(p)}$. The arguments leading to this are nearly the same as that for the fluid case. However, we additionally need to show that the general expression for the circulating transfer X_Δ for MHD should not contain $\mathbf{b(k)}$, $\mathbf{b(p)}$, $\mathbf{b(q)}$ and can also be given by Eq. (A.1)

In the previous section we showed that each term in X_Δ should depend on $\mathbf{u(k)}$, $\mathbf{u(p)}$, $\mathbf{u(q)}$ — this followed from the fundamentally three-mode feature of the interactions. The expression for the combined energy transfer to $\mathbf{u(k)}$ from $\mathbf{u(p)}$ and $\mathbf{u(q)}$ is identical for the fluid and for the MHD case. Hence, in the case of MHD also, each term in the circulating transfer between the velocity modes should be dependent on $\mathbf{u(k)}$, $\mathbf{u(p)}$, and $\mathbf{u(q)}$. Thus, the general expression for the circulating transfer between the velocity modes in MHD is the same as that for Fluid turbulence. The rest of the arguments leading to $X_\Delta = 0$ in MHD are identical to those in Section A.1.

Appendix B

Derivation of circulating transfer between the magnetic modes in a triad

In Section 3.7.2 we had shown that the mode-to-mode transfer from $\mathbf{b(p)}$ to $\mathbf{b(k)}$ can be written as $\mathcal{R}^{bb} = \mathcal{S}^{bb} + Y_\Delta$, where $\mathcal{S}^{bb}$ given by Eq. (3.49) is the effective transfer between the modes and Y_Δ is the circulating transfer. In this section we will derive the expression for the circulating transfer Y_Δ. The derivation for Y_Δ is similar to the derivation of X_Δ for fluid turbulence given in Appendix A.

Since the mode-to-mode transfer is a scalar, the circulating transfer Y_Δ will also be a scalar with a dependence on the wavenumbers $\mathbf{k}$, $\mathbf{p}$, $\mathbf{q}$ and the Fourier coefficients $\mathbf{u(k)}$, $\mathbf{u(p)}$, $\mathbf{u(q)}$, $\mathbf{b(k)}$, $\mathbf{b(p)}$, $\mathbf{b(q)}$. It should be linear in $\mathbf{k}$, $\mathbf{p}$ or $\mathbf{q}$ and cubic in the Fourier coefficients $\mathbf{u(k)}$, $\mathbf{u(p)}$, $\mathbf{u(q)}$, $\mathbf{b(k)}$, $\mathbf{b(p)}$, $\mathbf{b(q)}$ for dimensional reasons.

The most general form of Y_Δ that satisfies these properties can be written as

$$Y_\Delta = Y_\Delta^{(1)} + Y_\Delta^{(2)} + Y_\Delta^{(3)} + Y_\Delta^{(4)} \tag{B.1}$$

where

$$\begin{aligned} Y_\Delta^{(1)} = Re(\quad & [\mathbf{k.u(q)}] \quad \{[\mathbf{u(k).b(k)}]... + [\mathbf{u(k).b(p)}]... + [\mathbf{u(k).b(q)}]... + \\ & \qquad [\mathbf{u(p).b(k)}]... + [\mathbf{u(p).b(p)}]... + [\mathbf{u(p).b(q)}]... + \\ & \qquad \{[\mathbf{u(q).b(k)}]... + [\mathbf{u(q).b(p)}]... + [\mathbf{u(q).b(q)}]...\} + \\ & [\mathbf{k.u(p)}] \quad \{[\mathbf{u(k).b(k)}]... + ... + [\mathbf{u(k).b(q)}]... + ... + [\mathbf{u(q).b(k)}]... + ... + [\mathbf{u(q).b(} \end{aligned}$$

$$[p.u(k)] \quad \{[u(k).b(k)]... + ... + [u(p).b(q)]... + ... + [u(q).b(p)]... + ... + [u(q).b(q)]...\}$$

(B

$$Y_{\Delta}^{(2)} = R\epsilon(\quad [k.u(q)] \quad \{[b(k).b(k)] + [b(k).b(p)]\alpha + [b(k).b(q)]... +$$

$$[b(p).b(p)] + [b(p).b(q)]... + [b(q).b(q)]...\} +$$

$$[k.u(p)] \quad \{[b(k).b(k)]... + ... + [b(k).b(q)]\beta + ... + [b(q).b(q)]...\} +$$

$$[p.u(k)] \quad \{[b(k).b(k)]... + ... + [b(p).b(q)]\gamma + ... + [b(q).b(q)]...\})$$

(B.3)

$$= R\epsilon(\quad [k.b(q)] \quad \{[u(k).b(k)]... + [u(k).b(p)]\delta + [u(k).b(q)]... +$$

$$[u(p).b(k)]\eta + [u(p).b(p)]... + [u(p).b(q)]... +$$

$$\{[u(q).b(k)]... + [u(q).b(p)]... + [u(q).b(q)]...\} +$$

$$[k.b(p)] \quad \{[u(k).b(k)]... + ... + [u(k).b(q)]\mu + ... + [u(q).b(k)]\nu + ... + [u(q).b(q)]...\} +$$

$$[p.b(k)] \quad \{[u(k).b(k)]... + ... + [u(p).b(q)]\psi + ... + [u(q).b(p)]\chi + [u(q).b(q)]...\})$$

(B.

$$Y_{\Delta}^{(4)} = R\epsilon(\quad [k.b(q)] \quad \{[u(k).u(k)]... + [u(k).u(p)]\theta + [u(k).u(q)]... +$$

$$[u(p).u(p)]... + [u(p).u(q)]... + [u(q).u(q)]...\} +$$

$$\{[u(q).b(k)]... + [u(q).b(p)]... + [u(q).b(q)]...\} +$$

$$[k.b(p)] \quad \{[u(k).u(k)]... + [u(k).u(q)]\phi + ... + [u(q).u(q)]...\} +$$

$$[p.b(k)] \quad \{[u(k).u(k)]... + [u(p).u(q)]\xi + ... + [u(q).u(q)]...\})$$

(B.5)

Following Appendix A we consider explicitly only the real part, which is denoted by Re in the above equations. If we take a linear combination of the real and the imaginary parts instead, the derivation and the conclusions regarding Y_Δ will not change. In addition, terms of the $Re[\mathbf{k.u(q)}]Re[\mathbf{u(k).u(p)}]$, $Re[\mathbf{k.u(q)}]Re[\mathbf{u(k).b(p)}]$, etc. are not included as they violate galilean invariance - we had explained this in Appendix A in context of X_Δ. The three dots '...' in the above equations in front of some of the terms indicate that a coefficient multiplies each of these terms but which we have not shown explicitly as they do not enter most of the future discussion. The coefficients α, β, etc. in the above expressions for $Y_\Delta^{(1)}$... $Y_\Delta^{(4)}$ are non-dimensional functions of the wavenumbers $\mathbf{k}$, $\mathbf{p}$, $\mathbf{q}$ and of $\mathbf{u(k)}$, $\mathbf{u(p)}$, $\mathbf{u(q)}$, $\mathbf{b(k}$, $\mathbf{b(p)}$, $\mathbf{b(q)}$. To determine Y_Δ we should now determine these coefficients. Note that besides the terms of the kind $[\mathbf{k.u(q)}]\{...\}, [\mathbf{k.u(p)}]\{...\}, [\mathbf{p.u(k)}]\{...\}$ in Eqs. (B.2)-(B.5), there are also terms of the kind $[\mathbf{p.u(q)}]\{...\}, [\mathbf{q.u(p)}]\{...\}, [\mathbf{q.u(k)}]\{...\}$. However, using the incompressibility constraints $\mathbf{k.u(k)} = \mathbf{0}$ and the constraint $\mathbf{k} + \mathbf{p} + \mathbf{q} = \mathbf{0}$, we have absorbed the latter three terms into the former ones. Now we will impose a few restrictions on the form of Y_Δ.

The interactions between the magnetic modes fundamentally involve three-modes — the combined energy transfer to a magnetic mode, say $\mathbf{b(k)}$, depends on the Fourier coefficients at all three wavenumbers ($\mathbf{k}$, $\mathbf{p}$, $\mathbf{q}$). For example, the combined energy transfer to $\mathbf{b(k)}$ from $\mathbf{b(p)}$ and $\mathbf{b(q)}$, given by $S^{bb}(\mathbf{k}|\mathbf{p},\mathbf{q}) = -Re\,(i[\mathbf{k.u(q)}][\mathbf{b(k).b(p)}] + i[\mathbf{k.u(p)}][\mathbf{b(k).b(q)}])$, depends on $\mathbf{u(p)}$, $\mathbf{u(q)}$, $\mathbf{b(p)}$, $\mathbf{b(q)}$, and $\mathbf{b(k)}$. The mode-to-mode transfer should not break the fundamentally three-mode feature of these interactions, i.e., the mode-to-mode transfer should have Fourier coefficients from all wavenumbers $\mathbf{k}, \mathbf{p}, \mathbf{q}$. Hence we will drop all those terms from $Y_\Delta^{(1)}$ to $Y_\Delta^{(4)}$ which are independent of atleast one of the wavenumbers $\mathbf{k}, \mathbf{p}, \mathbf{q}$. Then, we get

$$Y_\Delta^{(1)} = Re(\quad [\mathbf{k.u(q)}]\,\{[\mathbf{u(k).b(p)}]... + [\mathbf{u(p).b(k)}]...\} \quad + [\mathbf{k.u(p)}]\,\{[\mathbf{u(k).b(q)}]... + [\mathbf{u(q).b(k)}]...\}$$
$$[\mathbf{p.u(k)}]\,\{[\mathbf{u(p).b(q)}]... + [\mathbf{u(q).b(p)}]...\}) \qquad \text{(B.}$$

$$Y_\Delta^{(2)} = Re(\quad [\mathbf{k.u(q)}][\mathbf{b(k).b(p)}]\alpha + [\mathbf{k.u(p)}][\mathbf{b(k).b(q)}]\beta + [\mathbf{p.u(k)}][\mathbf{b(p).b(q)}]\gamma) \tag{B.7}$$

$$\begin{aligned} Y_\Delta^{(3)} = Re(\quad & [\mathbf{k.b(q)}] \quad \{[\mathbf{u(k).b(p)}]\delta + [\mathbf{u(p).b(k)}]\eta\} + \\ & [\mathbf{k.b(p)}] \quad \{[\mathbf{u(k).b(q)}]\mu + [\mathbf{u(q).b(k)}]\nu\} + \\ & [\mathbf{p.b(k)}] \quad \{[\mathbf{u(p).b(q)}]\psi + [\mathbf{u(q).b(p)}]\chi\}) \end{aligned} \tag{B.8}$$

$$Y_\Delta^{(4)} = Re(\quad [\mathbf{k.b(q)}][\mathbf{u(k).u(p)}]\theta + [\mathbf{k.b(p)}][\mathbf{u(k).u(q)}]\phi + [\mathbf{p.b(k)}][\mathbf{u(k).u(k)}]... \quad) \tag{B.9}$$

We put the following additional restriction on the form of Y_Δ. If none of the magnetic modes in the triad are gaining/losing energy to the other two modes, i.e., if the combined energy transfer to each one of them is equal to zero, then even the circulating transfer should be equal to zero. We observe the following additional feature of the interactions. The combined energy transfer to every magnetic mode in the triad from the other two magnetic modes is equal to zero, if any two of $\mathbf{b(k)}, \mathbf{b(p)}, \mathbf{b(q)}$ are zero (see Eq. (3.36 in Chapter 2). The mode-to-mode transfer should also respect this feature of the interactions, i.e., the circulating transfer should be zero if {$\mathbf{b(k)}$, $\mathbf{b(p)=0}$}, or {$\mathbf{b(k)}$, $\mathbf{b(q)=0}$}, or {$\mathbf{b(p)}$, $\mathbf{b(q)=0}$}. Now, let us put $\mathbf{b(k)=0}$, $\mathbf{b(p)=0}$ in $Y_\Delta^{(1)}$ to $Y_\Delta^{(4)}$. It can easily shown that Y_Δ will be zero, for arbitrary values u's and b's, only if the all coefficients in $Y_\Delta^{(1)}$ and $Y_\Delta^{(4)}$ are themselves equal to zero. Hence we drop $Y_\Delta^{(1)}$ and $Y_\Delta^{(4)}$ from Y_Δ [Eq. (B.1)]. We get,

$$Y_\Delta = Y_\Delta^{(2)} + Y_\Delta^{(3)} \tag{B.10}$$

and

$$\begin{aligned} Y_\Delta^{(2)} = Re(\quad & [\mathbf{k.u(q)}][\mathbf{b(k).b(p)}]\alpha + \quad [\mathbf{k.u(p)}][\mathbf{b(k).b(q)}]\beta + \\ & [\mathbf{p.u(k)}][\mathbf{b(p).b(q)}]\gamma \quad) \end{aligned} \tag{B.11}$$

$$Y_\Delta^{(3)} = Re(\quad [\mathbf{k.b(q)}] \quad \{[\mathbf{u(k).b(p)}]\delta + [\mathbf{u(p).b(k)}]\eta\} +$$

$$[\mathbf{k.b(p)}]\ \{[\mathbf{u(k).b(q)}]\mu + [\mathbf{u(q).b(k)}]\nu\} +$$
$$[\mathbf{p.b(k)}]\ \{[\mathbf{u(p).b(q)}]\psi + [\mathbf{u(q).b(p)}]\lambda\}) \qquad \text{(B.12)}$$

In Appendix A we had considered the derivation of circulating transfer Y_Δ between the velocity modes. By imposing the condition of finiteness of the circulating transfer we had concluded that the coefficients should be independent of the magnitude of the wavenumbers and the Fourier coefficients $\mathbf{u(k)}$, etc. On imposing the constraint that Y_Δ should be finite and following the reasoning in Appendix A, we can conclude that the coefficients α, β, etc. should be independent of the magnitude of the wavenumbers and of the Fourier coefficients of the velocity and the magnetic fields. Therefore, we may write the coefficient $\alpha = f[\frac{\mathbf{k\,p}}{kp}, ..., \frac{\mathbf{k.u(p)}}{k|u(p)|}, \frac{\mathbf{k.b(p)}}{k|b(p)|}, ..., \frac{\mathbf{u(k).u(p)}}{|u(k)||u(p)|}, \frac{\mathbf{b(k).b(p)}}{|b(k)||b(p)|}, ..., \frac{\mathbf{u(k).b(p)}}{|u(k)||b(p)|}, ...]$. The other coefficients can also be written in the same manner.

We will now write the coefficients α, β, etc. as

$$\alpha = \alpha^{(0)} + \alpha^{(1)} + \alpha^{(2)} + \alpha^{(3)} + \alpha^{(4)}, \qquad \text{(B.13)}$$

where $\alpha^{(0)}$ is a constant, and

$$\alpha^{(1)} = \alpha_1^{(1)}\frac{\mathbf{k.p}}{kp} + \alpha_2^{(1)}\frac{\mathbf{k.q}}{kq} + \alpha_3^{(1)}\frac{\mathbf{p.q}}{pq}, \qquad \text{(B.14)}$$

$$\alpha^{(2)} = \alpha_1^{(2)}\frac{\mathbf{k.u(p)}}{k|\mathbf{u(p)}|} + \alpha_2^{(2)}\frac{\mathbf{k.u(q)}}{k|\mathbf{u(q)}|} + \alpha_3^{(2)}\frac{\mathbf{p.u(k)}}{p|\mathbf{u(k)}|} + \alpha_4^{(2)}\frac{\mathbf{p.u(q)}}{p|\mathbf{u(q)}|} + \alpha_5^{(2)}\frac{\mathbf{q.u(k)}}{q|\mathbf{u(k)}|} + \alpha_6^{(2)}\frac{\mathbf{q.u(p)}}{q|\mathbf{u(p)}|} +$$
$$\alpha_7^{(2)}\frac{\mathbf{k.b(p)}}{k|\mathbf{b(p)}|} + ... + \alpha_{12}^{(2)}\frac{\mathbf{q.b(p)}}{q|\mathbf{b(p)}|}, \qquad \text{(B.15)}$$

$$\alpha^{(3)} = \alpha_1^{(3)}\frac{\mathbf{u(k).u(p)}}{|\mathbf{u(k)}||\mathbf{u(p)}|} + \alpha_2^{(3)}\frac{\mathbf{u(k).u(q)}}{|\mathbf{u(k)}||\mathbf{u(q)}|} + \alpha_3^{(3)}\frac{\mathbf{u(p).u(q)}}{|\mathbf{u(p)}||\mathbf{u(q)}|} +$$
$$\alpha_4^{(3)}\frac{\mathbf{b(k).b(p)}}{|\mathbf{b(k)}||\mathbf{b(p)}|} + \alpha_5^{(3)}\frac{\mathbf{b(k).b(q)}}{|\mathbf{b(k)}||\mathbf{b(q)}|} + \alpha_6^{(3)}\frac{\mathbf{b(p).b(q)}}{|\mathbf{b(p)}||\mathbf{b(q)}|} +$$
$$\alpha_7^{(3)}\frac{\mathbf{u(k).b(k)}}{|\mathbf{u(k)}||\mathbf{b(k)}|} + \alpha_8^{(3)}\frac{\mathbf{u(k).b(p)}}{|\mathbf{u(k)}||\mathbf{b(p)}|} + ... + \alpha_{15}^{(3)}\frac{\mathbf{u(q).b(p)}}{|\mathbf{u(q)}||\mathbf{b(p)}|}. \qquad \text{(B.16)}$$

where $\alpha_1^{(1)}, \alpha_2^{(1)}, \alpha_1^{(2)}$, etc. are all unknown constants. The quantities $\alpha^{(1)}, \alpha^{(2)}, \alpha^{(3)}$ are 'linear' in the scalars of the type $\mathbf{k.p}/kp$, $\mathbf{k.u(p)}/k|\mathbf{u(p)}|$, $\mathbf{k.b(p)}/k|\mathbf{b(p)}|$, $\mathbf{u(k).u(p)}/|\mathbf{u(k)}||\mathbf{u(p)}|$.

$\mathbf{b(k).b(p)/|b(k)||b(p)|}$, and $\mathbf{u(k).b(p)/|u(k)||b(p)|}$. The quantity $\alpha^{(4)}$ contains higher order terms in these scalars like $(\mathbf{k.p})^2/k^2p^2$, $[\mathbf{k.u(p)}]^2/k^2([\mathbf{u(p).u(p)}]$, etc. All the other coefficients ζ, γ, ω, etc. in Eqs. (B.11)-(B.12) can be similarly divided into linear and non-linear terms.

The mode-to-mode transfer should be invariant under a galilean transformation. In Appendix A, we had given the transformation rules for the scalars of the type $\mathbf{k.p}$. $\mathbf{k.u(p)}$. $\mathbf{u(k).u(p)}$ and for a combination of these like $[\mathbf{k.u(p)}][\mathbf{u(k).u(q)}]$. For the present case we also need to consider the transformation properties of the magnetic field. MHD equations hold for low velocities and only quantities upto the order of v/c are included in the equations. Under this approximation the magnetic fields are equal in the two frames S and S' with a relative velocity $\mathbf{U_0}$. Then, the Fourier coefficient $\mathbf{b(k)}$ in the frame S and $\mathbf{b'(k)}$ in the frame S' are related as

$$\mathbf{b'(k)} = \mathbf{b(k)} \exp^{i(\mathbf{k.U_0})t} \tag{B.17}$$

This differs from the galilean transformation of $\mathbf{u(k)}$ by the term $\mathbf{U_0}\delta(\mathbf{k})$ only. Using the above relationship between between $\mathbf{b(k)}$ and $\mathbf{b'(k)}$ the transformation rules for $\mathbf{k.b(q)}$. $\mathbf{b(k).b(p)}$. $\mathbf{u(k).b(p)}$ are

$$\mathbf{k'.b'(q')} = \mathbf{k.b(q)} \exp^{i(\mathbf{q.U_0})t}, \tag{B.18}$$

$$\mathbf{b'(k').b'(p')} = \mathbf{b(k).b(p)} \exp^{i\mathbf{(k+p).U_0}t}, \tag{B.19}$$

$$\mathbf{u'(k').b'(p')} = \mathbf{u(k).b(p)} \exp^{i\mathbf{(k+p).U_0}t}. \tag{B.20}$$

These scalars are not galilean invariant (in Appendix A, we had likewise shown that the scalars of the type $\mathbf{k.u(p)}$, $\mathbf{u(k).u(p)}$ are not galilean invariant). It follows that $\alpha^{(2)}, \beta^{(2)}$, etc., $\alpha^{(3)}, \beta^{(3)}$, etc. are not invariant under a galilean transformation. To preserve the galilean invariance of Y_Δ, the coefficients $\alpha^{(2)}$, $\alpha^{(3)}$, $\beta^{(2)}$, $\beta^{(3)}$, and other such coefficients should be dropped from Eq. (B.13). The nonlinear quantity $\alpha^{(4)}$, $\beta^{(4)}$, etc. can be constructed in a galilean invariant form. Even then we will drop this term. We had also dropped this term

from the expression for X_Δ in Appendix A. Our derivation for Y_Δ, like the derivation of X_Δ in Appendix A, is is thus valid only upto the linear orders. After dropping the coefficients $\alpha^{(2)}$, $\alpha^{(3)}$, $\alpha^{(4)}$ and other coefficients of this type, Eq. (B.13) reduces to

$$\alpha = \alpha^{(0)} + \alpha^{(1)} \tag{B.21}$$

Using Eqs. (B.21) and (B.14) we can now write $Y_\Delta^{(2)}$ and $Y_\Delta^{(3)}$ in Eqs. (B.11)-(B.12) as

$$\begin{aligned} Y_\Delta^{(2)} = Re(\quad & [\mathbf{k.u(q)}][\mathbf{b(k).b(p)}]\{\alpha^{(0)} + \alpha_1 \tfrac{\mathbf{k.p}}{kp} + \alpha_2 \tfrac{\mathbf{k.q}}{kq} + \alpha_3 \tfrac{\mathbf{p.q}}{pq}\}+ \\ & [\mathbf{k.u(p)}][\mathbf{b(k).b(q)}]\{\beta^{(0)} + \beta_1 \tfrac{\mathbf{k.p}}{kp} + \beta_2 \tfrac{\mathbf{k.q}}{kq} + \beta_3 \tfrac{\mathbf{p.q}}{pq}\}+ \\ & [\mathbf{p.u(k)}][\mathbf{b(p).b(q)}]\{\gamma^{(0)} + \gamma_1 \tfrac{\mathbf{k.p}}{kp} + \gamma_2 \tfrac{\mathbf{k.q}}{kq} + \gamma_3 \tfrac{\mathbf{p.q}}{pq}\} \quad) \end{aligned} \tag{B.22}$$

$$\begin{aligned} Y_\Delta^{(3)} = Re(\quad & [\mathbf{k.b(q)}][\mathbf{u(k).b(p)}]\{\delta^{(0)} + \delta_1 \tfrac{\mathbf{k.p}}{kp} + \delta_2 \tfrac{\mathbf{k.q}}{kq} + \delta_3 \tfrac{\mathbf{p.q}}{pq}\}+ \\ & [\mathbf{k.b(q)}][\mathbf{u(p).b(k)}]\{\eta^{(0)} + \eta_1 \tfrac{\mathbf{k.p}}{kp} + \eta_2 \tfrac{\mathbf{k.q}}{kq} + \eta_3 \tfrac{\mathbf{p.q}}{pq}\}+ \\ & [\mathbf{k.b(p)}][\mathbf{u(k).b(q)}]\{\mu^{(0)} + \mu_1 \tfrac{\mathbf{k.p}}{kp} + \mu_2 \tfrac{\mathbf{k.q}}{kq} + \mu_3 \tfrac{\mathbf{p.q}}{pq}\}+ \\ & [\mathbf{k.b(p)}][\mathbf{u(q).b(k)}]\{\nu^{(0)} + \nu_1 \tfrac{\mathbf{k.p}}{kp} + \nu_2 \tfrac{\mathbf{k.q}}{kq} + \nu_3 \tfrac{\mathbf{p.q}}{pq}\}+ \\ & [\mathbf{p.b(k)}][\mathbf{u(p).b(q)}]\{\phi^{(0)} + \phi_1 \tfrac{\mathbf{k.p}}{kp} + \phi_2 \tfrac{\mathbf{k.q}}{kq} + \phi_3 \tfrac{\mathbf{p.q}}{pq}\}+ \\ & [\mathbf{p.b(k)}][\mathbf{u(q).b(p)}]\{\chi^{(0)} + \chi_1 \tfrac{\mathbf{k.p}}{kp} + \chi_2 \tfrac{\mathbf{k.q}}{kq} + \chi_3 \tfrac{\mathbf{p.q}}{pq}\} \quad) \end{aligned} \tag{B.23}$$

where the superscript '1' has been dropped from $\alpha^{(1)}$, $\alpha^{(2)}$, etc.

The quantity $Y_\Delta = Y_\Delta^{(2)} + Y_\Delta^{(3)}$ represents the energy circulating in the anti-clockwise direction, i.e. Y_Δ flows along $\mathbf{p} \to \mathbf{k} \to \mathbf{q} \to \mathbf{p}$ [see Fig. 3.10 in Section 3.7.2]. We will now denote the circulating transfer along $\mathbf{p} \to \mathbf{k}$ by $Y_\Delta(\mathbf{k}|\mathbf{p}|\mathbf{q})$, transfer along $\mathbf{k} \to \mathbf{q}$ by $Y_\Delta(\mathbf{q}|\mathbf{k}|\mathbf{p})$ and so on for the circulating transfer between each pair of modes. We take $Y_\Delta = Y_\Delta^{(2)} + Y_\Delta^{(3)}$ from Eqs. (B.22)-(B.23) to be the circulating transfer from $\mathbf{p}$ to $\mathbf{k}$, i.e., $Y_\Delta(\mathbf{k}|\mathbf{p}|\mathbf{q}|) \equiv Y_\Delta$ In the same manner $Y_\Delta(\mathbf{k}|\mathbf{q}|\mathbf{p})) = Y_\Delta^{(2)}(\mathbf{k}|\mathbf{q}|\mathbf{p}) + Y_\Delta^{(3)}(\mathbf{k}|\mathbf{q}|\mathbf{p})$ can be written as

$$\begin{aligned} Y_\Delta^{(2)}(\mathbf{k}|\mathbf{q}|\mathbf{p}) = Re(\quad & [\mathbf{k.u(p)}][\mathbf{b(k).b(q)}]\{\alpha^{(0)} + \alpha_1 \tfrac{\mathbf{k.q}}{kq} + \alpha_2 \tfrac{\mathbf{k.p}}{kp} + \alpha_3 \tfrac{\mathbf{p.q}}{pq}\}+ \\ & [\mathbf{k.u(q)}][\mathbf{b(k).b(p)}]\{\beta^{(0)} + \beta_1 \tfrac{\mathbf{k.q}}{kq} + \beta_2 \tfrac{\mathbf{k.p}}{kp} + \beta_3 \tfrac{\mathbf{p.q}}{pq}\}+ \\ & [\mathbf{q.u(k)}][\mathbf{b(p).b(q)}]\{\gamma^{(0)} + \gamma_1 \tfrac{\mathbf{k.q}}{kq} + \gamma_2 \tfrac{\mathbf{k.p}}{kp} + \gamma_3 \tfrac{\mathbf{p.q}}{pq}\} \quad) \end{aligned} \tag{B.24}$$

and

$$Y_{\Delta}^{(3)}(k|q|p) = Re(\quad [k.b(p)][u(k).b(q)]\{\delta^{(0)} + \delta_1\frac{k.q}{kq} + \delta_2\frac{k.p}{kp} + \delta_3\frac{p.q}{pq}\}+$$
$$[k.b(p)][u(q).b(k)]\{\eta^{(0)} + \eta_1\frac{k.q}{kq} + \eta_2\frac{k.p}{kp} + \eta_3\frac{p.q}{pq}\}+$$
$$[k.b(q)][u(k).b(p)]\{\mu^{(0)} + \mu_1\frac{k.q}{kq} + \mu_2\frac{k.p}{kp} + \mu_3\frac{p.q}{pq}\}+$$
$$[k.b(q)][u(p).b(k)]\{\nu^{(0)} + \nu_1\frac{k.q}{kq} + \nu_2\frac{k.p}{kp} + \nu_3\frac{p.q}{pq}\}+$$
$$[q.b(k)][u(q).b(p)]\{\phi^{(0)} + \phi_1\frac{k.q}{kq} + \phi_2\frac{k.p}{kp} + \phi_3\frac{p.q}{pq}\}+$$
$$[q.b(k)][u(p).b(q)]\{\chi^{(0)} + \chi_1\frac{k.q}{kq} + \chi_2\frac{k.p}{kp} + \chi_3\frac{p.q}{pq}\} \quad) \quad \text{(B.25)}$$

and the circulating transfer from p to k, $Y_{\Delta}(p|k|q)) = Y_{\Delta}^{(2)}(p|k|q) + Y_{\Delta}^{(3)}(p|k|q)$ can be written as

$$Y_{\Delta}^{(2)}(p|k|q) = Re(\quad [p.u(q)][b(k).b(p)]\{\alpha^{(0)} + \alpha_1\frac{k.p}{kp} + \alpha_2\frac{p.q}{pq} + \alpha_3\frac{k.q}{kq}\}+$$
$$[p.u(k)][b(p).b(q)]\{\beta^{(0)} + \beta_1\frac{k.p}{kp} + \beta_2\frac{p.q}{pq} + \beta_3\frac{k.q}{kq}\}+$$
$$[k.u(p)][b(k).b(q)]\{\gamma^{(0)} + \gamma_1\frac{k.p}{kp} + \gamma_2\frac{p.q}{kq} + \gamma_3\frac{k.q}{kq}\} \quad) \quad \text{(B.26)}$$

$$Y_{\Delta}^{(3)}(p|k|q) = Re(\quad [p.b(q)][u(p).b(k)]\{\delta^{(0)} + \delta_1\frac{k.p}{kp} + \delta_2\frac{p.q}{pq} + \delta_3\frac{k.q}{kq}\}+$$
$$[p.b(q)][u(k).b(p)]\{\eta^{(0)} + \eta_1\frac{k.p}{kp} + \eta_2\frac{p.q}{pq} + \eta_3\frac{k.q}{kq}\}+$$
$$[p.b(k)][u(p).b(q)]\{\mu^{(0)} + \mu_1\frac{k.p}{kp} + \mu_2\frac{p.q}{pq} + \mu_3\frac{k.q}{kq}\}+$$
$$[p.b(k)][u(q).b(p)]\{\nu^{(0)} + \nu_1\frac{k.p}{kp} + \nu_2\frac{p.q}{pq} + \nu_3\frac{k.q}{kq}\}+$$
$$[k.b(p)][u(k).b(q)]\{\phi^{(0)} + \phi_1\frac{k.p}{kp} + \phi_2\frac{p.q}{pq} + \phi_3\frac{k.q}{kq}\}+$$
$$[k.b(p)][u(q).b(k)]\{\chi^{(0)} + \chi_1\frac{k.p}{kp} + \chi_2\frac{p.q}{pq} + \chi_3\frac{k.q}{kq}\} \quad) \quad \text{(B.27)}$$

$Y_{\Delta}(k|p|q)$ flows along the anti-clockwise direction while $Y_{\Delta}(k|q|p)$ and $Y_{\Delta}(p|k|q)$ flow along the clockwise direction. The former should therefore be equal and opposite to the latter two transfers, i.e.,

$$Y_{\Delta}(k|p|q) + Y_{\Delta}(k|q|p) = 0, \quad \text{(B.28)}$$

and

$$Y_\Delta(\mathbf{k}|\mathbf{p}|\mathbf{q}) + Y_\Delta(\mathbf{p}|\mathbf{k}|\mathbf{q}) = 0. \tag{B.29}$$

Replacing the expression for $Y_\Delta(\mathbf{k}|\mathbf{p}|\mathbf{q})$ from Eqs. (B.22)-(B.23) and for $Y_\Delta(\mathbf{k}|\mathbf{q}|\mathbf{p})$ from Eqs. (B.24)-(B.25) into Eq. (B.28) we get

$$\begin{aligned}
&[\mathbf{k}.\mathbf{u}(\mathbf{q})][\mathbf{b}(\mathbf{k}).\mathbf{b}(\mathbf{p})]\{(\alpha^{(0)}+\beta^{(0)}) + (\alpha_1+\beta_2)\frac{\mathbf{k}.\mathbf{p}}{kp} + (\alpha_2+\beta_1)\frac{\mathbf{k}.\mathbf{q}}{kq} + (\alpha_3+\beta_3\frac{\mathbf{p}.\mathbf{q}}{pq}\}+\\
&[\mathbf{k}.\mathbf{u}(\mathbf{p})][\mathbf{b}(\mathbf{k}).\mathbf{b}(\mathbf{q})]\{(\beta^{(0)}+\alpha_{(0)}) + (\beta_1+\alpha_2)\frac{\mathbf{k}.\mathbf{p}}{kp} + (\beta_2+\alpha_1\frac{\mathbf{k}.\mathbf{q}}{kq} + \beta_3+\alpha_3\frac{\mathbf{p}.\mathbf{q}}{pq}\}+\\
&[\mathbf{p}.\mathbf{u}(\mathbf{k})][\mathbf{b}(\mathbf{p}).\mathbf{b}(\mathbf{q})]\{(\gamma_1-\gamma_2)\frac{\mathbf{k}.\mathbf{p}}{kp} + (\gamma_2-\gamma_1)\frac{\mathbf{k}.\mathbf{q}}{kq}+\\
&[\mathbf{k}.\mathbf{b}(\mathbf{q})][\mathbf{u}(\mathbf{k}).\mathbf{b}(\mathbf{p})]\{(\delta^{(0)}+\nu^{(0)}) + (\delta_1+\mu_2)\frac{\mathbf{k}.\mathbf{p}}{kp} + (\delta_2+\mu_1)\frac{\mathbf{k}.\mathbf{q}}{kq} + (\delta_3+\mu_3)\frac{\mathbf{p}.\mathbf{q}}{pq}\}+\\
&[\mathbf{k}.\mathbf{b}(\mathbf{q})][\mathbf{u}(\mathbf{p}).\mathbf{b}(\mathbf{k})]\{(\eta^{(0)}+\nu^{(0)})(\eta_1+\nu_2)\frac{\mathbf{k}.\mathbf{p}}{kp} + (\eta_2+\nu_1)\frac{\mathbf{k}.\mathbf{q}}{kq} + (\eta_3+\nu_3)\frac{\mathbf{p}.\mathbf{q}}{pq}\}+\\
&[\mathbf{k}.\mathbf{b}(\mathbf{p})][\mathbf{u}(\mathbf{k}).\mathbf{b}(\mathbf{q})]\{(\mu^{(0)}+\delta^{(0)}) + (\mu_1+\delta_2)\frac{\mathbf{k}.\mathbf{p}}{kp} + (\mu_2+\delta_1)\frac{\mathbf{k}.\mathbf{q}}{kq} + (\mu_3+\delta_3)\frac{\mathbf{p}.\mathbf{q}}{pq}\}+\\
&[\mathbf{k}.\mathbf{b}(\mathbf{p})][\mathbf{u}(\mathbf{q}).\mathbf{b}(\mathbf{k})]\{(\nu^{(0)}+\eta^{(0)}) + (\nu_1+\eta_2)\frac{\mathbf{k}.\mathbf{p}}{kp} + (\nu_2+\eta_1)\frac{\mathbf{k}.\mathbf{q}}{kq} + (\nu_3+\eta_3)\frac{\mathbf{p}.\mathbf{q}}{pq}\}+\\
&[\mathbf{p}.\mathbf{b}(\mathbf{k})][\mathbf{u}(\mathbf{p}).\mathbf{b}(\mathbf{q})]\{(\phi^{(0)}-\chi^{(0)}) + (\phi_1-\chi_2)\frac{\mathbf{k}.\mathbf{p}}{kp} + (\phi_2-\chi_1)\frac{\mathbf{k}.\mathbf{q}}{kq} + (\phi_3-\chi_3)\frac{\mathbf{p}.\mathbf{q}}{pq}\}+\\
&[\mathbf{p}.\mathbf{b}(\mathbf{k})][\mathbf{u}(\mathbf{q}).\mathbf{b}(\mathbf{p})]\{(\chi^{(0)}-\phi^{(0)}) + (\chi_1-\phi_2)\frac{\mathbf{k}.\mathbf{p}}{kp} + (\chi_2-\phi_1)\frac{\mathbf{k}.\mathbf{q}}{kq} + (\chi_3-\phi_3)\frac{\mathbf{p}.\mathbf{q}}{pq}\} = 0
\end{aligned} \tag{B.30}$$

and replacing the expression for $Y_\Delta(\mathbf{k}|\mathbf{p}|\mathbf{q})$ and $Y_\Delta(\mathbf{p}|\mathbf{k}|\mathbf{q})$ from Eqs. (B.26)-(B.27) into Eq.(B.29) we get

$$\begin{aligned}
&[\mathbf{k}.\mathbf{u}(\mathbf{q})][\mathbf{b}(\mathbf{k}).\mathbf{b}(\mathbf{p})]\{(\alpha_2-\alpha_3)\frac{\mathbf{k}.\mathbf{q}}{kq} + (\alpha_3-\alpha_2)\frac{\mathbf{p}.\mathbf{q}}{pq}\}+\\
&[\mathbf{k}.\mathbf{u}(\mathbf{p})][\mathbf{b}(\mathbf{k}).\mathbf{b}(\mathbf{q})]\{(\beta^{(0)}+\gamma^{(0)}) + (\beta_1+\gamma_2)\frac{\mathbf{k}.\mathbf{p}}{kp} + (\beta_2+\gamma_3\frac{\mathbf{k}.\mathbf{q}}{kq} + \beta_3+\gamma_2\frac{\mathbf{p}.\mathbf{q}}{pq}\}+\\
&[\mathbf{p}.\mathbf{u}(\mathbf{k})][\mathbf{b}(\mathbf{p}).\mathbf{b}(\mathbf{q})]\{(\gamma^{(0)}+\beta^{(0)}) + (\gamma_1+\beta_1)\frac{\mathbf{k}.\mathbf{p}}{kp} + (\gamma_2+\beta_3)\frac{\mathbf{k}.\mathbf{q}}{kq} + (\gamma_3+\beta_3)\frac{\mathbf{p}.\mathbf{q}}{pq}+\\
&[\mathbf{k}.\mathbf{b}(\mathbf{q})][\mathbf{u}(\mathbf{k}).\mathbf{b}(\mathbf{p})]\{(\delta^{(0)}-\eta^{(0)}) + (\delta_1-\eta_1)\frac{\mathbf{k}.\mathbf{p}}{kp} + (\delta_2-\eta_3)\frac{\mathbf{k}.\mathbf{q}}{kq} + (\delta_3-\eta_2)\frac{\mathbf{p}.\mathbf{q}}{pq}\}+\\
&[\mathbf{k}.\mathbf{b}(\mathbf{q})][\mathbf{u}(\mathbf{p}).\mathbf{b}(\mathbf{k})]\{(\eta^{(0)}-\delta^{(0)}) + (\eta_1-\delta_1)\frac{\mathbf{k}.\mathbf{p}}{kp} + (\eta_2-\delta_3)\frac{\mathbf{k}.\mathbf{q}}{kq} + (\eta_3-\delta_2)\frac{\mathbf{p}.\mathbf{q}}{pq}\}+
\end{aligned}$$

$$[\mathbf{k}.\mathbf{b}(\mathbf{p})][\mathbf{u}(\mathbf{k}).\mathbf{b}(\mathbf{q})]\{(\mu^{(0)}+\phi^{(0)})+(\mu_1+\phi_1)\frac{\mathbf{k}.\mathbf{p}}{kp}+(\mu_2+\phi_3)\frac{\mathbf{k}.\mathbf{q}}{kq}+(\mu_3+\phi_2)\frac{\mathbf{p}.\mathbf{q}}{pq}\}+$$
$$[\mathbf{k}.\mathbf{b}(\mathbf{p})][\mathbf{u}(\mathbf{q}).\mathbf{b}(\mathbf{k})]\{(\nu^{(0)}+\chi^{(0)})+(\nu_1+\chi_1)\frac{\mathbf{k}.\mathbf{p}}{kp}+(\nu_2+\chi_3)\frac{\mathbf{k}.\mathbf{q}}{kq}+(\nu_3+\chi_2)\frac{\mathbf{p}.\mathbf{q}}{pq}\}+$$
$$[\mathbf{p}.\mathbf{b}(\mathbf{k})][\mathbf{u}(\mathbf{p}).\mathbf{b}(\mathbf{q})]\{(\phi^{(0)}+\mu^{(0)})+(\phi_1+\mu_1)\frac{\mathbf{k}.\mathbf{p}}{kp}+(\phi_2+\mu_3)\frac{\mathbf{k}.\mathbf{q}}{kq}+(\phi_3+\mu_2)\frac{\mathbf{p}.\mathbf{q}}{pq}\}+$$
$$[\mathbf{p}.\mathbf{b}(\mathbf{k})][\mathbf{u}(\mathbf{q}).\mathbf{b}(\mathbf{p})]\{(\chi^{(0)}+\nu^{(0)})+(\chi_1+\nu_1)\frac{\mathbf{k}.\mathbf{p}}{kp}+(\chi_2+\nu_3)\frac{\mathbf{k}.\mathbf{q}}{kq}+(\chi_3+\nu_2)\frac{\mathbf{p}.\mathbf{q}}{pq}\}=0 \tag{B.31}$$

Since each term in the above equation has a different functional dependence on $\mathbf{u}(\mathbf{k})$, $\mathbf{u}(\mathbf{p})$, $\mathbf{u}(\mathbf{q})$, $\mathbf{b}(\mathbf{k})$, $\mathbf{b}(\mathbf{p})$, $\mathbf{b}(\mathbf{q})$, each term should be individually zero. It follows that the constants in the above equations should satisfy the following relationships : from Eq. (B.30) we get $\alpha^{(0)}+\beta^{(0)}=0, \alpha_1+\beta_2=0, \alpha_2+\beta_1=0, \alpha_3+\beta_3=0, \gamma_1-\gamma_2=0 \delta^{(0)}+\mu^{(0)}=0, \delta_1+\mu_2=0, \delta_2+\mu_1=0, \delta_3+\mu_3=0, \eta^{(0)}+\nu^{(0)}=0, \eta_1+\nu_2=0, \eta_2+\nu_1=0, \eta_3+\nu_3=0, \phi^{(0)}-\chi^{(0)}=0, \phi_1-\chi_2=0, \phi_2-\chi_1=0, \phi_3-\chi_3=0$, and from Eq. (B.31) we get $\alpha_2-\alpha_3=0, \beta^{(0)}+\gamma^{(0)}=0, \beta_1+\gamma_1=0, \beta_2+\gamma_3=0, \beta_3+\gamma_2=0, \delta^{(0)}-\eta^{(0)}=0, \delta_1-\eta_1=0, \delta_2-\eta_3=0, \delta_3-\eta_2=0, \mu^{(0)}+\phi^{(0)}=0, \mu_1+\phi_1=0, \mu_2+\phi_3=0, \mu_3+\phi_2=0, \nu^{(0)}+\chi^{(0)}=0, \nu_2+\chi_3=0, \mu_3+\phi_2=0$.

The above relationships can be arranged into the following groups: $\{\alpha^{(0)}=-\beta^{(0)}=\gamma^{(0)}\}$, $\{\delta^{(0)}=-\mu^{(0)}=\phi^{(0)}=\eta^{(0)}=-\nu^{(0)}=\chi^{(0)}\}$, $\{\alpha_1=-\beta_2=\gamma_3\}$, $\{\alpha_2=-\beta_1=\gamma_1=\gamma_2=\alpha_3=-\beta_3\}$, $\{\delta_1=-\mu_2=\phi_3=\chi_3=-\nu_2=\eta_1\}$, $\{\delta_2=-\mu_1=\phi_1=\chi_2=-\nu_3=\eta_3\}$, $\{\delta_3=-\mu_3=\phi_2=\chi_1=-\nu_1=\eta_2\}$.

Let us now consider a triad with $|\mathbf{p}|=|\mathbf{q}|$, $\mathbf{k}.\mathbf{p}=\mathbf{k}.\mathbf{q}$ and with the Fourier modes $\mathbf{u}(\mathbf{p}), \mathbf{u}(\mathbf{q}), \mathbf{b}(\mathbf{p}), \mathbf{b}(\mathbf{q})$ perpendicular to the plane formed by this triad. We argued in Appendix A that the circulating transfer should vanish for such a geometry. For this geometry we can write Y_Δ from Eq. (B.22) and (B.23) as

$$\begin{aligned} Y_\Delta = Re(\quad & [\mathbf{p}.\mathbf{u}(\mathbf{k})][\mathbf{b}(\mathbf{p}).\mathbf{b}(\mathbf{q})]\{\gamma^{(0)}+(\gamma_1+\gamma_2)\tfrac{\mathbf{k}.\mathbf{p}}{kp}+\gamma_3\tfrac{\mathbf{p}.\mathbf{q}}{pq}\}+ \\ & [\mathbf{p}.\mathbf{b}(\mathbf{k})][\mathbf{u}(\mathbf{p}).\mathbf{b}(\mathbf{q})]\{\phi^{(0)}+(\phi_1+\phi_2)\tfrac{\mathbf{k}.\mathbf{p}}{kp}+\phi_3\tfrac{\mathbf{p}.\mathbf{q}}{pq}\}+ \\ & [\mathbf{p}.\mathbf{b}(\mathbf{k})][\mathbf{u}(\mathbf{q}).\mathbf{b}(\mathbf{p})]\{\chi^{(0)}+(\chi_1+\chi_2)\tfrac{\mathbf{k}.\mathbf{p}}{kp}+\chi_3\tfrac{\mathbf{p}.\mathbf{q}}{pq}\} \quad) \end{aligned}$$

$$= 0 \tag{B.32}$$

The above equality should hold for all triads with $|\mathbf{p}| = |\mathbf{q}|$ and $\mathbf{k.p}=\mathbf{k.q}$. Therefore each term inside the curly brackets should be individually zero. This leads us to the following additional relationships between the various constants in the above equation: $\gamma^{(0)} = 0, \gamma_1 + \gamma_2 = 0, \gamma_3 = 0, \phi^{(0)} = 0, \phi_2 + \phi_3 = 0, \phi_1 = 0, \chi^{(0)} = 0, \chi_1 + \chi_3 = 0, \chi_2 = 0$. Similarly, by choosing $|\mathbf{k}| = |\mathbf{p}|$, and $\mathbf{u(k)}, \mathbf{u(p)}, \mathbf{b(k)}, \mathbf{b(p)}$ perpendicular to the triad plane we get the relationships $\alpha^{(0)} = 0, \alpha_1 = 0, \alpha_2 + \alpha_3 = 0, \delta^{(0)} = 0, \delta_1 = 0, \delta_2 + \delta_3 = 0, \eta^{(0)} = 0, \eta_1 = 0, \eta_2 + \eta_3 = 0$. and by choosing $|\mathbf{k}| = |\mathbf{q}|$, and $\mathbf{u(k)}, \mathbf{u(q)}, \mathbf{b(k)}, \mathbf{b(q)}$ perpendicular to the triad plane we get $\beta^{(0)} = 0, \beta_2 = 0, \beta_1 + \beta_3 = 0, \mu^{(0)} = 0, \mu_2 = 0, \mu_1 + \mu_3 = 0, \nu^{(0)} = 0, \nu_2 = 0, \nu_1 + \nu_3 = 0$

Using these relationships the above groups take the following values: $\{\alpha^{(0)} = -\beta^{(0)} = \gamma^{(0)} = 0\}$, $\{\delta^{(0)} = -\mu^{(0)} = \phi^{(0)} = \eta^{(0)} = -\nu^{(0)} = \chi^{(0)} = 0\}$, $\{\alpha_1 = -\beta_2 = \gamma_3 = 0\}$, $\{\alpha_2 = -\beta_1 = \gamma_1 = \gamma_2 = \alpha_3 = -\beta_3 = 0\}$, $\{\delta_1 = -\mu_2 = \phi_3 = \chi_3 = -\nu_2 = \eta_1 = 0\}$, $\{\delta_2 = -\mu_1 = \phi_1 = \chi_2 = -\nu_3 = \eta_3 = -\delta_3 = \mu_3 = -\phi_2 = -\chi_1 = \nu_1 = -\eta_2\}$. Hence, some of the constants are equal to zero, and all the non-zero constants are related to each other by just one undetermined constant which we will denote by 'C', i.e., $\{\delta_2 = -\mu_1 = ... = C\}$

Putting the values of these constants in the expressions for $Y_\Delta^{(2)}$ and $Y_\Delta^{(3)}$ in Eqs. (B.22)-(B.23) we get

$$Y_\Delta^{(2)} = 0 \tag{B.33}$$

$$\begin{aligned} Y_\Delta^{(3)} = Re(\quad & [\mathbf{k.b(q)}][\mathbf{u(k).b(p)}]\{C\tfrac{\mathbf{k.q}}{kq} - C\tfrac{\mathbf{p.q}}{pq}\} + [\mathbf{k.b(q)}][\mathbf{u(p).b(k)}]\{-C\tfrac{\mathbf{k.q}}{kq} + C\tfrac{\mathbf{p.q}}{pq}\} + \\ & [\mathbf{k.b(p)}][\mathbf{u(k).b(q)}]\{-C\tfrac{\mathbf{k.p}}{kp} + C\tfrac{\mathbf{p.q}}{pq}\} + [\mathbf{k.b(p)}][\mathbf{u(q).b(k)}]\{C\tfrac{\mathbf{k.p}}{kp} - C\tfrac{\mathbf{p.q}}{pq}\} + \\ & [\mathbf{p.b(k)}][\mathbf{u(p).b(q)}]\{C\tfrac{\mathbf{k.p}}{kp} - C\tfrac{\mathbf{k.q}}{kq}\} + [\mathbf{p.b(k)}][\mathbf{u(q).b(p)}]\{-C\tfrac{\mathbf{k.p}}{kp} + C\tfrac{\mathbf{k.q}}{kq}\} \quad) \end{aligned} \tag{B.34}$$

with a single undetermined constant.

For the determination of X_Δ in Appendix A, the above considerations were sufficient

to determine X_Δ. However, in the present case we are still left with one undetermined constant. We will now impose the constraint of locality which we state as follows: In the limit $\mathbf{k}, \mathbf{q} \to \infty >> \mathbf{p}$, Y_Δ should tend to zero. If Z_Δ remains finite then the noise, which is always inevitably present in any flow at the smallest scales, would interact directly with the large scales. Moreover, the locality constraint is also necessary in order that the circulating transfer is consistent with the effective transfer between $\mathbf{b(k)}$ and $\mathbf{b(q)}$ which goes to zero for in the above limit. Let us take $\mathbf{u(k)}$, $\mathbf{u(q)}$ to be perpendicular to the plane of the triad. Then we can write Y_Δ as

$$Y_\Delta^{(3)} = Re(\quad [\mathbf{k}.\mathbf{b}(\mathbf{p})][\mathbf{u}(\mathbf{k}).\mathbf{b}(\mathbf{q})]\{-C\tfrac{\mathbf{k}.\mathbf{p}}{kp} + C\tfrac{\mathbf{p}.\mathbf{q}}{pq}\} + [\mathbf{k}.\mathbf{b}(\mathbf{p})][\mathbf{u}(\mathbf{q}).\mathbf{b}(\mathbf{k})]\{C\tfrac{\mathbf{k}.\mathbf{p}}{kp} - C\tfrac{\mathbf{p}.\mathbf{q}}{pq}\} \quad) \tag{B.35}$$

which may be written in terms of the angles of the triangle formed by $\mathbf{k}$, $\mathbf{p}$, $\mathbf{q}$ [Fig. B] as

$$\begin{aligned} Y_\Delta^{(3)} = Re(\quad & \big[\hat{\mathbf{k}}.\mathbf{b}(\mathbf{p})\big][\mathbf{u}(\mathbf{k}).\mathbf{b}(\mathbf{q})]\{-Ck\cos(\psi) - Ck\cos(\theta)\} + \\ & \big[\hat{\mathbf{k}}.\mathbf{b}(\mathbf{p})\big][\mathbf{u}(\mathbf{q}).\mathbf{b}(\mathbf{k})]\{Ck\cos(\psi) + Ck\cos(\theta)\} \quad) \end{aligned} \tag{B.36}$$

We now take the limit $\mathbf{k}, \mathbf{q} \to \infty$, keeping ψ and $\mathbf{p}$ constant. In this limit $\phi \to 0$. Making use of the relationships $\theta = \pi - \psi - \phi$, $k/\sin\theta = p/\sin\phi$, and taking the limit $\phi \to 0$, we get for $Y_\Delta \to \big[\hat{\mathbf{k}}.\mathbf{b}(\mathbf{p})\big][\mathbf{u}(\mathbf{k}).\mathbf{b}(\mathbf{q})]\{-Cp\sin^2(\psi)\} + \big[\hat{\mathbf{k}}.\mathbf{b}(\mathbf{p})\big][\mathbf{u}(\mathbf{q}).\mathbf{b}(\mathbf{k})]\{Cp\sin^2(\psi)\}$. However, in this limit Y_Δ should tend to zero in order to satisfy locality. From this constraint we get $C = 0$. Putting the value of C in Eq. (B.34) gives $Y_\Delta^{(3)} = 0$.

Therefore we get $Y_\Delta = 0$. It follows that the mode-to-mode transfer $\mathcal{R}^{bb} = \mathcal{S}^{bb}$.

In the above proof we used rotational invariance, galilean invariance, finiteness of mode-to-mode transfer, the symmetry of Y_Δ with respect to $\mathbf{k}$, $\mathbf{p}$, $\mathbf{q}$, $\mathbf{u(k)}$, $\mathbf{u(p)}$, $\mathbf{u(q)}$, $\mathbf{b(k)}$, $\mathbf{b(p)}$, $\mathbf{b(q)}$, and the assumption that the circulating transfer should vanish if two of the wavenumbers approach infinity. This proof is valid only upto linear orders, as explained

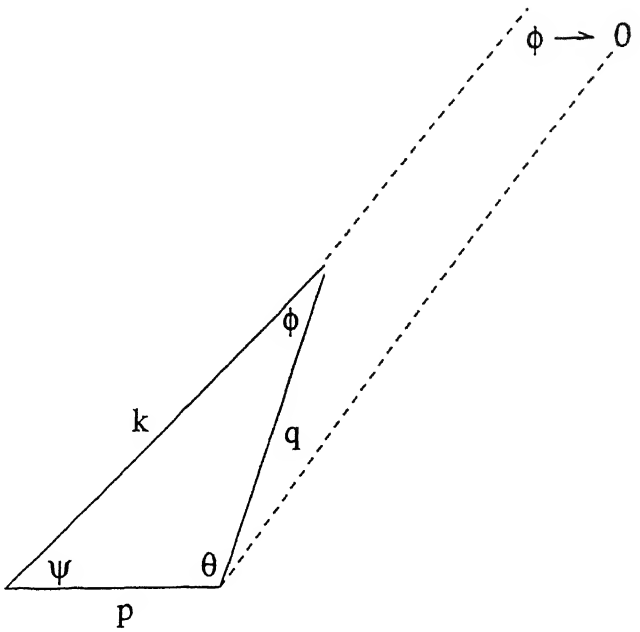

Figure B.1: In the wavenumber triad $\mathbf{k}, \mathbf{q} \rightarrow \infty >> \mathbf{p}$ the circulating transfer, $Y_\Delta = 0$ to avoid non-local transfer from very large wavenumbers to very small wavenumbers in comparison.

earlier in this appendix. A completely general proof without taking recourse to the linearity assumption is lacking at present.

Appendix C

Derivation of the circulating transfer between velocity modes and magnetic modes in a triad

In Section 3.7.3 we had shown that the energy transfer from $\mathbf{u}(\mathbf{p})$ to $\mathbf{b}(\mathbf{k})$ in the triad $(\mathbf{k}, \mathbf{p}, \mathbf{q})$ can be expressed as $\mathcal{T}^{bu}(\mathbf{k}|\mathbf{p}|\mathbf{q}) = \mathcal{S}^{bu}(\mathbf{k}|\mathbf{p}|\mathbf{q}) + Z_\Delta$. $\mathcal{S}^{bu}(\mathbf{k}|\mathbf{p}|\mathbf{q})$ is given by Eq. (3.76) of Section 3.7.3 was interpreted as the effective transfer from $\mathbf{u}(\mathbf{p})$ to $\mathbf{b}(\mathbf{k})$ and Z_Δ was interpreted as a circulating transfer between the velocity and magnetic modes belonging to a triad. We will follow the approach of Appendix A and Appendix B to determine Z_Δ in this Appendix. We will impose the following conditions on Z_Δ. It should not violate the fundamentally triad nature of the interactions, it should be finite, rotationally invariant, galilean invariant, and should vanish if $k/p \to \infty$.

The circulating transfer Z_Δ is a scalar with a dependence on atmost $\mathbf{k}$, $\mathbf{p}$, $\mathbf{q}$, $\mathbf{u}(\mathbf{k})$, $\mathbf{u}(\mathbf{p})$, $\mathbf{u}(\mathbf{q})$, $\mathbf{b}(\mathbf{k})$, $\mathbf{b}(\mathbf{p})$, $\mathbf{b}(\mathbf{q})$. We know from Appendix B that such a function can be expressed in the form given by Eqs. (B.1)-(B.5) of Appendix B. The interactions between the velocity and the magnetic modes are fundamentally three-mode, i.e., each term in the expression for combined energy transfer to a velocity or a magnetic mode depends on all the three wavenumbers $(\mathbf{k}, \mathbf{p}, \mathbf{q})$. the combined energy transfer to any of the velocity or the magnetic modes in the triad. Z_Δ should not violate this fundamental nature of the interactions. Hence we should drop all those terms from Eqs. (B.1)-(B.5) which are independent of atleast one of

the modes and then we get Eqs. (B.6)-(B.9) for Z_Δ. The combined energy transfer to velocity and magnetic modes in the triad are zero if $\{\mathbf{b(k)}, \mathbf{b(p)} = 0\}$, $\{\mathbf{b(k)}, \mathbf{b(q)} = 0\}$, or $\{\mathbf{b(p)}, \mathbf{b(q)} = 0\}$. The terms which are non-vanishing if one of the above set of Fourier coefficients are zero will be dropped from Eqs. (B.6)-(B.9), giving Eqs. (B.10)-(B.12) In Appendix B also we had imposed identical constraints on Eqs. (B.1)-(B.5) to get Eqs. (B.10)-(B.12). The dimensionless coefficients in these equations are $\mathbf{k}$, $\mathbf{p}$, $\mathbf{q}$, $\mathbf{u(k)}$, $\mathbf{u(p)}$, $\mathbf{u(q)}$, $\mathbf{b(k)}$, $\mathbf{b(p)}$, $\mathbf{b(q)}$ dependent and we will now attempt to determine these.

In Appendix B we had considered the consequences of finiteness and galilean invariance on Eqs. (B.10)-(B.12) of Appendix B. We will briefly summarise the conclusions now. To ensure the finiteness and galilean invariance of Eqs. (B.10)-(B.12) the dimensionless coefficients in these equations should be independent of the magnitudes of the wavenumbers and the Fourier coefficients. Then each coefficient in the equations can be written as $\alpha = \alpha^{(0)}+\alpha^{(1)}+\alpha^{(2)}+\alpha^{(3)}+\alpha^{(4)}$ where $\alpha^{(0)}$ is a constant, $\alpha^{(1)}, \alpha^{(2)}, \alpha^{(3)}$ defined in Eqs. (B.14)-(B.16) of Appendix B. are linear in terms of the kind $\mathbf{k.p}$, $\mathbf{k.u(p)}$, $\mathbf{u(k).u(p)}$ respectively, and $\alpha^{(4)}$ is nonlinear in these terms. $\alpha^{(2)}$, and $\alpha^{(3)}$ are not galilean invariant and would therefore lead to the non-invariance of Eqs. (B.14)-(B.16) of Appendix B. Hence, $\alpha^{(2)}$ and $\alpha^{(3)}$ should not be included in α. In Appendix B we had also dropped $\alpha^{(4)}$. Therefore, we get $\alpha = \alpha^{(0)} + \alpha^{(1)}$. Following Appendix B we will now write Z_Δ [given by Eqs. (B.10)-(B.12) in Appendix B]

$$Z^{bu}_{\Delta} = Z^{bu}_{2\Delta} + Z^{bu}_{3\Delta} \tag{C.1}$$

where

$$\begin{aligned} Z^{bu}_{2\Delta}(\mathbf{k}|\mathbf{p}|\mathbf{q}) = Re(\quad & [\mathbf{k.u(q)}][\mathbf{b(k).b(p)}]\{\alpha^{(0)} + \alpha^{(1)}_1\tfrac{\mathbf{k.p}}{kp} + \alpha^{(1)}_2\tfrac{\mathbf{k.q}}{kq} + \alpha^{(1)}_3\tfrac{\mathbf{p.q}}{pq}\}+ \\ & [\mathbf{k.u(p)}][\mathbf{b(k).b(q)}]\{\beta^{(0)} + \beta^{(1)}_1\tfrac{\mathbf{k.p}}{kp} + \beta^{(1)}_2\tfrac{\mathbf{k.q}}{kq} + \beta^{(1)}_3\tfrac{\mathbf{p.q}}{pq}\}+ \\ & [\mathbf{p.u(k)}][\mathbf{b(p).b(q)}]\{\gamma^{(0)} + \gamma^{(1)}_1\tfrac{\mathbf{k.p}}{kp} + \gamma^{(1)}_2\tfrac{\mathbf{k.q}}{kq} + \gamma^{(1)}_3\tfrac{\mathbf{p.q}}{pq}\} \quad) \end{aligned} \tag{C.2}$$

$$Z^{bu}_{3\Delta}(\mathbf{k}|\mathbf{p}|\mathbf{q}) = Re(\quad [\mathbf{k.b(q)}][\mathbf{u(k).b(p)}]\{\delta^{(0)} + \delta^{(1)}_1\tfrac{\mathbf{k.p}}{kp} + \delta^{(1)}_2\tfrac{\mathbf{k.q}}{kq} + \delta^{(1)}_3\tfrac{\mathbf{p.q}}{pq}\}+$$

$$
\begin{aligned}
&[\mathbf{k}.\mathbf{b}(\mathbf{q})][\mathbf{u}(\mathbf{p}).\mathbf{b}(\mathbf{k})]\{\eta^{(0)}+\eta_1^{(1)}\tfrac{\mathbf{k}.\mathbf{p}}{kp}+\eta_2^{(1)}\tfrac{\mathbf{k}.\mathbf{q}}{kq}+\eta_3^{(1)}\tfrac{\mathbf{p}.\mathbf{q}}{pq}\}+\\
&[\mathbf{k}.\mathbf{b}(\mathbf{p})][\mathbf{u}(\mathbf{k}).\mathbf{b}(\mathbf{q})]\{\mu^{(0)}+\mu_1^{(1)}\tfrac{\mathbf{k}.\mathbf{p}}{kp}+\mu_2^{(1)}\tfrac{\mathbf{k}.\mathbf{q}}{kq}+\mu_3^{(1)}\tfrac{\mathbf{p}.\mathbf{q}}{pq}\}+\\
&[\mathbf{k}.\mathbf{b}(\mathbf{p})][\mathbf{u}(\mathbf{q}).\mathbf{b}(\mathbf{k})]\{\nu^{(0)}+\nu_1^{(1)}\tfrac{\mathbf{k}.\mathbf{p}}{kp}+\nu_2^{(1)}\tfrac{\mathbf{k}.\mathbf{q}}{kq}+\nu_3^{(1)}\tfrac{\mathbf{p}.\mathbf{q}}{pq}\}+\\
&[\mathbf{p}.\mathbf{b}(\mathbf{k})][\mathbf{u}(\mathbf{p}).\mathbf{b}(\mathbf{q})]\{\phi^{(0)}+\phi_1^{(1)}\tfrac{\mathbf{k}.\mathbf{p}}{kp}+\phi_2^{(1)}\tfrac{\mathbf{k}.\mathbf{q}}{kq}+\phi_3^{(1)}\tfrac{\mathbf{p}.\mathbf{q}}{pq}\}+\\
&[\mathbf{p}.\mathbf{b}(\mathbf{k})][\mathbf{u}(\mathbf{q}).\mathbf{b}(\mathbf{p})]\{\chi^{(0)}+\chi_1^{(1)}\tfrac{\mathbf{k}.\mathbf{p}}{kp}+\chi_2^{(1)}\tfrac{\mathbf{k}.\mathbf{q}}{kq}+\chi_3^{(1)}\tfrac{\mathbf{p}.\mathbf{q}}{pq}\}\quad) \qquad \text{(C.3)}
\end{aligned}
$$

The quantities $Z_\Delta^{bu} = Z_{2\Delta}^{bu} + Z_{3\Delta}^{bu}$ represent the energy circulating from $\mathbf{u}(\mathbf{p}) \rightarrow \mathbf{b}(\mathbf{k}) \rightarrow \mathbf{u}(\mathbf{q}) \rightarrow \mathbf{b}(\mathbf{p}) \ldots \rightarrow \mathbf{u}(\mathbf{p})$ [see Fig. 3.12 in Section 3.7.3]. We will denote the circulating transfer from $\mathbf{u}(\mathbf{p}) \rightarrow \mathbf{b}(\mathbf{k})$ by $Z_\Delta^{bu}(\mathbf{k}|\mathbf{p}|\mathbf{q})$, from $\mathbf{b}(\mathbf{p}) \rightarrow \mathbf{u}(\mathbf{k})$ by $Z_\Delta^{ub}(\mathbf{k}|\mathbf{p}|\mathbf{q})$ and so on for the circulating transfer between other modes. We take $Z_\Delta^{bu} = Z_{2\Delta} +^{bu} Z_{3\Delta}^{bu}$ in Eqs. (C.2)-(C.3) to be the circulating transfer from $\mathbf{u}(\mathbf{p}) \rightarrow \mathbf{b}(\mathbf{k})$, i.e., $Z_\Delta^{bu}(\mathbf{k}|\mathbf{p}|\mathbf{q}) \equiv Z_\Delta$. Then by symmetry the circulating transfer from $\mathbf{u}(\mathbf{q})$ to $\mathbf{b}(\mathbf{k})$ can be written as

$$
Z_\Delta^{bu}(\mathbf{k}|\mathbf{q}|\mathbf{p}) = Z_{2\Delta}^{bu}(\mathbf{k}|\mathbf{q}|\mathbf{p}) + Z_{3\Delta}^{bu}(\mathbf{k}|\mathbf{q}|\mathbf{p}) \qquad \text{(C.4)}
$$

$$
\begin{aligned}
Z_{2\Delta}^{bu}(\mathbf{k}|\mathbf{q}|\mathbf{p}) = Re(\ &[\mathbf{k}.\mathbf{u}(\mathbf{p})][\mathbf{b}(\mathbf{k}).\mathbf{b}(\mathbf{q})]\{\alpha^{(0)}+\alpha_1\tfrac{\mathbf{k}.\mathbf{q}}{kq}+\alpha_2\tfrac{\mathbf{k}.\mathbf{p}}{kp}+\alpha_3\tfrac{\mathbf{p}.\mathbf{q}}{pq}\}+\\
&[\mathbf{k}.\mathbf{u}(\mathbf{q})][\mathbf{b}(\mathbf{k}).\mathbf{b}(\mathbf{p})]\{\beta^{(0)}+\beta_1\tfrac{\mathbf{k}.\mathbf{q}}{kq}+\beta_2\tfrac{\mathbf{k}.\mathbf{p}}{kp}+\beta_3\tfrac{\mathbf{p}.\mathbf{q}}{pq}\}+\\
&[\mathbf{q}.\mathbf{u}(\mathbf{k})][\mathbf{b}(\mathbf{p}).\mathbf{b}(\mathbf{q})]\{\gamma^{(0)}+\gamma_1\tfrac{\mathbf{k}.\mathbf{q}}{kq}+\gamma_2\tfrac{\mathbf{k}.\mathbf{p}}{kp}+\gamma_3\tfrac{\mathbf{p}.\mathbf{q}}{pq}\}\quad) \qquad \text{(C.5)}
\end{aligned}
$$

$$
\begin{aligned}
Z_{3\Delta}^{bu}(\mathbf{k}|\mathbf{q}|\mathbf{p}) = Re(\ &[\mathbf{k}.\mathbf{b}(\mathbf{p})][\mathbf{u}(\mathbf{k}).\mathbf{b}(\mathbf{q})]\{\delta^{(0)}+\delta_1\tfrac{\mathbf{k}.\mathbf{q}}{kq}+\delta_2\tfrac{\mathbf{k}.\mathbf{p}}{kp}+\delta_3\tfrac{\mathbf{p}.\mathbf{q}}{pq}\}+\\
&[\mathbf{k}.\mathbf{b}(\mathbf{p})][\mathbf{u}(\mathbf{q}).\mathbf{b}(\mathbf{k})]\{\eta^{(0)}+\eta_1\tfrac{\mathbf{k}.\mathbf{q}}{kq}+\eta_2\tfrac{\mathbf{k}.\mathbf{p}}{kp}+\eta_3\tfrac{\mathbf{p}.\mathbf{q}}{pq}\}+\\
&[\mathbf{k}.\mathbf{b}(\mathbf{q})][\mathbf{u}(\mathbf{q}).\mathbf{b}(\mathbf{k})]\{\mu^{(0)}+\mu_1\tfrac{\mathbf{k}.\mathbf{q}}{kq}+\mu_2\tfrac{\mathbf{k}.\mathbf{p}}{kp}+\mu_3\tfrac{\mathbf{p}.\mathbf{q}}{pq}\}+\\
&[\mathbf{k}.\mathbf{b}(\mathbf{q})][\mathbf{u}(\mathbf{k}).\mathbf{b}(\mathbf{q})]\{\nu^{(0)}+\nu_1\tfrac{\mathbf{k}.\mathbf{q}}{kq}+\nu_2\tfrac{\mathbf{k}.\mathbf{p}}{kp}+\nu_3\tfrac{\mathbf{p}.\mathbf{q}}{pq}\}+\\
&[\mathbf{q}.\mathbf{b}(\mathbf{k})][\mathbf{u}(\mathbf{q}).\mathbf{b}(\mathbf{p})]\{\phi^{(0)}+\phi_1\tfrac{\mathbf{k}.\mathbf{q}}{kq}+\phi_2\tfrac{\mathbf{k}.\mathbf{p}}{kp}+\phi_3\tfrac{\mathbf{p}.\mathbf{q}}{pq}\}+\\
&[\mathbf{q}.\mathbf{b}(\mathbf{k})][\mathbf{u}(\mathbf{p}).\mathbf{b}(\mathbf{q})]\{\chi^{(0)}+\chi_1\tfrac{\mathbf{k}.\mathbf{q}}{kq}+\chi_2\tfrac{\mathbf{k}.\mathbf{p}}{kp}+\chi_3\tfrac{\mathbf{p}.\mathbf{q}}{pq}\}\quad) \qquad \text{(C.6)}
\end{aligned}
$$

We have dropped the superscript '1' in the above equations. $Z_\Delta^{bu}(\mathbf{k}|\mathbf{p}|\mathbf{q})$ and $Z_\Delta^{ub}(\mathbf{p}|\mathbf{k}|\mathbf{q})$ are physically the same transfers, but the former represents the transfer from $\mathbf{u}(\mathbf{p})$ to $\mathbf{b}(\mathbf{k})$ and

the latter represents the same transfer from $\mathbf{b(k)}$ to $\mathbf{u(p)}$ The former should therefore be equal and opposite in sign to the latter, i.e.,

$$Z^{bu}_{\Delta}(\mathbf{k|p|q}) + Z^{ub}_{\Delta}(\mathbf{p|k|q}) = 0 \tag{C.7}$$

$Z^{ub}_{\Delta}(\mathbf{p|k|q})$ is thus given by the negative of Eqs. (C.1)-(C.3). Using the expression for $Z^{ub}_{\Delta}(\mathbf{p|k|q})$ we can write $Z^{ub}_{\Delta}(\mathbf{k|p|q})$ to be

$$Z^{ub}_{\Delta}(\mathbf{k|p|q}) = Z^{ub}_{2\Delta}(\mathbf{k|p|q}) + Z^{ub}_{3\Delta}(\mathbf{k|p|q}) \tag{C.8}$$

$$\begin{aligned} Z^{ub}_{2\Delta}(\mathbf{k|p|q}) = Re(\quad & -[\mathbf{k.u(p)}][\mathbf{b(k).b(q)}]\{\gamma^{(0)} + \gamma_1 \tfrac{\mathbf{k.p}}{kp} + \gamma_2 \tfrac{\mathbf{p.q}}{pq} + \gamma_3 \tfrac{\mathbf{k.q}}{kq}\} \\ & +[\mathbf{k.u(q)}][\mathbf{b(k).b(p)}]\{\alpha^{(0)} + \alpha_1 \tfrac{\mathbf{k.p}}{kp} + \alpha_2 \tfrac{\mathbf{p.q}}{pq} + \alpha_3 \tfrac{\mathbf{k.q}}{kq}\} \\ & -[\mathbf{p.u(k)}][\mathbf{b(p).b(q)}]\{\beta^{(0)} + \beta_1 \tfrac{\mathbf{k.p}}{kp} + \beta_2 \tfrac{\mathbf{p.q}}{pq} + \beta_3 \tfrac{\mathbf{k.q}}{kq}\} \quad) \end{aligned} \tag{C.9}$$

$$\begin{aligned} Z^{ub}_{3\Delta}(\mathbf{k|p|q}) = Re(\quad & -[\mathbf{k.b(p)}][\mathbf{u(k).b(q)}]\{\phi^{(0)} + \phi_1 \tfrac{\mathbf{k.p}}{kp} + \phi_2 \tfrac{\mathbf{p.q}}{pq} + \phi_3 \tfrac{\mathbf{k.q}}{kq}\} \\ & -[\mathbf{k.b(p)}][\mathbf{u(q).b(k)}]\{\chi^{(0)} + \chi_1 \tfrac{\mathbf{k.p}}{kp} + \chi_2 \tfrac{\mathbf{p.q}}{pq} + \chi_3 \tfrac{\mathbf{k.q}}{kq}\} \\ & +[\mathbf{k.b(q)}][\mathbf{u(p).b(k)}]\{\delta^{(0)} + \delta_1 \tfrac{\mathbf{k.p}}{kp} + \delta_2 \tfrac{\mathbf{p.q}}{pq} + \delta_3 \tfrac{\mathbf{k.q}}{kq}\} \\ & +[\mathbf{k.b(q)}][\mathbf{u(k).b(p)}]\{\eta^{(0)} + \eta_1 \tfrac{\mathbf{k.p}}{kp} + \eta_2 \tfrac{\mathbf{p.q}}{pq} + \eta_3 \tfrac{\mathbf{k.q}}{kq}\} \\ & -[\mathbf{p.b(k)}][\mathbf{u(p).b(q)}]\{\mu^{(0)} + \mu_1 \tfrac{\mathbf{k.p}}{kp} + \mu_2 \tfrac{\mathbf{p.q}}{pq} + \mu_3 \tfrac{\mathbf{k.q}}{kq}\} \\ & -[\mathbf{p.b(k)}][\mathbf{u(q).b(p)}]\{\nu^{(0)} + \nu_1 \tfrac{\mathbf{k.p}}{kp} + \nu_2 \tfrac{\mathbf{p.q}}{pq} + \nu_3 \tfrac{\mathbf{k.q}}{kq}\} \quad) \end{aligned} \tag{C.10}$$

and $Z^{ub}_{\Delta}(\mathbf{k|q|p})$ is given by

$$Z^{ub}_{\Delta}(\mathbf{k|q|p}) = Z^{ub}_{2\Delta}(\mathbf{k|q|p}) + Z^{ub}_{3\Delta}(\mathbf{k|q|p}) \tag{C.11}$$

$$\begin{aligned} Z^{ub}_{2\Delta}(\mathbf{k|q|p}) = Re(\quad & -[\mathbf{k.u(q)}][\mathbf{b(k).b(p)}]\{\gamma^{(0)} + \gamma_1 \tfrac{\mathbf{k.q}}{kq} + \gamma_2 \tfrac{\mathbf{p.q}}{pq} + \gamma_3 \tfrac{\mathbf{k.p}}{kp}\} \\ & +[\mathbf{k.u(p)}][\mathbf{b(k).b(q)}]\{\alpha^{(0)} + \alpha_1 \tfrac{\mathbf{k.q}}{kq} + \alpha_2 \tfrac{\mathbf{p.q}}{pq} + \alpha_3 \tfrac{\mathbf{k.p}}{kp}\} \\ & -[\mathbf{q.u(k)}][\mathbf{b(p).b(q)}]\{\beta^{(0)} + \beta_1 \tfrac{\mathbf{k.q}}{kq} + \beta_2 \tfrac{\mathbf{p.q}}{pq} + \beta_3 \tfrac{\mathbf{k.p}}{kp}\} \quad) \end{aligned}$$

(C.12)

$$
\begin{aligned}
Z^{ub}_{3\Delta}(\mathbf{k}|\mathbf{q}|\mathbf{p}) = Re(\quad & -[\mathbf{k}.\mathbf{b}(\mathbf{q})][\mathbf{u}(\mathbf{k}).\mathbf{b}(\mathbf{p})]\{\phi^{(0)} + \phi_1\tfrac{\mathbf{k}.\mathbf{q}}{kq} + \phi_2\tfrac{\mathbf{p}.\mathbf{q}}{pq} + \phi_3\tfrac{\mathbf{k}.\mathbf{p}}{kp}\} \\
& -[\mathbf{k}.\mathbf{b}(\mathbf{q})][\mathbf{u}(\mathbf{p}).\mathbf{b}(\mathbf{k})]\{\chi^{(0)} + \chi_1\tfrac{\mathbf{k}.\mathbf{q}}{kq} + \chi_2\tfrac{\mathbf{p}.\mathbf{q}}{pq} + \chi_3\tfrac{\mathbf{k}.\mathbf{p}}{kp}\} \\
& +[\mathbf{k}.\mathbf{b}(\mathbf{p})][\mathbf{u}(\mathbf{q}).\mathbf{b}(\mathbf{k})]\{\delta^{(0)} + \delta_1\tfrac{\mathbf{k}.\mathbf{q}}{kq} + \delta_2\tfrac{\mathbf{p}.\mathbf{q}}{pq} + \delta_3\tfrac{\mathbf{k}.\mathbf{p}}{kp}\} \\
& +[\mathbf{k}.\mathbf{b}(\mathbf{p})][\mathbf{u}(\mathbf{k}).\mathbf{b}(\mathbf{q})]\{\eta^{(0)} + \eta_1\tfrac{\mathbf{k}.\mathbf{q}}{kq} + \eta_2\tfrac{\mathbf{p}.\mathbf{q}}{pq} + \eta_3\tfrac{\mathbf{k}.\mathbf{p}}{kp}\} \\
& -[\mathbf{q}.\mathbf{b}(\mathbf{k})][\mathbf{u}(\mathbf{q}).\mathbf{b}(\mathbf{p})]\{\mu^{(0)} + \mu_1\tfrac{\mathbf{k}.\mathbf{q}}{kq} + \mu_2\tfrac{\mathbf{p}.\mathbf{q}}{pq} + \mu_3\tfrac{\mathbf{k}.\mathbf{p}}{kp}\} \\
& -[\mathbf{q}.\mathbf{b}(\mathbf{k})][\mathbf{u}(\mathbf{p}).\mathbf{b}(\mathbf{q})]\{\nu^{(0)} + \nu_1\tfrac{\mathbf{k}.\mathbf{q}}{kq} + \nu_2\tfrac{\mathbf{p}.\mathbf{q}}{pq} + \nu_3\tfrac{\mathbf{k}.\mathbf{p}}{kp}\} \quad)
\end{aligned}
$$

(C.13)

The sum of the circulating transfer to $\mathbf{b}(\mathbf{k})$ from $\mathbf{u}(\mathbf{p})$ and from $\mathbf{u}(\mathbf{q})$ should be zero. i.e.,

$$Z^{bu}_{\Delta}(\mathbf{k}|\mathbf{p}|\mathbf{q}) + Z^{bu}_{\Delta}(\mathbf{k}|\mathbf{q}|\mathbf{p}) = 0 \tag{C.14}$$

and similarly the sum of the circulating transfer to $\mathbf{u}(\mathbf{k})$ from $\mathbf{b}(\mathbf{p})$ and from $\mathbf{b}(\mathbf{q})$ should also be equal to zero. i.e.,

$$Z^{ub}_{\Delta}(\mathbf{k}|\mathbf{p}|\mathbf{q}) + Z^{ub}_{\Delta}(\mathbf{k}|\mathbf{q}|\mathbf{p}) = 0 \tag{C.15}$$

Replacing $Z^{bu}_{\Delta}(\mathbf{k}|\mathbf{p}|\mathbf{q})$ and $Z^{bu}_{\Delta}(\mathbf{k}|\mathbf{q}|\mathbf{p})$ from Eqs. (C.1)-(C.3) and Eqs. (C.4)-(C.6) into Eq. (C.14) we get the following relationships between the constants: α, β, etc. $\alpha^{(0)} + \beta^{(0)} = 0, \alpha_1 + \beta_2 = 0, \alpha_2 + \beta_1 = 0, \alpha_3 + \beta_3 = 0, \gamma_1 - \gamma_2 = 0, \delta^{(0)} + \mu^{(0)} = 0, \delta_1 + \mu_2 = 0, \delta_2 + \mu_1 = 0, \delta_3 + \mu_3 = 0, \eta^{(0)} + \nu^{(0)} = 0, \eta_1 + \nu_2 = 0, \eta_2 + \nu_1 = 0, \eta_3 + \nu_3 = 0, \phi^{(0)} - \chi^{(0)} = 0, \phi_1 - \chi_2 = 0, \phi_2 - \chi_1 = 0, \phi_3 - \chi_3 = 0$. After replacing $Z^{ub}_{\Delta}(\mathbf{k}|\mathbf{p}|\mathbf{q})$ and $Z^{ub}_{\Delta}(\mathbf{k}|\mathbf{q}|\mathbf{p})$ from Eqs. (C.1)-(C.3) and Eqs. (C.11)-(C.13) into Eq. (C.15) we get the following relationships: $\alpha_2 - \alpha_3 = 0, \beta^{(0)} + \gamma^{(0)} = 0, \beta_1 + \gamma_1 = 0, \beta_2 + \gamma_3 = 0, \beta_3 + \gamma_2 = 0, \delta^{(0)} - \eta^{(0)} = 0, \delta_1 - \eta_1 = 0, \delta_2 - \eta_3 = 0, \delta_3 - \eta_2 = 0, \mu^{(0)} + \phi^{(0)} = 0, \mu_1 + \phi_1 = 0, \mu_2 + \phi_3 = 0, \mu_3 + \phi_2 = 0, \nu^{(0)} + \chi^{(0)} = 0, \nu_2 + \chi_3 = 0, \mu_3 + \phi_2 = 0$.

Let us now consider the following geometry: the three wavenumbers in the triad form an

isosceles triangle, and we choose Fourier coefficients at the two wavenumbers of equal lengths to be perpendicular to **k**, **p**, **q**. We had considered this kind of geometry in Appendix A and Appendix B. We had argued that because of the symmetry between the two wavenumbers of equal length, the circulating transfer should vanish for this geometry. This constraint had given us an additional set of relationships between the constants in Y_Δ. Z_Δ^{bu} should also be equal to zero for this geometry. Since Z_Δ^{bu} and Y_Δ have the same functional form, given by Eq. (B.22)-(B.23) of Appendix B and Eq. (C.1)-(C.3) of this appendix respectively, hence imposition of this constraint on Z_Δ^{bu} would give the same set of relationships, i.e., $\gamma^{(0)} = 0, \gamma_1 + \gamma_2 = 0, \gamma_3 = 0, \phi^{(0)} = 0, \phi_2 + \phi_3 = 0, \phi_1 = 0, \chi^{(0)} = 0, \chi_1 + \chi_3 = 0, \chi_2 = 0, \alpha^{(0)} = 0, \alpha_1 = 0, \alpha_2 + \alpha_3 = 0, \delta^{(0)} = 0, \delta_1 = 0, \delta_2 + \delta_3 = 0, \eta^{(0)} = 0, \eta_1 = 0, \eta_2 + \eta_3 = 0, \beta^{(0)} = 0, \beta_2 = 0, \beta_1 + \beta_3 = 0, \mu^{(0)} = 0, \mu_2 = 0, \mu_1 + \mu_3 = 0, \nu^{(0)} = 0, \nu_2 = 0, \nu_1 + \nu_3 = 0$.

The above relationships between the constants in Eqs. (C.2)-(C.3) are identical to the relationships between the constants in Eqs. (B.22)-(B.23) of Appendix B. We know from Appendix B that these relationships can be expressed more clearly as follows: $\{\alpha^{(0)} = -\beta^{(0)} = \gamma^{(0)} = 0\}$, $\{\delta^{(0)} = -\mu^{(0)} = \phi^{(0)} = \eta^{(0)} = -\nu^{(0)} = \chi^{(0)} = 0\}$, $\{\alpha_1 = -\beta_2 = \gamma_3 = 0\}$, $\{\alpha_2 = -\beta_1 = \gamma_1 = \gamma_2 = \alpha_3 = -\beta_3 = 0\}$, $\{\delta_1 = -\mu_2 = \phi_3 = \chi_3 = -\nu_2 = \eta_1 = 0\}$, $\{\delta_2 = -\mu_1 = \phi_1 = \chi_2 = -\nu_3 = \eta_3 = -\delta_3 = \mu_3 = -\phi_2 = -\chi_1 = \nu_1 = -\eta_2\}$. There is just one undetermined constant which we will denote by 'C', i.e., $\{\delta_2 = -\mu_1 = ... = C\}$. Expressing Z_Δ^{bu} [Eqs. (C.2)-(C.3)] in terms of this single constant, we get

$$Z_{2\Delta} = 0 \tag{C.16}$$

$$\begin{aligned} Z_{3\Delta} = Re(\quad & [\mathbf{k}.\mathbf{b}(\mathbf{q})][\mathbf{u}(\mathbf{k}).\mathbf{b}(\mathbf{p})]\{C\tfrac{\mathbf{k}.\mathbf{q}}{kq} - C\tfrac{\mathbf{p}.\mathbf{q}}{pq}\} + [\mathbf{k}.\mathbf{b}(\mathbf{q})][\mathbf{u}(\mathbf{p}).\mathbf{b}(\mathbf{k})]\{-C\tfrac{\mathbf{k}.\mathbf{q}}{kq} + C\tfrac{\mathbf{p}.\mathbf{q}}{pq}\} + \\ & [\mathbf{k}.\mathbf{b}(\mathbf{p})][\mathbf{u}(\mathbf{k}).\mathbf{b}(\mathbf{q})]\{-C\tfrac{\mathbf{k}.\mathbf{p}}{kp} + C\tfrac{\mathbf{p}.\mathbf{q}}{pq}\} + [\mathbf{k}.\mathbf{b}(\mathbf{p})][\mathbf{u}(\mathbf{q}).\mathbf{b}(\mathbf{k})]\{C\tfrac{\mathbf{k}.\mathbf{p}}{kp} + -C\tfrac{\mathbf{p}.\mathbf{q}}{pq}\} + \\ & [\mathbf{p}.\mathbf{b}(\mathbf{k})][\mathbf{u}(\mathbf{p}).\mathbf{b}(\mathbf{q})]\{C\tfrac{\mathbf{k}.\mathbf{p}}{kp} - C\tfrac{\mathbf{k}.\mathbf{q}}{kq}\} + [\mathbf{p}.\mathbf{b}(\mathbf{k})][\mathbf{u}(\mathbf{q}).\mathbf{b}(\mathbf{p})]\{-C\tfrac{\mathbf{k}.\mathbf{p}}{kp} + C\tfrac{\mathbf{k}.\mathbf{q}}{kq}\} \quad) \end{aligned} \tag{C.17}$$

which is the same as the expression for for Y_Δ in Eqs. (B.33)-(B.34) of Appendix B.

If k/p and $q/p \rightarrow \infty$, while $\mathbf{p}$ is kept constant the circulating transfer Z_Δ should tend to zero. This constraint was also applied on the circulating transfer between magnetic modes, Y_Δ in Appendix B. We had shown that the constant $C = 0$ for this constraint to be satisfied. Putting $C = 0$ in Eqs. (C.16)-(C.17) we get $Z^{bu}_\Delta = Z^{bu}_{2\Delta} + Z^{bu}_{3\Delta}$ equal to zero.

The circulating transfer between the velocity and the magnetic modes in the triad is equal to zero and the mode-to-mode transfer $\mathcal{R}^{bu}(\mathbf{k}|\mathbf{p}|\mathbf{q}) = \mathcal{S}^{bu}(\mathbf{k}|\mathbf{p}|\mathbf{q})$.

The derivation of Z^{bu}_Δ, however took the coefficients to be linear. A completely general derivation for Z^{bu}_Δ will require imposition of additional symmetry and invariance or some other constraints, which we have ignored here.

Appendix D

Equivalence of Kraichnan's formula and our formula for the Kinetic energy flux

In this appendix we will show that the flux formula (3.30) based on the effective mode-to-mode transfer is equivalent to Eq. (3.28) derived by Kraichnan.

Kraichnan[95] showed that the kinetic energy flux in terms of the combined energy transfer S^{uu} given by

$$\Pi^{u<}_{u>}(K) = -\sum_{|\mathbf{k}|<\mathbf{K}} \sum_{\mathbf{p}}^{\Delta} \frac{1}{2} S^{uu}(\mathbf{k}|\mathbf{p},\mathbf{q}) \tag{D.1}$$

Our formula for flux in terms of the effective mode-to-mode transfer $\mathcal{S}^{uu}$ is given by

$$\Pi^{u<}_{u>}(K) = -\sum_{|\mathbf{k}|<K} \sum_{|\mathbf{p}|>K}^{\Delta} \mathcal{S}^{uu}(\mathbf{k}|\mathbf{p}|\mathbf{q}). \tag{D.2}$$

The equation (D.1) can be written in terms of $\mathcal{S}$'s as follows:

$$\Pi^{u<}_{u>}(K) = \sum_{|\mathbf{k}|<\mathbf{K}} \sum_{\mathbf{p}}^{\Delta} \frac{1}{2} \left(\mathcal{S}^{uu}(\mathbf{k}|\mathbf{p}|\mathbf{q}) + \mathcal{S}^{uu}(\mathbf{k}|\mathbf{q}|\mathbf{p})\right) \tag{D.3}$$

which can be further split up as

$$\begin{aligned}\Pi^{u<}_{u>}(K) \;=\; & \\ & \sum_{|\mathbf{k}|<\mathbf{K}} \sum_{|\mathbf{p}|,|\mathbf{q}|<K}^{\Delta} \frac{1}{2} \left(\mathcal{S}^{uu}(\mathbf{k}|\mathbf{p}|\mathbf{q}) + \mathcal{S}^{uu}(\mathbf{k}|\mathbf{q}|\mathbf{p})\right) \\ + & \sum_{|\mathbf{k}|<\mathbf{K}} \sum_{|\mathbf{p}|,|\mathbf{q}|>K}^{\Delta} \frac{1}{2} \left(\mathcal{S}^{uu}(\mathbf{k}|\mathbf{p}|\mathbf{q}) + \mathcal{S}^{uu}(\mathbf{k}|\mathbf{q}|\mathbf{p})\right)\end{aligned}$$

$$+ \sum_{|\mathbf{k}|<\mathbf{K}} \sum_{|\mathbf{p}|<K,|\mathbf{q}|>K}^{\Delta} \frac{1}{2}(\mathcal{S}^{uu}(\mathbf{k}|\mathbf{p}|\mathbf{q}) + \mathcal{S}^{uu}(\mathbf{k}|\mathbf{q}|\mathbf{p}))$$

$$+ \sum_{|\mathbf{k}|<\mathbf{K}} \sum_{|\mathbf{p}|>K,|\mathbf{q}|<K}^{\Delta} \frac{1}{2}(\mathcal{S}^{uu}(\mathbf{k}|\mathbf{p}|\mathbf{q}) + \mathcal{S}^{uu}(\mathbf{k}|\mathbf{q}|\mathbf{p})) \tag{D.4}$$

These transfers are shown in Fig. D.1.

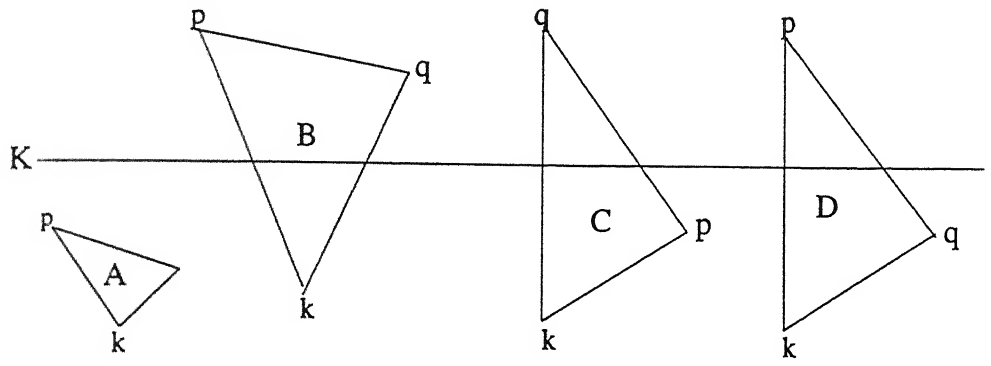

Figure D.1: The various triads involved in the terms in Eq. (D.4). Triad of type A does not contribute to energy flux. Triad of type C and D are equivalent and contribute the same amount.

Making use of symmetries between $\mathbf{k}, \mathbf{p}, \mathbf{q}$ in the summations we get the following relationships. Since $\mathbf{p}$, $\mathbf{q}$ are interchangeable we get

$$\sum_{|\mathbf{k}|<\mathbf{K}} \sum_{|\mathbf{p}|,|\mathbf{q}|>K}^{\Delta} \mathcal{S}^{uu}(\mathbf{k}|\mathbf{p}|\mathbf{q}) = \sum_{|\mathbf{k}|<\mathbf{K}} \sum_{|\mathbf{p}|,|\mathbf{q}|>K}^{\Delta} \mathcal{S}^{uu}(\mathbf{k}|\mathbf{q}|\mathbf{p}), \tag{D.5}$$

since $\mathbf{k}$, $\mathbf{p}$ are interchangeable,

$$\sum_{|\mathbf{k}|<\mathbf{K}} \sum_{|\mathbf{p}|<K,|\mathbf{q}|>K}^{\Delta} \mathcal{S}^{uu}(\mathbf{k}|\mathbf{p}|\mathbf{q}) = \sum_{|\mathbf{k}|<\mathbf{K}} \sum_{|\mathbf{p}|<K,|\mathbf{q}|>K}^{\Delta} \mathcal{S}^{uu}(\mathbf{p}|\mathbf{k}|\mathbf{q}), \tag{D.6}$$

since $\mathbf{k}$, $\mathbf{q}$ are interchangeable,

$$\sum_{|\mathbf{k}|<\mathbf{K}} \sum_{|\mathbf{q}|<K,|\mathbf{p}|>K}^{\Delta} \mathcal{S}^{uu}(\mathbf{k}|\mathbf{q}|\mathbf{p}) = \sum_{|\mathbf{k}|<\mathbf{K}} \sum_{|\mathbf{q}|<K,|\mathbf{p}|>K}^{\Delta} \mathcal{S}^{uu}(\mathbf{q}|\mathbf{k}|\mathbf{p}). \tag{D.7}$$

The sum $\sum_{|\mathbf{k}|<\mathbf{K}} \sum^{\Delta}_{|\mathbf{p}|<K,|\mathbf{q}|>K} \frac{1}{2}\mathcal{S}^{uu}(\mathbf{k}|\mathbf{p}|\mathbf{q})$ involves transfers from $\mathbf{k} \to \mathbf{p}$ and also from $\mathbf{p} \to \mathbf{k}$.

which are equal and opposite. Therefore

$$\sum_{|\mathbf{k}|<\mathbf{K}} \sum_{|\mathbf{p}|<\mathbf{K},|\mathbf{q}|>K}^{\Delta} \frac{1}{2}\mathcal{S}^{uu}(\mathbf{k}|\mathbf{p}|\mathbf{q}) = 0. \tag{D.8}$$

Similarly,

$$\sum_{|\mathbf{k}|<\mathbf{K}} \sum_{|\mathbf{p}|>\mathbf{K},|\mathbf{q}|<K}^{\Delta} \frac{1}{2}\mathcal{S}^{uu}(\mathbf{k}|\mathbf{q}|\mathbf{p}) = 0, \tag{D.9}$$

and,

$$\sum_{|\mathbf{k}|<\mathbf{K}} \sum_{|\mathbf{p}|<\mathbf{K},|\mathbf{q}|<K}^{\Delta} \frac{1}{2}\mathcal{S}^{uu}(\mathbf{k}|\mathbf{q}|\mathbf{p}) = 0, \tag{D.10}$$

In other words all terms except both legs of Fig. D.1, $\mathbf{p} \to \mathbf{k}$ legs of Fig. D.1, and $\mathbf{q} \to \mathbf{k}$ legs of Fig. D.1 survive. We use these results to rewrite $\Pi_{u>}^{u<}(K)$ as

$$\begin{aligned}\Pi_{u>}^{u<}(K) &= \sum_{|\mathbf{k}|<\mathbf{K}} \sum_{|\mathbf{p}|,|\mathbf{q}|>K}^{\Delta} \mathcal{S}^{uu}(\mathbf{k}|\mathbf{p}|\mathbf{q}) + \sum_{|\mathbf{k}|<\mathbf{K}} \sum_{|\mathbf{p}|<K,|\mathbf{q}|>K}^{\Delta} \frac{1}{2}\mathcal{S}^{uu}(\mathbf{k}|\mathbf{q}|\mathbf{p}) \\ &+ \sum_{|\mathbf{k}|<\mathbf{K}} \sum_{|\mathbf{q}|<K,|\mathbf{p}|>K}^{\Delta} \frac{1}{2}\mathcal{S}^{uu}(\mathbf{k}|\mathbf{p}|\mathbf{q})\end{aligned} \tag{D.11}$$

Using symmetry between $\mathbf{p}$ and $\mathbf{q}$ we get,

$$\sum_{|\mathbf{k}|<\mathbf{K}} \sum_{|\mathbf{p}|<\mathbf{K},|\mathbf{q}|>K}^{\Delta} \frac{1}{2}\mathcal{S}^{uu}(\mathbf{k}|\mathbf{q}|\mathbf{p}) = \sum_{|\mathbf{k}|<\mathbf{K}} \sum_{|\mathbf{q}|<\mathbf{K},|\mathbf{p}|>K}^{\Delta} \frac{1}{2}\mathcal{S}^{uu}(\mathbf{k}|\mathbf{p}|\mathbf{q}) \tag{D.12}$$

Hence, we can write,

$$\begin{aligned}\Pi_{u>}^{u<} &= \sum_{|\mathbf{k}|<\mathbf{K}} \sum_{|\mathbf{p}|,|\mathbf{q}|>K}^{\Delta} \mathcal{S}^{uu}(\mathbf{k}|\mathbf{p}|\mathbf{q}) + \sum_{|\mathbf{k}|<\mathbf{K}} \sum_{|\mathbf{q}|<K,|\mathbf{p}|<K}^{\Delta} \mathcal{S}^{uu}(\mathbf{k}|\mathbf{p}|\mathbf{q}) \\ &= \sum_{|\mathbf{k}|<\mathbf{K}} \sum_{|\mathbf{p}|>K}^{\Delta} \mathcal{S}^{uu}(\mathbf{k}|\mathbf{p}|\mathbf{q})\end{aligned} \tag{D.13}$$

This is the same as $\Pi_{u>}^{u<}$ of Eq. (3.28). Thus, we have shown that Kraichnan's formula for flux is the same as our formula based on the mode-to-mode transfer.

Bibliography

[1] R. H. Kraichnan. *Phys. Fluids*, 8:1385, 1965.

[2] P. S. Iroshnikov. *Astron. Zh.*, 40:742, 1963.

[3] M. Dobrowolny, A. Mangeney, and P. Veltri. *Phys. Rev. Lett.*, 45:144, 1980.

[4] R. Grappin, A. Pouquet, and J. Leorat. *Astron. Astrophys.*, 126:51, 1983.

[5] E. Marsch. In *Reviews in Modern Astronomy*, editor, G. Klare, volume 4, page 43. Heidelberg : Springer Verlag, 1990.

[6] W. H. Matthaeus and Y. Zhou. *Phys. Fluids*, 31:3634, 1988.

[7] Y. Zhou and W. H. Matthaeus. *J. Geophys. Res.*, 95:14881, 1990.

[8] D. Biskamp and H. Welter. *Phys. Fluids B*, 1:1964, 1989.

[9] A. Pouquet, P. L. Sulem, and M. Meneguzzi. *Phys. Fluids*, 31:2635, 1988.

[10] H. Politano, A. Pouquet, and P. L. Sulem. *Phys. Fluids*, 1:2330, 1989.

[11] M. K. Verma, D. A. Roberts, M. L. Golstein, S. Ghosh, and W. T. Stribling. *J. Geophys. Res.*, 101:21619, 1996.

[12] H. Politano, A. Pouquet, and V. Carbone. *Europhys. Lett.*, 43:516, 1998.

[13] W. Muller and D. Biskamp. physics/9906003, 1999.

[14] E. Marsch and C.-Y. Tu. *J. Geophys. Res.*, 95:8211, 1990.

[15] W. H. Matthaeus and M. L. Goldstein. *J. Geophys. Res.*, 87:6011, 1982.

[16] C.-Y. Tu, E. Marsch, and K. M. Thieme. *J. Geophys. Res.*, 94:11739, 1989.

[17] A. Pouquet, U. Frisch, and J. Leorat. *J. Fluid Mech.*, 77:321, 1976.

[18] A. Pouquet. *J. Fluid Mech.*, 88:1, 1978.

[19] A. Ishizawa and Y. Hattori. *chao-dyn/9810036*, 1998.

[20] A. Ishizawa and Y. Hattori. *J. Phys. Soc. Jpn.*, 67:441, 1998.

[21] A. Pouquet and G. S. Patterson. *J. Fluid Mech.*, 85:395, 1978.

[22] E. G. Zweibel. *Phys. Plasma*, 6:1725, 1999.

[23] E. Marsch. In R. Schwenn and E. Marsch, editors, *Physics of the Inner Heliosphere*, page 159. Heidelberg : Springer Verlag.

[24] Ya. B. Zeldovich, A. A. Ruzmaikin, and D. D. Sokoloff. *Magnetic fields in Astrophysics*. Gordon and Breach Science Publishers, 1983.

[25] A. N. Kolmogorov. *Dokl. Akad. Nauk SSSR*, 30:9, 1941.

[26] M. K. Verma. *Phys. Plasma*, 6, 1999.

[27] M. K. Verma and G. Dar. In *Proceedings of Nonlinear dynamics and computational physics conference*, editors, V. B. Sheorey, page 192. Narosa, New Delhi, 1999.

[28] F. F. Chen. *Introduction to Plasma Physics*. Plenum Press, 1974.

[29] W. H. Matthaeus, M. L. Goldstein, and D. C. Montgomery. *Phys. Rev. Lett.*, 51:1484, 1984.

[30] W. H. Matthaeus and D. Montgomery. In*Statistical Physics and chaos in Fusion Plasmas*, editors, C. W. J. Horton and L. E. Reichl, page 285. Wiley, New York, 1984.

[31] A. C. Ting, W. H. Matthaeus, and D. Montgomery. *Phys. Fluids*, 29:9695, 1986.

[32] T. Stribling and W. H. Matthaeus. *Phys. Fluids B*, 2:1979, 1990.

[33] T. Stribling and W. H. Matthaeus. *Phys. Fluids B*, 3:1848, 1991.

[34] R. Kinney, J. C. Mcwilliams, and T. Tajima. *Phys. Plasma*, 2:3623, 1995.

[35] D. C. Leslie. *Developments in the theory of turbulence.* Oxford University Press, 1973.

[36] M. M. Stanisic. *The Mathematical Theory of Turbulence.* Springer-Verlag, 1985.

[37] A. M. Obukhov. *Dokl. Akad. Nauk SSSR*, 32:22, 1941.

[38] U. Frisch. *Turbulence the legacy of A. N. Kolmogorov.* Cambridge University Press. 1995.

[39] J. A. Domaradzki and R. S. Rogallo. *Phys. Fluids A*, 2:413, 1990.

[40] J. A. Domaradzki. *Phys. Fluids*, 31:2747, 1988.

[41] Y. Zhou. *Phys. Fluids A*, 5:1092, 1993.

[42] Y. Zhou. *Phys. Fluids A*, 5:2511, 1993.

[43] K. Ohkitani and S. Kida. *Phys. Fluids A*, 4:794, 1992.

[44] M. Lesieur. *Turbulence in Fluids - Stochastic and Numerical Modelling.* Kluwer Academic Publishers, 1990.

[45] R. H. Kraichnan. *Phys. Fluids*, 10:1417, 1967.

[46] M. Nelkin. *chao-dyn/9906023*, 1999.

[47] G. K. Batchelor. *Phys. Fluid Suppl. II*, 12:233, 1969.

[48] R. H. Kraichnan and D. Montgomery. *Rep. Prog. Phys.*, 43:547, 1980.

[49] P. S. Iroshnikov. *Sov. Astron.*, 7:566, 1964.

[50] M. K. Verma and J. K. Bhattacharjee. *Europhys. Lett.*, 31:195, 1995.

[51] A. Basu, A. Sain, S. K. Dhar, and R. Pandit. *Phys. Rev. Lett.*, 81:2687, 1998.

[52] R. Benzi, S. Ciliberto, C. Tripiccione, C. Baudet, F. Massaioli, and S. Succi. *Phys. Rev. E*, 48:R29, 1993.

[53] R. Benzi, S. Ciliberto, C. Baudet, G. R. Chavarria, and C. Tripiccione. *Europhys. Lett.*, 24:275, 1993.

[54] R. Benzi, S. Ciliberto, C. Baudet, and G. R. Chavarria. *Physica D*, 80:385, 1995.

[55] S. K. Dhar, A. Sain, and R. Pandit. *Phys. Rev. Lett.*, 78:2964, 1997.

[56] V. Carbone, R. Bruno, and P. Veltri. *Geophys. Res. Lett.*, 23:121, 1996.

[57] C.-Y. Tu, E. Marsch, and H. Rosebauer. *Ann. Geophysicae*, 14:270, 1996.

[58] A. N. Kolmogorov. *Dokl. Akad. Nauk SSSR*, 32:16, 1941.

[59] H. Politano and A. Pouquet. *Geophys. Res. Lett.*, 25:273, 1998.

[60] H. Politano and A. Pouquet. *Phys. Rev. E*, 57:R21, 1998.

[61] L. F. Burlaga. *J. Geophys. Res.*, 96:5847, 1991.

[62] L. F. Burlaga. *J. Geophys. Res.*, 97:4283, 1992.

[63] E. Marsch and S. Liu. *Ann. Geophys.*, 11:227, 1993.

[64] D. Biskamp. *Nonlinear Magnetohydrodynamics*. Cambridge University Press, 1993.

[65] Z. S. She and E. Leveque. *Phys. Rev. Lett.*, 72:336, 1994.

[66] R. Grauer, J. Krug, and C. Marliani. *Phys. Lett. A*, 95:335, 1994.

[67] H. Politano and A. Pouquet. *Phys. Rev. E*, 52:636, 1995.

[68] W. D. McComb. *The Physics of Fluid Turbulence.* Cambridge Press. Oxford, 1990.

[69] J. D. Fournier, P. L. Sulem, and A. Pouquet. *J. Phys. A: Math Gen.*, 15:1393, 1982.

[70] S. J. Camargo and H. Tasso. *Phys. Fluids B*, 4:1199, 1992.

[71] M. K. Verma. *PhD thesis.* University of Maryland, 1994.

[72] G. K. Batchelor. *Proc. Roy. Soc. (London)*, 2:413, 1950.

[73] D. Fyfe and D. Montgomery. *J. Plasma Phys.*, 16:181, 1976.

[74] M. Hossain, W. H. Matthaeus, and D. Montogomery. *J. Plasma Phys.*, 30:479, 1983.

[75] D. Biskamp and U. Bremer. *Phys. Rev. Lett.*, 72:3819, 1993.

[76] H. Tennekes and J. L. Lumley. *A first course in turbulence.* MIT press, 1972.

[77] P. Frick and D. Sokoloff. *Phys. Rev. E*, 57:4155, 1998.

[78] R.S.Miller, F.Mashayek, V.Adumitroaie, and P.Givi. *Phys. Fluids*, 3:3304, 1996.

[79] M. Meneguzzi, U. Frisch, and A. Pouquett. *Phys. Rev. Lett.*, 47:1060, 1981.

[80] J. Leorat, A. Pouquet, and U. Frisch. *J. Fluid Mech.*, 104:419, 1981.

[81] M. K. Moffatt. *Magnetic field generation in electrically conducting fluids.* Cambridge University Press, 1978.

[82] Ya. B. Zeldovich. *Sov. Phys. JETP*, 4:460, 1957.

[83] L. W. Klein, D. A. Roberts, and M. L. Goldstein. *J. Geophys. Res.*, 96:3779, 1991.

[84] J. V. Shebalin, W. H. Matthaeus, and D. Montgomery. *J. Plasma Phys.*, 29:525, 1983.

[85] S. Oughton, E. R. Priest, and W. H. Matthaeus. *J. Fluid Mech.*, 280:95, 1994.

[86] D. Montgomery and L. Turner. *Phys. Fluids*, 24:825, 1981.

[87] S. Oughton, W. H. Matthaeus, and S. Ghosh. *Phys. Plasma*, 5:4235, 1998.

[88] W. H. Matthaeus, S. Oughton, S. Ghosh, and M. Hossain. *Phys. Rev. Lett.*, 81:2056, 1998.

[89] R. M. Kinney and J. C. McWilliams. *Phys. Rev. E*, 57:7111, 1998.

[90] R. Grappin, U. Frisch, J. Leorat, and A. Pouquet. *Astron. Astrophys.*, 105:6, 1982.

[91] C. Canuto, M. Y. Hussaini, A. Quarteroni, and T. A. Zang. *Spectral Methods in Fluid Mechanics*. Springer-Verlag, New York, 1988.

[92] D. Biskamp, E. Schwarz, and A. Celani. *Phys. Rev. Lett.*, 81:4855, 1998.

[93] R. H. Kraichnan. *J. Atmos. Sci.*, 33:1521, 1976.

[94] J. A. Domaradzki, R. W. Metcalfe, R. S. Rogallo, and J. J. Riley. *Phys. Rev. Lett.*, 58:547, 1987.

[95] R. H. Kraichnan. *J. Fluid Mech.*, 5:497, 1959.

[96] G. Dar, M. K. Verma, and V. Eswaran. *Phys. Plasma*, 5:2528, 1998.

[97] D. A. Roberts, L. W. Klein, M. L. Goldstein, and W. H. Matthaeus. *J. Geophys. Res.*, 92:11021, 1987a.

[98] D. A. Roberts, L. W. Klein, M. L. Goldstein, and W. H. Matthaeus. *J. Geophys. Res.*, 92:12023, 1987b.

[99] M. K. Verma, D. A. Roberts, and M. L. Golstein. *J. Geophys. Res.*, 100:19839, 1995.